General Disclaimer

One or more of the Following Statements may affect this Document

- This document has been reproduced from the best copy furnished by the organizational source. It is being released in the interest of making available as much information as possible.

- This document may contain data, which exceeds the sheet parameters. It was furnished in this condition by the organizational source and is the best copy available.

- This document may contain tone-on-tone or color graphs, charts and/or pictures, which have been reproduced in black and white.

- This document is paginated as submitted by the original source.

- Portions of this document are not fully legible due to the historical nature of some of the material. However, it is the best reproduction available from the original submission.
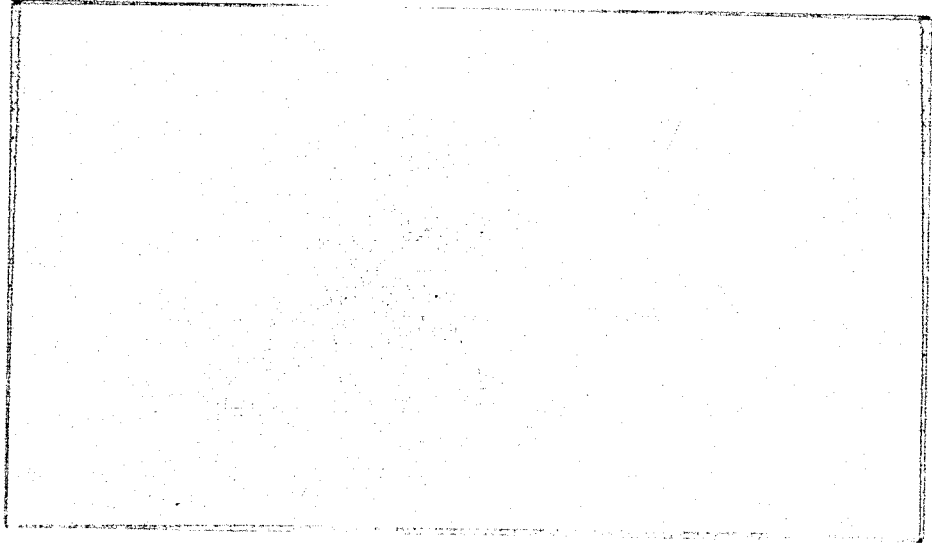
Department of

ELECTRICAL ENGINEERING

UNIVERSITY OF NOTRE DAME, NOTRE DAME, INDIANA

Annual Technical Report

to the

National Aeronautics and Space Administration

on

NASA Grant NSG-3048*

ALTERNATIVES FOR JET ENGINE CONTROL

March 1, 1978 - February 28, 1979

*Under the Direction of

Dr. Michael K. Sain
Department of Electrical Engineering
University of Notre Dame
Notre Dame, Indiana 46556

TABLE OF CONTENTS

ABSTRACT

This report deals with progress made on the Grant NSG-3048 during the calendar year beginning March 1, 1978 and ending February 28, 1979. The NASA Technical Officer for this period was Dr. Kurt Seldner of Lewis Research Center. The directors of the research at the University of Notre Dame were Dr. Michael K. Sain, for the duration of the year and Dr. R. Jeffrey Leake, for the initial six month period.

General goals of the research have been classified in two categories. The first category involves the use of modern multivariable frequency domain methods for control of engine models in the neighborhood of a set-point. The second category involves the use of nonlinear modelling and optimization techniques for control of engine models over a more extensive part of the flight envelope.

Progress in the first category has included the extension of CARDIAD (Complex Acceptability Region for DIAgonal Dominance) methods developed with the help of the grant to the case of engine models with four inputs and four outputs. A suitable bounding procedure for the dominance function has been determined. The bound is quadratic in the compensator elements, and can be helpful in the general case of multiple inputs and outputs even when the Hessian matrix is indefinite. In addition, improvements have been made on the 370 CARDIAD software; and a beginning in the process of developing interactive CARDIAD software on a recently acquired PDP-11/60 has been made. These steps are expected to enhance grant impact in the area of noninteractive engine control design.

1

Progress in the second category has had its principal focus on automatic nonlinear model generation. The approach consists of using the general form

$$\dot{x} = A(x,u) \ (x - g(u))$$

in which steady state measurements of x, A, and B in a linearized model are used to determine values of $A(x,u)$, $g(u)$, and $\partial g(u)/\partial u$ at setpoints. A Hermite polynomial interpolation scheme has been employed to determine global extensions of $A(x,u)$ and $g(u)$. Simulations of these models have produced satisfactory results where compared with the NASA DYNGEN digital engine deck. Studies have been begun to apply time-optimal control computational techniques to the new models and to compare these results with those of prior studies under this support.

I. GENERAL BACKGROUND

The following sections describe researches under Grant NSG-3048 during the calendar year March 1, 1978 - February 28, 1979. In this section, we make a number of preliminary and general remarks and lay some of the ground-work for those sections.

Initiation of Grant NSG-3048 in March 1975 was timed with developments in the engine industry, which was beginning to experience some limitations in the application of classical hydromechanical control technique as the primary base technology for modern engines with ever increasing sophistication. At the same time, milestone developments in digital hardware began to open realistic possibilities for onboard computation to an extent not heretofore possible. This confluence of events led directly to the concept of increasing the role of electronics in engine control. In turn, the availability of digital electronics itself created a wide variety of opportunity for application of new control design philosophy and technique. Among the earliest of such studies is the F100 Multivariable Control Synthesis Program [1] sponsored by the National Aeronautics and Space Administration, Lewis Research Center and the Air Force Aero-Propulsion Laboratory, Wright-Patterson Air Force Base. This program has recently completed the test phase.

The advent of digital technology on the engine scene offers not only the opportunity to control more engine variables but also the possibility of integrating engine and airframe control. Studies of this type have also begun.

Primary tools in the F100 Multivariable Control Synthesis Program were linear quadratic regulator (LQR) theory in the linear case. For the global control, nonlinear optimal methods were not directly applied.

The purpose of Grant NSG-3048 has been to evaluate alternatives to LQR in the linear case and to examine nonlinear modelling and optimization approaches for global control.

Context for the studies is set by the DYNGEN digital simulator [2]. Based upon earlier computer codes GENENG [3] and GENENG II [4], DYNGEN has the combined capabilities of [3] and [4], for calculating steady-state performance, together with the further capability for calculating transient performance. DYNGEN uses a modified Euler method to solve the differential equations which model the dynamics of the engine. This modified Euler method permits the user to specify large time steps, for example a tenth of a second; and this can result in considerable savings of execution time. On the other hand, convergence problems are sometimes encountered with DYNGEN when small time steps are used.

The DYNGEN digital simulation is particularized to a given situation by a process of loading data for the various maps associated with a given engine. The maps for the Grant NSG-3048 have been provided by engineering personnel at Lewis Research Center. These maps correspond to a paper engine, which is not closely identified with any current engine. But the data do correspond in a broad, general sense to realistic two spool turbofan engines. The simulation provides for two essential controls, main burner fuel flow and jet exhaust area. Portions of the envelope which can be used for linear or nonlinear experimentation are limited by

the convergence capabilities of the available engine data on DYNGEN.

As mentioned in the Final Report for NASA Grant NSG-3048, Supplement No. 1, a promising new technique for designing dynamical compensation began to develop in the Fall of 1976. This methodology, built upon what are currently being called CARDIAD plots, was only being tentatively considered in October, 1976 when the continuation proposal for NASA Grant NSG-3048, Supplement No. 2, was being written. Based upon favorable preliminary reaction by personnel from NASA Lewis Research Center, a decision was made to investigate further the use of CARDIAD plots as a design aid for turbofan engine control in the frequency domain. In essence, this study proved to be successful enough that it really dominated the remaining time period of Supplement No. 1 and has continued through seccessive study periods.

A great deal of the power of the CARDIAD plot arises from its simplicity. For each frequency, a circle is constructed on a planar plot. Data for the center and radius of this circle is obtained from the complex transfer function matrix of the plant. The circle may be solid or dashed. If solid, the inside of the circle defines the acceptable complex region for the value of a frequency dependent compensator element in order to achieve dominance. If dashed, the outside of the circle defines the acceptable region. As the frequency follows a standard Nyquist pattern, these circles result in a CARDIAD plot. (Complex Acceptability Region for DIAgonal Dominance). This plot has been shown to speak constructively to the issue of compensator choice to reduce interaction.

Examples of the use of CARDIAD plots utilizing a two-input, five-

state, two-output engine model in which the inputs are fuel flow and noz-
zle area, the states are compressor speed, fan speed, burner exit pres-
sure, after-burner exit pressure, and high turbine inlet energy, and the
outputs are thrust and high turbine inlet temperature, may be found in
the Final Report for Grant NSG-3048, Supplement No. 2.

Though linear multivariable frequency domain techniques are very prac-
tical as a part of an overall engine design, there is always the task of
integrating them into an overall controller which is nonlinear and which
operates over a substantial flight envelope. One approach to this need
has been to design a type of model following control system in which a
nonlinear model generates trajectories which can then be tracked by the
actual engine. Linear multivariable controllers are often helpful for
local adjustments to this tracking process. It follows that the model
which generates the trajectories to be tracked is of major importance in
any design.

Some desirable features of such models are accurate steady-state be-
havior and acceptable dynamical behavior. After consideration of several
modelling ideas over the history of this study, Dr. R.J. Leake and J.G.
Comiskey have suggested a form

$$\dot{x} = A(x,u) \ (x - g(u))$$

where $g(u)$ can be developed to yield steady-state accuracy and $A(x,u)$
can be determined for dynamical purposes. Moreover, the process of
gathering data to identify these functions is well suited to digital eng-
ine simulations.

II. SUMMARY OF RESEARCH RESULTS

This section provides a brief technical summary of the research results associated with the calendar year ending February 28, 1979. Further information on the ideas discussed here may be found in Sections III and IV, and in their referenced appendices.

1. The CARDIAD design method was applied to a turbofan engine model having four inputs, four outputs, and six states. This was a major test for a graphical, interactive method, inasmuch as the engine model has only two major inputs, with the other inputs intended for a less major role. The application was successful.

2. A suitable quadratic bound for the diagonal dominance function has been selected. This should make it possible to study the CARDIAD method in a general n-input, n-output case.

3. It has been found that the bound above can be governed in engine models by a Hessian matrix which is indefinite. A method to design in that case has been proposed.

4. Software for CARDIAD design on the 370 computer has been improved and modularized. The CARDIAD method is being prepared for use on a PDP-11/60 computer with graphics interface. This is expected to reduce design time by orders of magnitude. Previous CARDIAD plots came by Calcomp on the 370 machine.

5. The nonlinear modelling class

$$\dot{x} = A(x,u) \ (x - g(u))$$

described in the previous Annual Technical Report has been applied to

the DYNGEN digital simulator. Responses of the models agree well with those of the digital deck.

6. A Hermite interpolation scheme has been proposed to extend this class of models to a region of finite extent on the available DYNGEN envelope. Application of the method indicates acceptable results, but only within the region of the original data.

7. A program of testing these models under time-optimal feedback control and comparing their performance with that of the DYNGEN deck has been begun.

8. Numerous technical improvements have been made in the mathematical programming for the time-optimal problem. These will be reported in the final version of an M.S. Thesis by J.G. Comiskey.

III. LOCAL MULTIVARIABLE FREQUENCY DOMAIN METHODS

In accordance with discussions carried out with engineering personnel at Lewis Research Center, a decision was made in the latter part of summer, 1978, to begin a gradual phasing out of grant researches having to do with multivariable frequency domain methods. The motivation for this decision grew out of the feeling that grant activities had provided already a substantial stimulus to work in this area. See, for example, Grant NSG-3048 Annual Technical Reports for the last three years. Correspondingly, an increase of emphasis upon nonlinear modelling and control was stated as a grant goal.

Because of the promise afforded by the CARDIAD method to achieve diagonal dominance in turbofan engine models, it was also decided to place the remaining frequency domain emphasis in the grant upon this method.

Primary efforts have been those of R.M. Schafer, under the direction of Dr. M.K. Sain. The report on this work is divided into two six-month portions.

1. First Six Months

During the six-month period beginning on March 1, 1978, the CARDIAD method for design to achieve diagonal dominance has been advanced to the case in which plants have four inputs and four outputs. The following paragraphs review this progress and illustrate it with design examples.

The figures for this discussion are many in numbers, and have been included as Appendix B.

Recall that in the CARDIAD plot approach, column dominance may be achieved by using only precompensation. The general form of this precompensator, K(s) is given by

$$K(s) = \begin{bmatrix} 1 & k_{12}(s) & k_{13}(s) & k_{14}(s) \\ k_{21}(s) & 1 & k_{23}(s) & k_{24}(s) \\ k_{31}(s) & k_{32}(s) & 1 & k_{34}(s) \\ k_{41}(s) & k_{42}(s) & k_{43}(s) & 1 \end{bmatrix}$$

An exception to this general form is the use of a K matrix to interchange columns of the system to facilitate achieving dominance. This procedure is explicated in the first design example.

Let G(s) be the transfer function matrix of the uncompensated system. With the above form of K(s), dominance in each column of the compensated system, Q(s) = G(s) K(s), is a function of the off-diagonal entries in the corresponding column of K(s). Hence, the goal is to design the off-diagonal entries of a column of K(s) in such a way that Q(s) is dominant in that column.

To choose the off-diagonal entries, the system is evaluated over a range of frequencies. At each frequency, the off-diagonal entries in each column of the compensator $K(s)\big|_{s=j\omega}$ are complex numbers; and a sufficient condition for dominance can be expressed as an inequality. If x is defined as a vector of the real and imaginary parts of the off-diagonal entries in a column, then that column of the system will be dominant at the frequency of evaluation if

$$f(x) > 0,$$

where $f(x)$ is a function of the system evaluated at a frequency.

Two approaches are used to maximize $f(x)$ and achieve dominance. The first approach is to draw the CARDIAD plots for each off-diagonal entry

in a column under the assumption that the other off-diagonal entries in that column of K(s) are zero. This is called the standard or Type 1 analysis and is a partial gradient analysis of $f(\underset{\sim}{x})$. Implicit in this type analysis is the fact that it is being attempted to achieve dominance using only one off-diagonal entry in each column. When dominance cannot be achieved using Type 1 analysis, a full gradient or Type 2 analysis is performed on $f(\underset{\sim}{x})$. In Type 2 analysis, all off-diagonal entries are used to achieve dominance in the column.

In each type of analysis, the CARDIAD plots describe the choice of off-diagonal entries that will achieve dominance. Before proceeding with the design examples, a review of the features of CARDIAD plots is in order.

Consider first the Type 1 analysis. The extrema found in the CARDIAD plot analysis are plotted in the complex plane using one of three different symbols, two of which have circles associated with them. These are a '+' with a solid circle around it and an 'x' with a dashed circle around it. The former case occurs when a maximum is found and is such that $f(\underset{\sim}{x})\big|_{\underset{\sim}{x}=\underset{\sim}{x}_{max}} > 0$. The solid circle then encloses the region where the choice of any complex value inside the circle will achieve dominance at the frequency associated with that circle. Similarly, the 'x' and the dashed circle are drawn when the acceptable region lies outside the circle. Hence, in the Type 1 analysis, choosing an off-diagonal entry $k_{ij}(s)$ which, at each frequency, is inside the circle if it is solid, or outside the circle if it is dashed, will achieve dominance. In the simplest case, there is a point on the real line which satisfies the above condition, and dominance can be achieved in the column with constant compensation.

It is not always possible to achieve dominance using only one off-diagonal entry in a column. At frequencies at which this occurs, a 'Δ' is plotted. The 'Δ' indicates the best choice of a compensator at a given frequency, but the one entry alone will not be sufficient to make $f(x) > 0$.

The occurrence of this 'Δ' symbol in Type 1 analysis plots will have one of 2 effects. If, for instance, some of the plots for a column of the system contain triangles, and others do not, dominance can be achieved by choosing an entry to fit one of the plots without triangles and letting the other entries remain zero. If, however, all the plots for a given column contain some triangles, no one entry will be sufficient to achieve dominance; and Type 2 analysis must be used.

In the Type 2 analysis, the type of the center and circle drawn is decided in the same way as in Type 1 analysis, that is, under the assumption that the other off-diagonal entries are zero. The reason the gradient values are not used in this determination is to avoid misleading the designer. If the gradient values were used, the region indicated by a solid circle in one plot would only be valid of the centers of the other plots for that column were fit exactly. Hence, when using Type 2 analysis, the strategy is to fit the compensators to all the plots and then use Type 1 analysis to check for dominance.

Notice carefully that, although the type (+,x,Δ) of the center and the type (solid, dashed) of the circle are determined by Type 1 analysis, the location of the center is determined by full gradient (Type 2) analysis.

We now turn to the discussion of some design examples.

The model used for the design examples was taken from a paper by Peczkowski and Sain[6] . A state feedback model is used with inputs WFMB, A_j, CIVV, RCVV; states N_1, N_2, P_7, $T_{4.5hi}$, $T_{4.5lo}$. The states fed back are N_1, N_2, P_7, $T_{4.5hi}$ and $T_{4.5lo}$. This model was made dominant using CARDIAD plot analysis with two different approaches.

In the first approach, the first step in the design procedure was to switch the first and third columns by choosing as a first compensator

$$K = \begin{bmatrix} 0 & 0 & 1 & 0 \\ 0 & 1 & 0 & 0 \\ 1 & 0 & 0 & 0 \\ 0 & 0 & 0 & 1 \end{bmatrix} .$$

While this choice happens to make the first column dominant, it was chosen to facilitate achieving dominance in the third and fourth columns. Regardless of what column switch is used, dominance is easily achieved in the first two columns of most jet engine models since fuel flow and exhaust area have a dominant effect on all states and outputs of a jet engine. The improvement gained by the column switch, as will be seen later, is the simple shapes of the Type 2 analysis of the third column.

The Type 1 analysis plots for the system with the column switch are given in Figures 1 - 24. Analysis of these plots proceeds as follows.

The first column of the system, Figures 1 - 6, is dominant without further compensation. This can be seen from the fact that in each plot, the origin is included by all solid circles and excluded by all dashed circles. Thus, the plots indicate that an acceptable choice for any one off-diagonal entry (assuming the other off-diagonal entries are zero since

this is Type 1 analysis) is zero. Hence, all further compensation of the first column will be the first column of the identity matrix.

The second column, Figures 7 - 12, is not dominant; and the (1,2) and (3,2) plots each have triangles at high frequencies, indicating that dominance cannot be achieved by using either one of these entries by themselves. However, the (4,2) entry, Figures 11 & 12, contains no triangles; and therefore dominance can be achieved by judicious selection of this entry.

In the third column, Figures 13 - 18, all the plots contain triangles. This says that no one entry in the column will achieve dominance, and Type 2 analysis will be necessary.

The fourth column plots, Figures 19 - 24, also all contain triangles; but the (2,4) entry has solid or dashed circles at frequencies of $\omega \geq 40$. Hence, dominance can be achieved at these higher frequencies by designing for this entry.

The Type 2 analysis plots of column 3 are given in Figures 25 - 30. Recall that when using Type 2 analysis, all three off-diagonal entries will be designed. The semi-circular shapes of the Type 2 analysis plots indicate that designing to fit the shapes will not be difficult. These easily designed shapes are the reason that the column switch was chosen as it was.

From this analysis, the following entries in the compensator were designed.

The (4,2) entry of K(s) was chosen to be

$$k_{42}(s) = \frac{.97s - 89.1}{.033s + 1} \ .$$

Referring to Figures 11 and 12, this entry, as a function of frequency, starts on the real line to the left of the low frequency dashed circles, and moves clockwise through the complex plane such that at each frequency, the value is outside the circle at that frequency if it is dashed, or inside if it is solid. Note that there is no point on the real axis which is inside all solid circles and outside all dashed circles. Hence, there is no constant entry which will suffice.

The three off-diagonal entries in the third column were chosen to be first order and designed to fit the shapes of the triangles of the Type 2 analysis plots (Figures 25 - 30). The resulting entries are

$$k_{13}(s) = \frac{-.00019s - .0084}{-.01137s + 1} \ ,$$

$$k_{23}(s) = \frac{-.00008s - .00049}{-.0113s + 1} \ ,$$

$$k_{43}(s) = \frac{.00003s + .000137}{-.0108s + 1} \ .$$

Finally, the (2,4) entry was designed to achieve dominance for $\omega \geq 40$. This entry was designed to start at the $\omega = 0$ triangle, center on the $\omega = 40$ solid circle, and remain outside the dashed circles which occur thereafter. The resulting entry is

$$k_{24}(s) = \frac{-.00806s + .0212}{-.0172s + 1} \ .$$

The resulting compensator is

$$K_1(s) = \begin{bmatrix} 1 & 0 & \dfrac{-.00019s - .0084}{-.01137s + 1} & 0 \\[2em] 0 & 1 & \dfrac{-.00008s - .00049}{-.0113s + 1} & \dfrac{-.00806s + .0212}{-.0172s + 1} \\[2em] 0 & 0 & 1 & 0 \\[2em] 0 & \dfrac{.97s - 89.1}{.033s + 1} & \dfrac{.00003s + .000137}{-.0108s + 1} & 1 \end{bmatrix}$$

and the overall compensation thus far is $K(s) = K\, K_1(s)$. This compensator is labeled KMP3 on the plots.

The Type 1 analysis plots of the system compensated with $K(s)$ equal to $K\, K_1(s)$ are given in Figures 31 - 54. The plots of the first three columns show that these columns are now dominant at all frequencies. This is true since in each CARDIAD plot of the first three columns, the origin is included by all solid circles and excluded by all dashed circles. The fourth column is not dominant at all frequencies, but is dominant at frequencies of $\omega \geq 40$ as expected. Thus, further compensation is necessary only in the fourth column.

Since the Type 1 analysis plots of the fourth column, Figures 49 - 54, all contain triangles at lower frequencies, Type 2 analysis will be used to further compensate the column. The Type 2 analysis plots are given in Figures 55 - 60.

Considering the (3,4) entry (Figures 59,60) first, we see that all of the centers are located at approximately 57.3 on the real axis. Hence, this value was chosen for the (3,4) entry. In a similar spirit, the (1,4) entry was chosen to be the value at $\omega = 0$, namely .9. The next compensator chosen was

$$K_2 = \begin{bmatrix} 1 & 0 & 0 & .9 \\ 0 & 1 & 0 & 0 \\ 0 & 0 & 1 & 57.3 \\ 0 & 0 & 0 & 1 \end{bmatrix}.$$

The overall compensation is now $K(s) = K\,K_1(s)\,K_2$. The only column that is affected by K_2 is the fourth column. By considering the relative magnitudes of the fourth column entries of $K_1(s)\,K_2$, it was decided that an approximation could be made. The effect of this approximation is that the zeros in the (1,4) and (3.4) entries of $K_1(s)$ could be replaced by .9 and 57.3 respectively with the result being approximately the same as the full product result. Thus, the fourth column of $K_1(s)$ became

$$\begin{bmatrix} .9 \\ \dfrac{.00806s + .0212}{-.0172s + 1} \\ 57.3 \\ 1 \end{bmatrix}$$

The fourth column was replotted with $K_1(s)$ changed as above. The plots are labeled KMP4 and are shown in Figures 61 - 66.

Analyzing these plots, we see that the (1,4) entry now contains no triangles. Though the column is not yet dominant, dominance can now be achieved by fitting a frequency dependent entry to the solid circles of the (1,4) entry plot. The entry which fits these circles is

$$k_{14}(s) = \frac{.232s + .4104}{.1127s + 1}$$

and the next compensator was

$$\begin{bmatrix} 1 & 0 & 0 & \dfrac{.232s + .4104}{.1127s + 1.} \\ 0 & 1 & 0 & 0 \\ 0 & 0 & 1 & 0 \\ 0 & 0 & 0 & 1 \end{bmatrix}$$

Again, this only changes the fourth column which becomes

$$\begin{bmatrix} \dfrac{.232s + .4104}{.1127s + 1} + .9 \\ \dfrac{-.00806s + .0212}{-.0172s + 1} \\ 57.3 \\ 1 \end{bmatrix}$$

The overall compensation is $K(s) = K \; \hat{K}(s)$ where

$$K = \begin{bmatrix} 0 & 0 & 1 & 0 \\ 0 & 1 & 0 & 0 \\ 1 & 0 & 0 & 0 \\ 0 & 0 & 0 & 1 \end{bmatrix}$$

and

$$\hat{K}(s) = \begin{bmatrix} 1 & 0 & \dfrac{-.00019s - .0084}{-.01137s + 1} & \dfrac{.334s + 1.3104}{.1127s + 1} \\ 0 & 1 & \dfrac{-.00008s - .00049}{-.0113s + 1} & \dfrac{-.00806s + .0212}{.0172s + 1} \\ 0 & 0 & 1 & 57.3 \\ 0 & \dfrac{.97s - 89.1}{.033s + 1} & \dfrac{.00003s + .000137}{-.0108s + 1} & 1 \end{bmatrix}$$

Figures 67 - 72 are the Type 1 analysis plots of the fourth column with the above compensation and are labeled KMP5. Dominance has been achieved.

Using the same model, a second approach was used to achieve dominance. The second approach proved considerably more direct than the first approach. The starting point of the approach is to choose $G^{-1}(0)$ as a first compensator instead of the column switch that was used in the first approach. In this case, dominance was easily achieved by using this approach.

With regards to the labeling of the plots, the following should be noted. Analysis Type 11 is analysis Type 1 with $G^{-1}(0)$ as a first compensator. Type 12 is Type 2 with $G^{-1}(0)$ as a first compensator.

Figures 73 - 96 are the CARDIAD plot Type 1 analyses compensated by $G^{-1}(0)$.

$$G^{-1}(0) = K_1 = \begin{bmatrix} & & \\ & - & \\ & & \end{bmatrix} .$$

Analysis of the columns is as follows.

The first column (Figures 73 - 78) is not dominant, but there exists a point on the real line in the plot of the (4,1) entry, Figures 77 - 78, which is included by all the solid circles. Hence, dominance can be achieved in this column by choosing $k_{41} = .076$.

The second column (Figures 79 - 84) is not dominant, but the plot of the (1,2) entry contains no triangles. A simple first order compensator was chosen to fit the solid circles of the plot. The entry chosen was

$$k_{12}(s) = \frac{.1s}{.178s + 1} .$$

The third column plots, Figures 85 - 90, show that the column is not dominant and that Type 2 analysis will be necessary since all plots contain triangles.

The fourth column plots, Figures 91 - 96, show that the fourth column is dominant without further compensation.

Figures 97 - 102 are the Type 2 analysis plots of the third column of the system already compensated by $G^{-1}(0)$. The plots are all very regular in shape, and first order compensators were fit to each plot. The three entries chosen were

$$k_{13}(s) = \frac{-6.627s}{.0639s + 1} \quad ,$$

$$k_{23}(s) = \frac{-3.806s}{.0639s + 1} \quad ,$$

$$k_{43}(s) = \frac{-1.182s}{.0640s + 1} \quad .$$

The overall compensator is

$$K(s) = \begin{bmatrix} 1 & \frac{.1s}{.178s + 1} & \frac{-6.627s}{.0639s + 1} & 0 \\ 0 & 1 & \frac{-3.806s}{.0639s + 1} & 0 \\ 0 & 0 & 1 & 0 \\ .076 & 0 & \frac{-1.182s}{.064s + 1} & 1 \end{bmatrix}$$

The plots for the system with compensation $K_1 K(s)$ are given in Figures 103 - 126. As can be seen from the plots, the system is dominant.

It should be mentioned that the second of these two design examples was completed in about thirty minutes terminal time, though final plots

had to be awaited in a longer time frame. Moreover, the four input,
four output case is definitely nontrivial for current models of jet engines.

Accordingly, the results support additional efforts to complete the
development and refinement of CARDIAD methods.

2. Second Six Months

During the six-month period beginning on September 1, 1978, work on
the CARDIAD method was primarily divided into two areas. The first area
involved a theoretical study of the dominance equation used in the analy-
sis and a general proof of the bound that is employed. The second area in-
volved software generalization and initial development work on the inter-
active graphics software package.

Before proceeding with the discussion of the theoretical aspects,
some preliminary development is in order. Recall that the basis of the
CARDIAD method is the definition of diagonal dominance which states that
the jth column of an $n \times n$ matrix $Z(s)$ will be dominant at a point
$s \in C$ if and only if

$$\left| z_{jj}(s) \right| > \sum_{\substack{i=1 \\ i \neq j}}^{n} \left| z_{ij}(s) \right| . \tag{1}$$

Let $G(s)$ be the transfer function matrix of the uncompensated
plant. Let $K(s)$ be a precompensator of a form having 1's on the main
diagonal and general frequency-dependent entries off the main diagonal.
If $Q(s) = G(s) K(s)$, then the condition for the jth column of the com-
pensated plant to be dominant as s is

$$\left| q_{jj}(s) \right| > \sum_{\substack{i=1 \\ i \neq j}}^{n} \left| q_{ij}(s) \right| . \tag{2}$$

Recall that the initial step in the development of the dominance equation by the CARDIAD method was to square (2). This gives the following condition for dominance,

$$\left| q_{jj}(s) \right|^2 > \left[\sum_{\substack{i=1 \\ i \neq j}}^{n} \left| q_{ij}(s) \right| \right]^2 . \tag{3}$$

The next step in the procedure was to replace the condition in (3) with a simpler formulation involving a bound that results in a sufficient condition for dominance. Using the bound, the jth column of $Q(s)$ will be dominant at s if

$$\left| q_{jj}(s) \right|^2 - (n-1) \sum_{\substack{i=1 \\ i \neq j}}^{n} \left| q_{ij}(s) \right|^2 > 0 . \tag{4}$$

To prove the validity of this bound in the general case, it is necessary to show that

$$M \sum_{i=1}^{M} \alpha_i^2 \geq \left[\sum_{i=1}^{M} \alpha_i \right]^2 \tag{5}$$

for all real α_i and for $M = 2,3,4...$ To do this, we shall first show that

$$\sum_{i=1}^{M} \alpha_i^2 + \sum_{i=1}^{M-1} \sum_{j=i+1}^{M} (\alpha_i^2 + \alpha_j^2) \geq \left[\sum_{i=1}^{M} \alpha_i \right]^2 . \tag{6}$$

This is a consequence of the following calculations.

$$(\alpha_i - \alpha_j)^2 \geq 0$$

$$\rightarrow \alpha_i^2 + \alpha_j^2 - 2\alpha_i \alpha_j \geq 0$$

$$\rightarrow \quad \alpha_i^2 + \alpha_j^2 \geq 2\alpha_i \alpha_j$$

Thus, with the aid of this observation, it follows that

$$\sum_{i=1}^{M-1} \sum_{j=i+1}^{M} [\alpha_i^2 + \alpha_j^2] \geq \sum_{i=1}^{M-1} \sum_{j=i+1}^{M} 2\alpha_i \alpha_j. \tag{7}$$

Adding the same term to each side of (7) preserves the inequality; and we get the relationship

$$\sum_{i=1}^{M} \alpha_i^2 + \sum_{i=1}^{M-1} \sum_{j=i+1}^{M} [\alpha_i^2 + \alpha_j^2] \geq \sum_{i=1}^{M} \alpha_i^2$$

$$+ \sum_{i=1}^{M-1} \sum_{j=i+1}^{M} 2\alpha_i \alpha_j. \tag{8}$$

However, the right-hand member summation expression is

$$\sum_{i=1}^{M} \alpha_i^2 + \sum_{i=1}^{M-1} \sum_{j=i+1}^{M} 2\alpha_i \alpha_j = [\sum_{i=1}^{M} \alpha_i]^2. \tag{9}$$

With the completion of this preliminary step, it remains to show that

$$M \sum_{i=1}^{M} \alpha_i^2 = \sum_{i=1}^{M} \alpha_i^2 + \sum_{i=1}^{M-1} \sum_{j=i+1}^{M} [\alpha_i^2 + \alpha_j^2] \tag{10}$$

for all $M \geq 2$. The proof is by induction. Consider the $M = 2$ case. For $M = 2$, (10) becomes

$$2 \sum_{i=1}^{2} \alpha_i^2 = \sum_{i=1}^{2} \alpha_i^2 + \sum_{i=1}^{1} \sum_{j=2}^{2} [\alpha_i^2 + \alpha_j^2] \tag{11}$$

which becomes

$$2 \alpha_1^2 + 2 \alpha_2^2 = \alpha_1^2 + \alpha_2^2 + \alpha_1^2 + \alpha_2^2$$

$$= 2 \alpha_1^2 + 2 \alpha_2^2,$$

and thus the relationship has been shown for $M = 2$. Next we will show that, if (10) is assumed true for $M \geq 2$, it is also true for $M + 1$;

and the proof will be complete. Assume

$$M \sum_{i=1}^{M} \alpha_i^2 = \sum_{i=1}^{M} \alpha_i^2 + \sum_{i=1}^{M-1} \sum_{j=i+1}^{M} (\alpha_i^2 + \alpha_j^2) \, .$$

Adding identical terms to each member yields

$$M \sum_{i=1}^{M} \alpha_i^2 + M \alpha_{M+1}^2 = \sum_{i=1}^{M} \alpha_i^2 + \sum_{i=1}^{M-1} \sum_{j=i+1}^{M} (\alpha_i^2 + \alpha_j^2)$$

$$+ M \alpha_{M+1}^2 \, .$$

Again, adding another term results in

$$M \sum_{i=1}^{M+1} \alpha_i^2 + \sum_{i=1}^{M+1} \alpha_i^2 = \sum_{i=1}^{M} \alpha_i^2 + \sum_{i=1}^{M-1} \sum_{j=i+1}^{M} (\alpha_i^2 + \alpha_j^2)$$

$$+ M \alpha_{M+1}^2 + \sum_{i=1}^{M+1} \alpha_i^2 \, .$$

Now, manipulating the equation, we get

$$(M+1) \sum_{i=1}^{M+1} \alpha_i^2 = \sum_{i=1}^{M} \alpha_i^2 + \sum_{i=1}^{M-1} \sum_{j=i+1}^{M} (\alpha_i^2 + \alpha_j^2)$$

$$+ M \alpha_{M+1}^2 + \sum_{i=1}^{M} \alpha_i^2 + \alpha_{M+1}^2$$

$$= \sum_{i=1}^{M+1} \alpha_i^2 + \sum_{i=1}^{M-1} \sum_{j=i+1}^{M} (\alpha_i^2 + \alpha_j^2) + \sum_{i=1}^{M} (\alpha_i^2 + \alpha_{M+1}^2)$$

$$= \sum_{i=1}^{M+1} \alpha_i^2 + \sum_{i=1}^{M} \sum_{j=i+1}^{M+1} (\alpha_i^2 + \alpha_j^2) \, .$$

Finally, letting $L = M + 1$, we see that

$$L \sum_{i=1}^{L} \alpha_i^2 = \sum_{i=1}^{L} \alpha_i^2 + \sum_{i=1}^{L-1} \sum_{j=i+1}^{L} (\alpha_i^2 + \alpha_j^2) \, ;$$

thus, if (10) is true for $M \geq 2$, it is true also for $M + 1$. Hence,

by induction, the bound is valid.

Thus, we have as a sufficient condition for the jth column of $Q(s)$ to be dominant at a frequency ω_0 that

$$|q_{jj}(j\omega_0)|^2 - (n-1) \sum_{\substack{i=1 \\ i \neq j}}^{n} |q_{ij}(j\omega_0)|^2 > 0.$$

After considerable algebraic manipulation, a more useful expression of the dominance equation can be shown to be of the form

$$f_j(\underset{\sim}{x}) = \underset{\sim}{x}^t A \underset{\sim}{x} + \underset{\sim}{x}^t b + c > 0.$$

In this equation, A, B, and c are respectively a 2n-2 by 2n-2 matrix, a 2n-2 vector, and a scalar; and each are functions of the plant transfer function matrix evaluated at a specific frequency. All entries are real, and the matrix A is Hermitian. The subscript j indicates that dominance in the jth column is being considered. This subscript will henceforth be dropped, with the understanding that the equation refers to dominance in only one column. The vector $\underset{\sim}{x}$ is a 2n-2 vector composed of the real and imaginary parts of the off-diagonal entries of the compensator in the column being considered. Consider, for example, the first column. The associated column of the compensator matrix $K(s)$ is:

$$K_1(s) = [1, k_{21}(s), k_{31}(s), \ldots]^t.$$

If we let $k_{ij}(s)\big|_{s=j\omega} = \alpha_{ij} + j\beta_{ij}$, then the vector $\underset{\sim}{x}$ is

$$\underset{\sim}{x} = [\alpha_{21}, \beta_{21}, \alpha_{31}, \beta_{31}, \ldots]^t.$$

By choosing $\underset{\sim}{x}$ such that $f(\underset{\sim}{x})$ is positive, one is selecting the values of the off-diagonal entries of the compensator that achieve dominance at the frequency being considered.

Within the framework of the quadratic form, it is easy to demonstrate how the various types of analysis are performed. In the case of Type 1 or partial gradient analysis, all of the entries in $\underset{\sim}{x}$ are set to zero except for one (α, β) pair; then the gradient of $f(\underset{\sim}{x})$ is set to zero, and a solution for the non-zero entries (α, β) is found. In the case of Type 2 analysis, the standard gradient is taken. This results in the expression

$$\frac{\partial f(\underset{\sim}{x})}{\partial \underset{\sim}{x}} = (A + A^t)\, \underset{\sim}{x} + b = 0.$$

Since A is symmetric, the solution for $\underset{\sim}{x}$ is:

$$\underset{\sim}{x} = -1/2\ A^{-1} b.$$

One significant change was made in Type 2 analysis, and that was in the manner in which the circle types and radii are chosen. In the past, the centers of the circles were the gradient value but the type and size of the circle was decided in the same manner as in Type 1 analysis. Thus, the type and size of the circle were decided under the assumption that the other off-diagonal entries were zero. In Type 2 analysis this is not the case, and thus the designer was advised to ignore the circles when using Type 2 analysis and just try to fit a frequency dependent entry to the centers.

In the present software, the circle types and radii are decided in the following manner. For a given center in one plot. a deviation of a specified percentage is made in a worst case direction from the gradient values (i.e. circle centers) in all the other plots for the column. Then, the center type and radius are decided for the remaining entry. Consider a deviation of 10%. If a given plot has a very large circle at

a frequency, this implies that if the other entries are designed to be within 10% of the centers at this frequency, there is a lot of freedom in the remaining entry; and the designer does not have to fit this entry very precisely. If a very small circle results, the designer has to be very precise. In the case where a triangle results, it means that no value will achieve dominance in this entry at the frequency being considered if the other entries are 10% or more away from their gradient values. With this new way of deciding the circle types and radii, the designer is afforded more information as to how closely each of the entries need to be fit.

A third means of making $f(\underset{\sim}{x})$ positive was studied during this period. In Type 2 analysis, if the Hessian, which in this case is the matrix 2A, is negative definite, then the solution found by the gradient analysis is a global maximum. If the Hessian is positive definite, the solution is a global minimum. However, in the case where A is indefinite, the solution found is a saddle point; and Type 2 analysis cannot be used to achieve dominance.

If A is indefinite, a solution for $\underset{\sim}{x}$ that will make $f(\underset{\sim}{x})$ positive is a scalar times the eigenvector of A associated with one of the positive eigenvalues of A. Let k be a positive scalar. Then

$$f(k\underset{\sim}{e}) = k^2 \underset{\sim}{e}^t A\underset{\sim}{e} + k \underset{\sim}{e}^t b + c.$$

Because $\underset{\sim}{e}$ is an eigenvector associated with a positive eigenvalue of A, the quadratic term will be positive; and the function can be made arbitrarily positive. Thus, in the case of an indefinite Hessian, the eigenvectors serve as a guide to a solution that achieves dominance. This method of achieving dominance is still under study and is in the process of being implemented.

A considerable amount of time during this six-month period was spent on software. The first area of work involved the generalization of the 370 version of the CARDIAD software. The principal changes involved generalizing the subroutine which solves for the values in A, b, and c of the quadratic form. Previous to this time, a different subroutine was called depending on the number of inputs and outputs of the problem; and the expressions for the entries were quite complex. At present, one sub-routine is able to solve for these values for any size plant, with the only limiting factor being the size of dimensioned arrays. Other changes on this software included modularizing certain activities, polishing some code that was quickly written in the original software, and adding soft-ware to perform the new Type 2 analysis of circle type and radii.

A large amount of time was involved with the development and initial implementation of an interactive graphics version of the CARDIAD software on a PDP-11/60 recently acquired by the Department of Electrical Engineer-ing. Much of the work was preliminary in nature because there was lead time involved with getting acquainted with the features of a new machine. Current plans include a package whereby the designer can draw the CARDIAD plot on the graphics terminal and fit a design to the plot, by selecting the order and type of complex entry that he desires and picking design values from the displayed plot. The designer will then be able to draw the locus of the entry over the CARDIAD plot to determine if it is a good candidate for achieving dominance. Having chosen an entry, the designer can then redraw the CARDIAD plot with the compensator and determine if dominance has been achieved. The CARDIAD method is by nature an inter-

active tool, and the necessity of having to wait for Calcomp plots has

been a great hindrance in the past. It is hoped the interactive software

will greatly reduce the time necessary to achieve dominance.

IV. GLOBAL NONLINEAR OPTIMAL METHODS

As discussed in the preceding section, the future investigations on this grant will begin to decrease the emphasis on multivariable frequency domain methods and start a gradual increase of the effort placed on non-linear work.

The present studies underway on the DYNGEN digital engine simulator are to be completed.

1. First Six Months

During this period, the primary efforts were those of J.G. Comiskey, under the direction of Dr. R.J. Leake.

With respect to nonlinear modelling and optimization, the emphasis has been twofold: to develop good analytical nonlinear models of the jet engine and to use these models in conjunction with techniques of mathe-matical programming in order to develop advances to global control over significant reaches of the flight envelope.

In general, there are several aspects to this part of the investi-gation. First, it is possible to conceive the basic differential equa-tions from fundamental principles. In this case, there are usually about sixteen nonlinear differential equations, as well as a large number of nonlinear static functions which serve as part of the coupling between the equations. These functions often have more than one argument. If the equations arise in this fashion, then there is a significant need to identify the parameters. This must normally be done from the DYNGEN digital simulation. Second, it is possible to assume a general form for the nonlinear differential equations in such a way that fundamental prin-

30

ciples are not ignored but that added emphasis is placed upon general mathematical form. If this general form is chosen according to a scheme designed to make maximum use of the type of data which is directly available from the digital simulation, then a type of "automatic" nonlinear model generation becomes possible. Third, whether the first or second modelling procedure is employed, there is almost always a need to consider the problem of reducing the order of the models. Though order reduction can often be highly mathematical in nature, it is almost always the case that the reduced order model depends upon the scaling of the equations. As a result, the final reduced models often depend in a nontrivial way upon physical insight, as well as mathematical method.

Work on this grant has focused especially upon the first and second aspects of the modelling problem, with a gradual specialization toward automatic model generation.

Insofar as optimization is concerned, the stress has been placed upon time optimal control, and considerable effort has been invested in specialized programming methodology designed to take maximum advantage of the particular features of jet engine models.

The main effort during this six-month period has been in the area of model development. Fundamentals of the approach have been described in the Final Report for Supplement No. 2. For completeness, however, they are briefly sketched here.

These models are based upon the general form

$$\dot{x} = f(x,u)$$

where

$$f(x,u) = A(x,u) \ (x-g(u)).$$

the equation

$$x = g(u)$$

, governs the important steady state analysis. Moreover, if a program such as DYGABCD [5] is available, it is shown in the Final Report for Supplement No. 2 that information concerning

$$A(x,u), \ g(u), \ \partial g(u)/\partial u$$

can then be numerically generated from DYNGEN.

It should be noted that interpolation on $g(u)$ from its points and derivatives involves a sort of Hermite problem, which is discussed in the following section.

A feature of the approach is its authenticity with regard to equilibrium values, state matrix A, and DC gain values.

At this point an M.S. Thesis was outlined for the purposes of comparing this class of models with earlier modelling ideas studied on the grant and of using it for time optimal control calculations and simulations.

The Table of Contents as originally planned is attached to this report as Appendix C.

2. Second Six Months

During this period, the primary efforts were again those of J.G. Comiskey, but this time under the direction of Dr. M.K. Sain.

Production of the M.S. Thesis planned according to Appendix C was begun. Appendix D contains Chapters I through V of this document. The contents closely follow the plan of Appendix C.

A discovery of this part of the work is that the accuracy of the numerical models can degrade rapidly outside the range of their data points. This means that the designer must be sure to include steady state and dynamic data from the entire area of state and control space that he or she wishes to explore.

These results are not unusual in the theory of polynomic approximation in general. However, in view of the conceptual challenges encountered in the interpolation steps, it may be that the indications are toward the study of different types of nonlinear modelling methods.

The beginning of such a new type of modelling idea is scheduled for the continuation of this grant. In addition, the completion of the Comiskey work will appear as part of the semi-annual report associated with that continuation.

V. SPECIAL INITIATIVES RELATED TO GRANT WORK

One of the biggest related efforts to work on Grant NSG-3048 was the International Forum on Alternatives for Linear Multivariable Control, sponsored by the National Engineering Consortium in Chicago during October 1977. Dr. M.K. Sain served as Program Chairman and devised with the help of an advisory committee a Theme Problem based upon turbofan engine control for use by participants in the Forum.

Dr. T.F. Edgar, Program Chairman for the 1979 Joint Automatic Control Conference, expressed interest in a continuation of the Forum idea at the JACC. Dr. Sain contacted all the Forum attendees and asked them to indicate their interest in the project. As a result, three sessions entitled "Further Alternatives for Linear Multivariable Control" are planned for the 1979 JACC.

Preliminary information on these sessions is included here.

1979 JACC

FURTHER ALTERNATIVES FOR LINEAR MULTIVARIABLE CONTROL

Chairman and Organizer: Michael K. Sain
University of Notre Dame

Session I

1. Regulator Design for the F100 Turbofan Engine

    S. Engell and N. Munro
    University of Manchester

2. Frequency Dependent Precompensation for Dominance in a Four Input/
    Output Theme Problem Model

    R.M. Schafer and M.K. Sain
    University of Notre Dame

3. On Hidden Stability Margins in Multivariable Control

    Z.V. Rekasius
    Northwestern University

4. Stability and Homotopy II

    R. Saeks and J. Murray
    Texas Tech University

Session II

5. Design of a Turbofan Engine Controller Via Eigenvalue/Eigenvector
    Assignment: A New Sensitivity Formulation

    S.R. Liberty, R.A. Maynard, and R.R. Mielke
    Old Dominion University

6. Quasi-Upper Triangular Decomposition Applied to the Linearized Control
    of a Turbofan Engine--Further Results

    W.E. Holley and W. Chung
    Oregon State University

7. **Design of Flight Control Systems Via Robust Decoupled Servomechanism Theory**

   S.-H. Wang, University of Maryland and
   E.J. Davison, University of Toronto

8. **Computer Aided Design of Control Systems Via Optimization**

   D.Q. Mayne
   Imperial College

Session III

9. **Inverse Systems in Multivariable Control**

   J.L. Peczkowski, Bendix Corporation,
   M.K. Sain, University of Notre Dame, and
   R.J. Leake, Fresno State University

10. **Failure Accommodation in Gas Turbine Engines**

    R.K. Sahgal and R.J. Miller
    Pratt & Whitney Aircraft

11. **Model Algorithmic Control: Extensions and Further Applications**

    R.K. Mehra, A. Rault, and R. Rouhani
    Scientific Systems, Inc.

12. **An Application of Model Following Control**

    J.D. Aplevich
    University of Waterloo

VI. REFERENCES

1. R.L. De Hoff, W. Earl Hall, Jr., R.J. Adams, and N.K. Gupta, "F100 Multivariable Control Synthesis Program", Vols. I and II, Technical Report AFAPL-TR-77-35, June 1977.

2. J.F. Sellers and C.J. Daniele, "DYNGEN-A Program for Calculating Steady-State and Transient Performance of Turbojet and Turbofan Engines", NASA Technical Note TN D-7901, April 1975.

3. R.W. Koenig and L.H. Fishbach, "GENENG-A Program for Calculating Design and Off-Design Performance for Turbojet and Turbofan Engines", NASA Technical Note TN D-6552, February 1972.

4. L.H. Fishbach and R.W. Koenig, "GENENG II-A Program for Calculating Design and Off-Design Performance of Two and Three Spool Turbofans with as Many as Three Nozzles", NASA Technical Note TN D-6553, February 1972.

5. "DYGABCD - A Program for Calculating A, B, C, and D Matrices for Linear Descriptions of Simulated Turbojet and Turbofan Engines", NASA Lewis Research Center, Preliminary Report.

6. Joseph L. Peczkowski and Michael K. Sain, "Linear Multivariable Synthesis with Transfer Functions," in _Alternatives for Linear Multivariable Control_, M.K. Sain, J.L. Peczkowski, and J.L. Melsa, eds. Chicago: National Engineering Consortium, 1978, pp. 71-87.

APPENDIX A

GRANT BIBLIOGRAPHY, INCEPTION TO PRESENT

(1) R.J. Leake, J.L. Melsa, and M.K. Sain, "Preliminary Proposal on Modern Approaches to Jet Engine Control", November 1, 1974.

(2) R.J. Leake, M.K. Sain, and J.L. Melsa, "Proposal to NASA for Support of a Work Entitled 'Alternatives for Jet Engine Control'", November 27, 1974.

(3) R.J. Leake and M.K. Sain, "Semi-Annual Status Report on NASA Grant NSG-3048, 'Alternatives for Jet Engine Control'", March 1, 1975 - August 31, 1975.

(4) R.J. Leake, M.K. Sain, and J.L. Melsa, "Proposal for Continuation of NASA Grant NSG-3048, 'Alternatives for Jet Engine Control'", October 1, 1975.

(5) J.C. Shearer, "An IBM 370/158 Installation and User's Guide for the DYNGEN Jet Engine Simulator", M.S. Thesis, November 1975.

(6) T.C. Brennan and R.J. Leake, "Simplified Simulation Models for Control Studies of Turbojet Engines", Technical Report EE 757, University of Notre Dame, November 1975.

(7) R.J. Leake, M.K. Sain, and J.L. Melsa, "Final Technical Report on NASA Grant NSG-3048, 'Alternatives for Jet Engine Control'", March 1, 1975 - February 29, 1976.

(8) R.R. Gejji and M.K. Sain, "Polynomial Techniques Applied to Multivariable Control of Jet Engines", Technical Report EE 761, March 1976.

(9) V. Seshadri and M.K. Sain, "Multivariable System Compensation Including Characteristic Methods for Jet Engine Control", Technical Report EE 763, May 1976.

(10) A.J. Maloney III, "Graphics Analysis of Dominance in Jet Engine Control Models", Technical Report EE 765, June 1976.

(11) M.K. Sain, R.J. Leake, R. Basso, R. Gejji, A. Maloney, and V. Seshadri, "Alternative Methods for the Design of Jet Engine Control Systems", Proceedings Fifteenth Joint Automatic Control Conference, pp. 133-142, July 1976.

(12) J.C. Shearer, W.E. Longenbaker, Jr., and R.J. Leake, "An IBM 370/158 Installation and User's Guide to the DYNGEN Jet Engine Simulator", Technical Report EE 766, July 1976.

(13) R.R. Gejji and M.K. Sain, "A Jet Engine Control Problem for Evaluating Minimal Design Software", Proceedings Midwest Symposium on Circuits and Systems, pp. 238-243, August 1976.

(14) V. Seshadri and M.K. Sain, "Interaction Studies on a Jet Engine Model by Characteristic Methodologies", Proceedings Midwest Symposium on Circuits and Systems, pp. 232-237, August 1976.

(15) R.J. Leake and M.K. Sain, "Semi-Annual Status Report on NASA Grant NSG-3048, 'Alternatives for Jet Engine Control', Supplement No. 1", March 1, 1976-August 31, 1976.

(16) R. Basso and R.J. Leake, "Computational Alternatives to Obtain Time-Optimal Jet Engine Control", Technical Report EE 767, September 1976.

(17) R. Basso and R.J. Leake, "Computational Methods to Obtain Time-Optimal Jet Engine Control", Proceedings Fourteenth Allerton Conference on Circuit and System Theory, pp. 652-661, September 1976.

(18) M.K. Sain and V. Seshadri, "A Result on Pole Assignment by Exterior Algebra", Proceedings Fourteenth Allerton Conference on Circuit and System Theory, pp. 399-407, September 1976.

(19) R.R. Gejji, "A Computer Program to Find the Kernel of a Polynomial Operator", Proceedings Fourteenth Allerton Conference on Circuit and System Theory, pp. 1091-1100, September 1976.

(20) R.J. Leake and M.K. Sain, "Proposal for Continuation of NASA Grant NSG-3048, 'Alternatives for Jet Engine Control'", October 25, 1976.

(21) R.M. Schafer, W.E. Longenbaker, and M.K. Sain, "System Dominance: A Preliminary Report on an Alternate Approach", Technical Report, University of Notre Dame, November 25, 1976.

(22) R.J. Leake and M.K. Sain, "Final Technical Report, NASA Grant NSG-3048, 'Alternatives for Jet Engine Control', Supplement No. 1", March 1, 1976 - February 28, 1977.

(23) R.J. Leake, J.G. Allen, and R.S. Schlunt, "Optimal Regulators and Follow-Up Systems Determined from Input-Output Signal Monitoring", Proceedings IEEE International Symposium on Circuits and Systems, April 1977.

(24) R.M. Schafer, "A Graphical Approach to System Dominance", Technical Report EE 772, University of Notre Dame, April 1, 1977.

(25) W.E. Longenbaker and R.J. Leake, "Hierarchy of Simulation Models for a Turbofan Gas Engine", Proceedings Eighth Annual Pittsburgh Conference on Modeling and Simulation, April 1977.

(26) P.W. Hoppner, "The Direct Approach to Compensation of Multivariable

Jet Engine Models", Technical Report EE 774, University of Notre Dame, May 1977.

(27) R.R. Gejji and R.J. Leake, "Time-Optimal Control of a Single Spool Turbojet Engine Using a Linear Affine Model", Technical Report EE 7711, University of Notre Dame, June 1977.

(28) R.M. Schafer, R.R. Gejji, P.W. Hoppner, W.E. Longenbaker, and M.K. Sain, "Frequency Domain Compensation of a DYNGEN Turbofan Engine Model", Proceedings Sixteenth Joint Automatic Control Conference, pp. 1013-1018, June 1977.

(29) R.R. Gejji and M.K. Sain, "Application of Polynomial Techniques to Multivariable Control of Jet Engines", Proceedings Fourth IFAC Symposium on Multivariable Technological Systems, pp. 421-429, July 1977.

(30) R.R. Gejji, "Use of DYGABCD Program at Off-Design Points", Technical Report EE 7703, University of Notre Dame, July 1977.

(31) E.A. Sheridan and R.J. Leake, "Non-Interactive State Request Jet Engine Control with Non-Singular B Matrix", Proceedings Twentieth Midwest Symposium on Circuits and Systems, pp. 539-543, August 1977.

(32) R. Gejji, R.M. Schafer, M.K. Sain, and P. Hoppner, "A Comparison of Frequency Domain Techniques for Jet Engine Control System Design", Proceedings Twentieth Midwest Symposium on Circuits and Systems, pp. 680-685, August 1977.

(33) W.E. Longenbaker and R.J. Leake, "Time Optimal Control of a Two-Spool Turbofan Jet Engine", Technical Report EE 7714, University of Notre Dame, September 1977.

(34) R.J. Leake and J.G. Comiskey, "A Direct Method for Obtaining Non-linear Analytical Models of a Jet Engine", Proceedings International Forum on Alternatives for Linear Multivariable Control, National Electronics Conference, Chicago, pp. 203-212, October 1977.

(35) M.K. Sain and R.J. Leake, "Proposal for Continuation of NASA Grant NSG-3048, 'Alternatives for Jet Engine Control'", October 25, 1977.

(36) J.A. Ortega and R.J. Leake, "Discrete Maximum Principle with State Constrained Control", SIAM Journal on Control and Optimization, Vol. 15, No. 6, pp. 109-115, November 1977.

(37) Michael K. Sain and V. Seshadri, "Pole Assignment and a Theorem from Exterior Algebra", Proceedings IEEE Conference on Decision and Control, pp. 291-295, December 1977.

(38) R. Michael Schafer and Michael K. Sain, "Some Features of CARDIAD Plots for System Dominance", Proceedings IEEE Conference on Decision

and Control, pp. 801-806, December 1977.

(39) M.K. Sain, "The Theme Problem", in <u>Alternatives for Linear Multivariable Control</u>, M.K. Sain, J.L. Peczkowski and J.L. Melsa, Editors. Chicago: National Engineering Consortium, 1978, pp. 20-30.

(40) R.M. Schafer and M.K. Sain, "Input Compensation for Dominance of Turbofan Models", in <u>Alternatives for Linear Multivariable Control</u>, M.K. Sain, J.L. Peczkowski, and J.L. Melsa, Editors. Chicago: National Engineering Consortium, 1978, pp. 156-169.

(41) J.L. Peczkowski and M.K. Sain, "Linear Multivariable Synthesis with Transfer Functions", in <u>Alternatives for Linear Multivariable Control</u>, M.K. Sain, J.L. Peczkowski, and J.L. Melsa, Editors. Chicago: National Engineering Consortium, 1978, pp. 71-87.

(42) R.J. Leake and M.K. Sain, "Semi-Annual Status Report, NASA Grant NSG-3048, 'Alternatives for Jet Engine Control', Supplement No. 2", March 1, 1977 - August 31, 1977.

(43) R.J. Leake and M.K. Sain, "Final Technical Report, NASA Grant NSG-3048, 'Alternatives for Jet Engine Control', Supplement No. 2", March 1, 1977 - February 28, 1978.

(44) M.K. Sain and R.J. Leake, "Semi-Annual Status Report, NASA Grant NSG-3048, 'Alternatives for Jet Engine Control'", March 1, 1978 - August 31, 1978.

(45) R.J. Leake, J.L. Peczkowski, and M.K. Sain, "Step Trackable Linear Multivariable Plants", Technical Report EE 789, September 1978.

(46) R.M. Schafer and M.K. Sain, "CARDIAD Design: Progress in the Four Input/Output Case", <u>Proceedings Sixteenth Allerton Conference on Communication, Control, and Computing</u>, p. 567, October 1978.

(47) M.K. Sain, "Proposal for Continuation of NASA Grant NSG-3048, 'Alternatives for Jet Engine Control'", November 1, 1978.

(48) M.K. Sain, "On Exosubsets and Internal Models", <u>Proceedings IEEE Conference on Decision and Control</u>, pp. 1069-1073, January 1979.

(49) M.K. Sain, "Annual Technical Report, NASA Grant NSG-3048, 'Alternatives for Jet Engine Control'", March 1, 1978 - February 28, 1979.

Figure 1

IMAGINARY PART

REAL PART
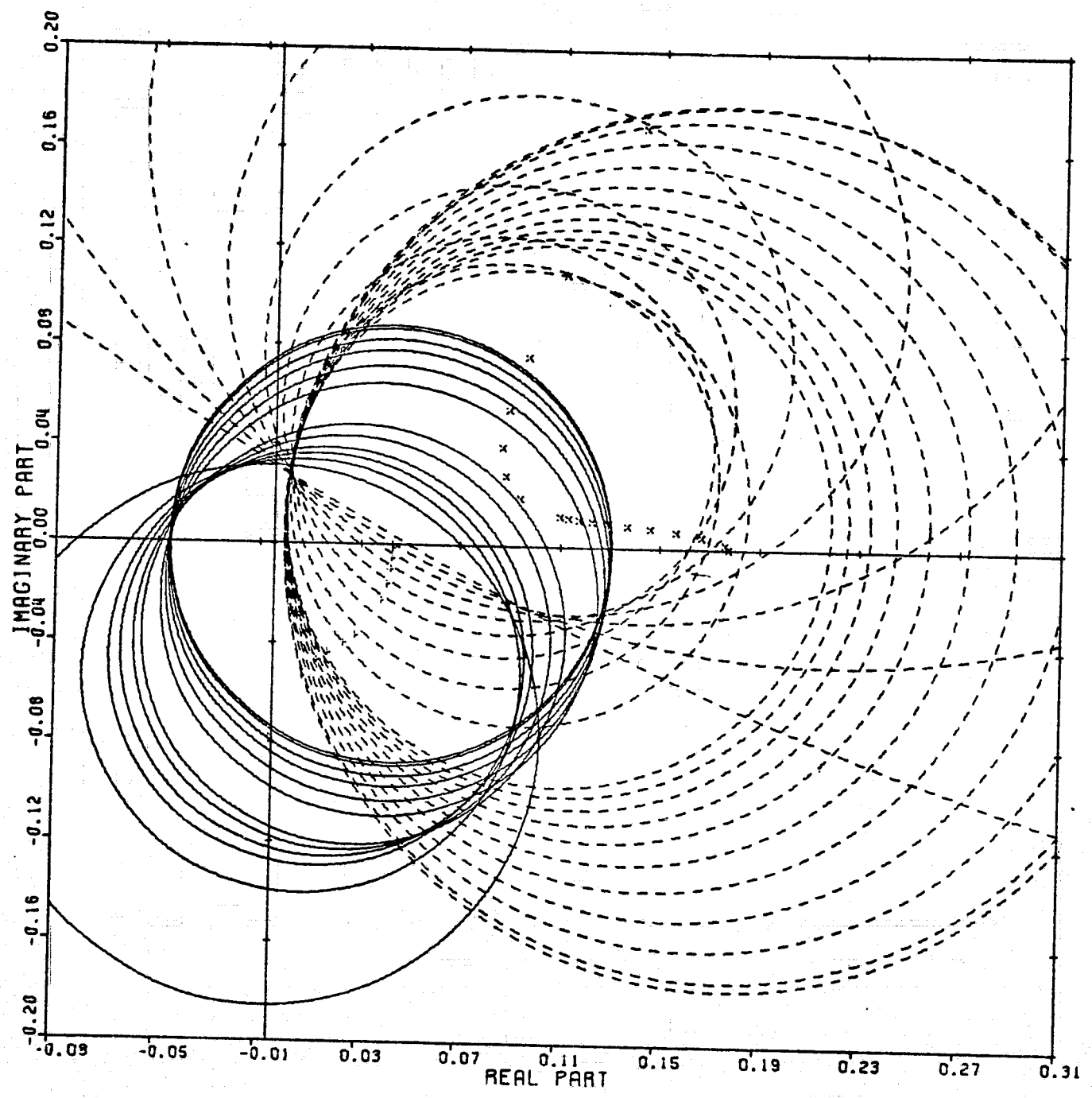
CARDIAD PLOT: 2.1 ENTRY: COLUMN SWITCH, 6/14/78.

INPUTS = 4, SYSTEM ORDER = 6, ANALYSIS TYPE = 1
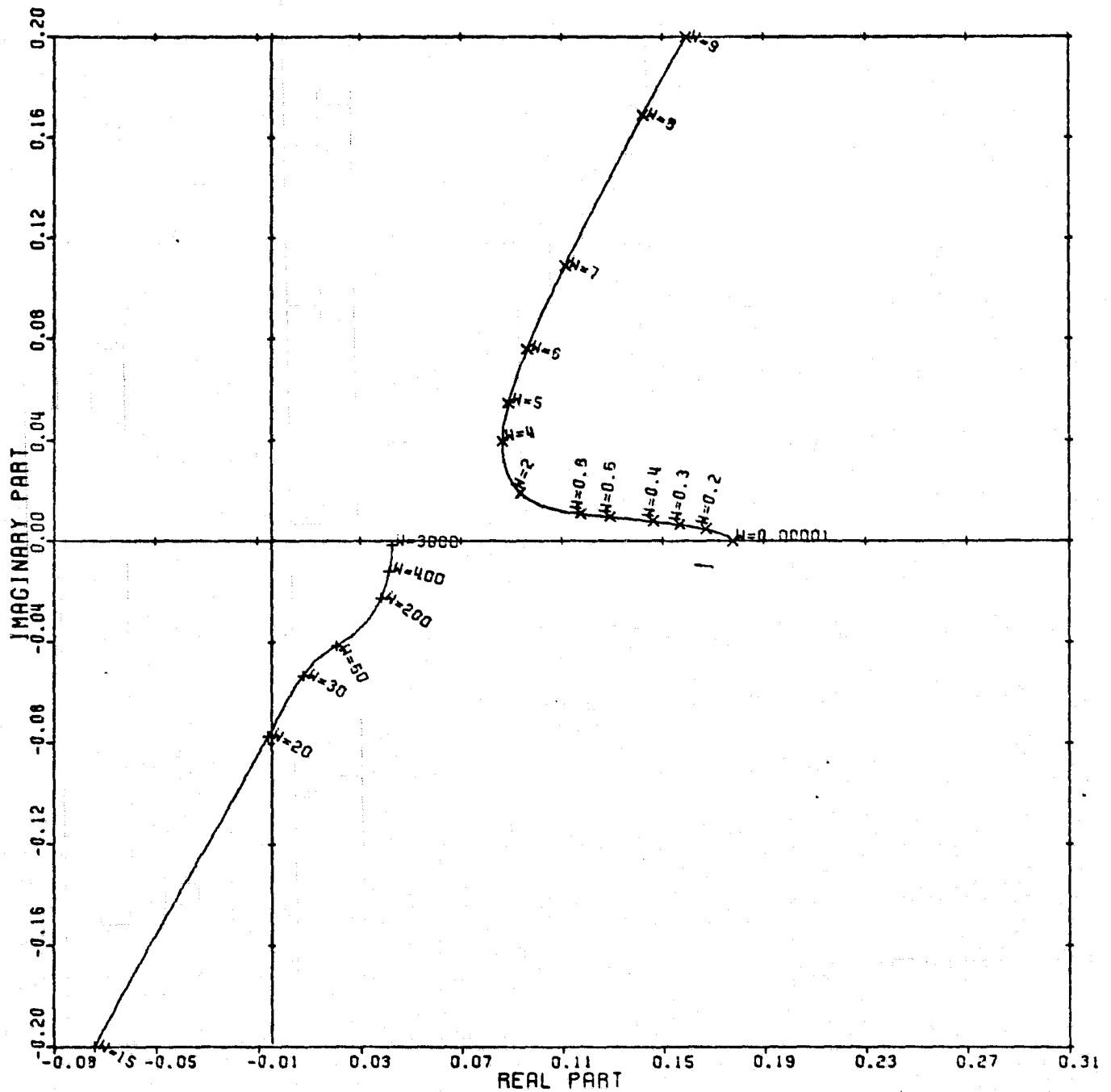
Figure 2

LOCUS OF CENTERS PLOT: 2,1 ENTRY: COLUMN SWITCH, 6/14/78.

INPUTS = 4, SYSTEM ORDER = 6, ANALYSIS TYPE = 1
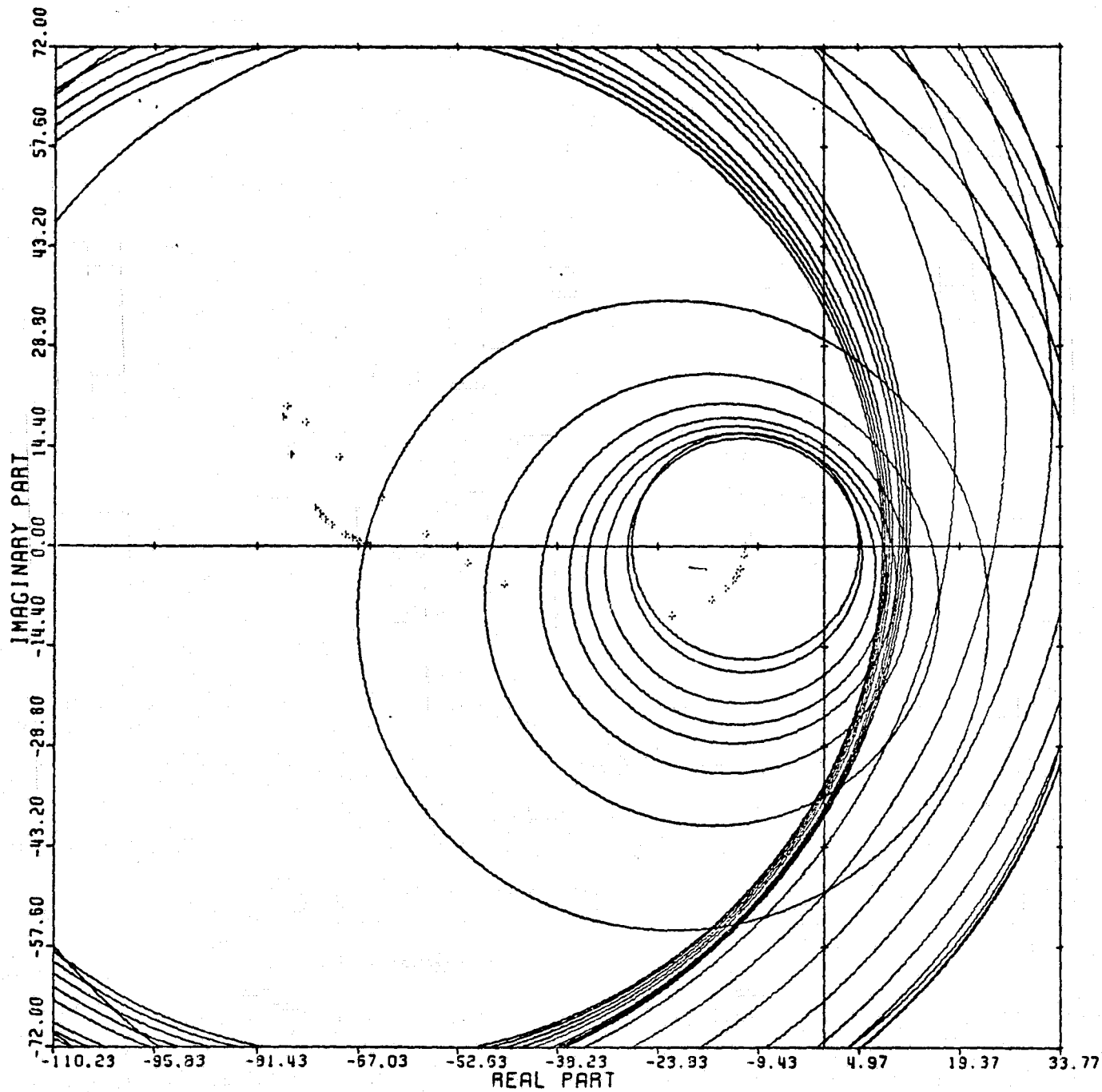
Figure 3

CARDIAD PLOT: 3,1 ENTRY: COLUMN SWITCH. 6/14/78.

INPUTS = 4, SYSTEM ORDER = 6, ANALYSIS TYPE = 1
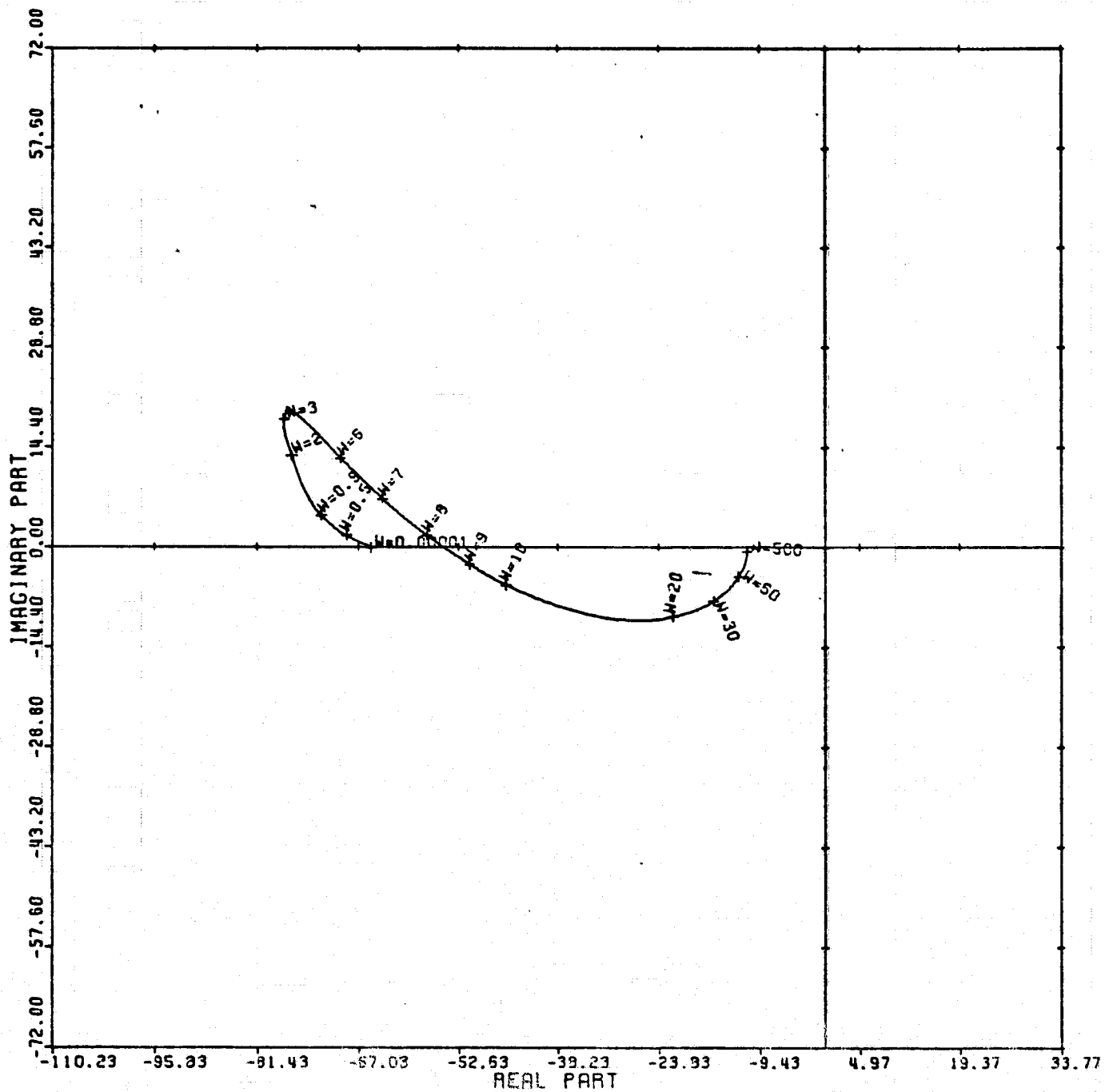
Figure 4

LOCUS OF CENTERS PLOT: 3,1 ENTRY: COLUMN SWITCH, 6/14/78.

INPUTS = 4, SYSTEM ORDER = 6, ANALYSIS TYPE = 1
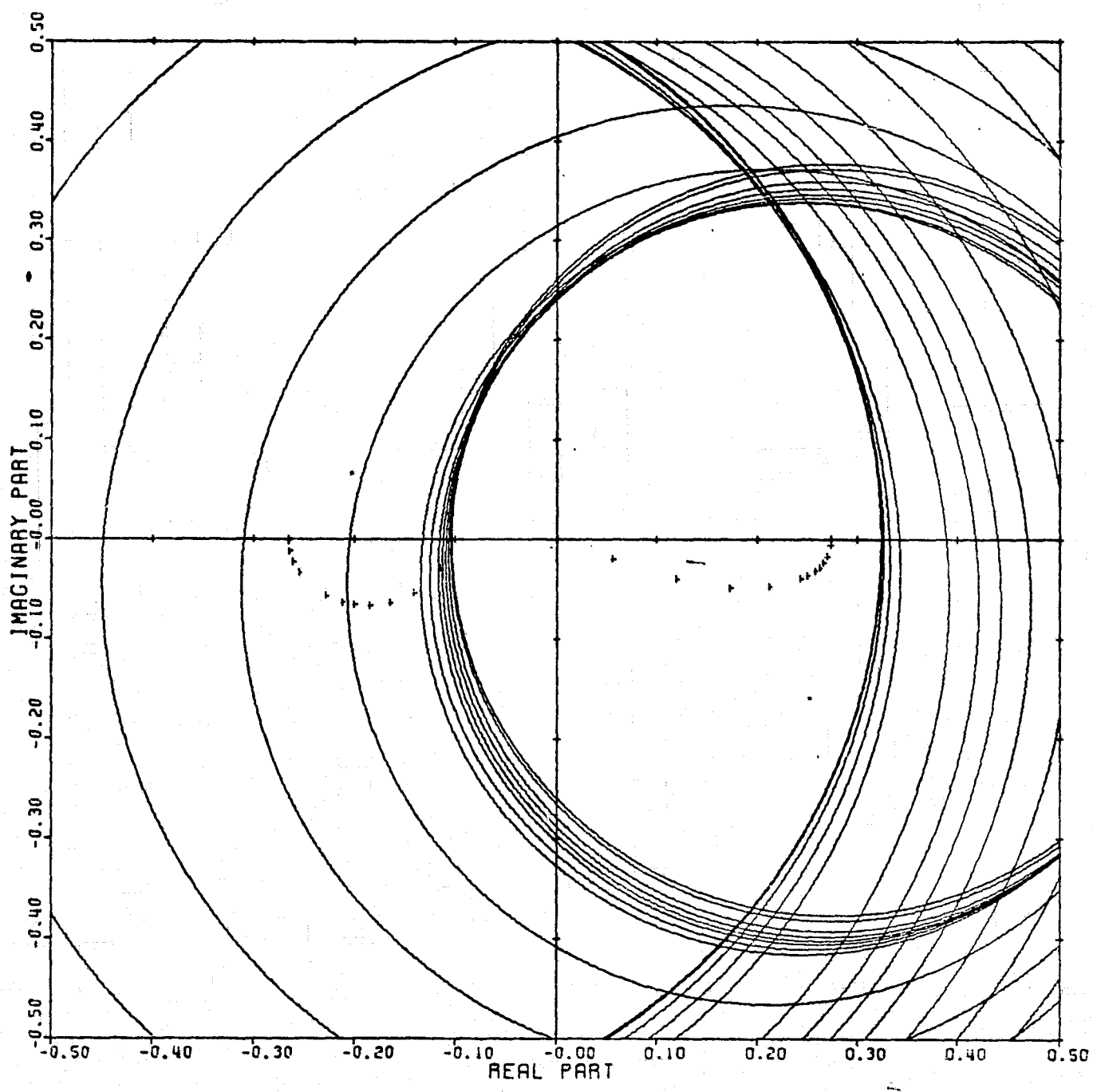
Figure 5

CARDIAD PLOT: 4.1 ENTRY: COLUMN SWITCH, 6/14/78.

INPUTS = 4, SYSTEM ORDER = .6, ANALYSIS TYPE = 1
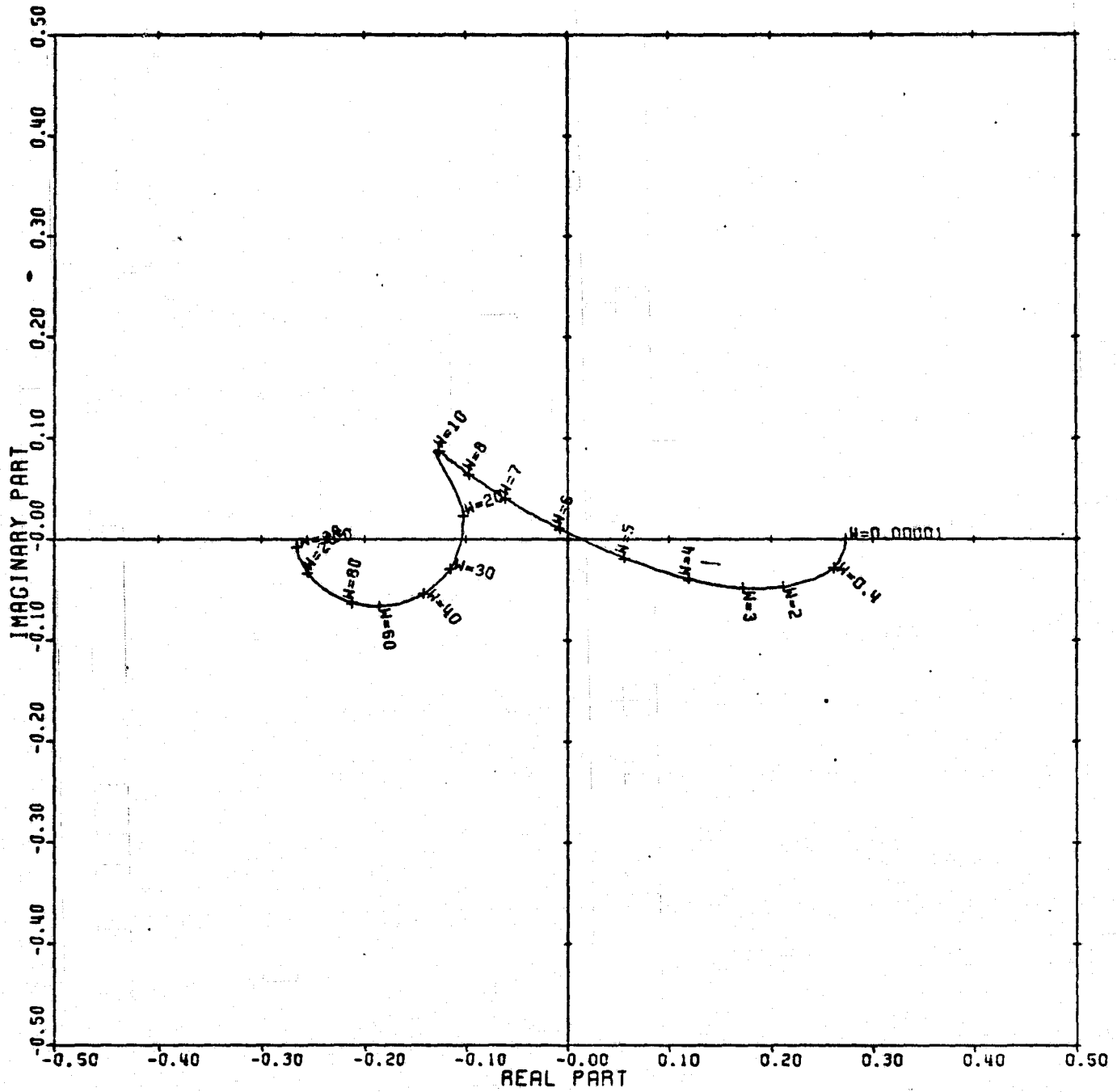
Figure 6

LOCUS OF CENTERS PLOT: 4,1 ENTRY: COLUMN SWITCH, 6/14/78.

INPUTS = 4, SYSTEM ORDER = .6, ANALYSIS TYPE = 1
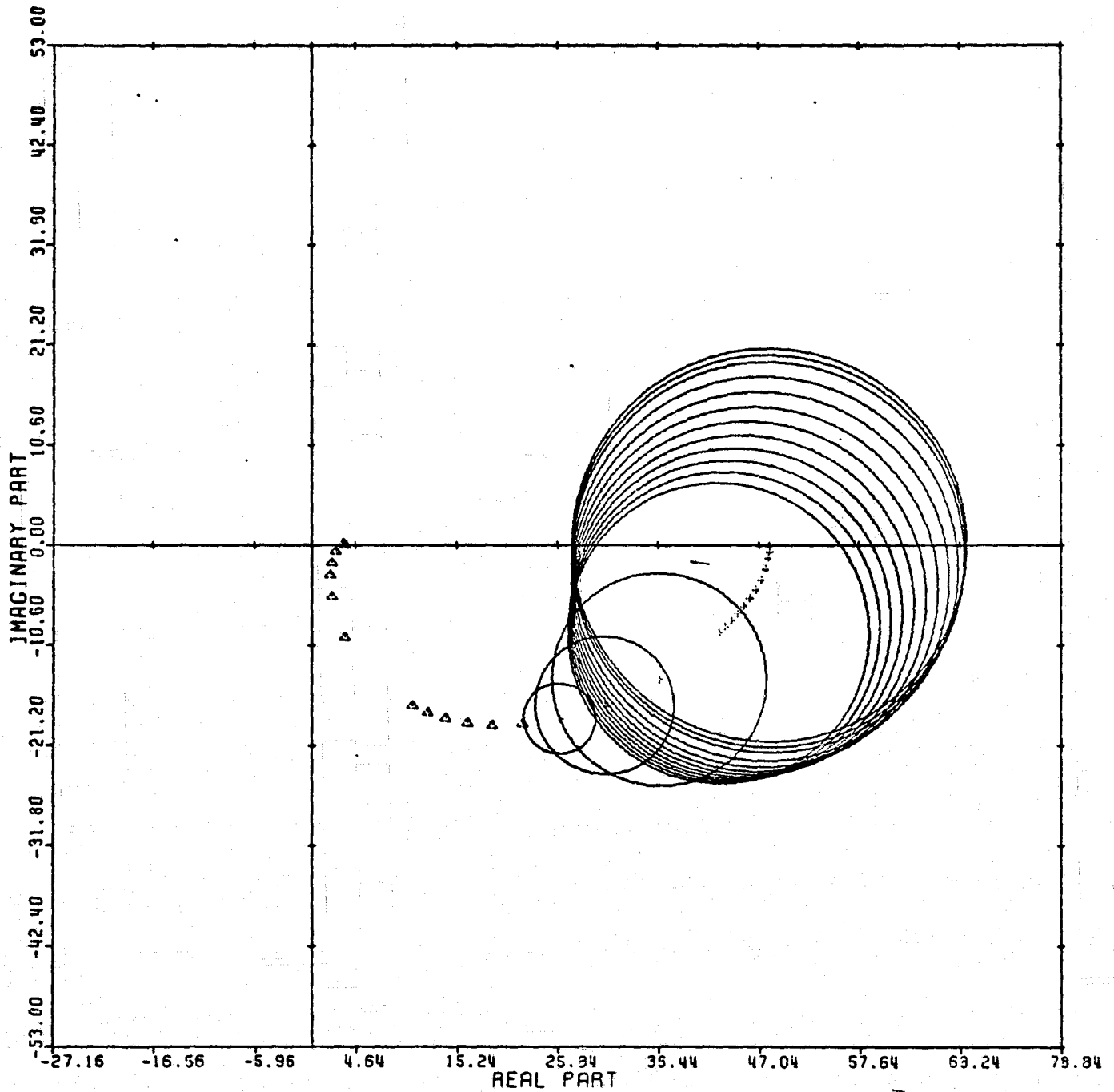
Figure 7

CARDIAD PLOT: 1,2 ENTRY: COLUMN SWITCH, 6/14/78.

INPUTS = 4, SYSTEM ORDER = 6, ANALYSIS TYPE = 1

Figure 8
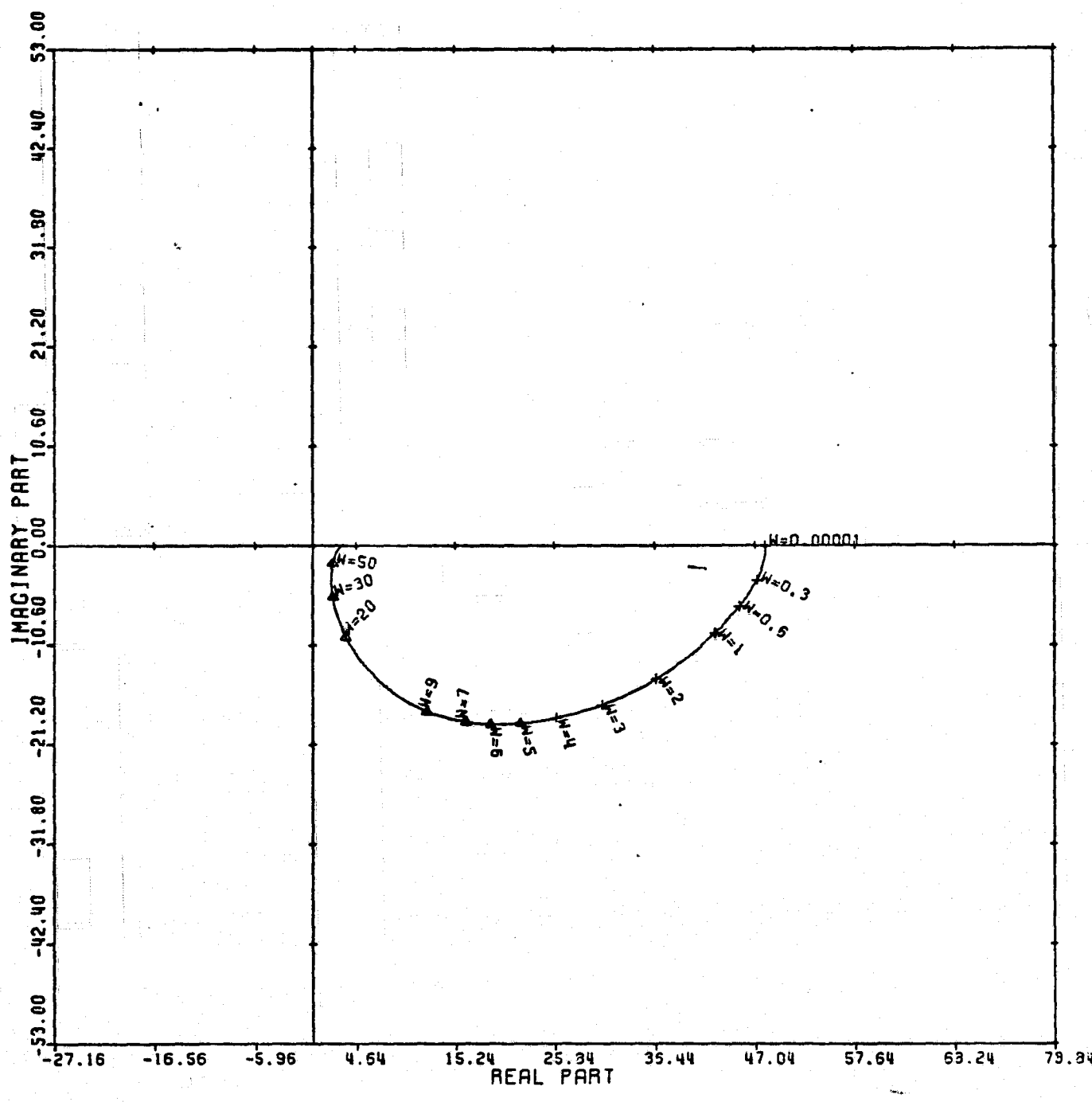
LOCUS OF CENTERS PLOT: 1,2 ENTRY: COLUMN SWITCH, 6/14/78.

INPUTS = 4, SYSTEM ORDER = 6, ANALYSIS TYPE = 1

Figure 9
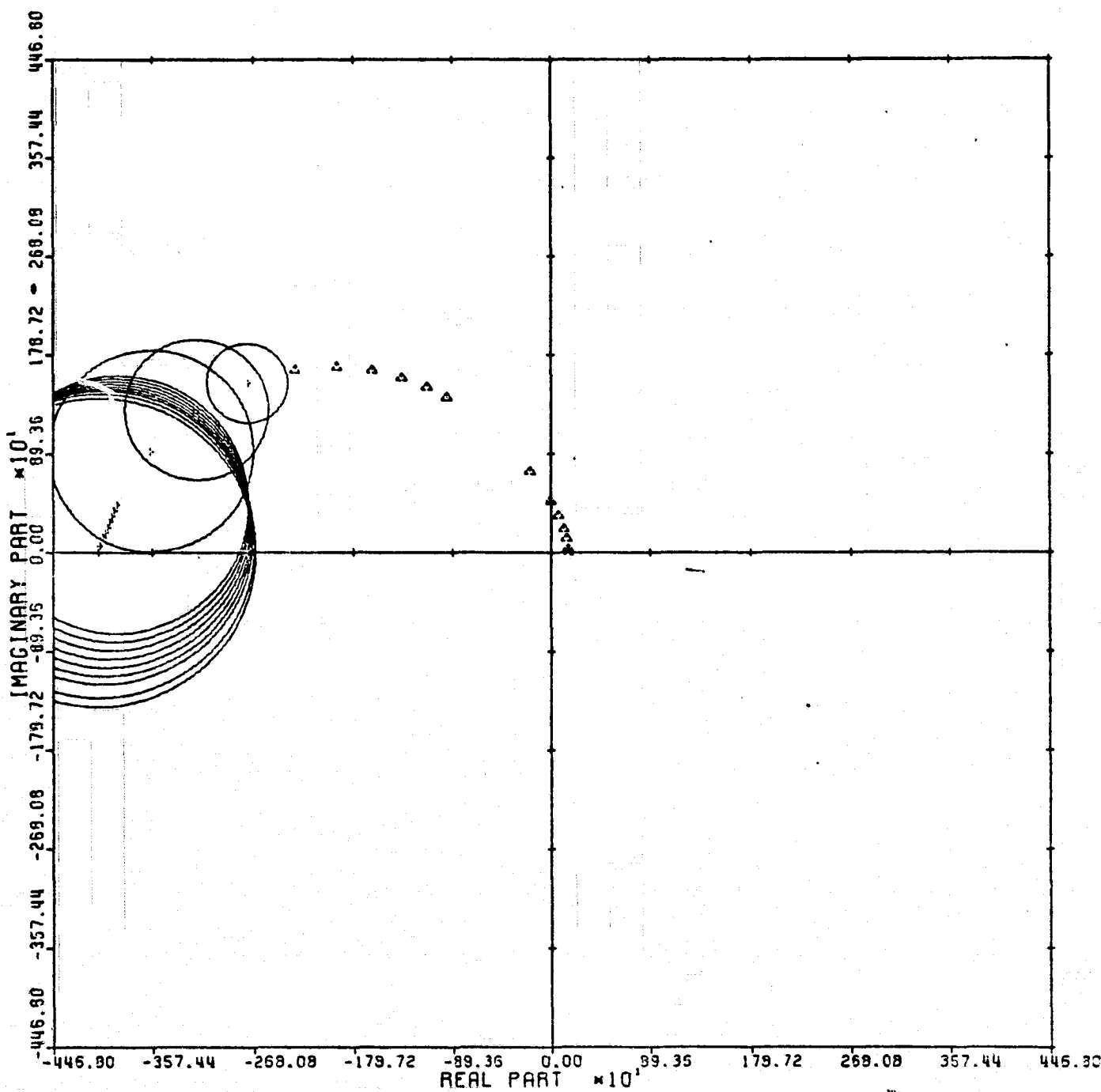
CARDIAD PLOT: 3,2 ENTRY: COLUMN SWITCH, 6/14/78.

INPUTS = 4, SYSTEM ORDER = 6, ANALYSIS TYPE = 1

Figure 10
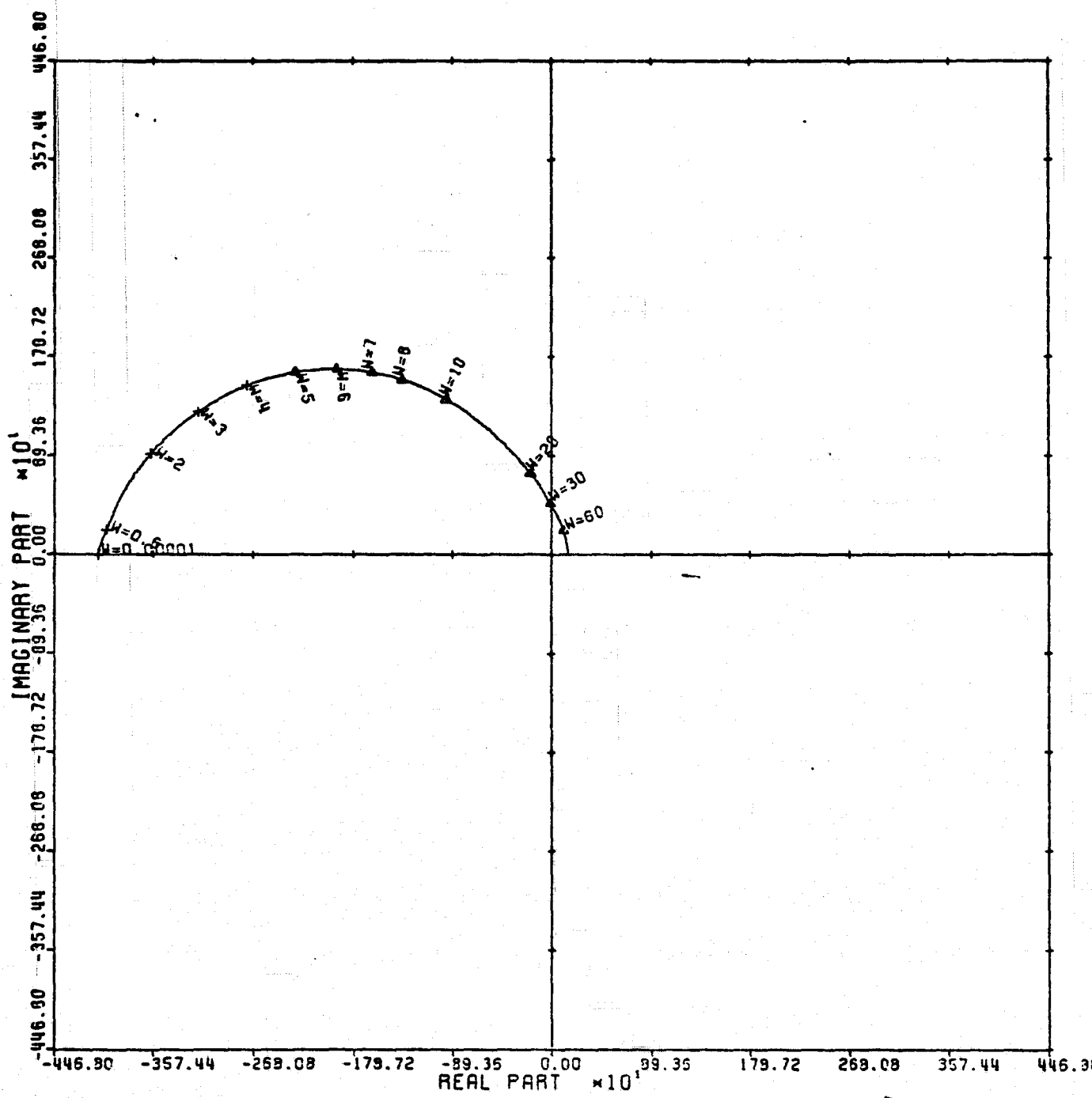
LOCUS OF CENTERS PLOT: 3.2 ENTRY: COLUMN SWITCH. 6/14/78.

INPUTS = 4. SYSTEM ORDER = 6. ANALYSIS TYPE = 1
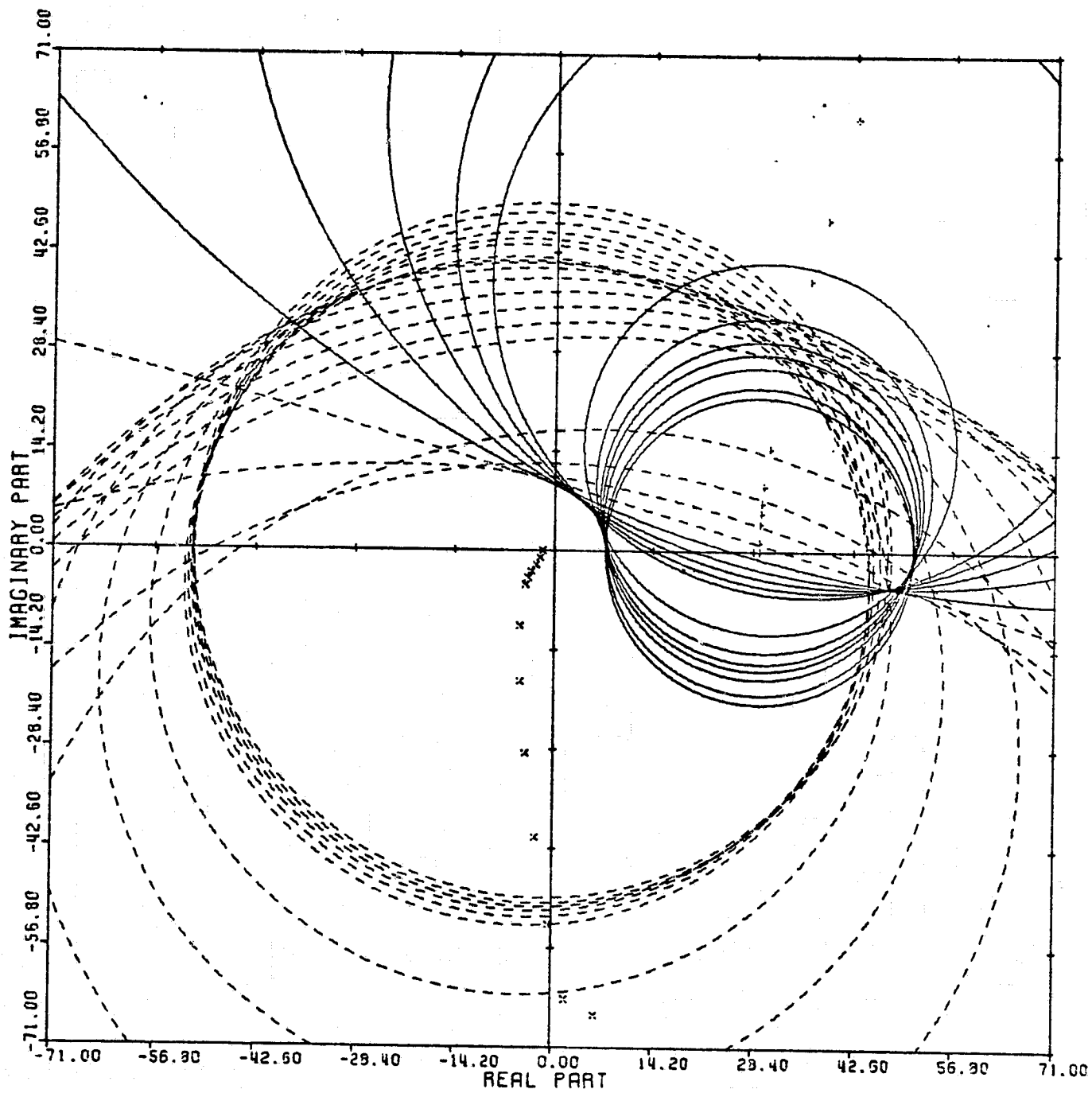
Figure 11

CARDIAD PLOT: 4,2 ENTRY: COLUMN SWITCH. 6/14/78.

INPUTS = 4, SYSTEM ORDER = 6, ANALYSIS TYPE = 1

Figure 12
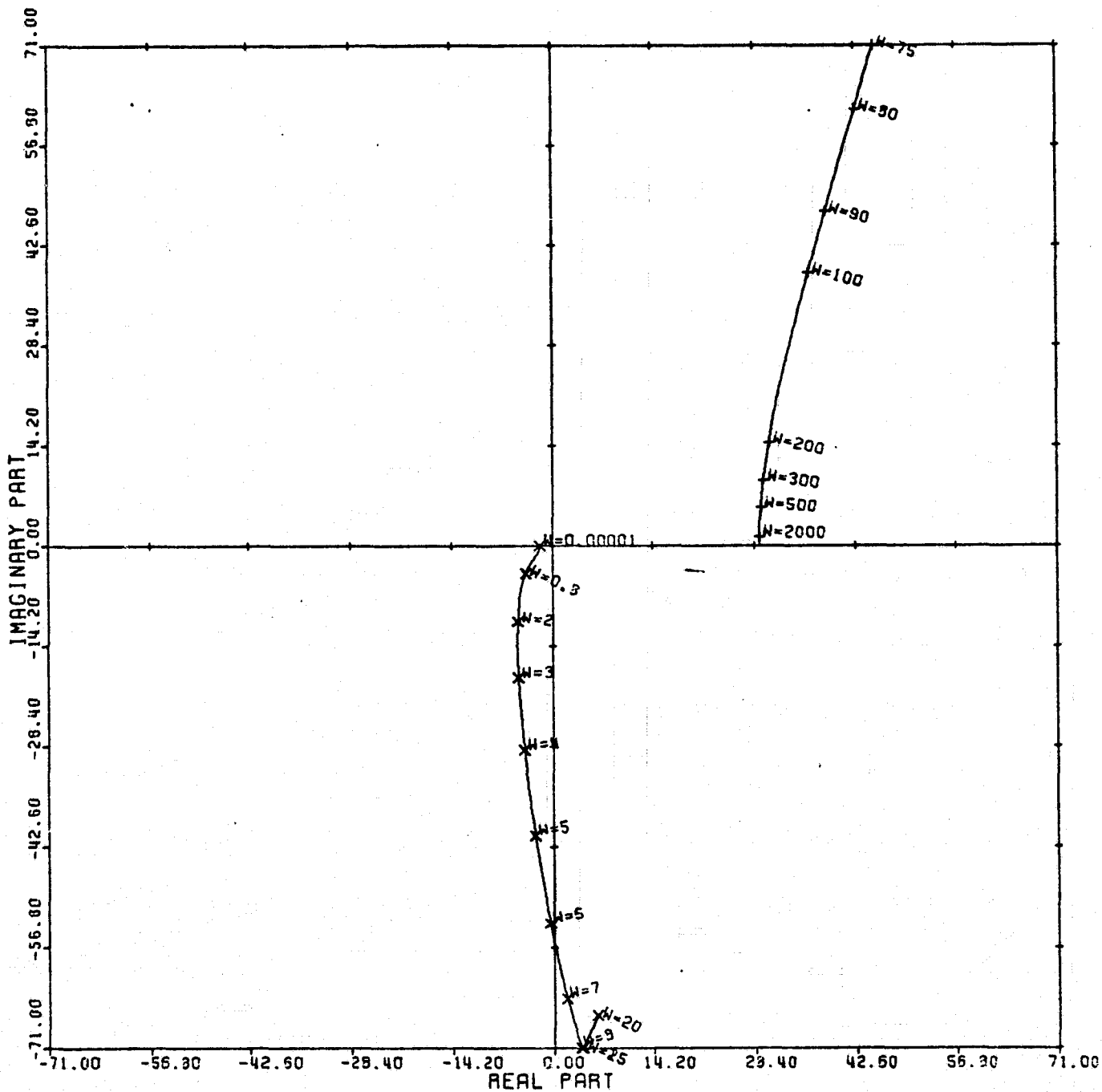
LOCUS OF CENTERS PLOT: 4,2 ENTRY: COLUMN SWITCH, 6/14/78.

INPUTS = 4, SYSTEM ORDER = 6, ANALYSIS TYPE = 1

Figure 13
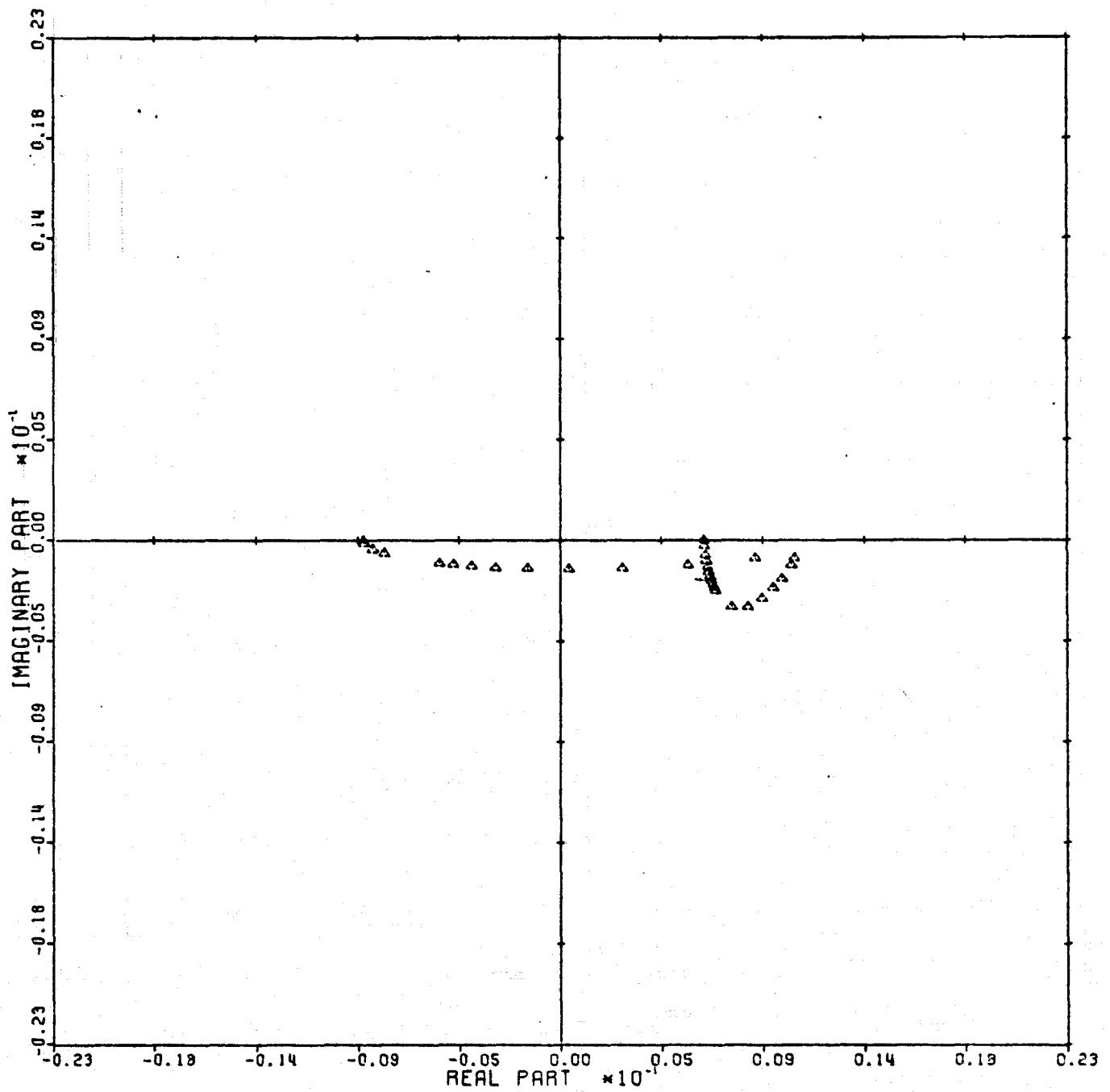
CARDIAD PLOT: 1,3 ENTRY: COLUMN SWITCH, 6/14/78.

INPUTS = 4, SYSTEM ORDER = 6, ANALYSIS TYPE = 1

Figure 14
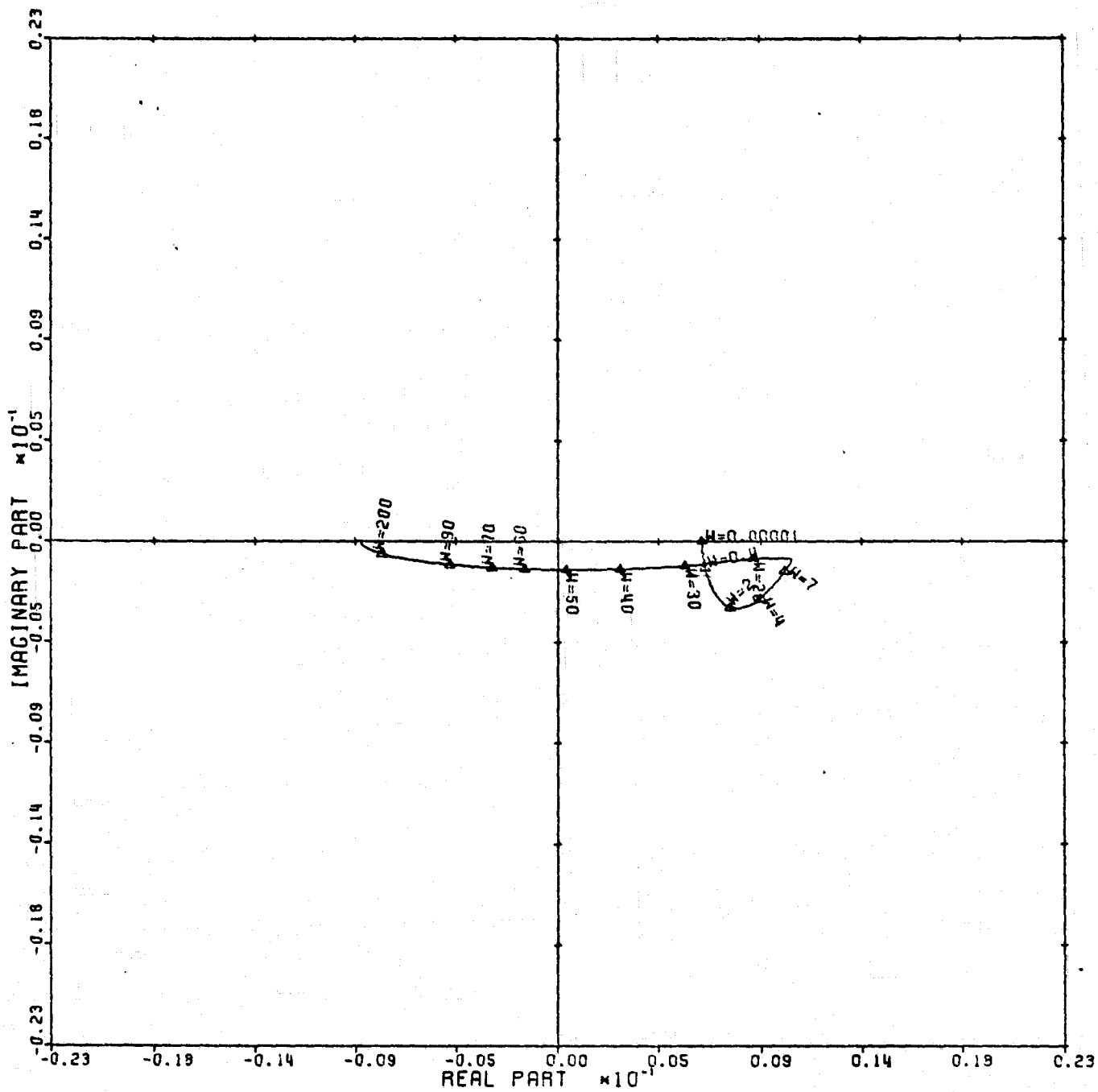
LOCUS OF CENTERS PLOT: 1,3 ENTRY: COLUMN SWITCH, 6/14/78.

INPUTS = 4, SYSTEM ORDER = 6, ANALYSIS TYPE = 1

Figure 15
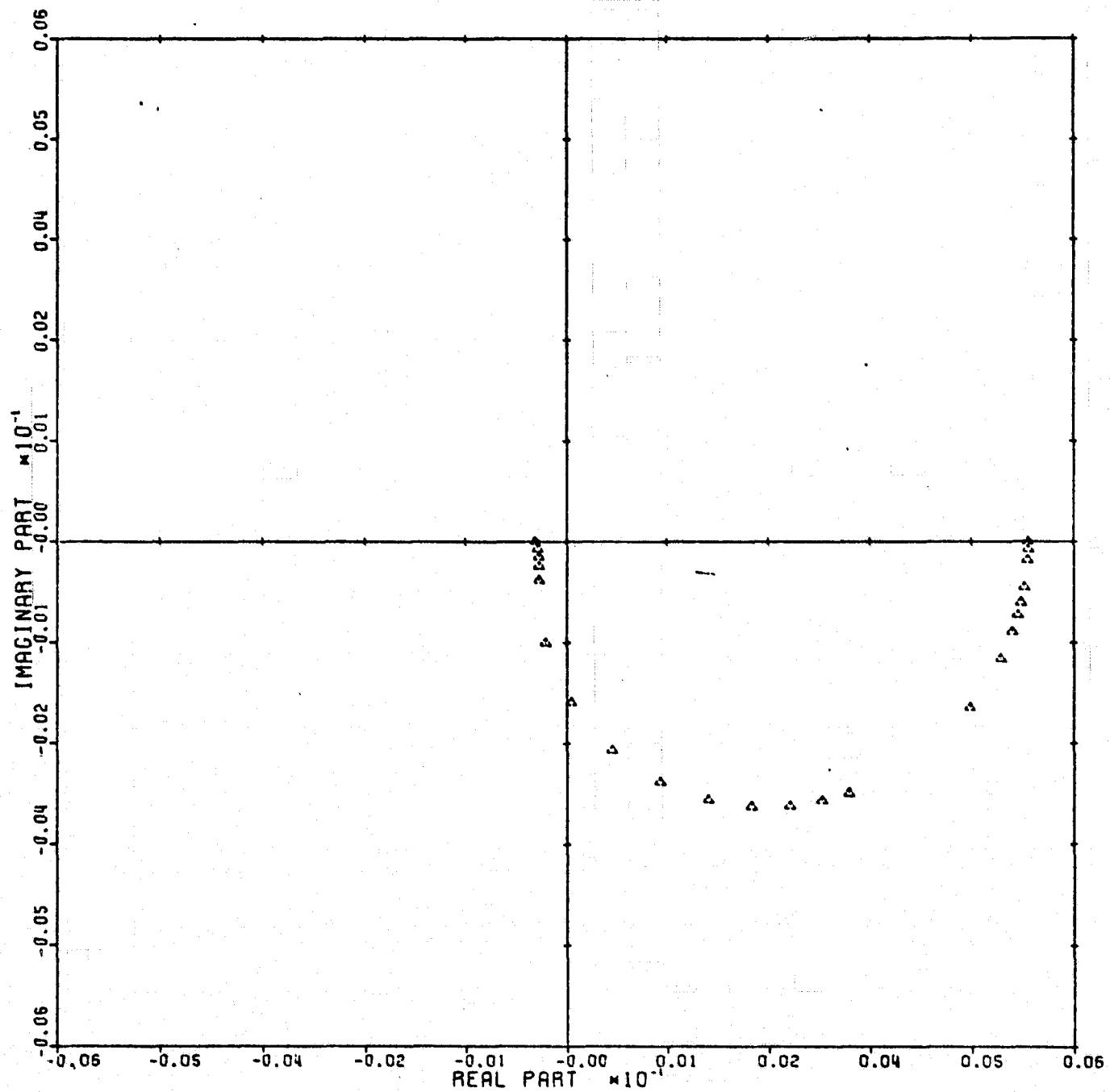
CARDIAD PLOT: 2,3 ENTRY: COLUMN SWITCH, 6/14/78.

INPUTS = 4, SYSTEM ORDER = 6, ANALYSIS TYPE = 1

Figure 16
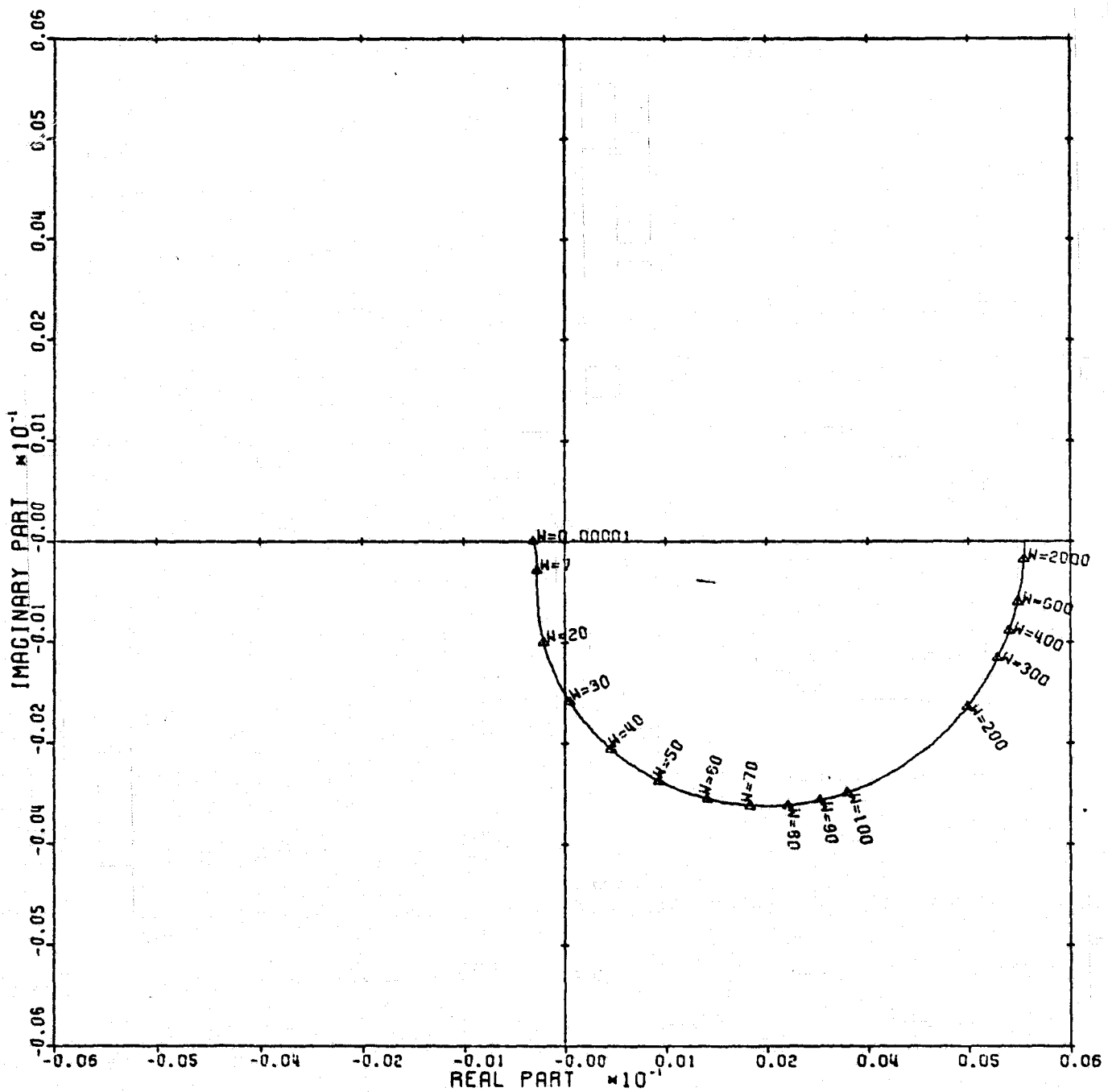
LOCUS OF CENTERS PLOT: 2,3 ENTRY: COLUMN SWITCH, 6/14/78.

INPUTS = 4, SYSTEM ORDER = 6, ANALYSIS TYPE = 1

Figure 17
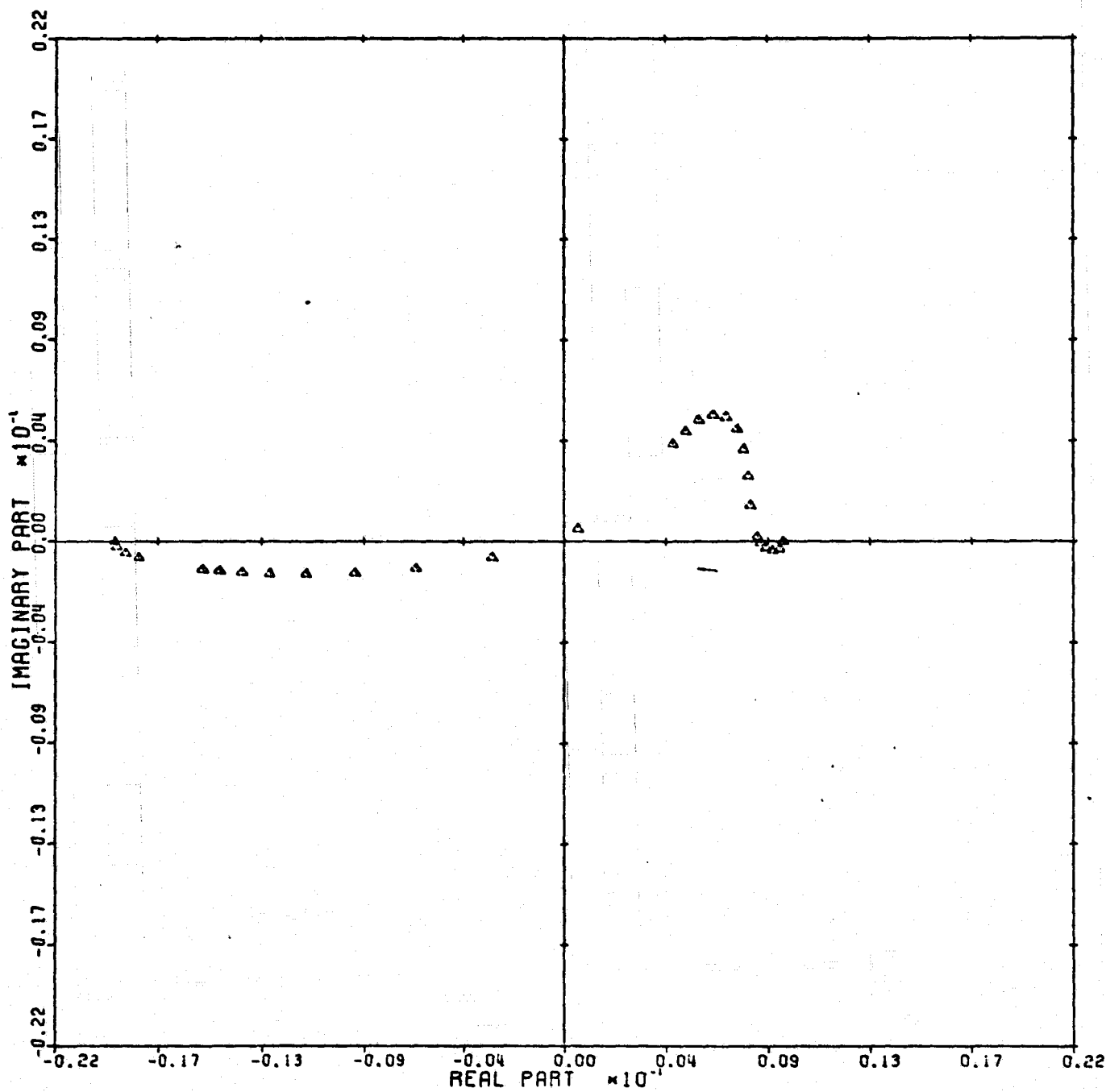
CARDIAD PLOT: 4,3 ENTRY: COLUMN SWITCH, 6/14/78.

INPUTS = 4, SYSTEM ORDER = 6, ANALYSIS TYPE = 1

Figure 18
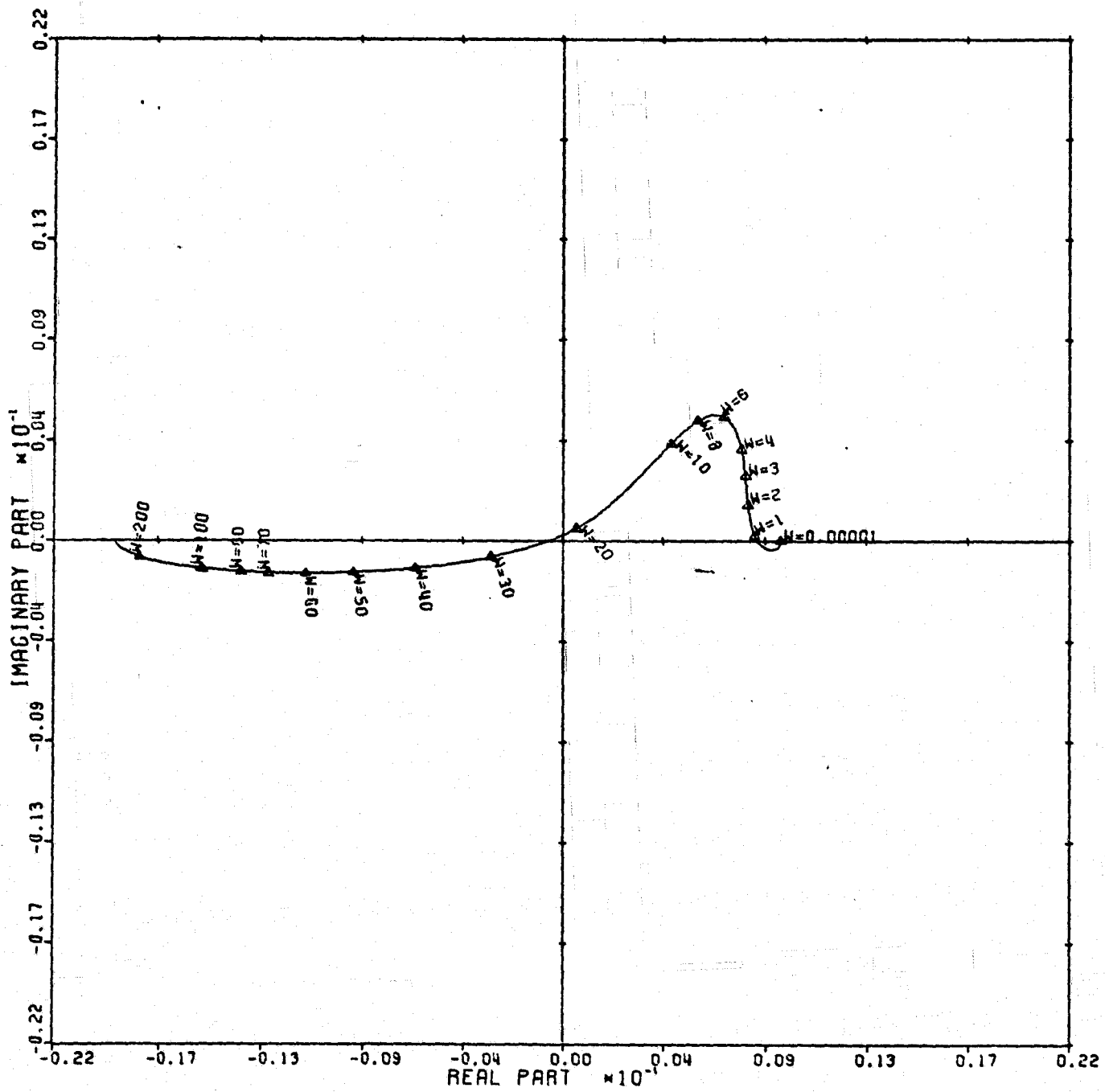
LOCUS OF CENTERS PLOT: 4,3 ENTRY: COLUMN SWITCH. 6/14/78.

INPUTS = 4, SYSTEM ORDER = 6, ANALYSIS TYPE = 1

Figure 19
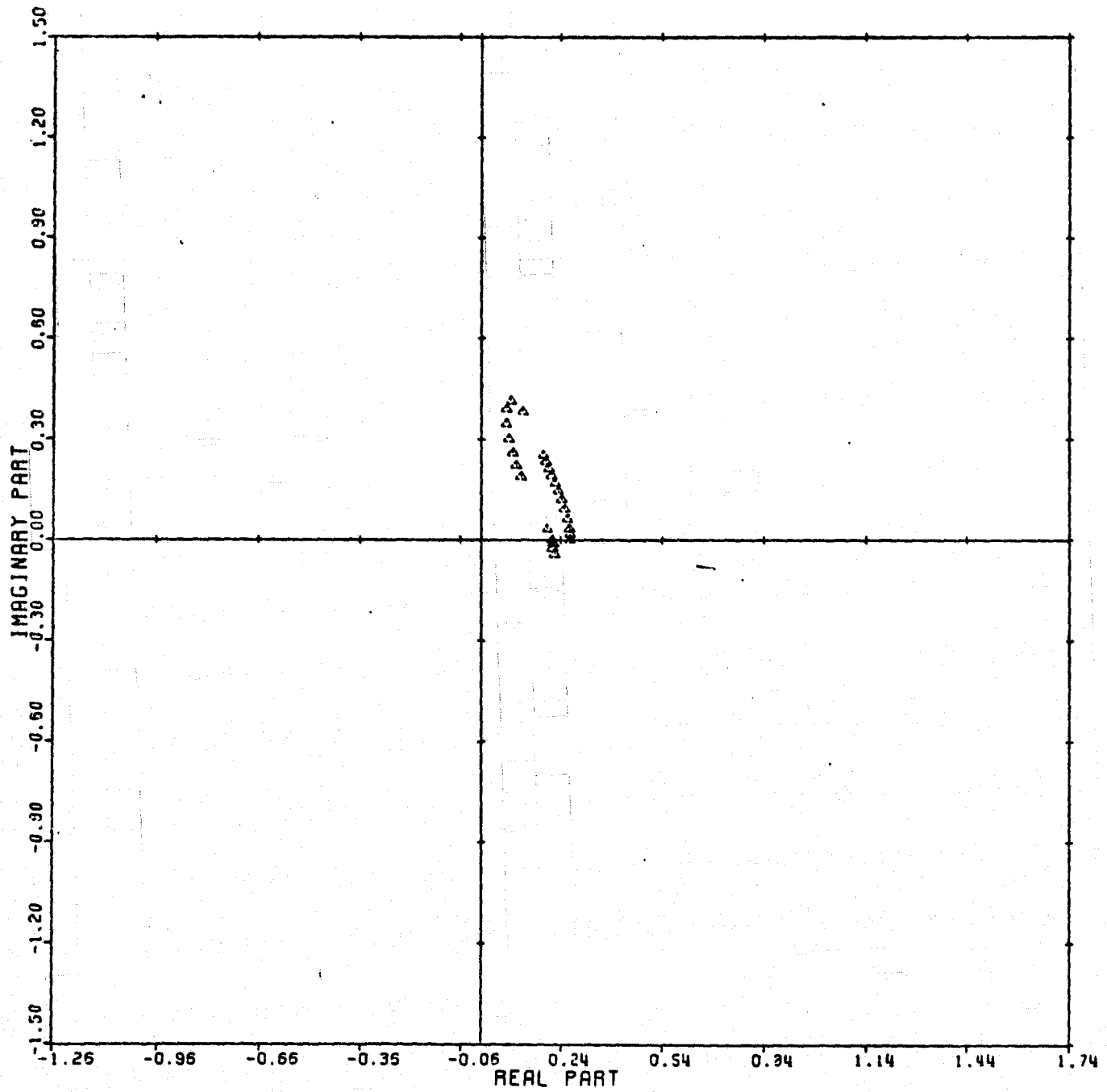
CARDIAD PLOT: 1.4 ENTRY: COLUMN SWITCH, 6/14/78.

INPUTS = 4, SYSTEM ORDER = 6, ANALYSIS TYPE = 1

Figure 20
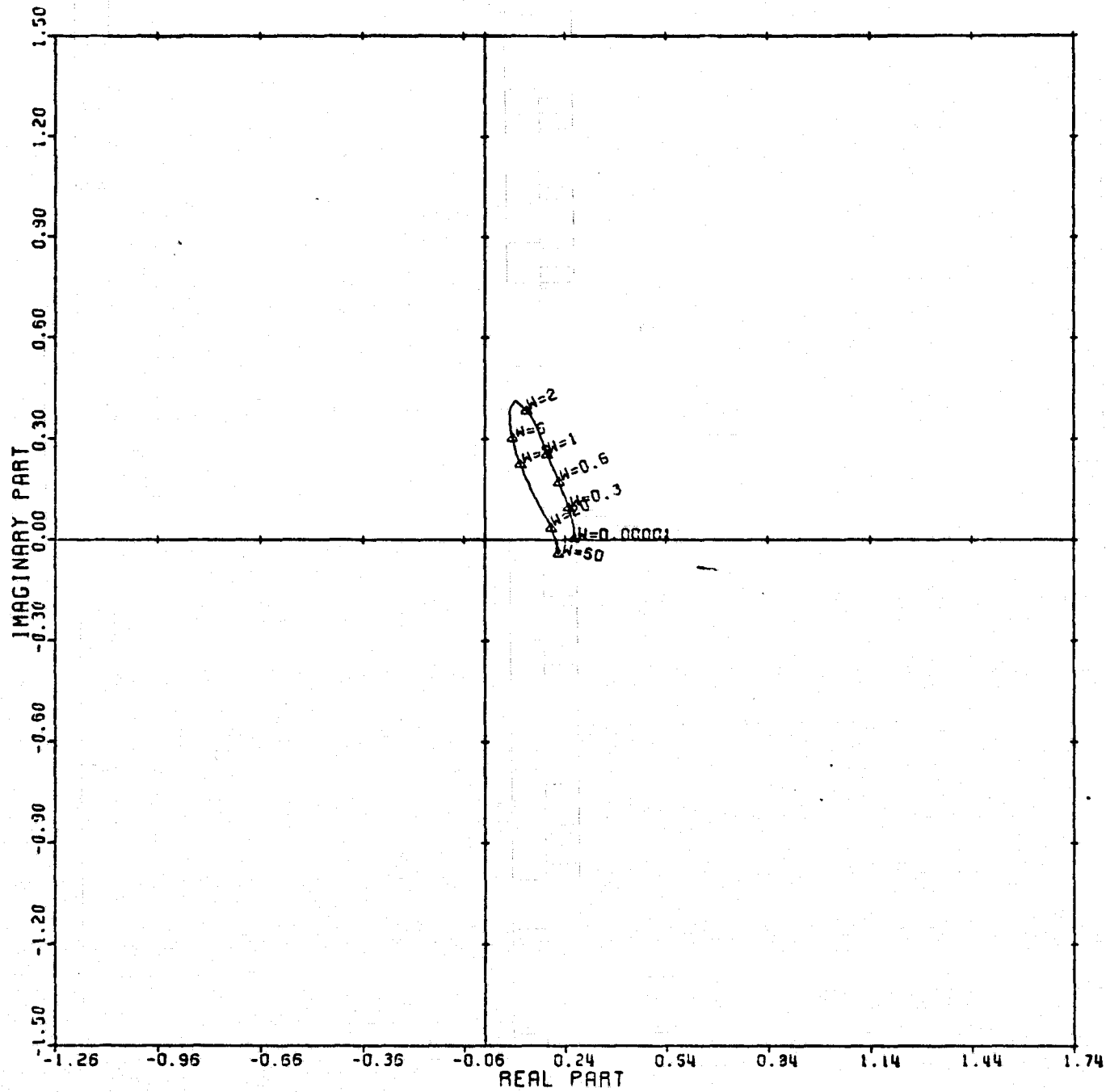
LOCUS OF CENTERS PLOT: 1,4 ENTRY: COLUMN SWITCH, 6/14/78.

INPUTS = 4, SYSTEM ORDER = 6, ANALYSIS TYPE = 1

Figure 21
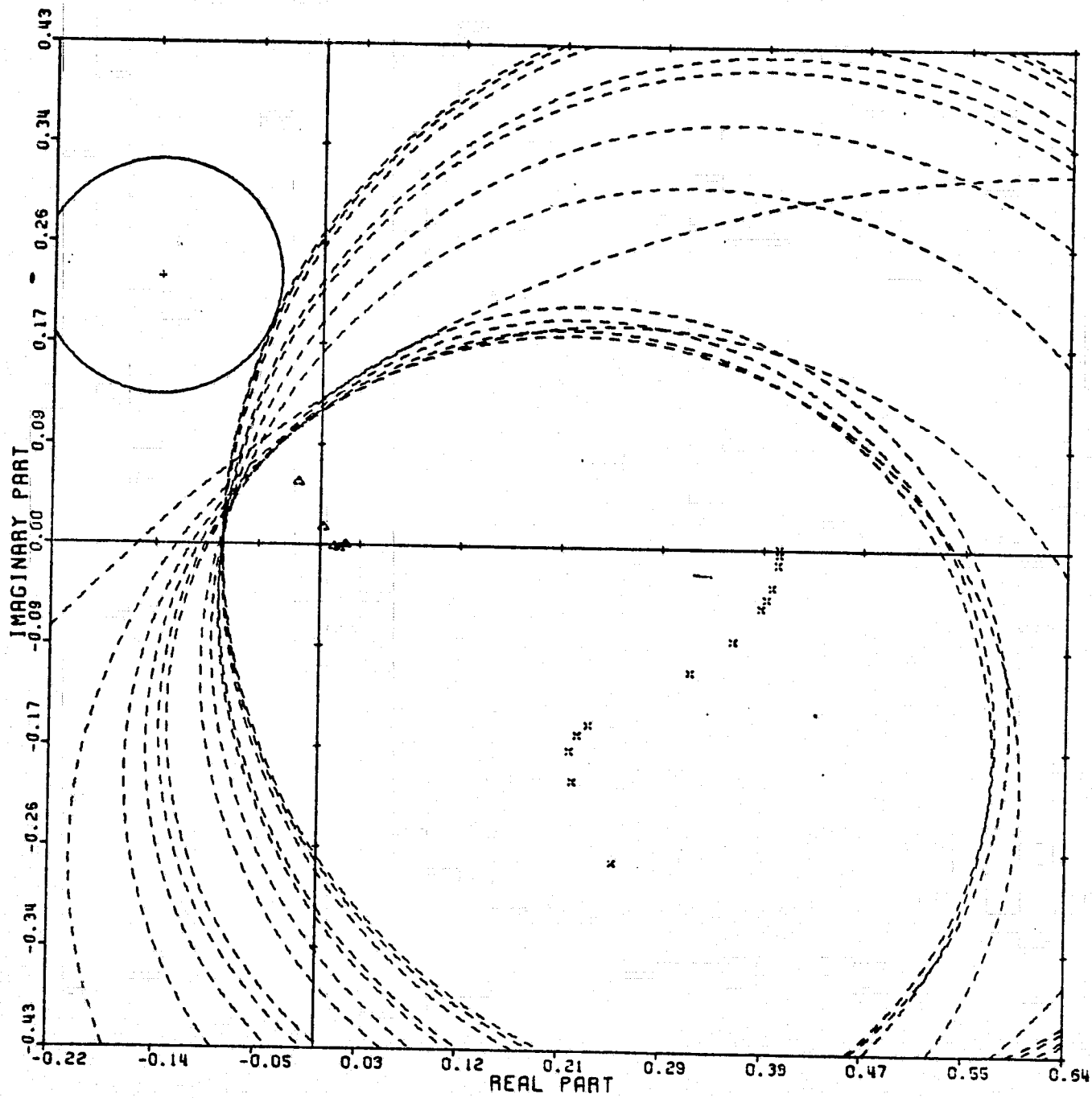
CARDIAD PLOT: 2,4 ENTRY: COLUMN SWITCH, 6/14/78.

INPUTS = 4, SYSTEM ORDER = .6, ANALYSIS TYPE = 1

Figure 22
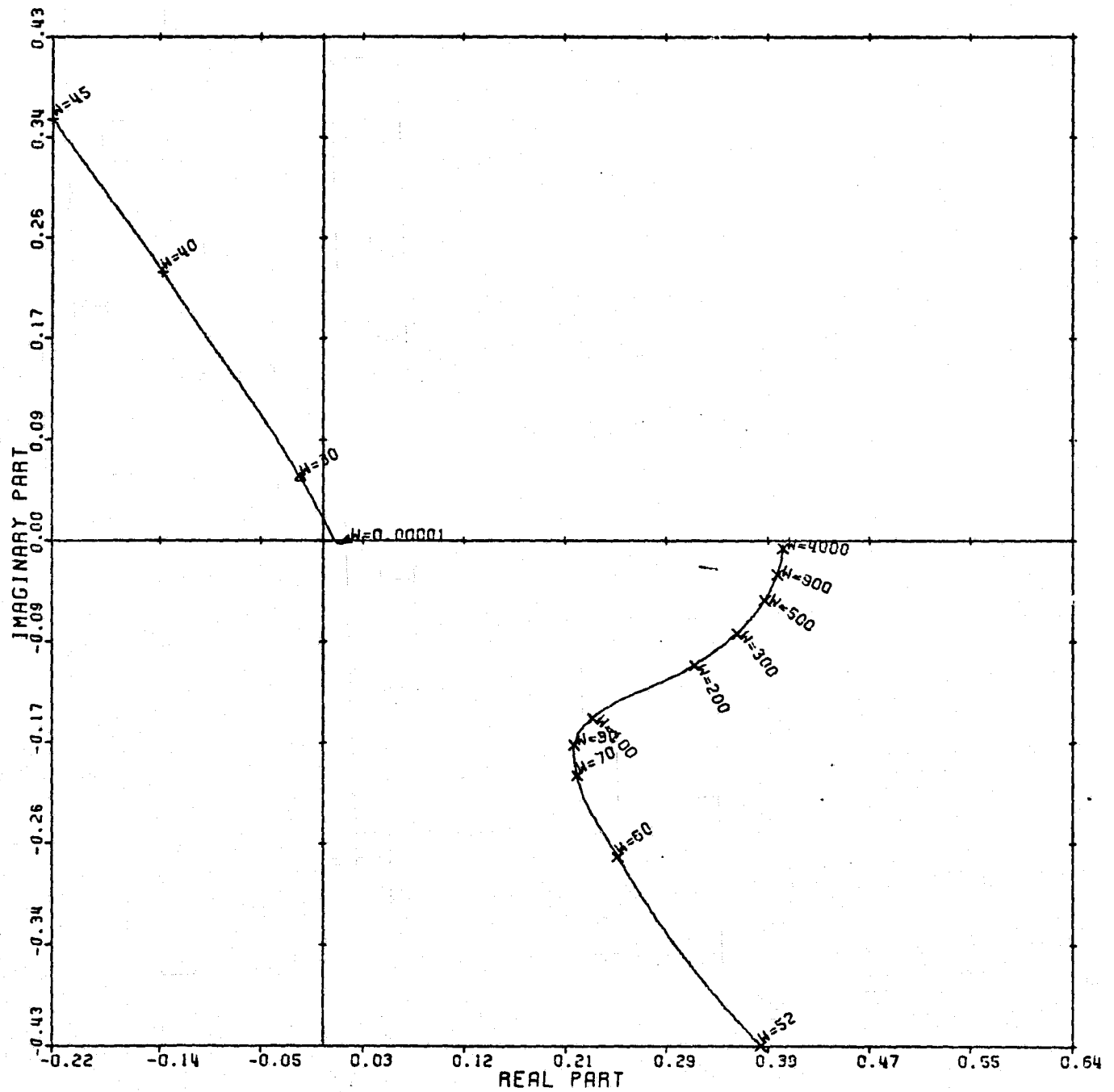
LOCUS OF CENTERS PLOT: 2,4 ENTRY: COLUMN SWITCH. 6/14/78.

INPUTS = 4, SYSTEM ORDER = 6, ANALYSIS TYPE = 1

Figure 23
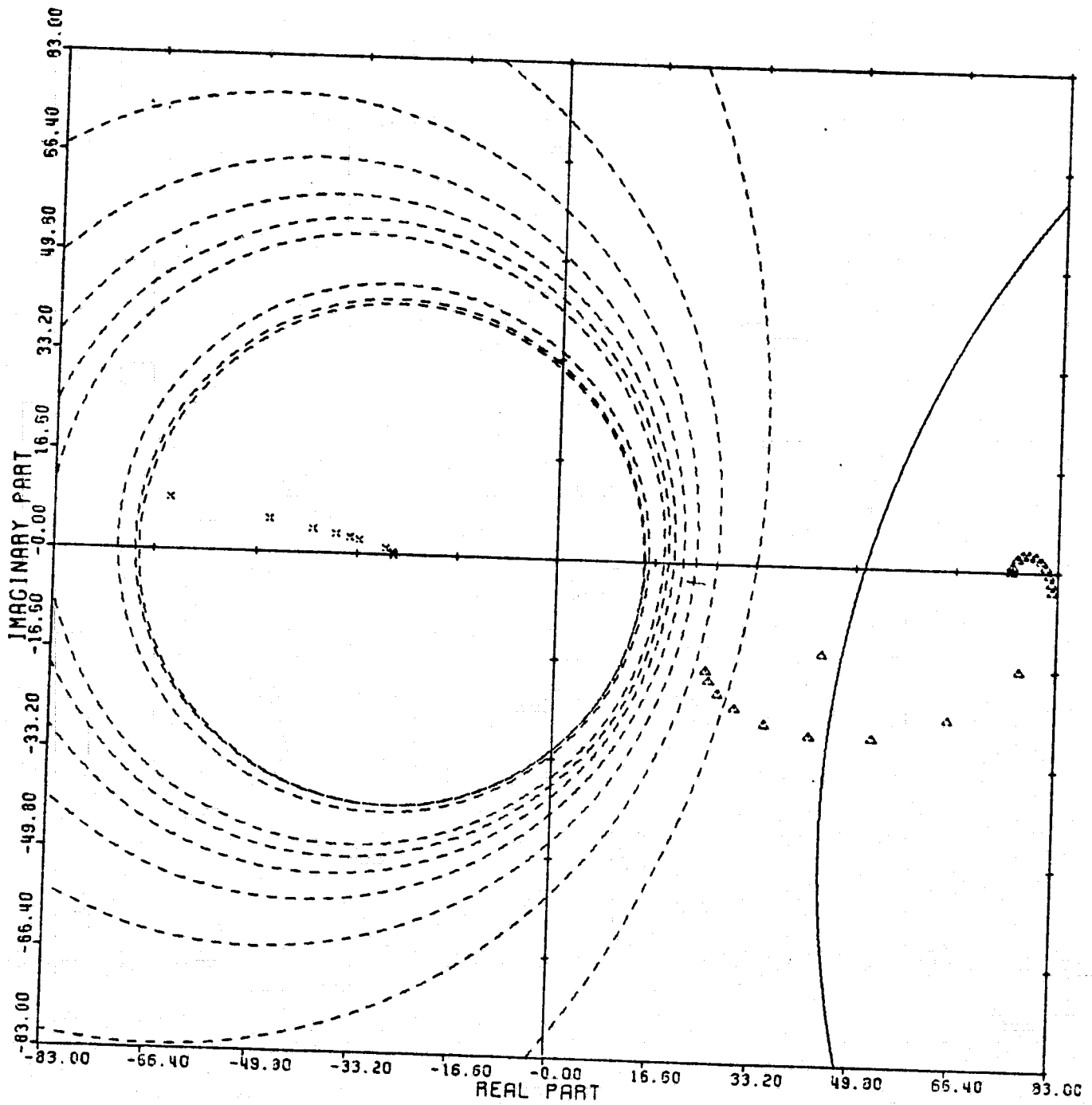
CARDIAC PLOT: 3.4 ENTRY: COLUMN SWITCH. 6/14/78.

INPUTS = 4. SYSTEM ORDER = 6. ANALYSIS TYPE = 1

Figure 24
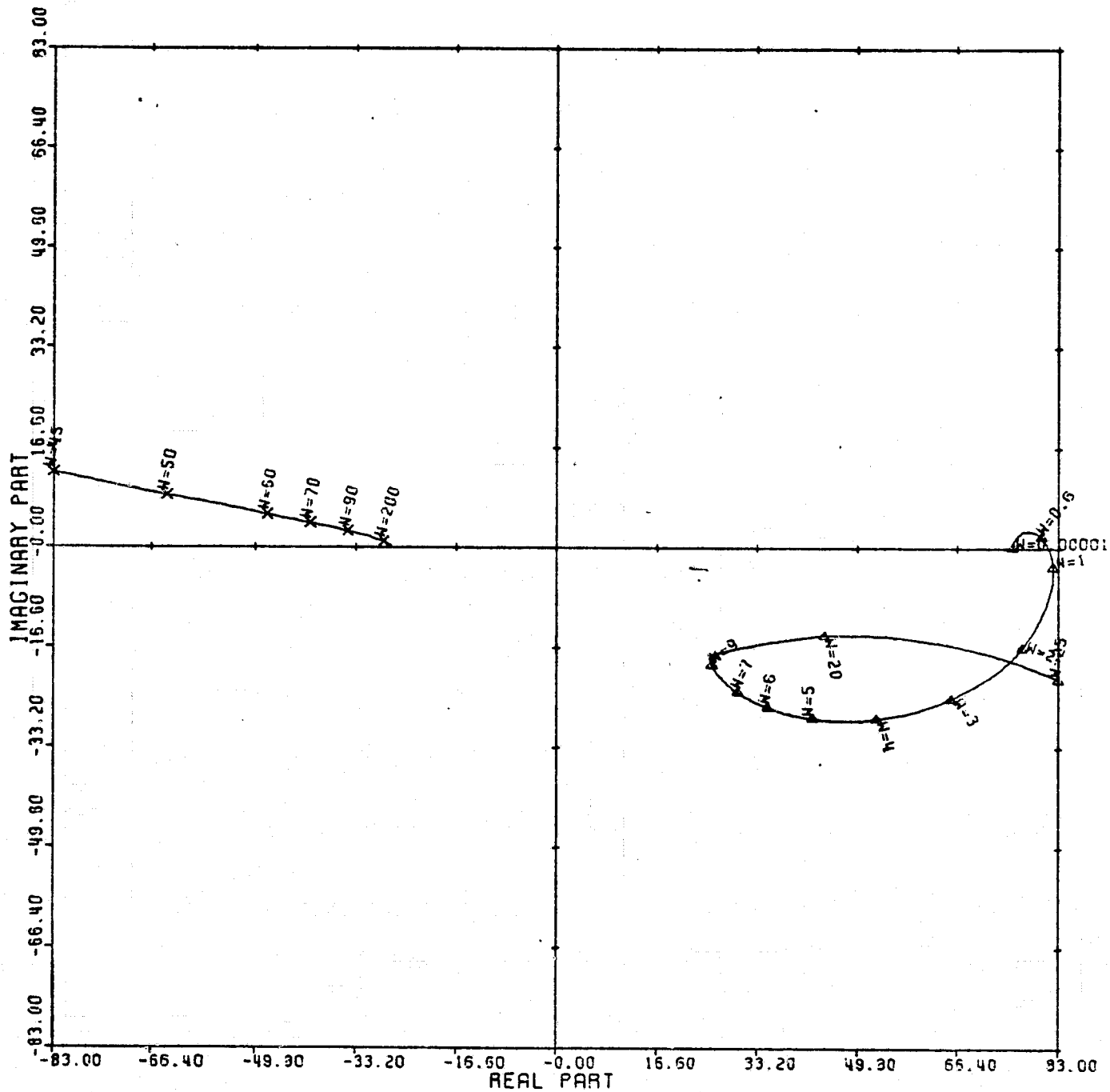
LOCUS OF CENTERS PLOT: 3,4 ENTRY: COLUMN SWITCH, 6/14/78.

INPUTS = 4, SYSTEM ORDER = 6, ANALYSIS TYPE = 1

Figure 25
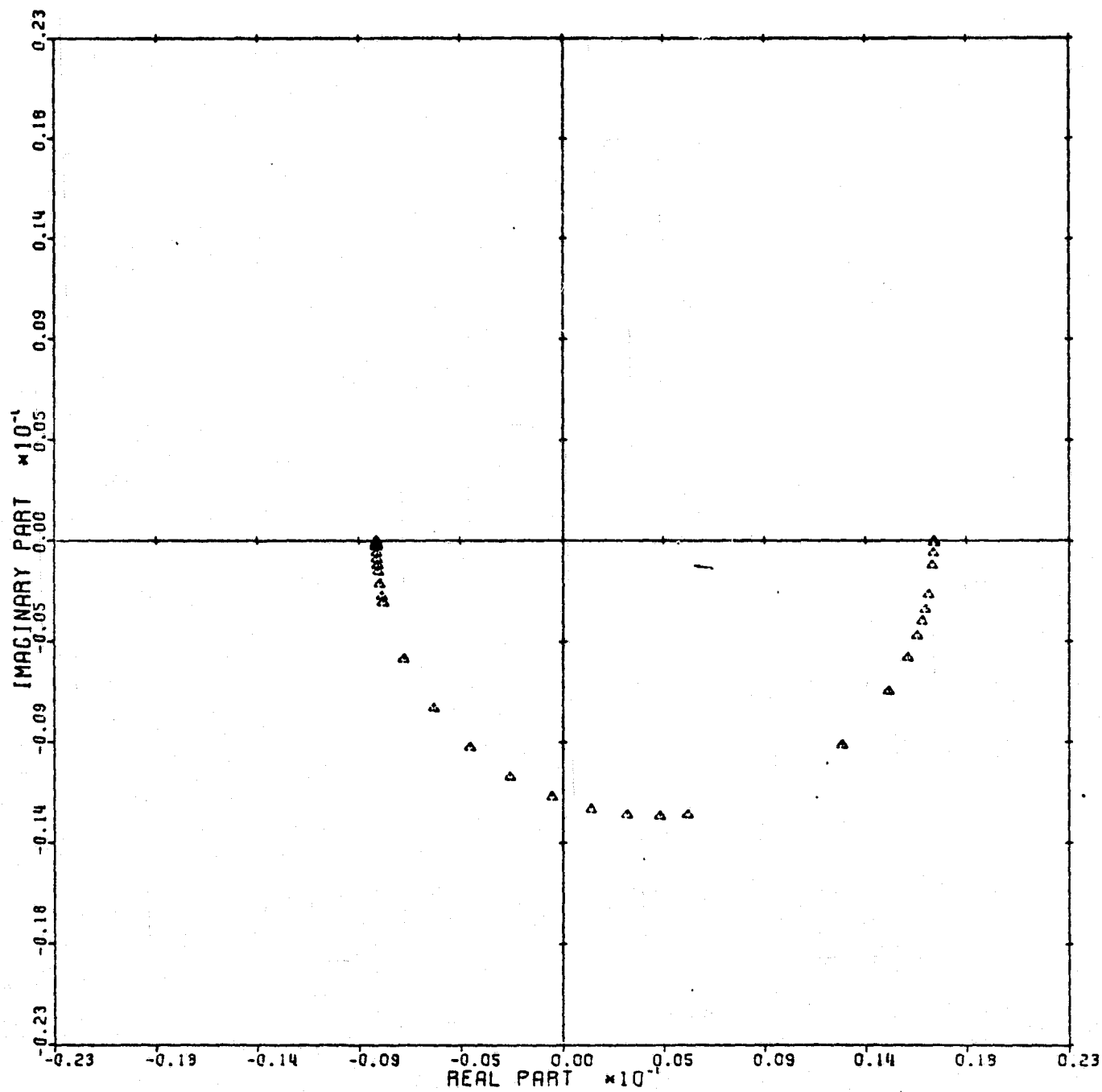
CARDIAD PLOT: 1,3 ENTRY: COLUMN SWITCH. 6/14/78.

INPUTS = 4, SYSTEM ORDER = 6, ANALYSIS TYPE = 2

Figure 26
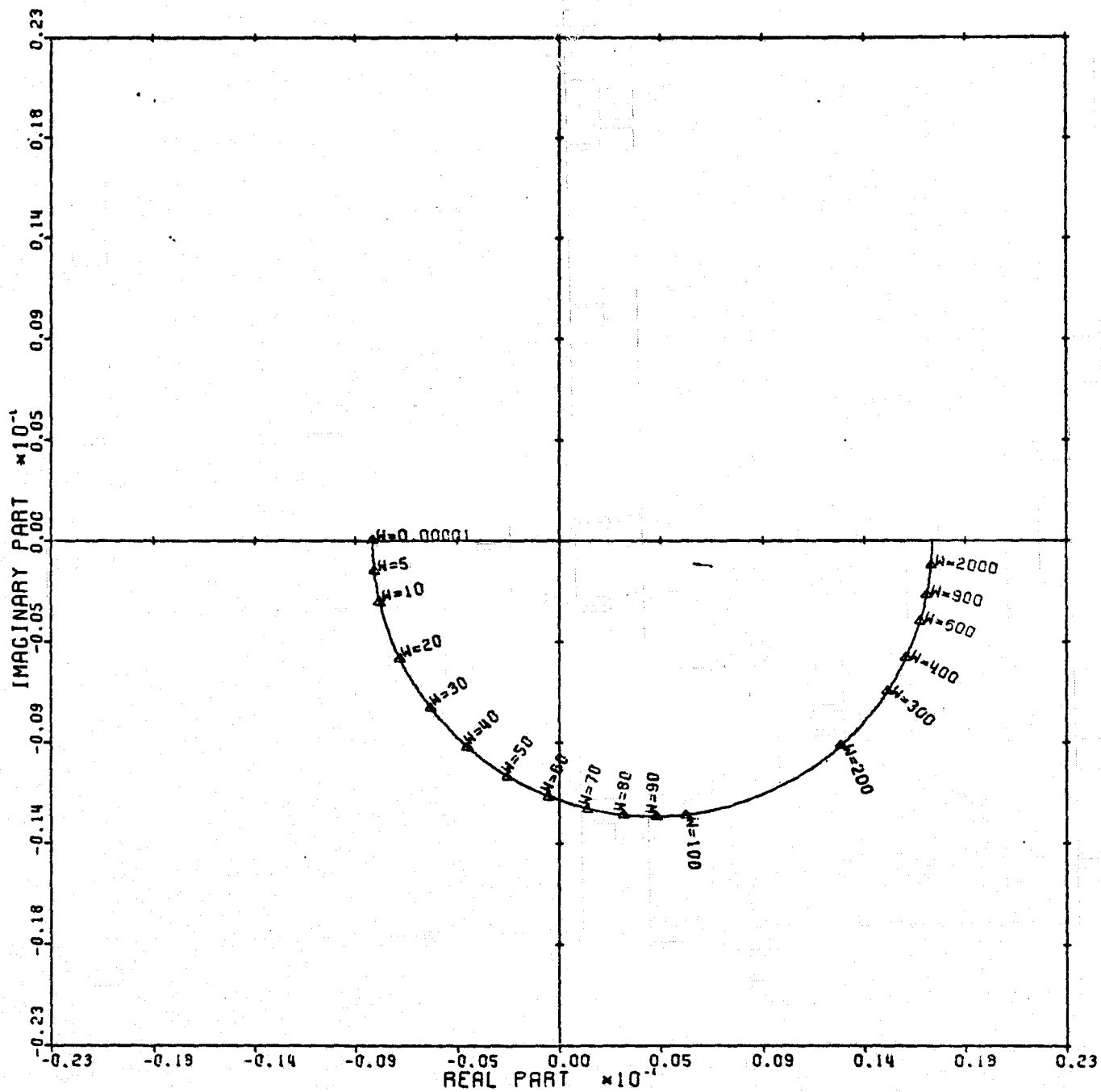
LOCUS OF CENTERS PLOT: 1,3 ENTRY: COLUMN SWITCH. 6/14/78.

INPUTS = 4, SYSTEM ORDER = 6, ANALYSIS TYPE = 2

Figure 27
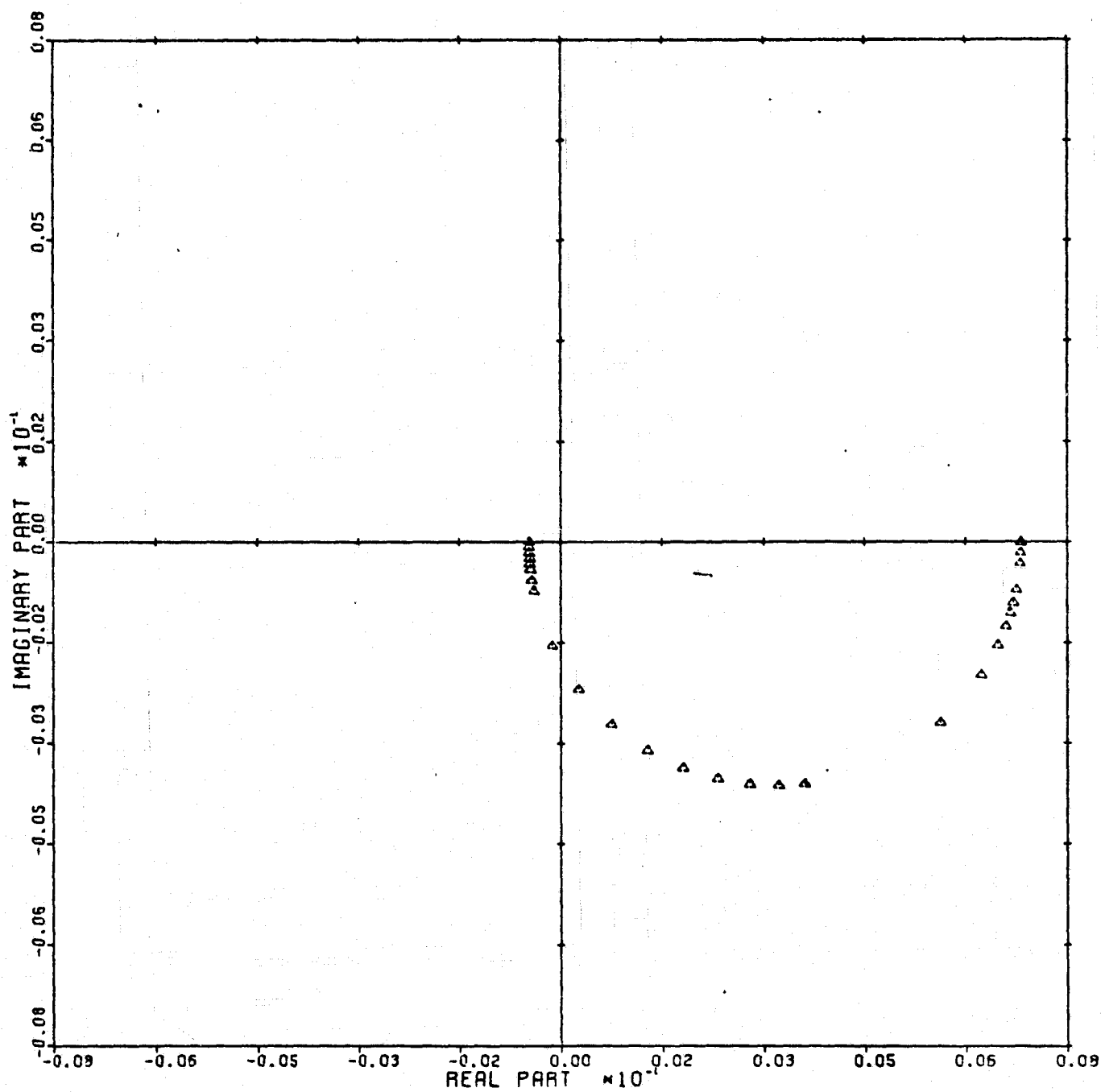
CARDIAD PLOT: 2.3 ENTRY: COLUMN SWITCH. 6/14/78.

INPUTS = 4, SYSTEM ORDER = 6, ANALYSIS TYPE = 2

Figure 28
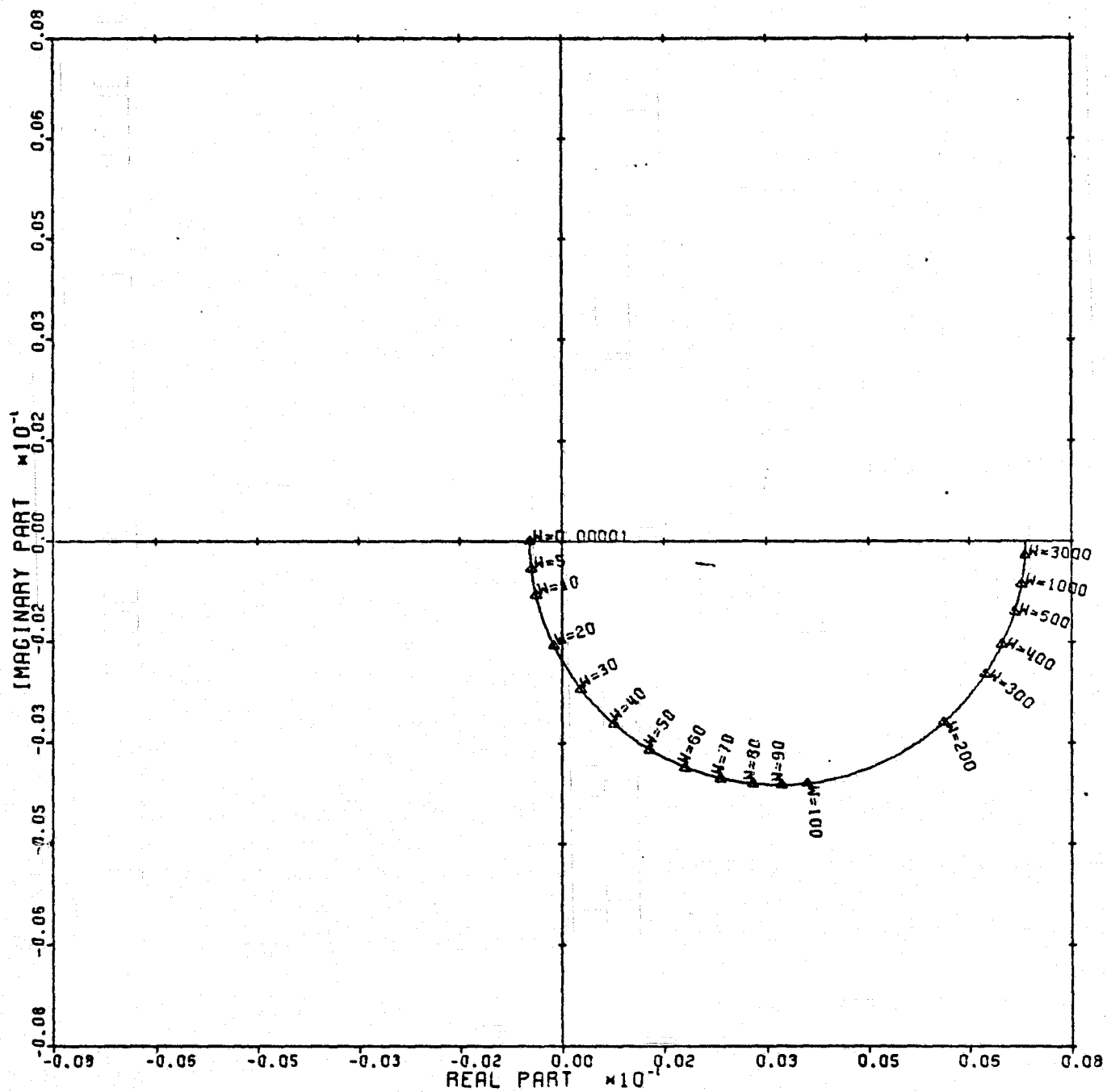
LOCUS OF CENTERS PLOT: 2,3 ENTRY: COLUMN SWITCH, 6/14/78.

INPUTS = 4, SYSTEM ORDER = 6, ANALYSIS TYPE = 2

Figure 29
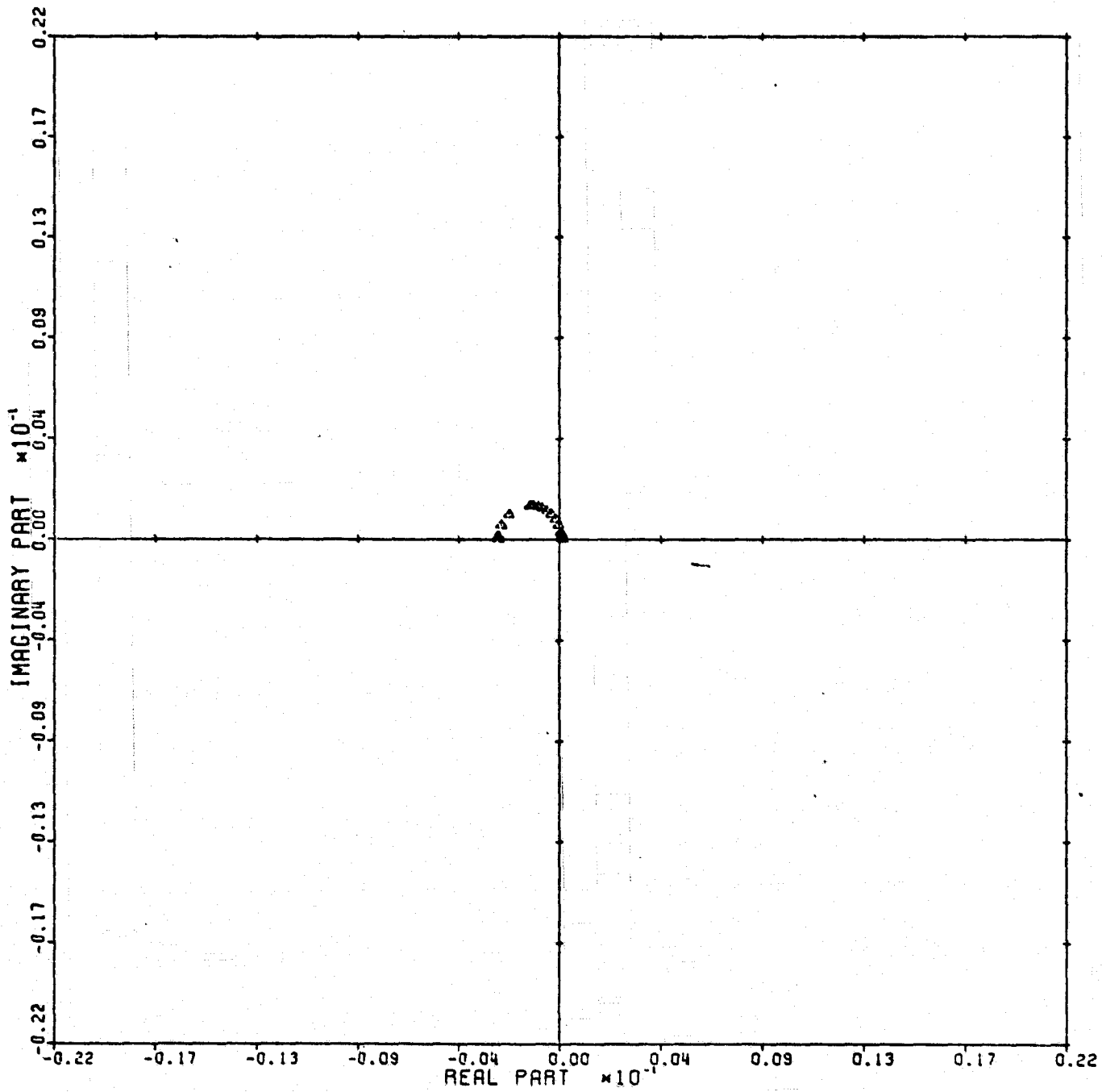
CARDIAO PLOT: 4,3 ENTRY: COLUMN SWITCH, 6/14/78.

INPUTS = 4, SYSTEM ORDER = 6, ANALYSIS TYPE = 2

Figure 30
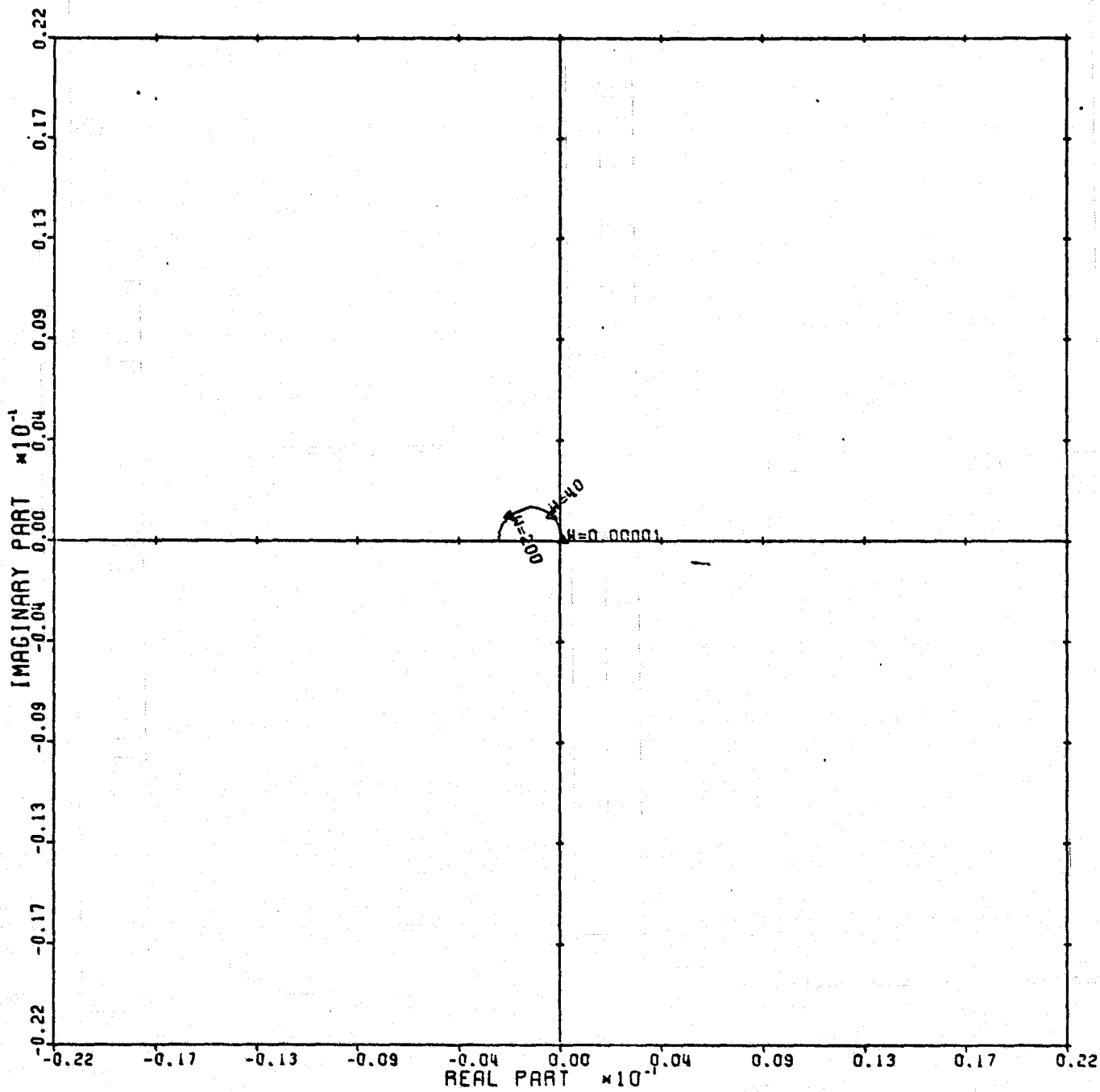
LOCUS OF CENTERS PLOT: 4.3 ENTRY: COLUMN SWITCH. 6/14/78.

INPUTS = 4, SYSTEM ORDER = 6, ANALYSIS TYPE = 2

Figure 31
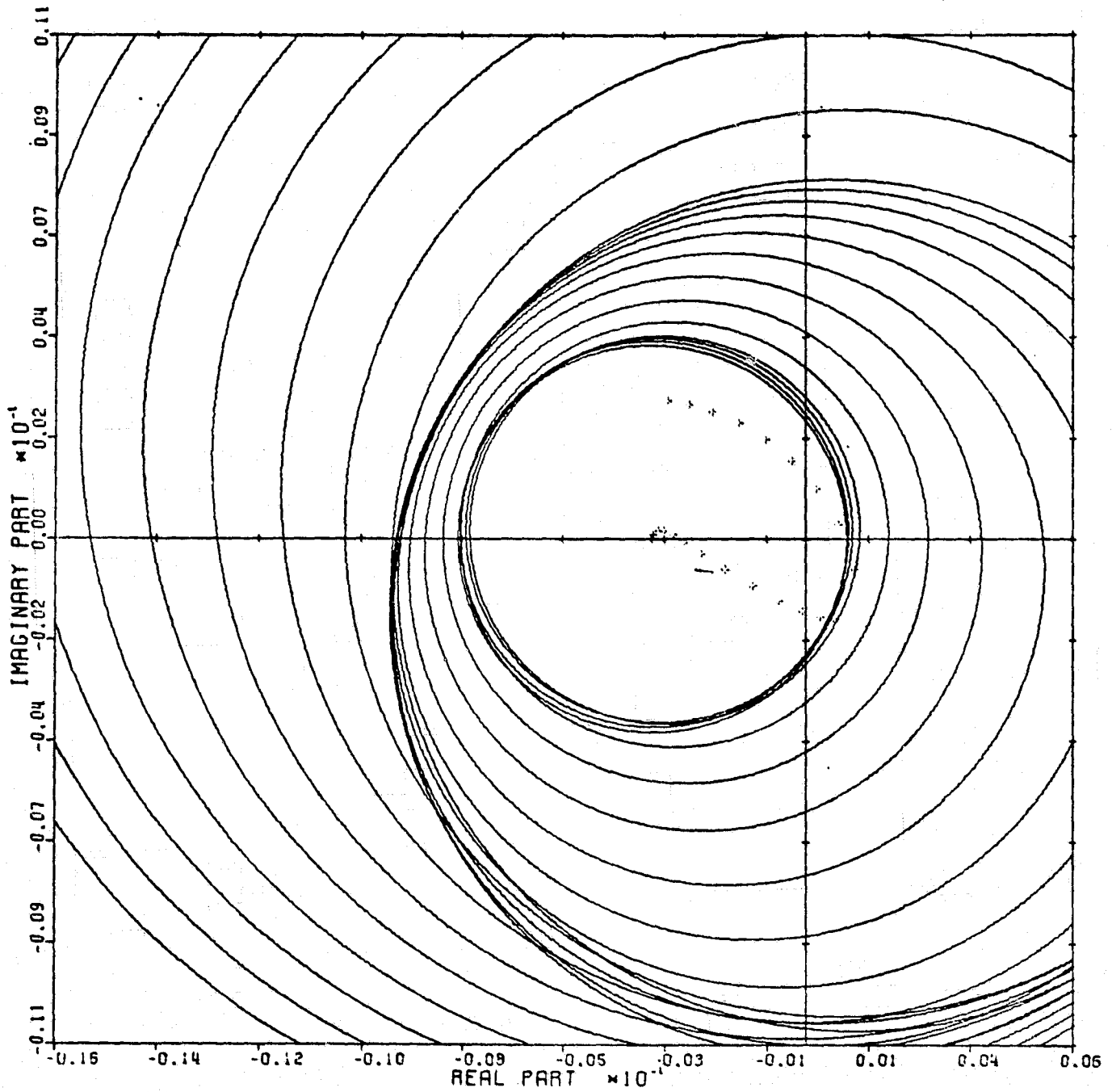
CARDIAO PLOT: 2.1 ENTRY: KMP3, 6/20/78.

INPUTS = 4, SYSTEM ORDER = 6, ANALYSIS TYPE = 1

Figure 32
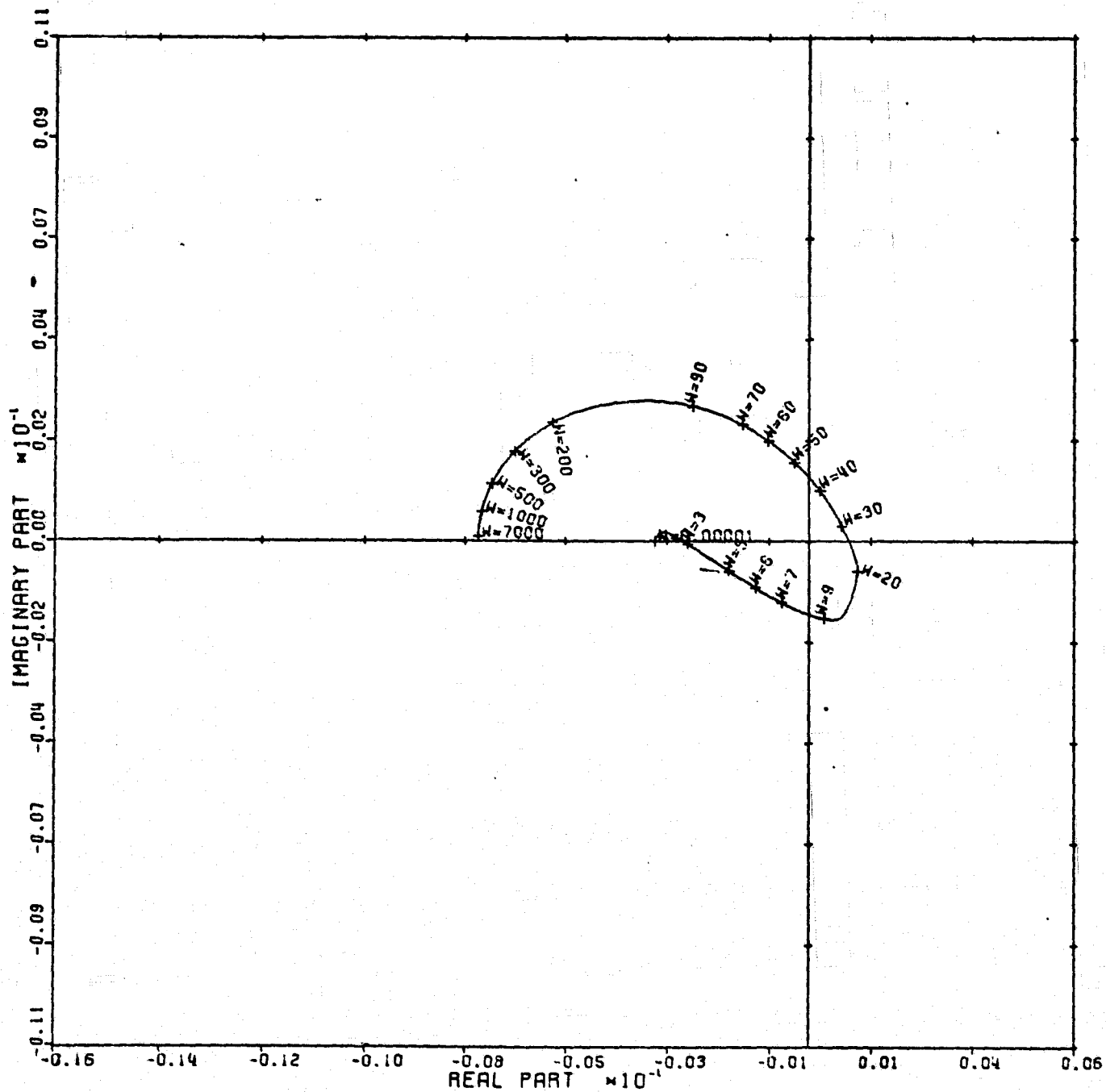
LOCUS OF CENTERS PLOT: 2.1 ENTRY: KMP3, 6/20/78.

INPUTS = 4, SYSTEM ORDER = 6, ANALYSIS TYPE = 1

Figure 33
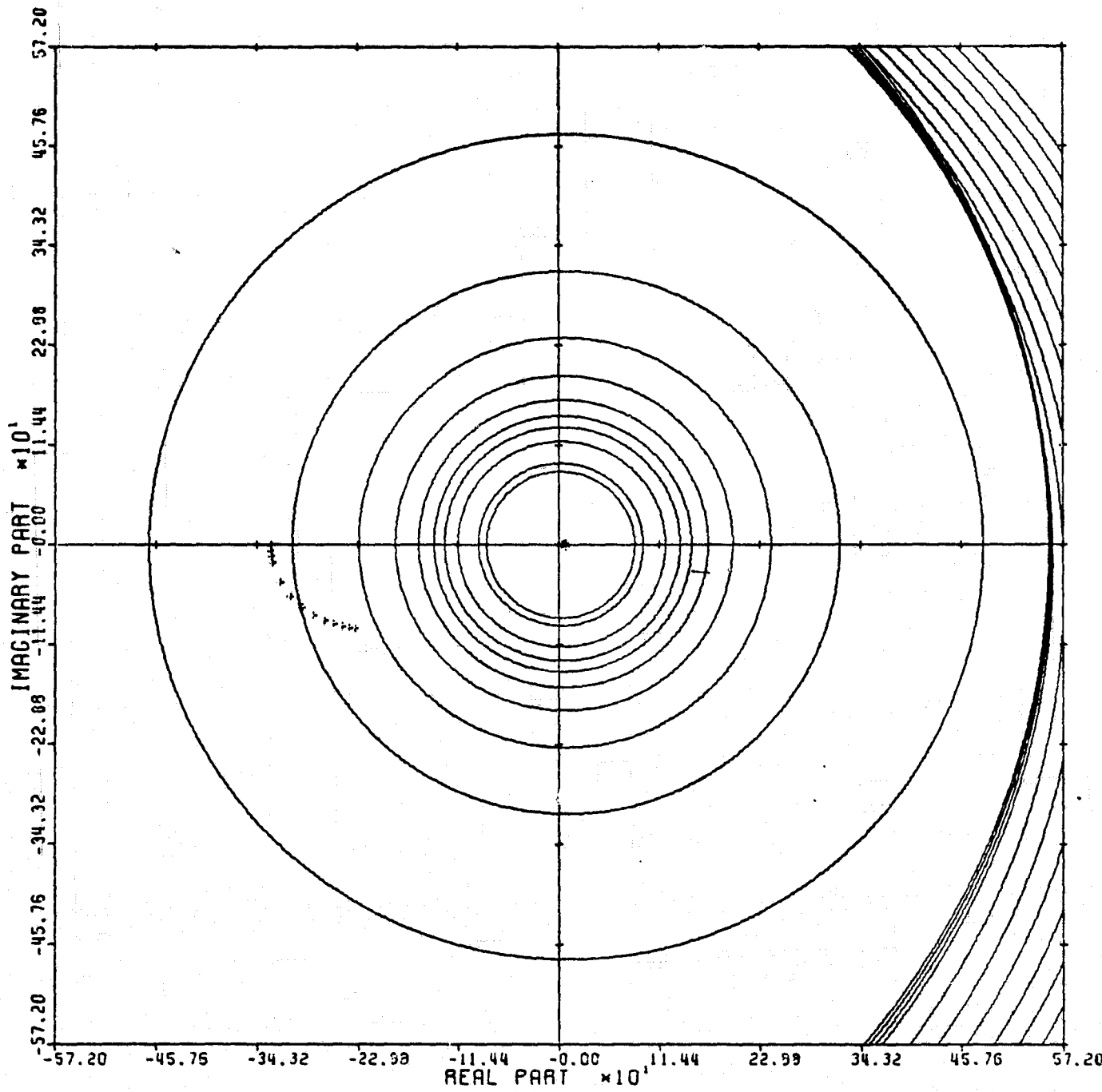
CARDIAD PLOT: 3.1 ENTRY: KMP3, 6/20/78.

INPUTS = 4, SYSTEM ORDER = 6, ANALYSIS TYPE = 1

Figure 34
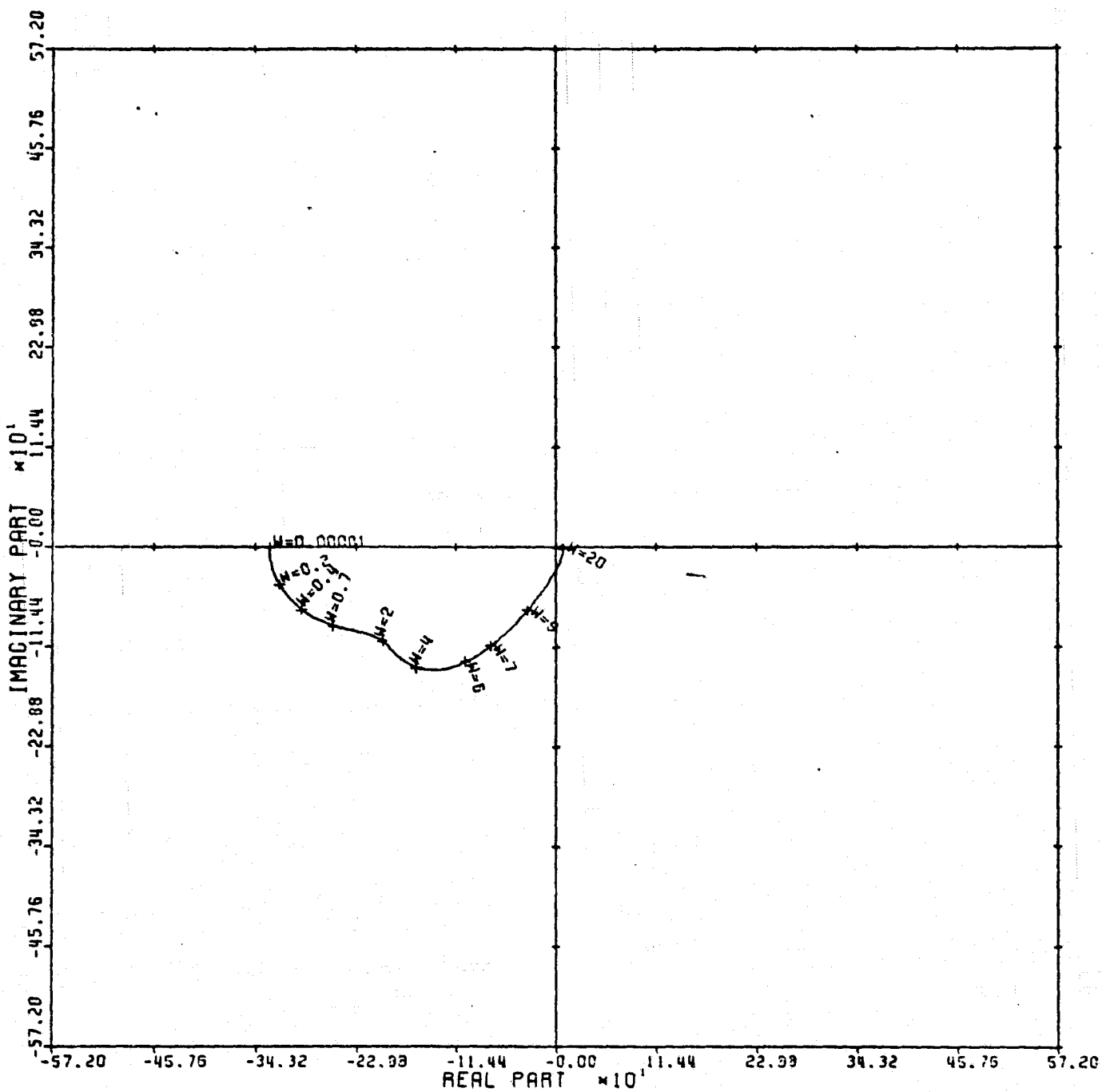
LOCUS OF CENTERS PLOT: 3,1 ENTRY: KMP3, 6/20/78.

INPUTS = 4, SYSTEM ORDER = 6, ANALYSIS TYPE = 1

Figure 35
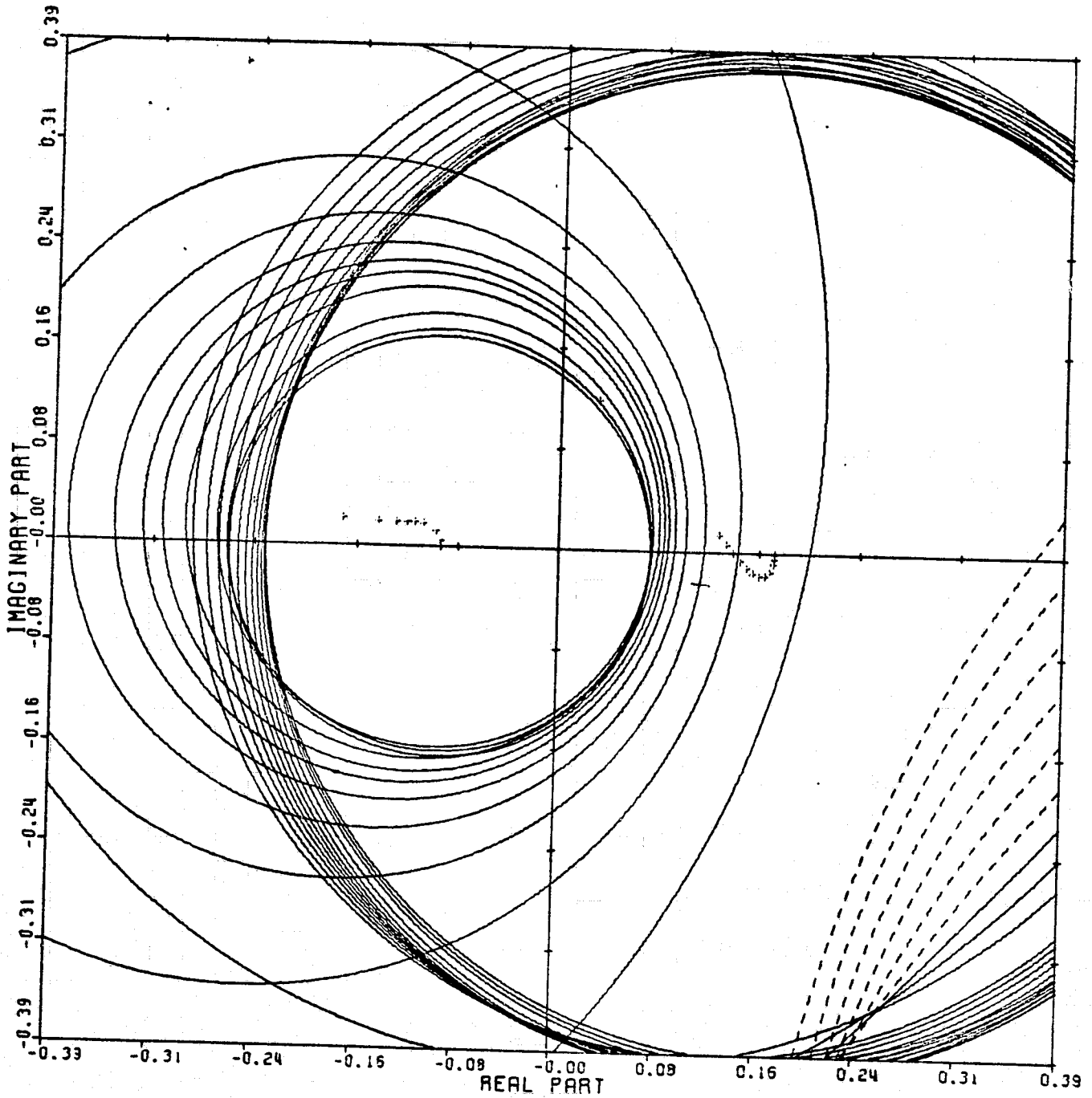
CARDIAD PLOT: 4,1 ENTRY: KMP3, 6/20/78.

INPUTS = 4, SYSTEM ORDER = 6, ANALYSIS TYPE = 1

Figure 36
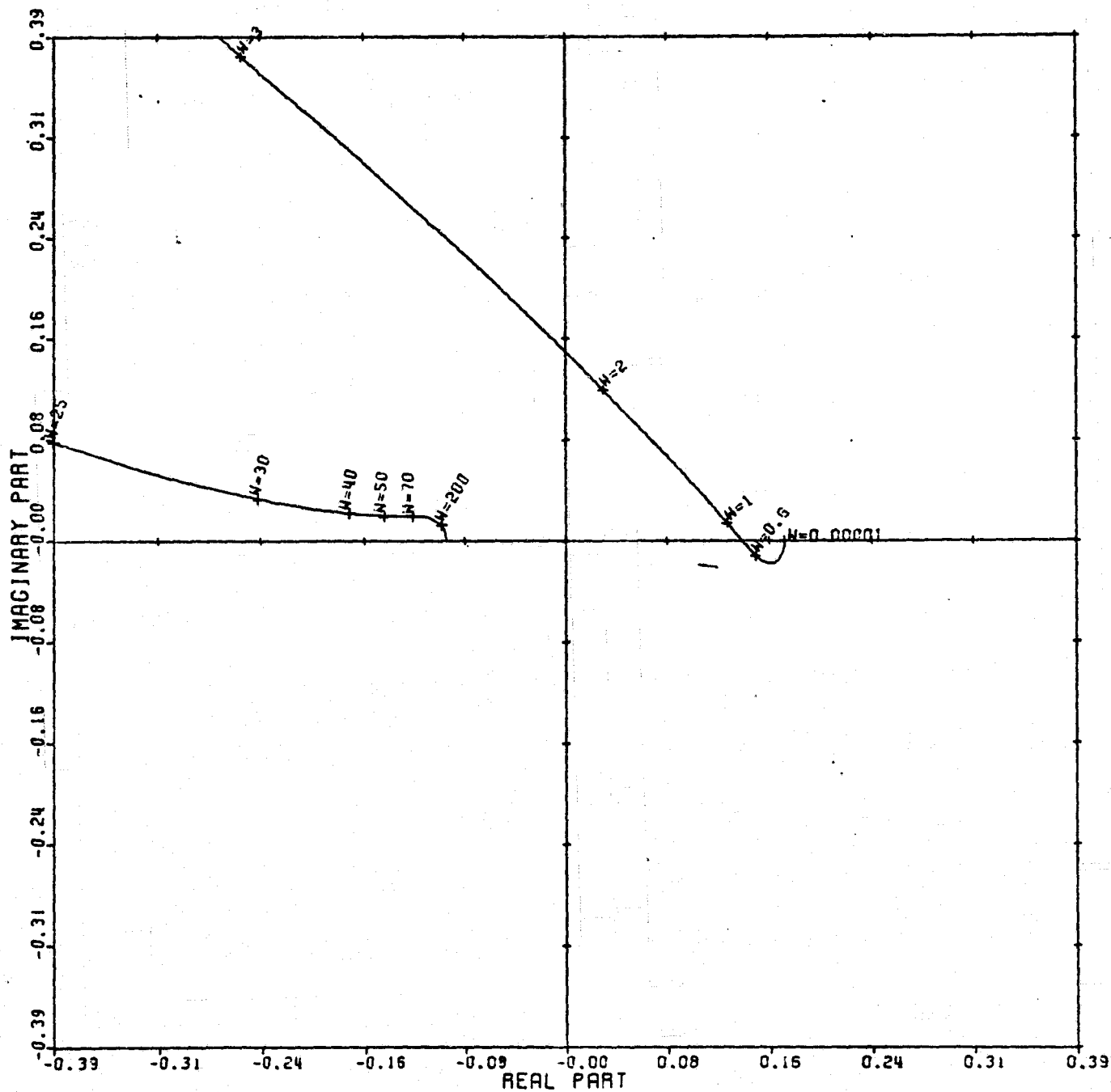
LOCUS OF CENTERS PLOT: 4.1 ENTRY: KMP3. 6/20/78.

INPUTS = 4. SYSTEM ORDER = 6. ANALYSIS TYPE = 1

Figure 37
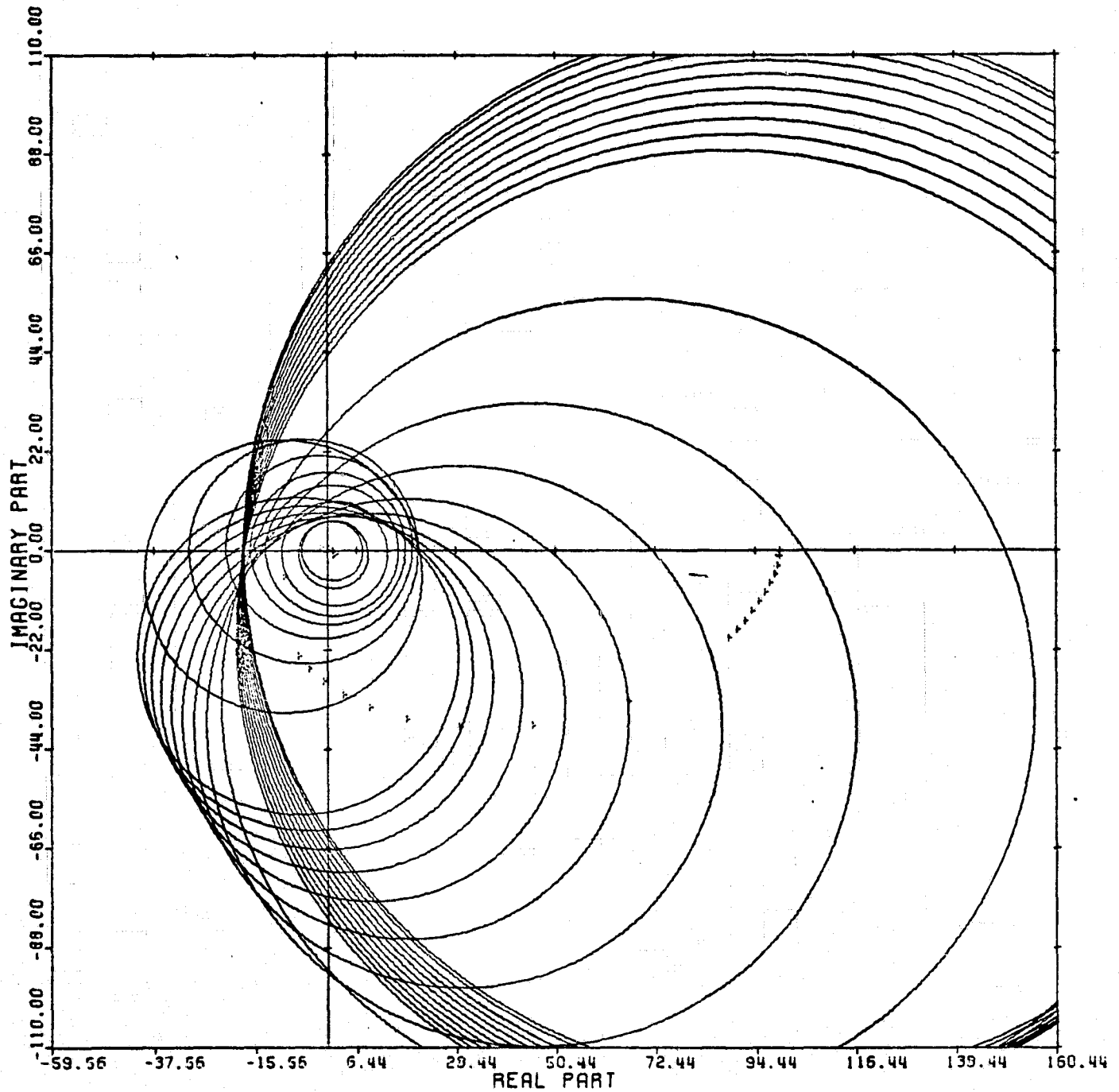
CARDIAD PLOT: 1,2 ENTRY: KMP3. 6/20/78.

INPUTS = 4, SYSTEM ORDER = 6, ANALYSIS TYPE = 1

Figure 38
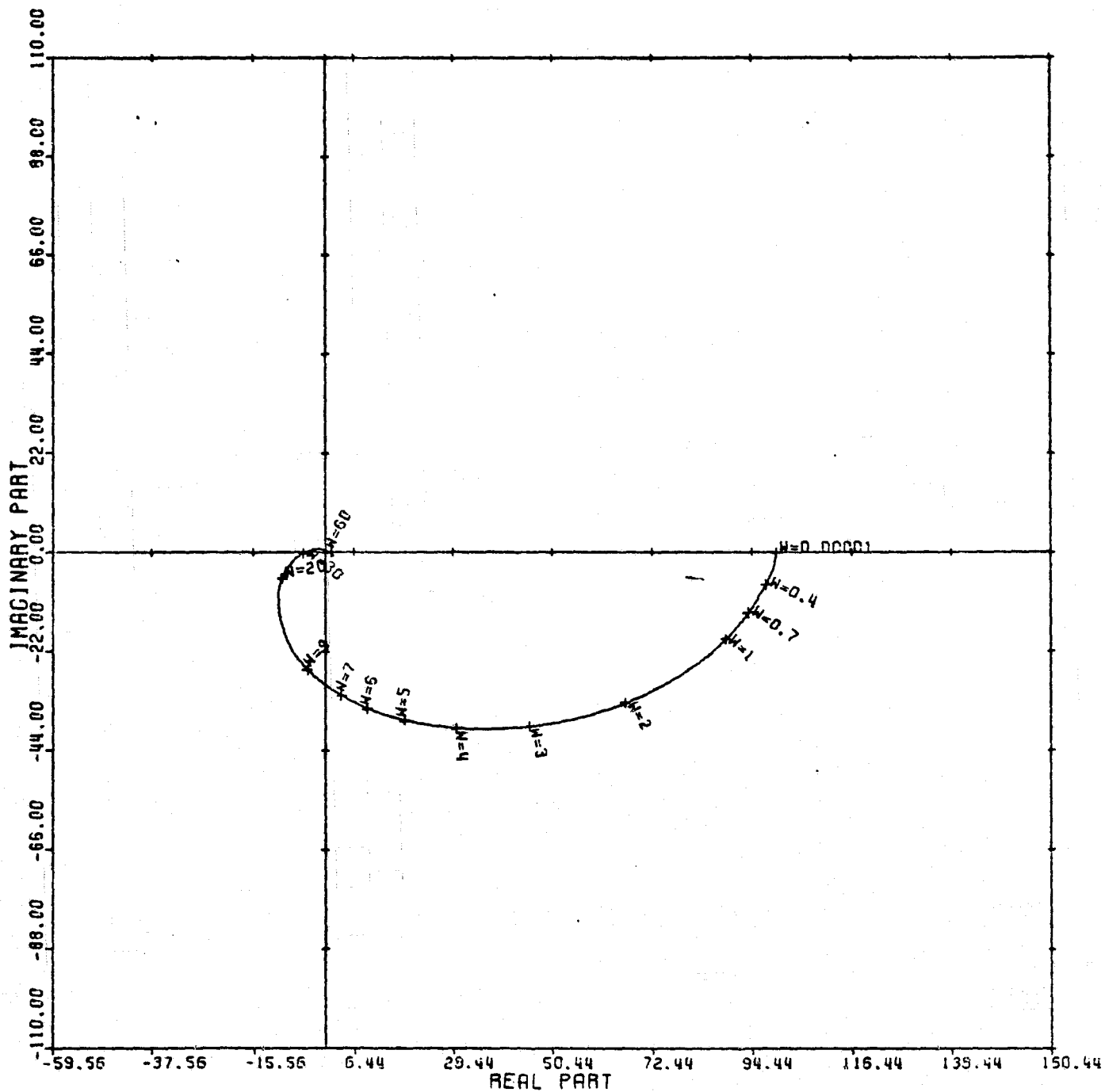
LOCUS OF CENTERS PLOT: 1,2 ENTRY: KMP3, 6/20/78.

INPUTS = 4, SYSTEM ORDER = 6, ANALYSIS TYPE = 1

Figure 39
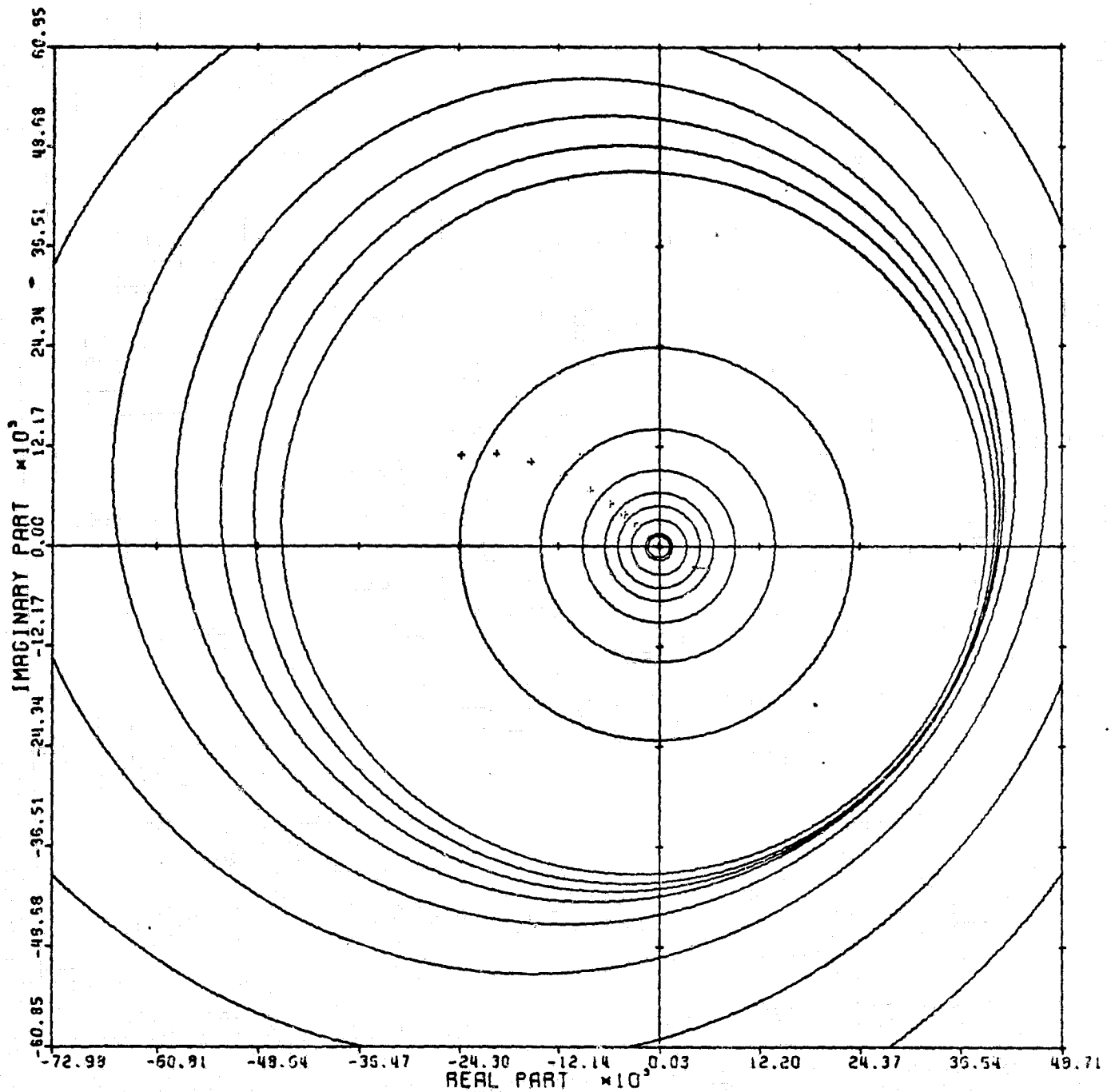
CARDIAD PLOT: 3.2 ENTRY: KMP3, 6/20/78.

INPUTS = 4, SYSTEM ORDER = 6, ANALYSIS TYPE = 1

Figure 40
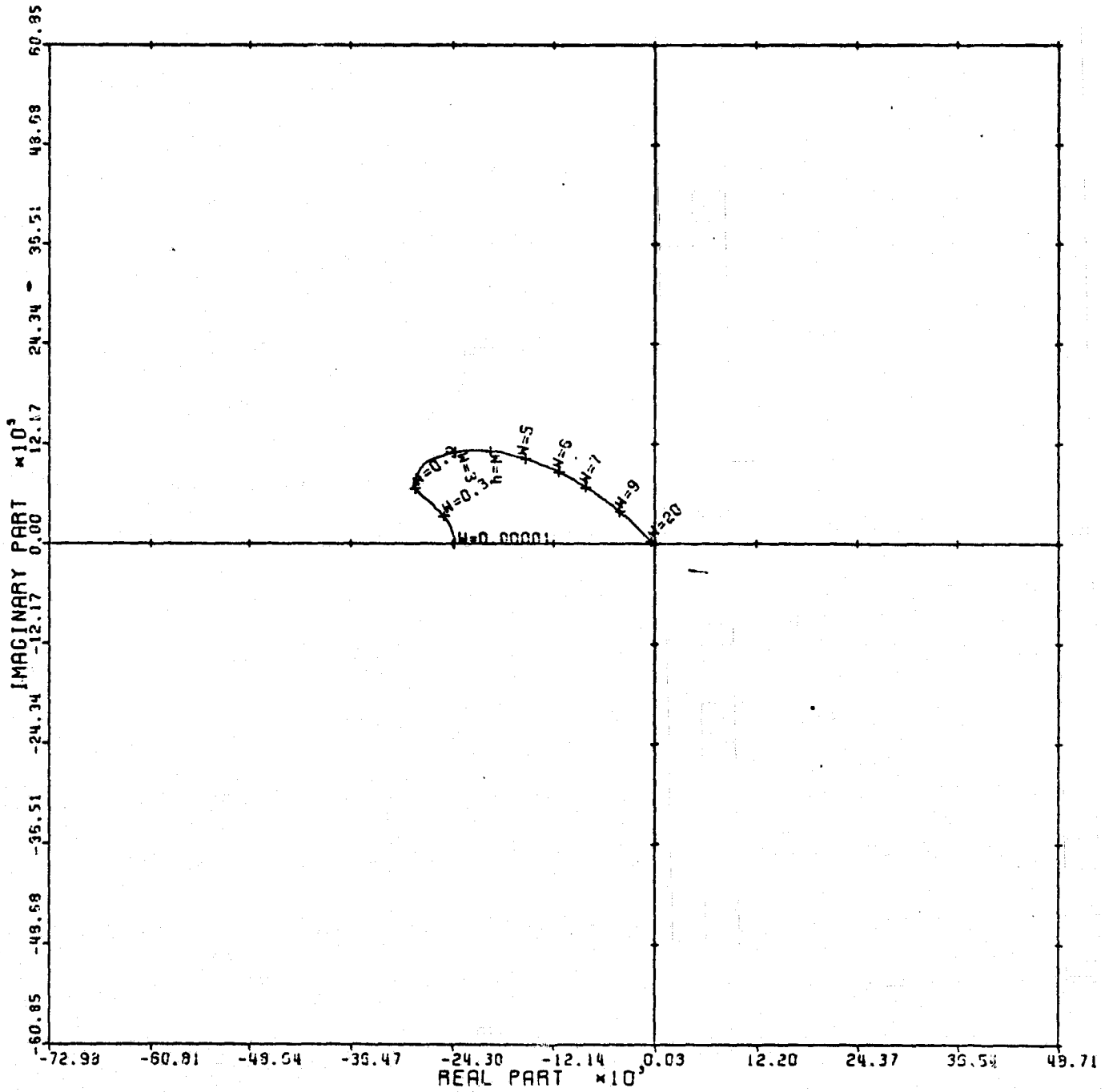
LOCUS OF CENTERS PLOT: 3.2 ENTRY: KMP3, 6/20/78.

INPUTS = 4, SYSTEM ORDER = 6, ANALYSIS TYPE = 1

Figure 41
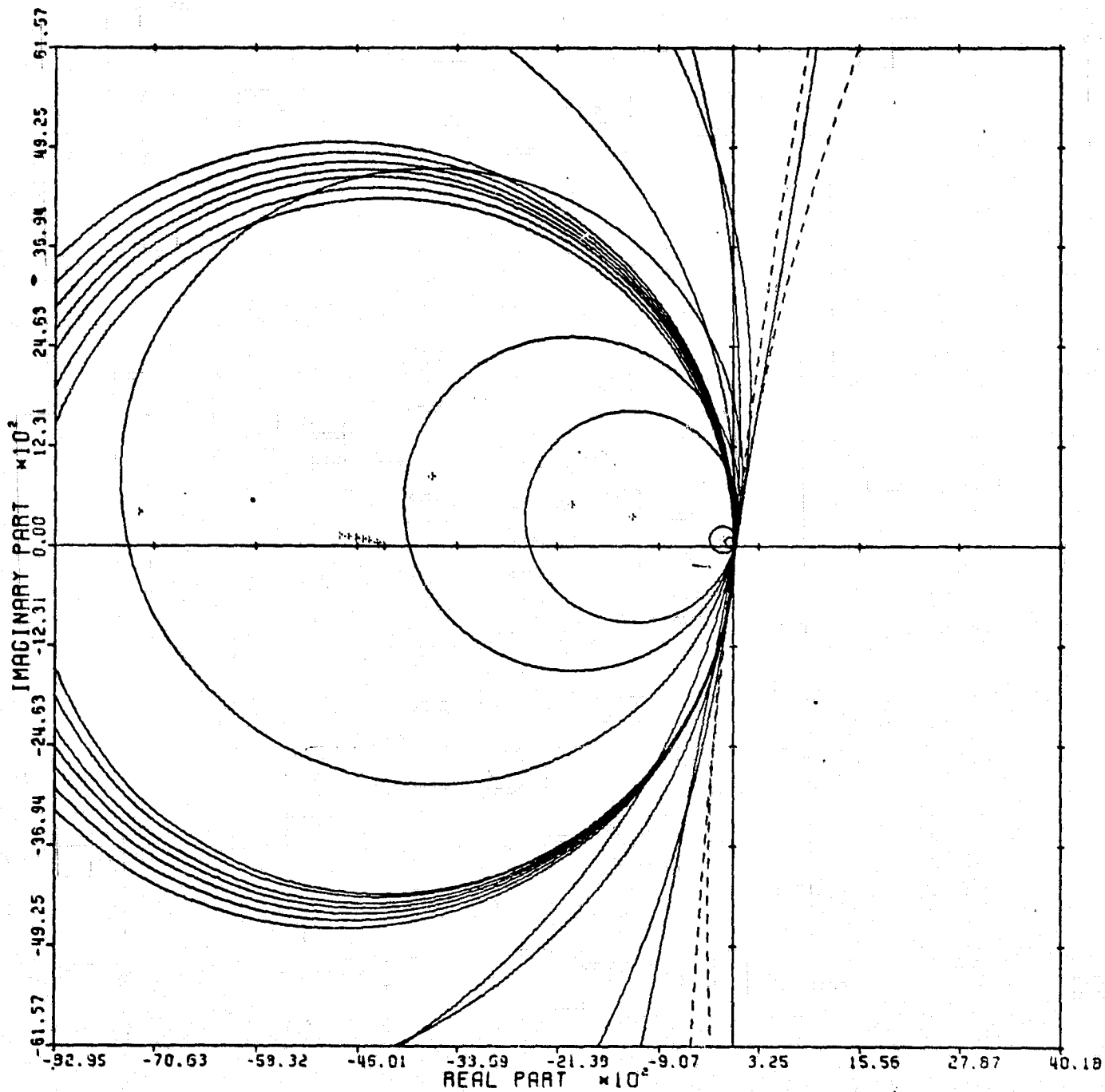
CARDIAD PLOT: 4,2 ENTRY: KMP3, 6/20/78.

INPUTS = 4, SYSTEM ORDER = 6, ANALYSIS TYPE = 1

Figure 42
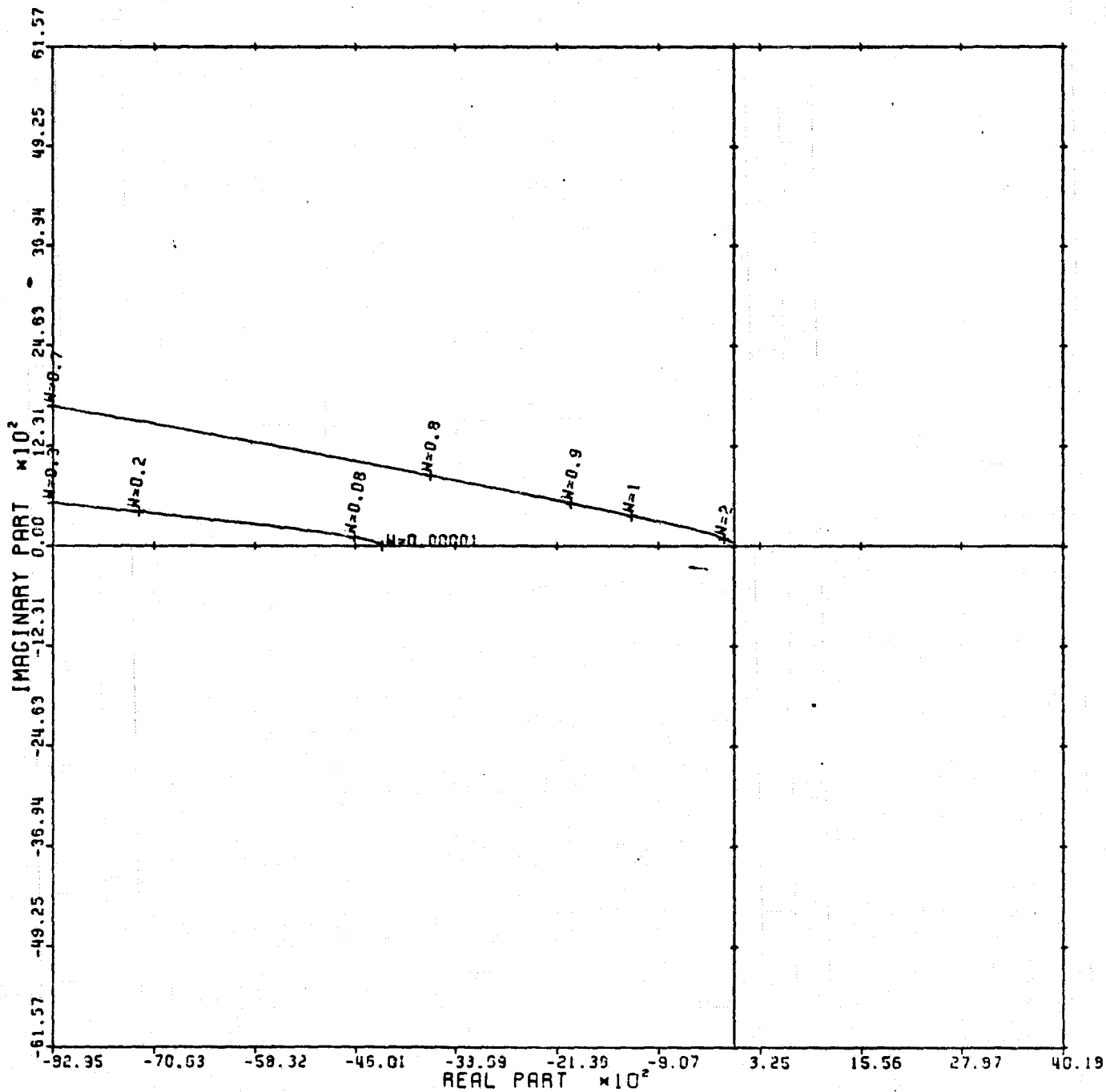
LOCUS OF CENTERS PLOT: 4.2 ENTRY: KMP3. 6/20/78.

INPUTS = 4, SYSTEM ORDER = 6. ANALYSIS TYPE = 1

Figure 43
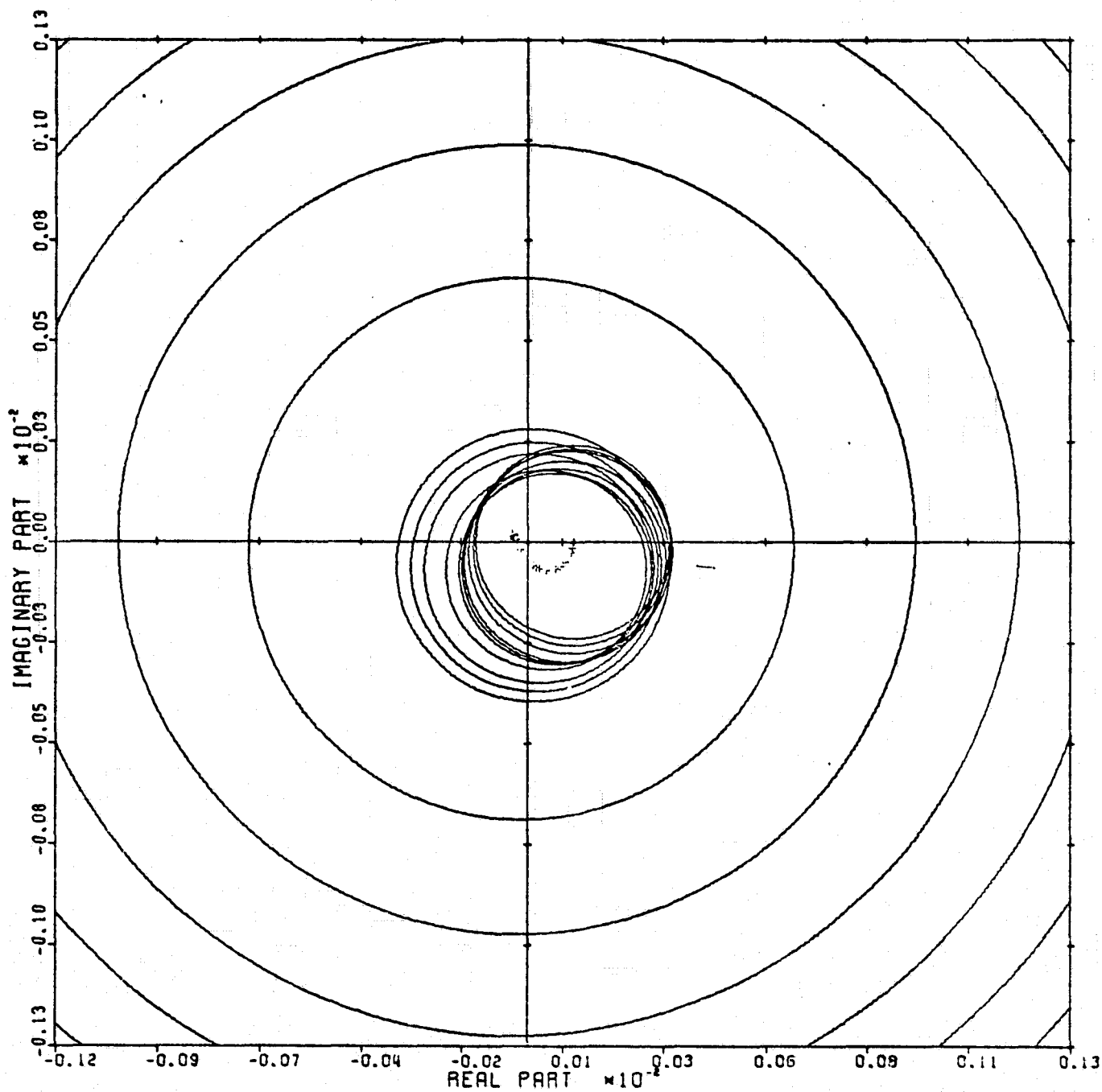
CARDIAD PLOT: 1,3 ENTRY: KMP3, 6/20/78.

INPUTS = 4, SYSTEM ORDER = 6, ANALYSIS TYPE = 1

Figure 44
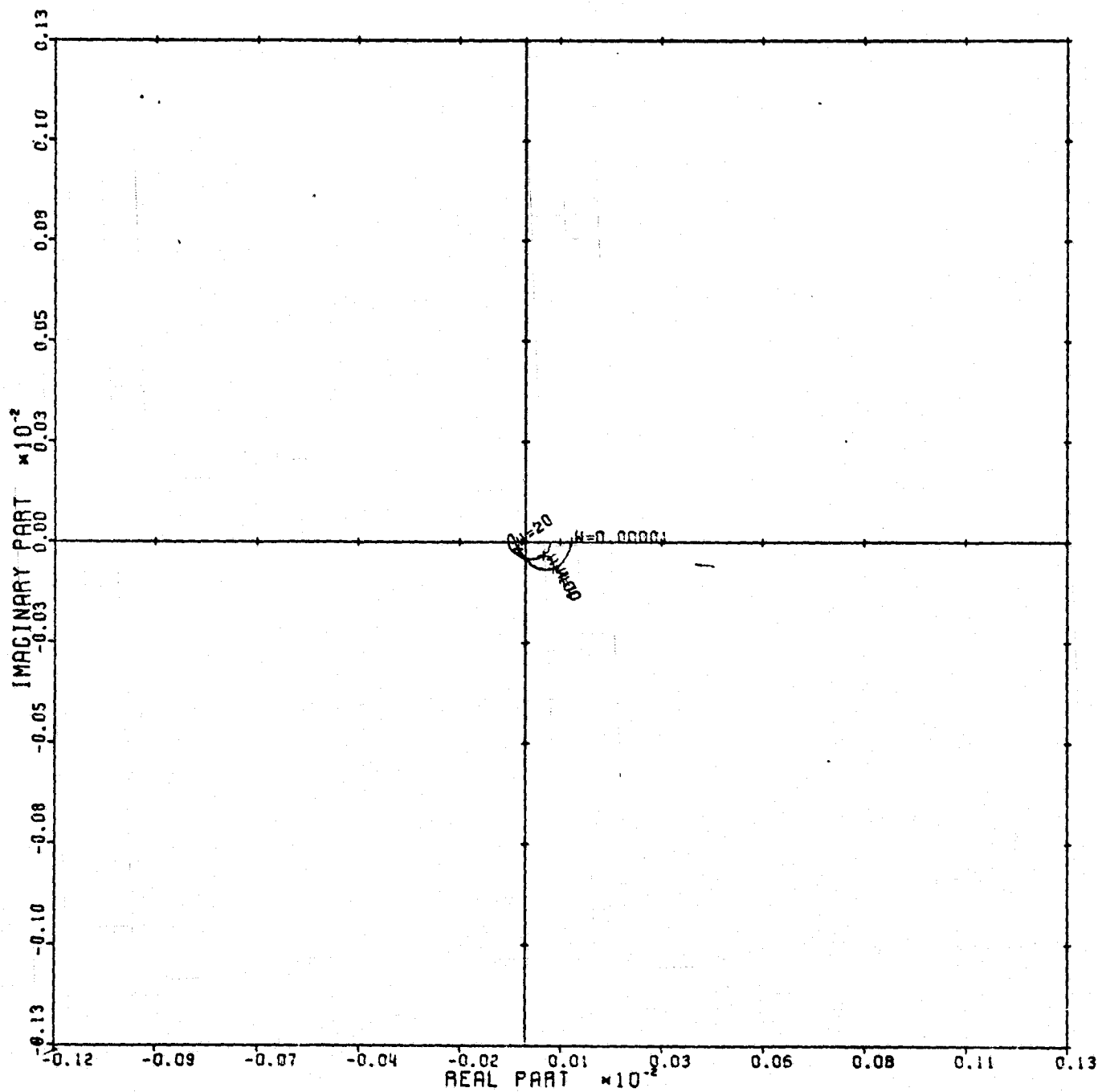
LOCUS OF CENTERS PLOT: 1,3 ENTRY: KMP3, 6/20/78.

INPUTS = 4, SYSTEM ORDER = 6, ANALYSIS TYPE = 1

Figure 45
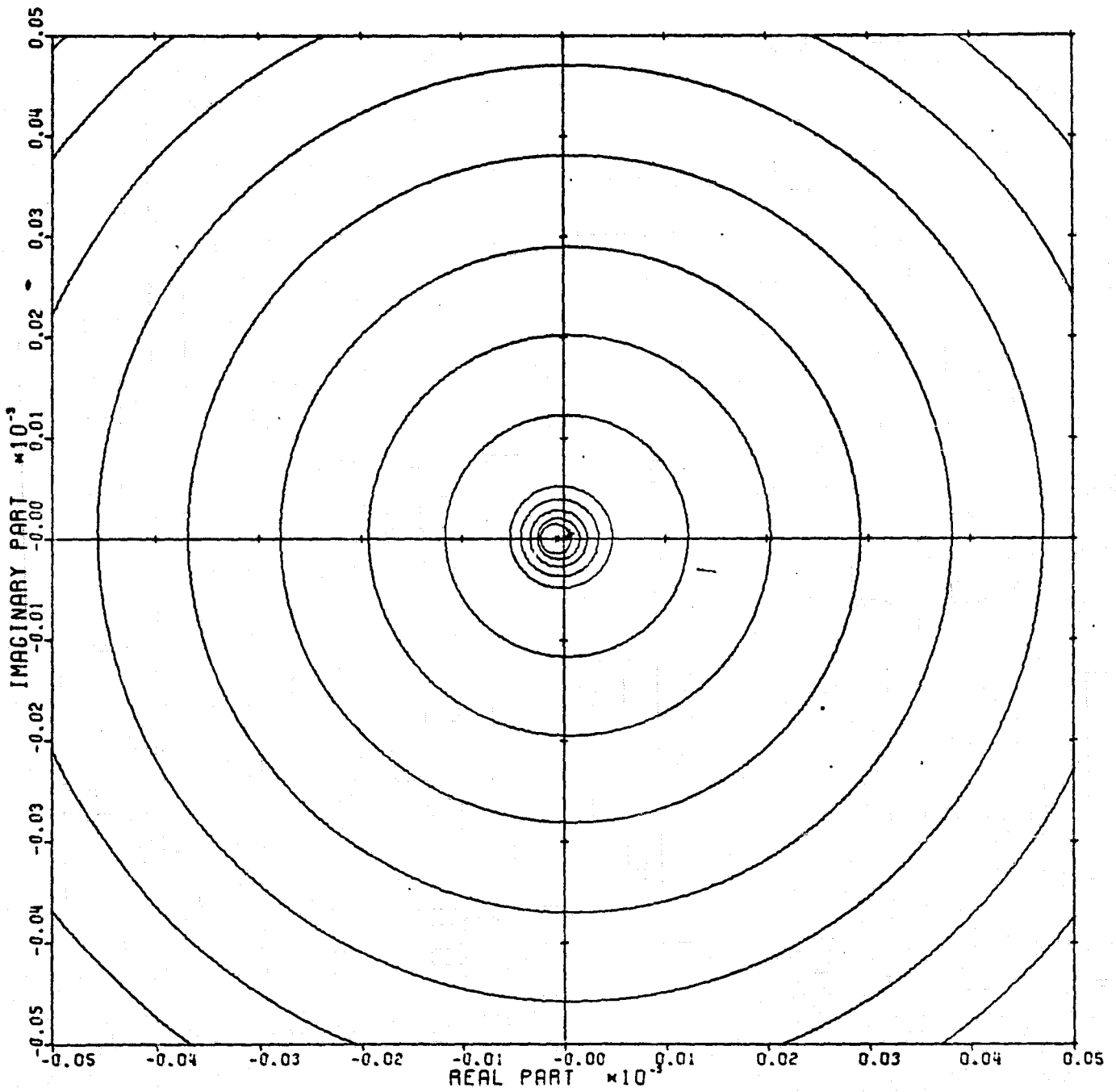
CARDIAD PLOT: 2,3 ENTRY: KMP3, 6/20/78.

INPUTS = 4, SYSTEM ORDER = 6, ANALYSIS TYPE = 1

Figure 46
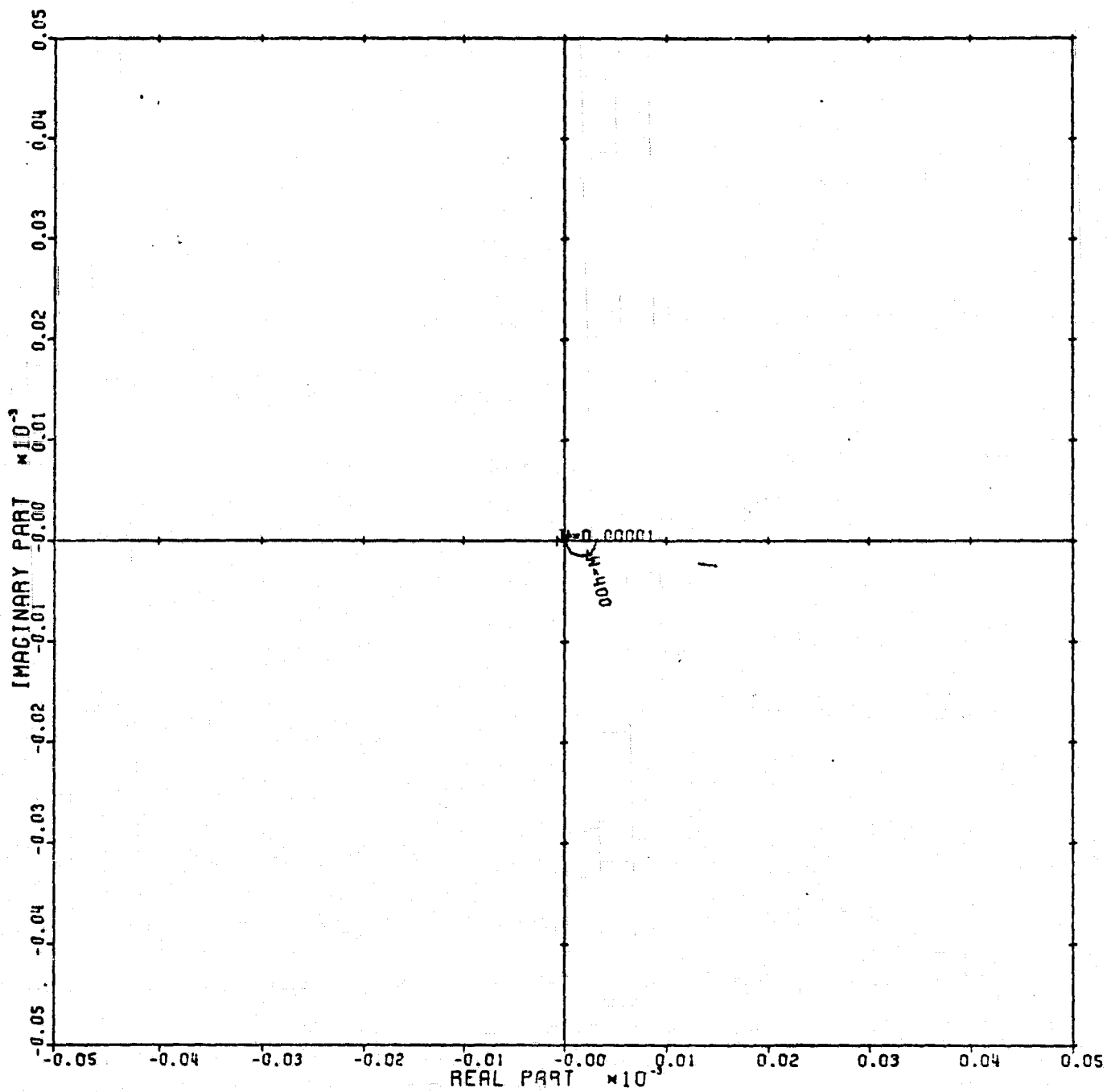
LOCUS OF CENTERS PLOT: 2.3 ENTRY: KMP3, 6/20/78.

INPUTS = 4, SYSTEM ORDER = 6, ANALYSIS TYPE = 1

Figure 47
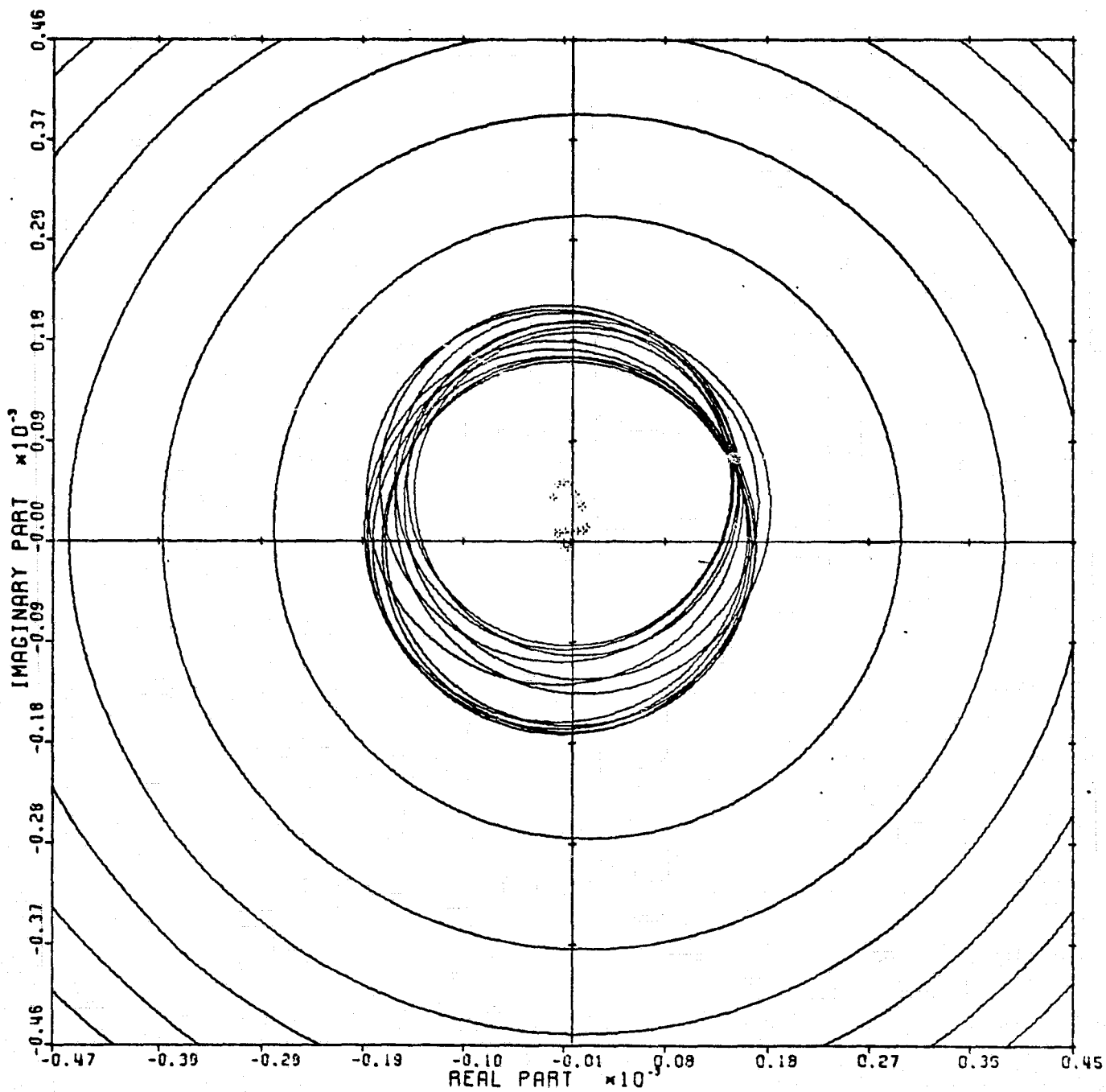
CARDIAD PLOT: 4,3 ENTRY: KMP3, 6/20/78.

INPUTS = 4, SYSTEM ORDER = 6, ANALYSIS TYPE = 1

Figure 48
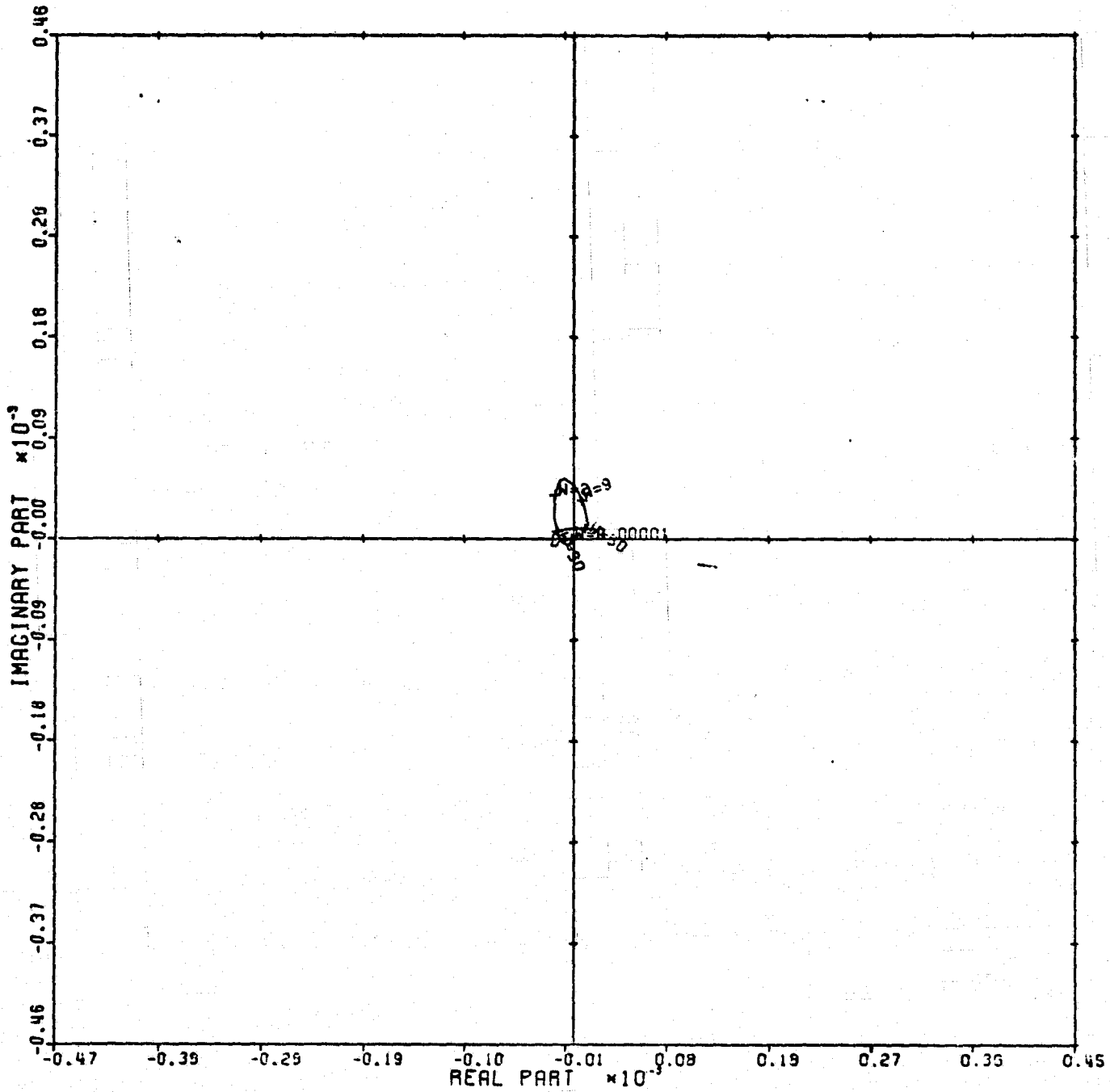
LOCUS OF CENTERS PLOT: 4,3 ENTRY: KMP3, 6/20/78.

INPUTS = 4, SYSTEM ORDER = 6, ANALYSIS TYPE = 1

Figure 49
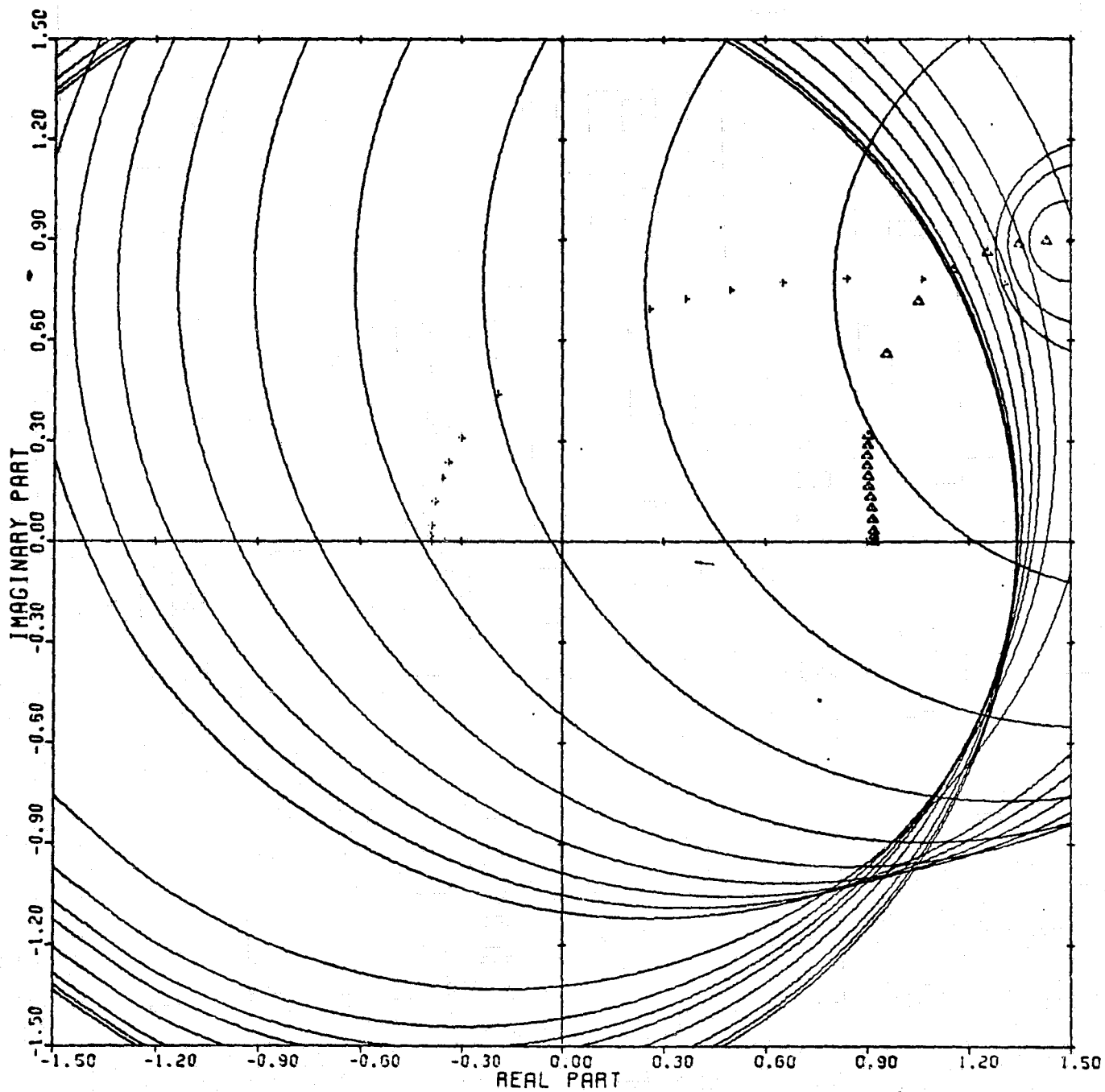
CARDIAD PLOT: 1,4 ENTRY: KMP3, 6/20/78.

INPUTS = 4, SYSTEM ORDER = 6, ANALYSIS TYPE = 1

Figure 50
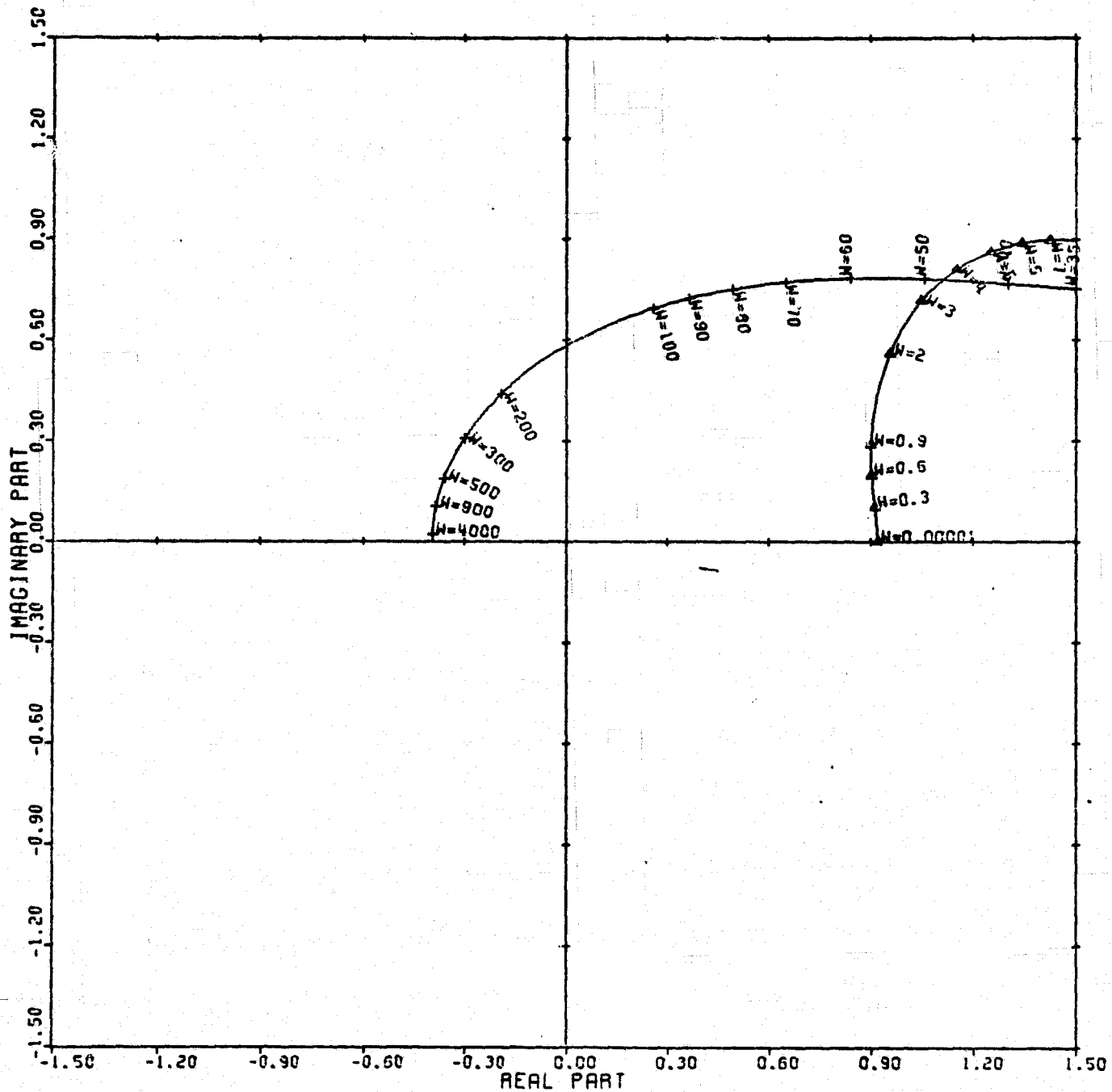
LOCUS OF CENTERS PLOT: 1.4 ENTRY: KMP3, 6/20/78.

INPUTS = 4, SYSTEM ORDER = 6, ANALYSIS TYPE = 1

Figure 51
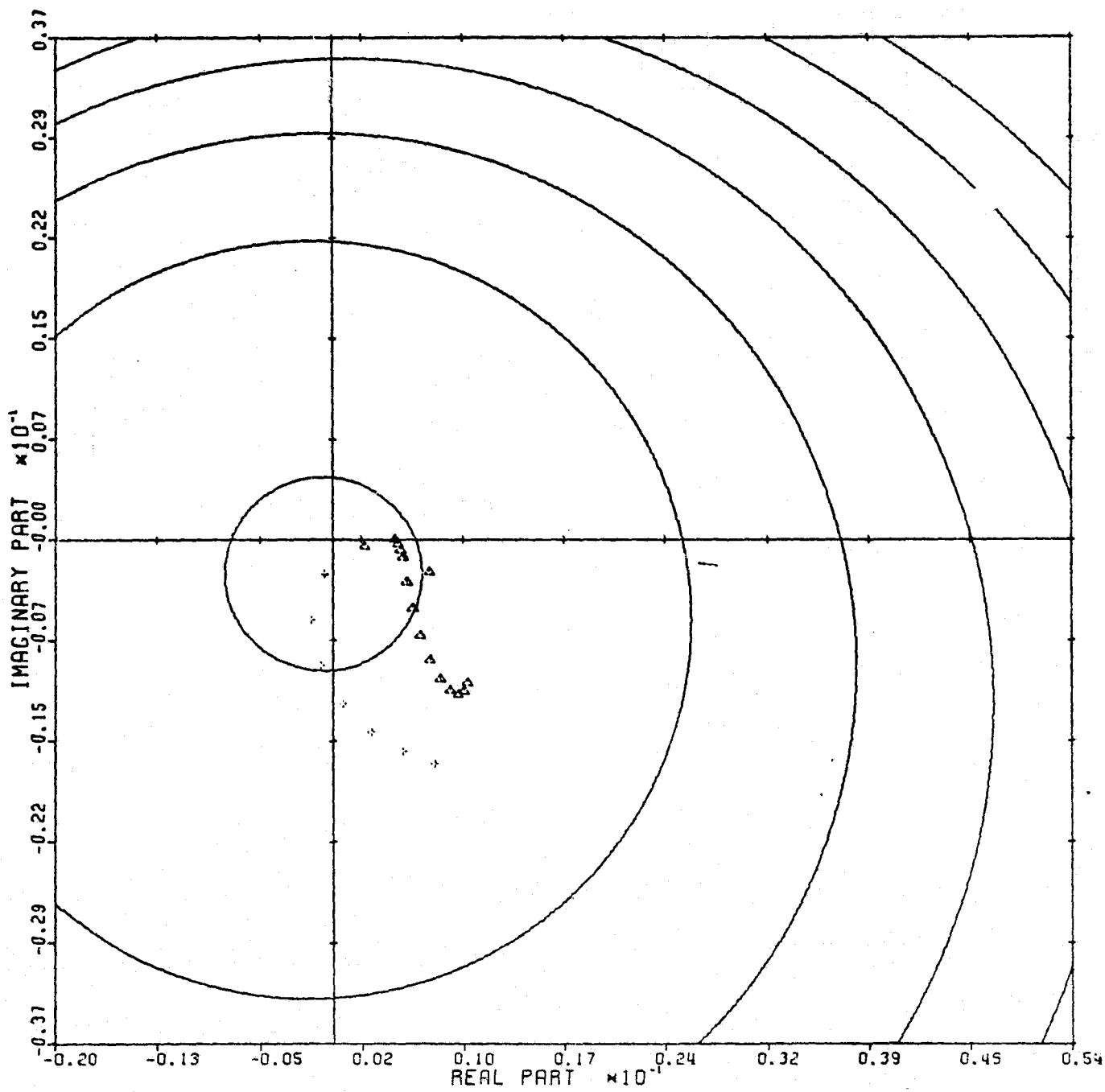
CARDIAD PLOT: 2.4 ENTRY: KMP3, 6/20/78.

INPUTS = 4, SYSTEM ORDER = 6, ANALYSIS TYPE = 1

Figure 52
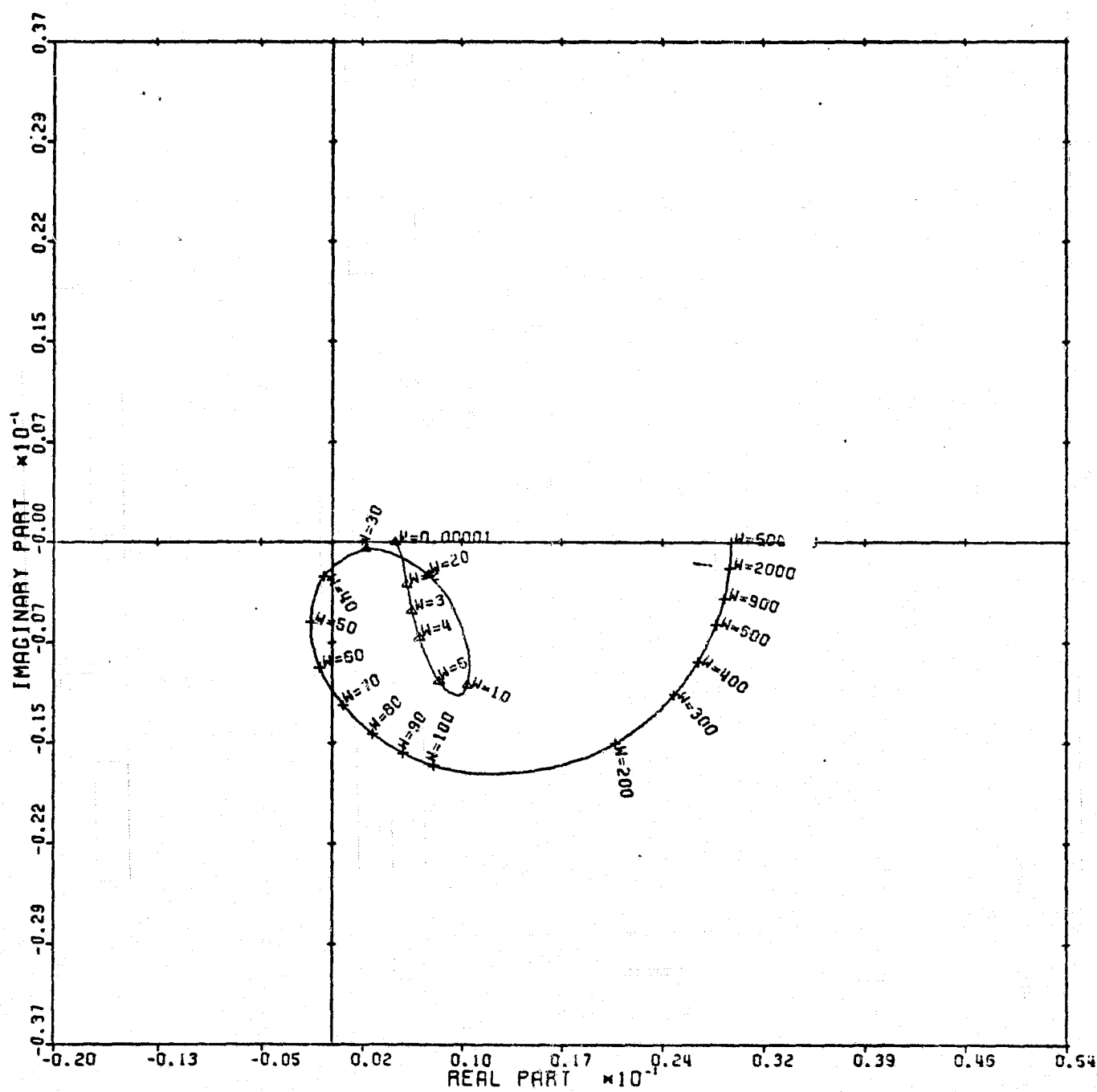
LOCUS OF CENTERS PLOT: 2.4 ENTRY: KMP3. 6/20/78.

INPUTS = 4, SYSTEM ORDER = 6, ANALYSIS TYPE = 1

Figure 53
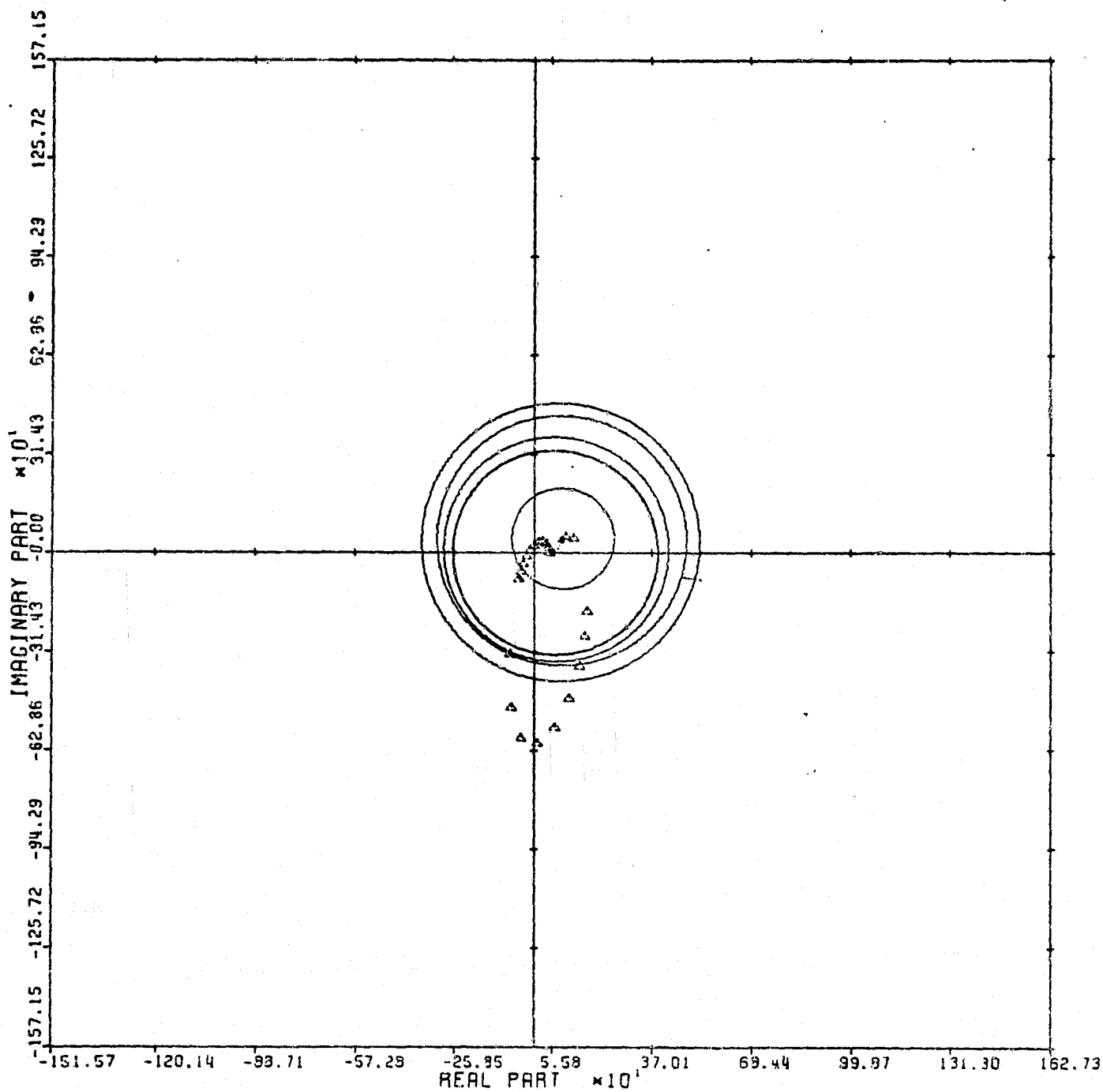
CARDIAD PLOT: 3,4 ENTRY: KMP3, 6/20/78.

INPUTS = 4, SYSTEM ORDER = 6, ANALYSIS TYPE = 1

Figure 54
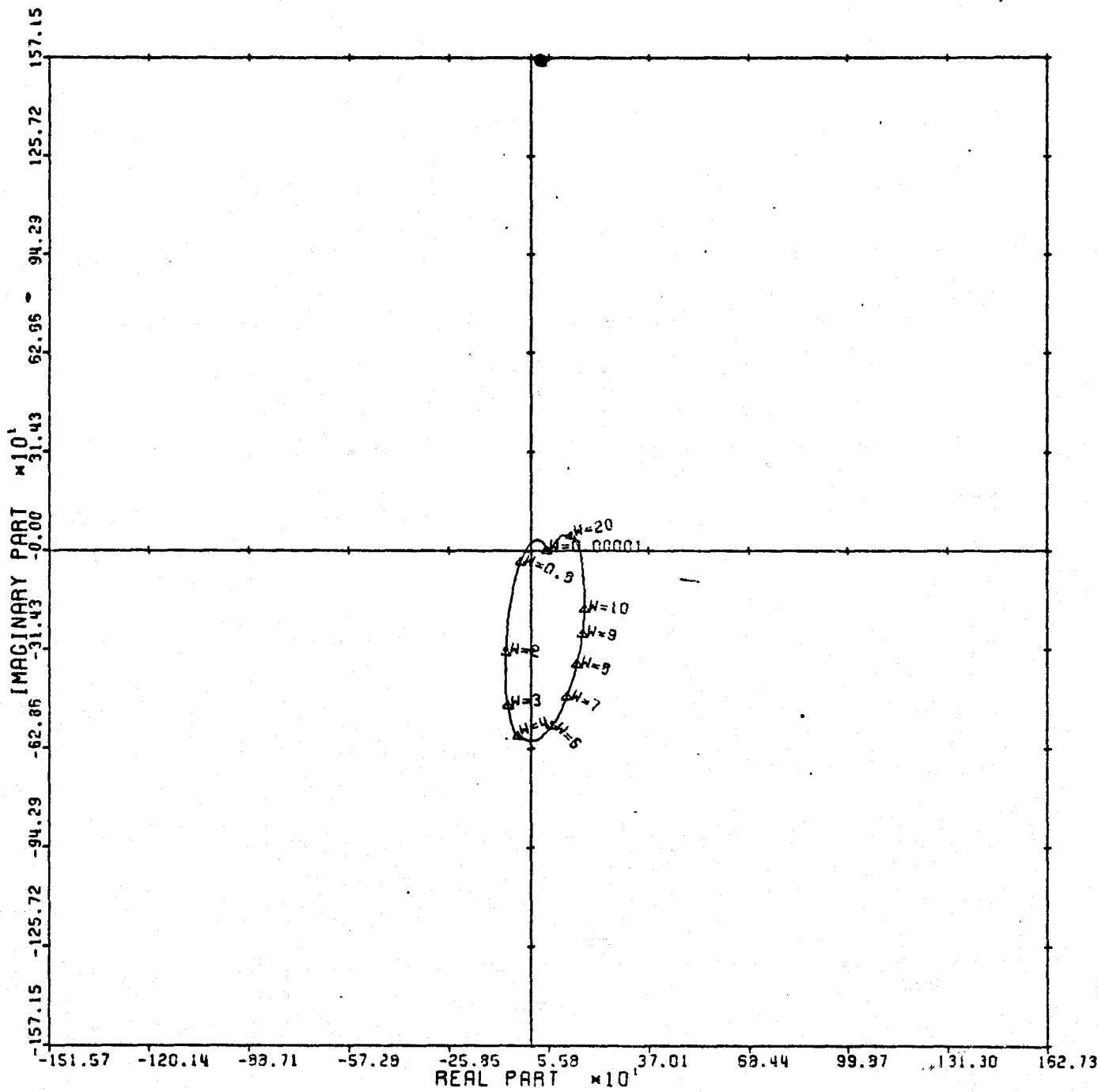
LOCUS OF CENTERS PLOT: 3.4 ENTRY: KMP3. 6/20/78.

INPUTS = 4, SYSTEM ORDER = 6, ANALYSIS TYPE = 1

C-2

Figure 55
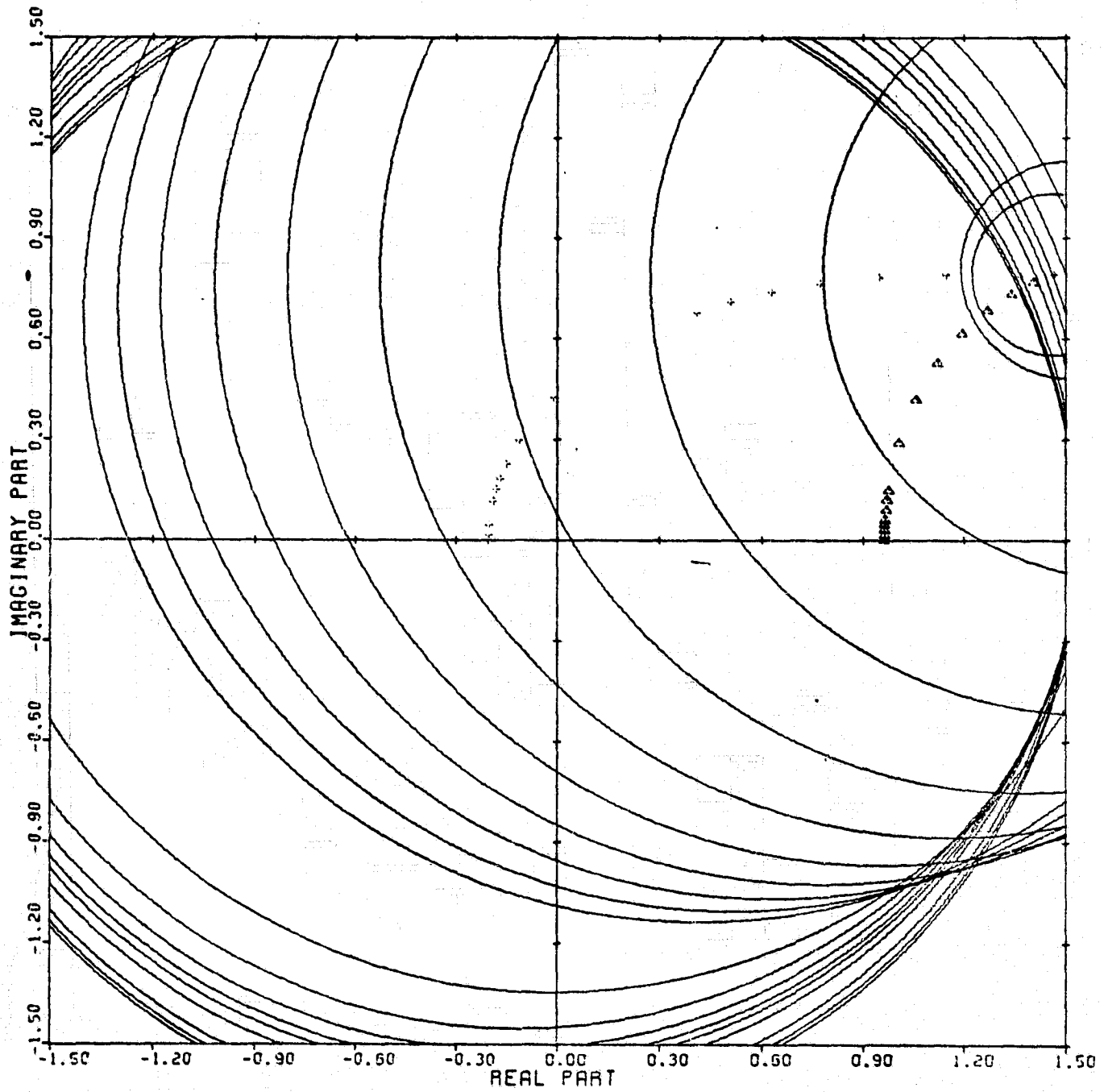
CARDIAD PLOT: 1,4 ENTRY: KMP3, 6/20/78.

INPUTS = 4, SYSTEM ORDER = .6, ANALYSIS TYPE = 2

Figure 56
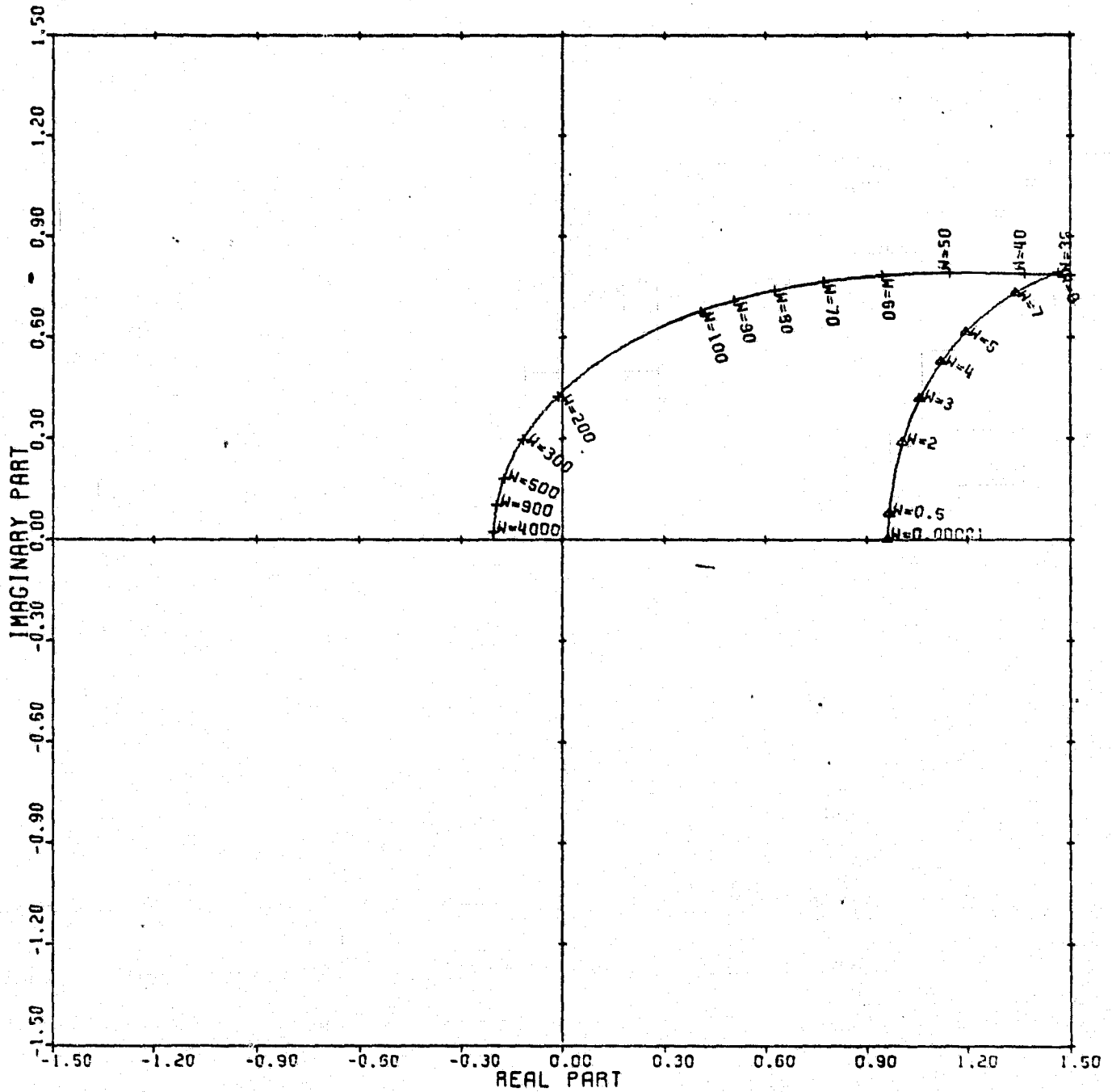
LOCUS OF CENTERS PLOT: 1.4 ENTRY: KMP3, 6/20/78.

INPUTS = 4, SYSTEM ORDER = 6, ANALYSIS TYPE = 2

Figure 57
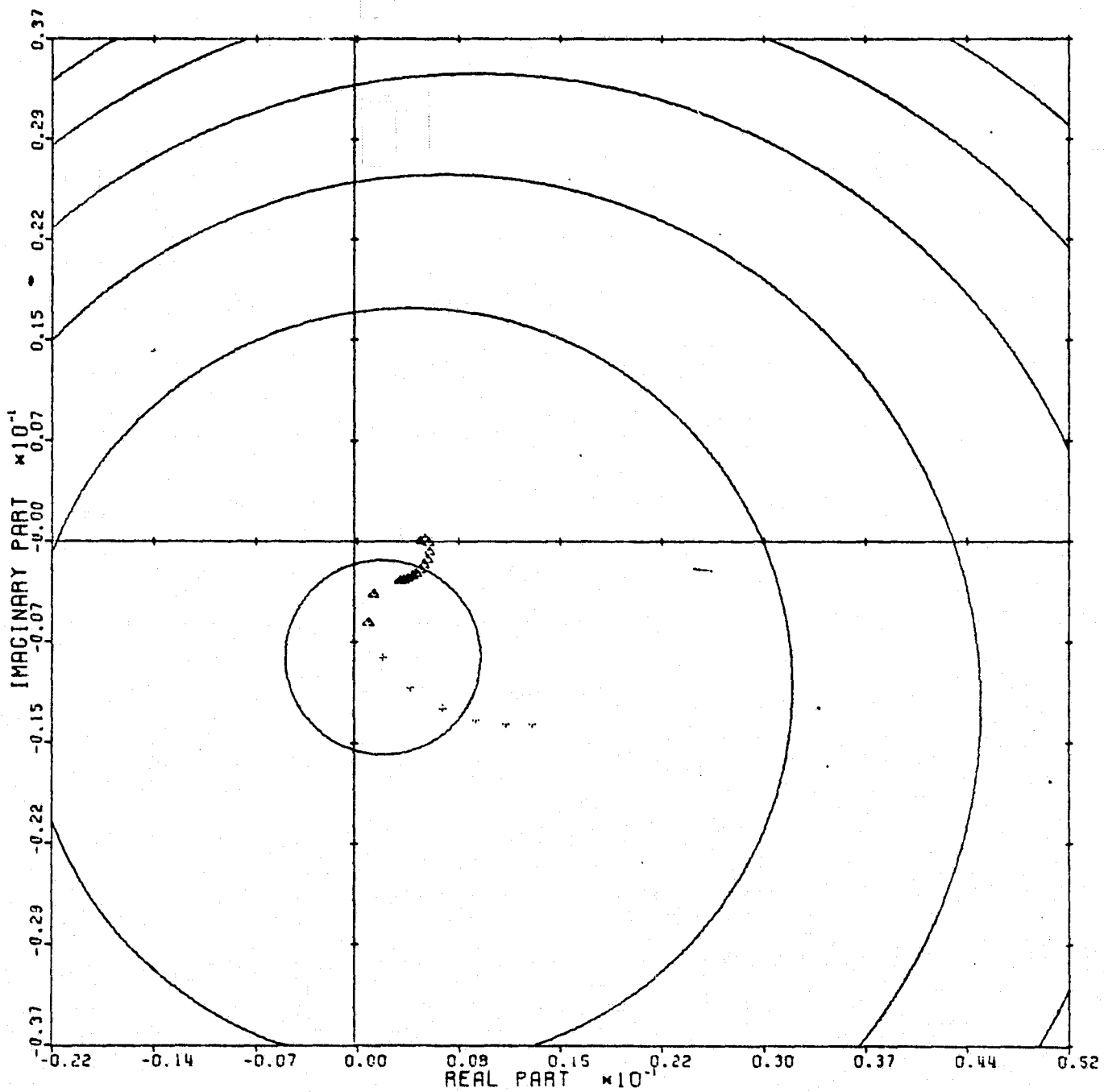
CARDIAD PLOT: 2.4 ENTRY: KMP3. 6/20/78.

INPUTS = 4. SYSTEM ORDER = 6. ANALYSIS TYPE = 2

Figure 58
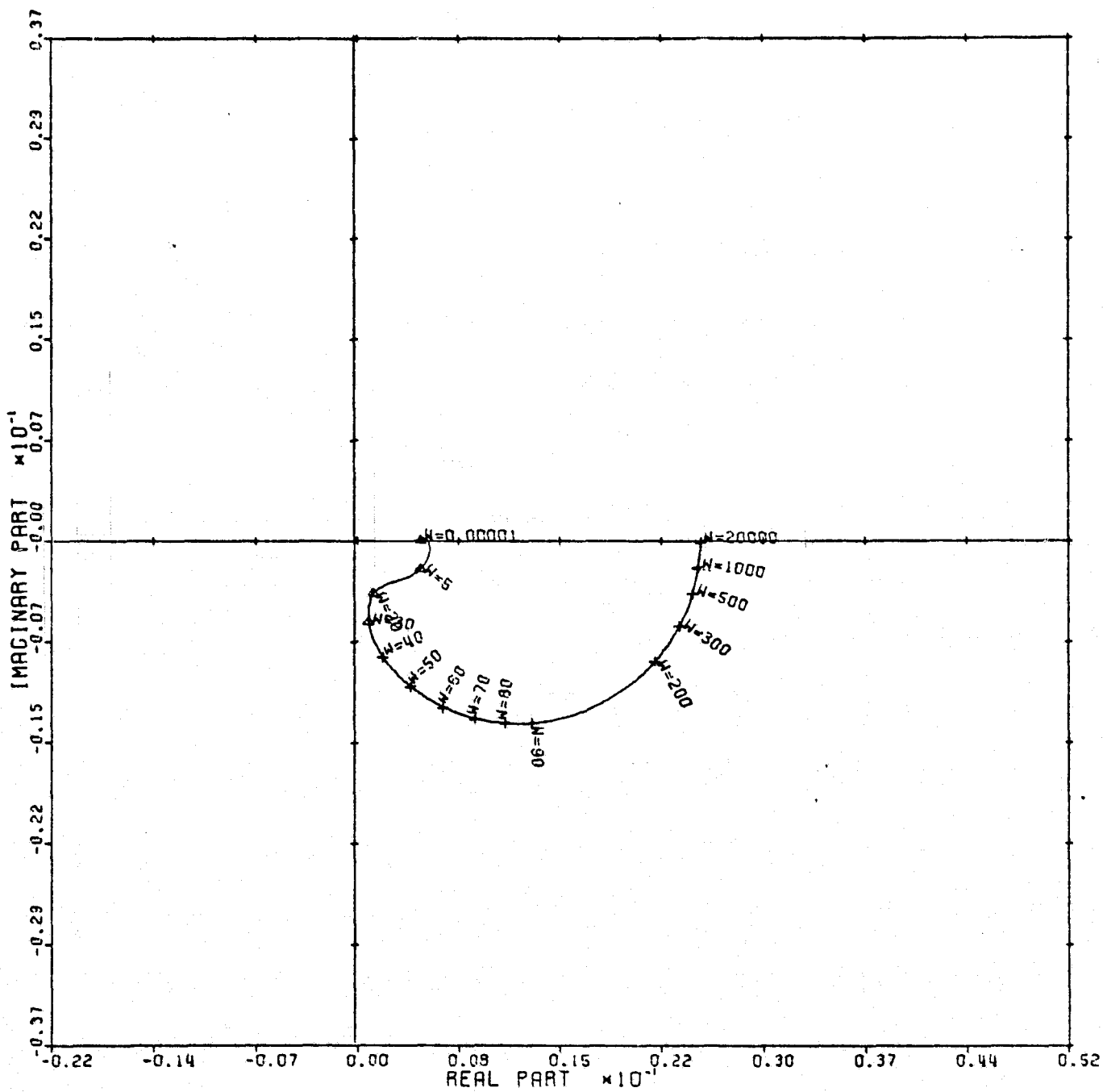
LOCUS OF CENTERS PLOT: 2,4 ENTRY: KMP3, 6/20/78.

INPUTS = 4, SYSTEM ORDER = 6, ANALYSIS TYPE = 2

Figure 59
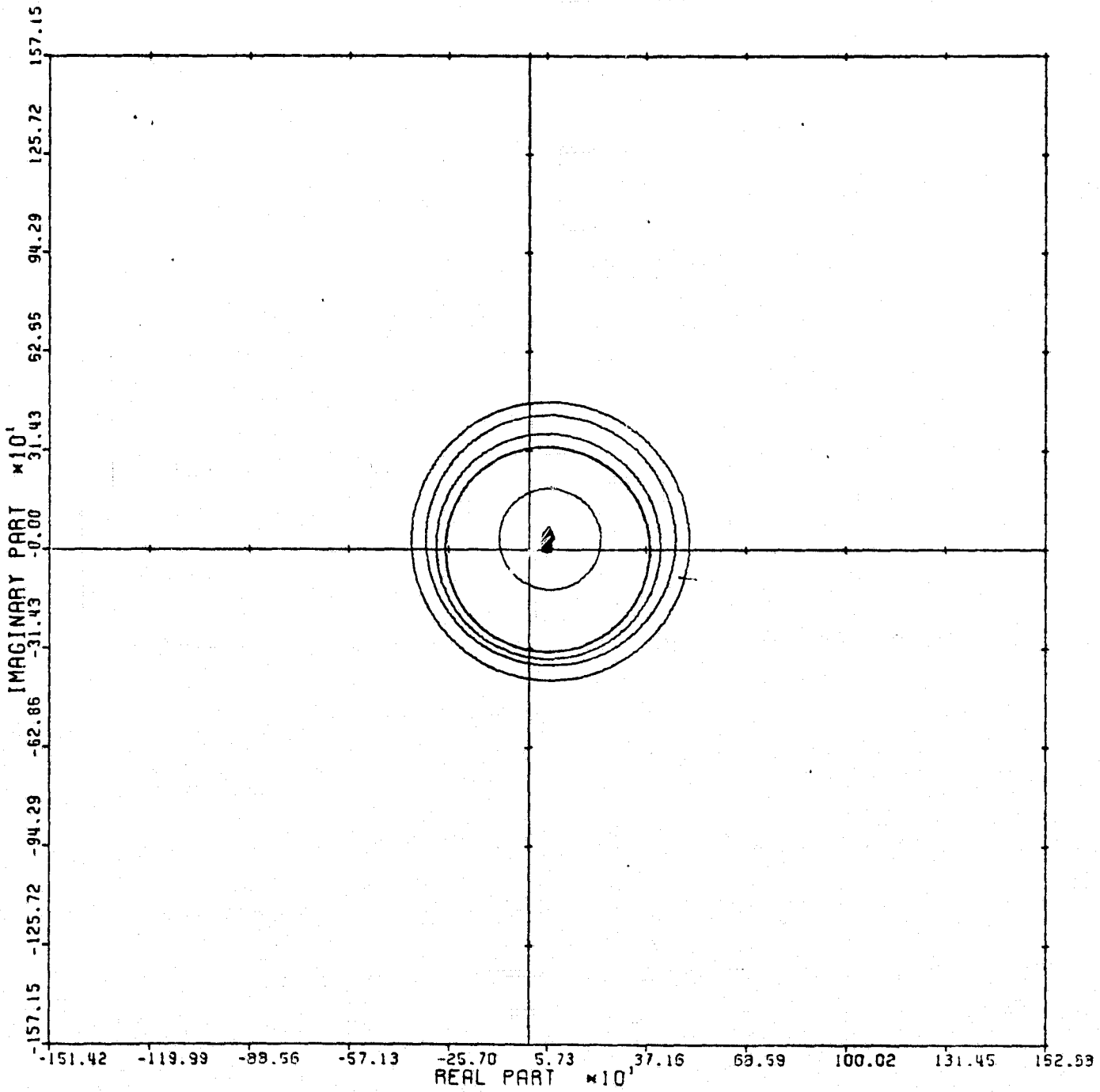
CARDIAC PLOT: 3,4 ENTRY: KMP3, 6/20/78.

INPUTS = 4, SYSTEM ORDER = 6, ANALYSIS TYPE = 2

Figure 60
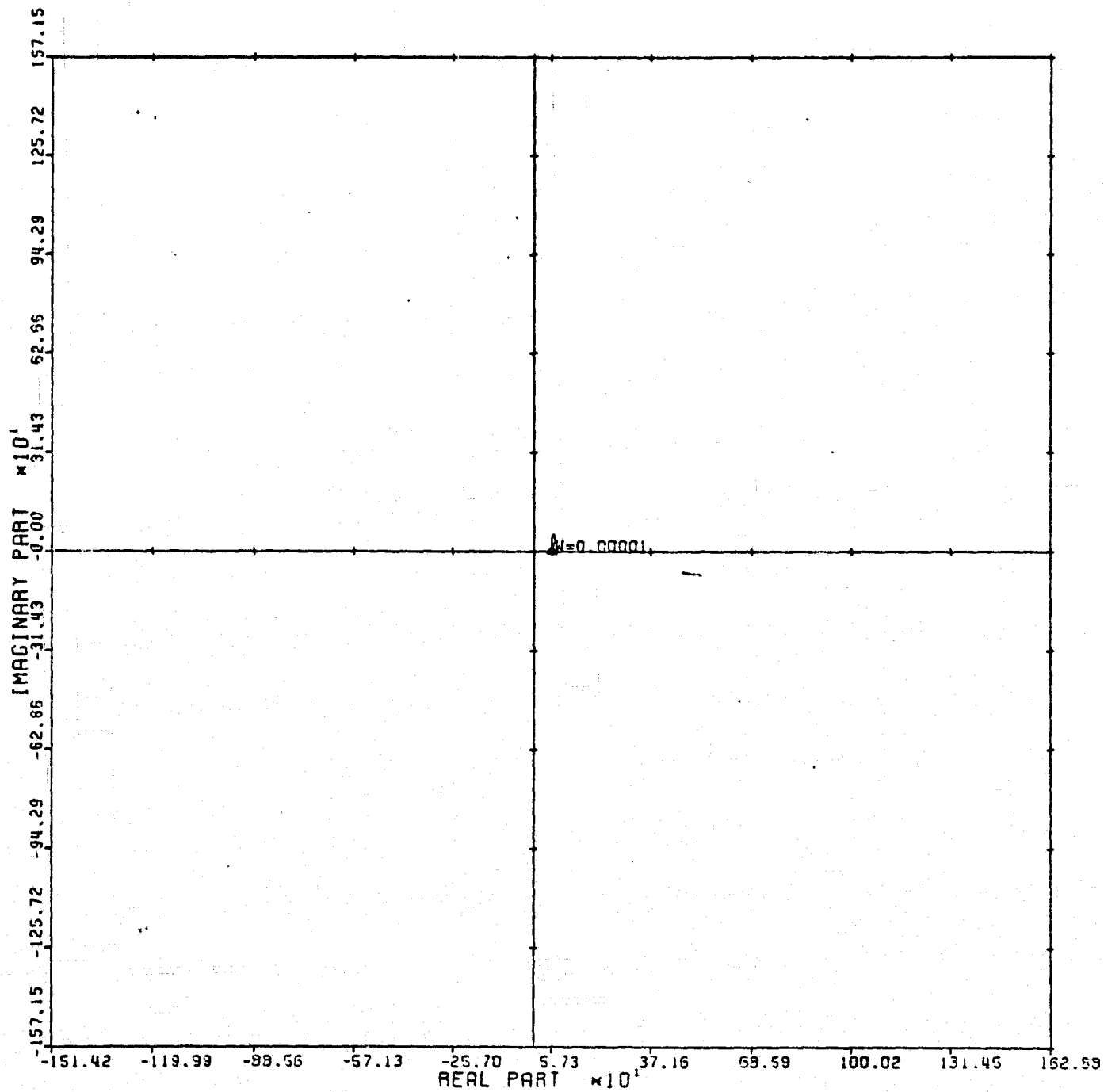
LOCUS OF CENTERS PLOT: 3,4 ENTRY: KMP3, 6/20/78.

INFUTS = 4, SYSTEM ORDER = 6, ANALYSIS TYPE = 2

Figure 61
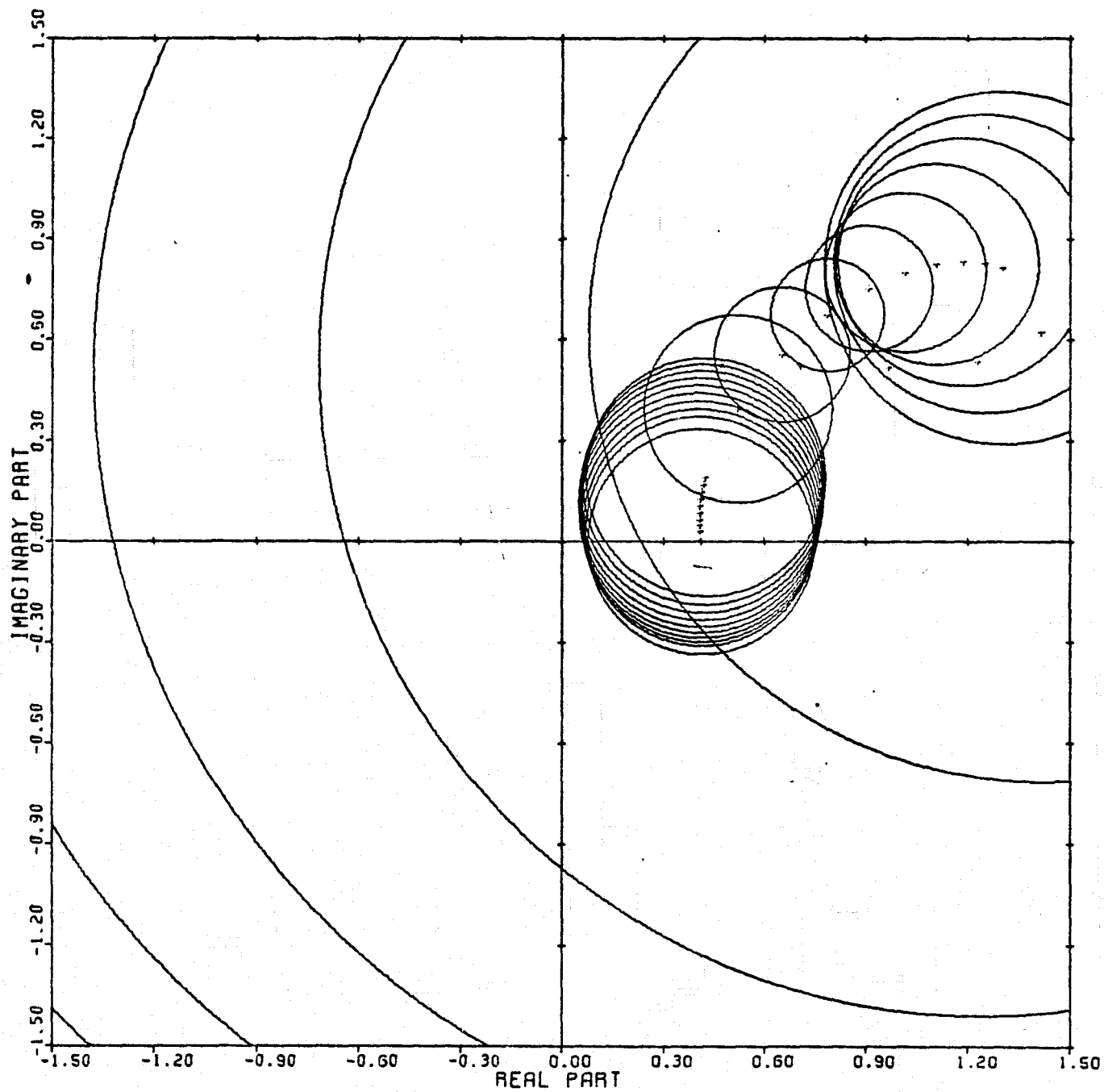
CARDIAD PLOT: 1,4 ENTRY: KMP 4, 6/22/78.

INPUTS = 4, SYSTEM ORDER =.6, ANALYSIS TYPE = 1

Figure 62
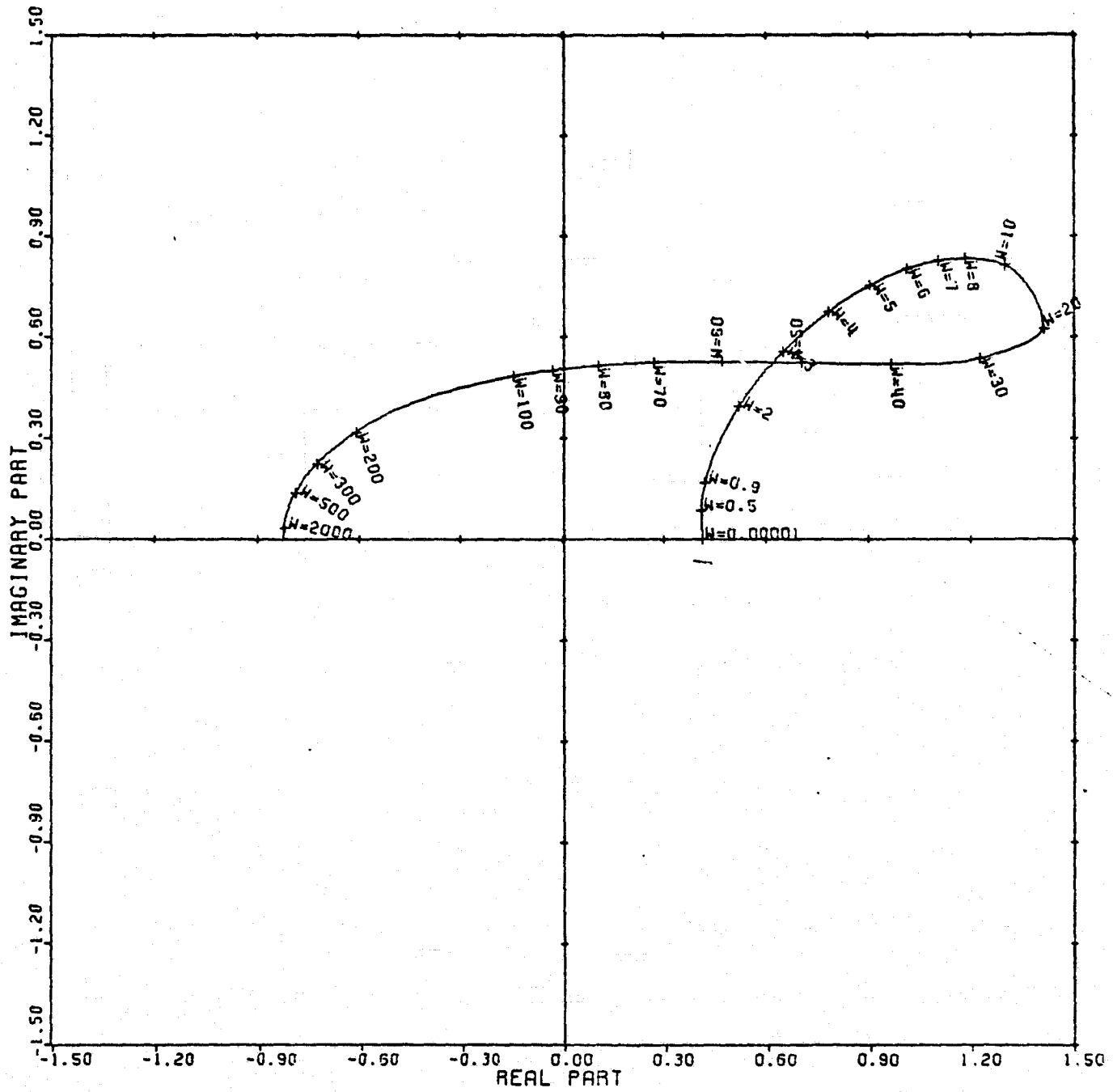
LOCUS OF CENTERS PLOT: 1,4 ENTRY: KMP 4, 6/22/78.

INPUTS = 4, SYSTEM ORDER = 6, ANALYSIS TYPE = 1

Figure 63
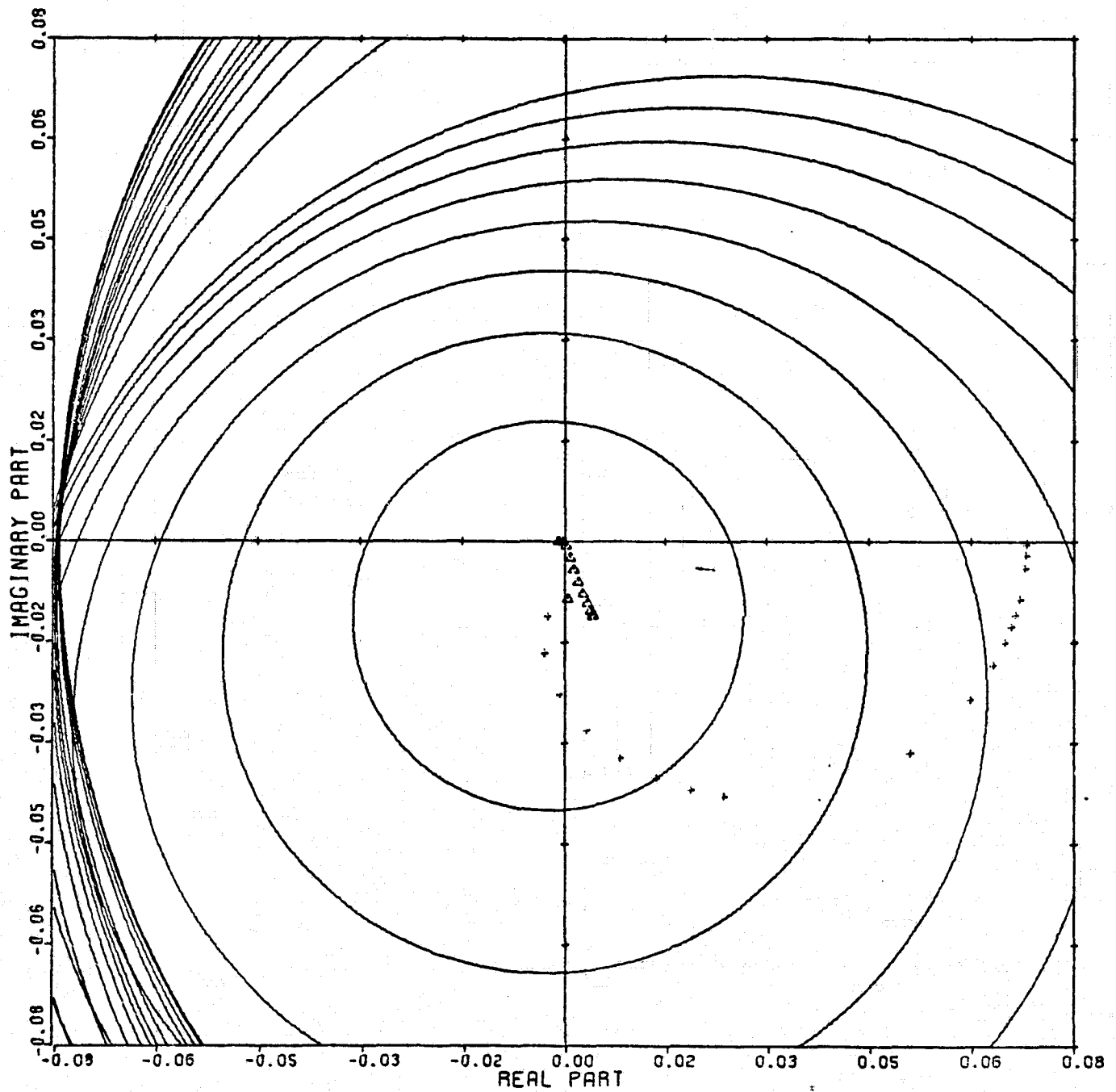
CARDIAO PLOT: 2,4 ENTRY: KMP 4, 6/22/78.

INPUTS = 4, SYSTEM ORDER = 6, ANALYSIS TYPE = 1

Figure 64
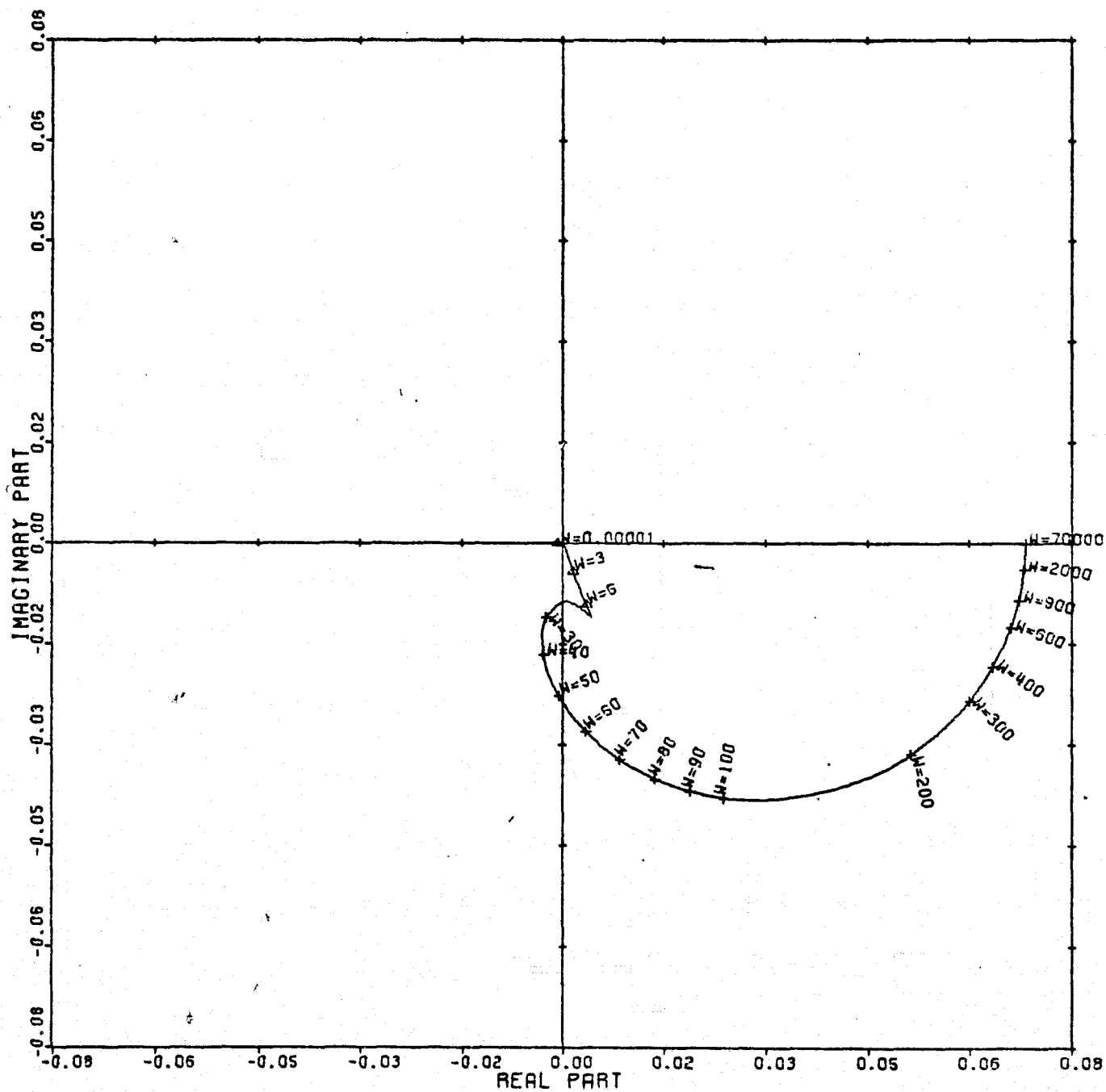
LOCUS OF CENTERS PLOT: 2.4 ENTRY: KMP 4, 6/22/78.

INPUTS = 4, SYSTEM ORDER = 6, ANALYSIS TYPE = 1

Figure 65
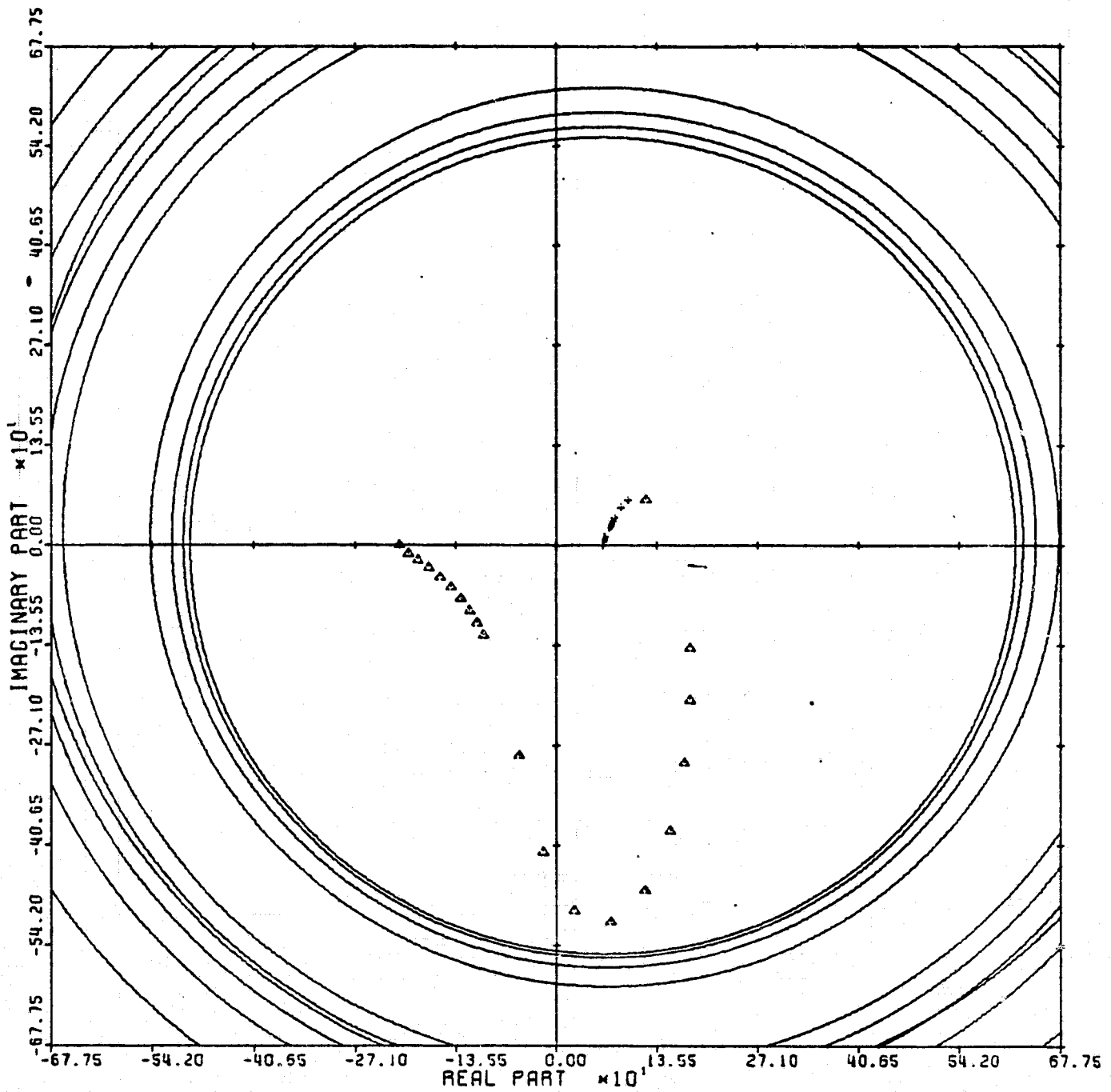
CARDIAD PLOT: 3,4 ENTRY: KMP 4, 6/22/78.

INPUTS = 4, SYSTEM ORDER = .6, ANALYSIS TYPE = 1

Figure 66
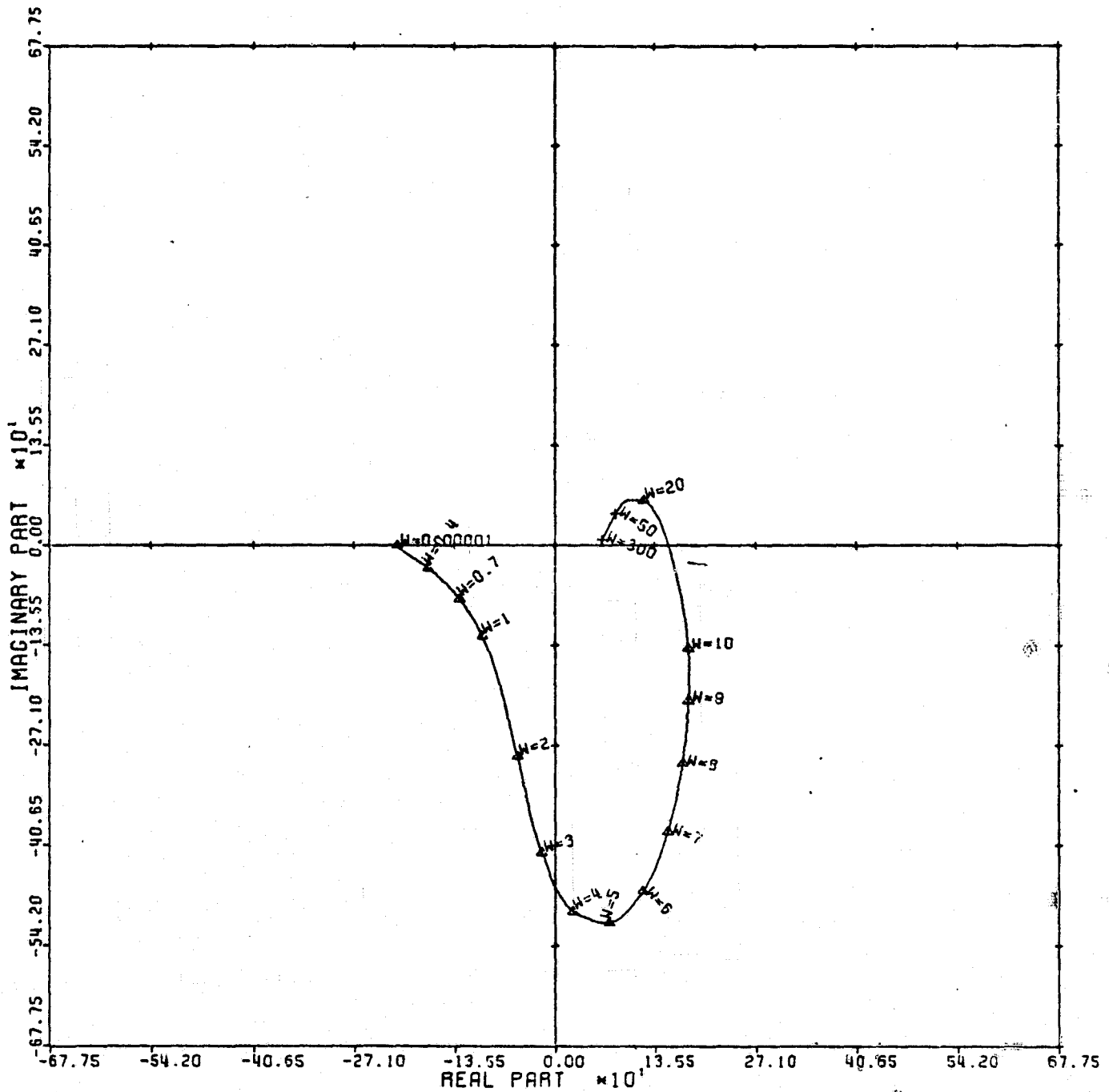
LOCUS OF CENTERS PLOT: 3,4 ENTRY: KMP 4, 6/22/78.

INPUTS = 4, SYSTEM ORDER = 6, ANALYSIS TYPE = 1

Figure 67
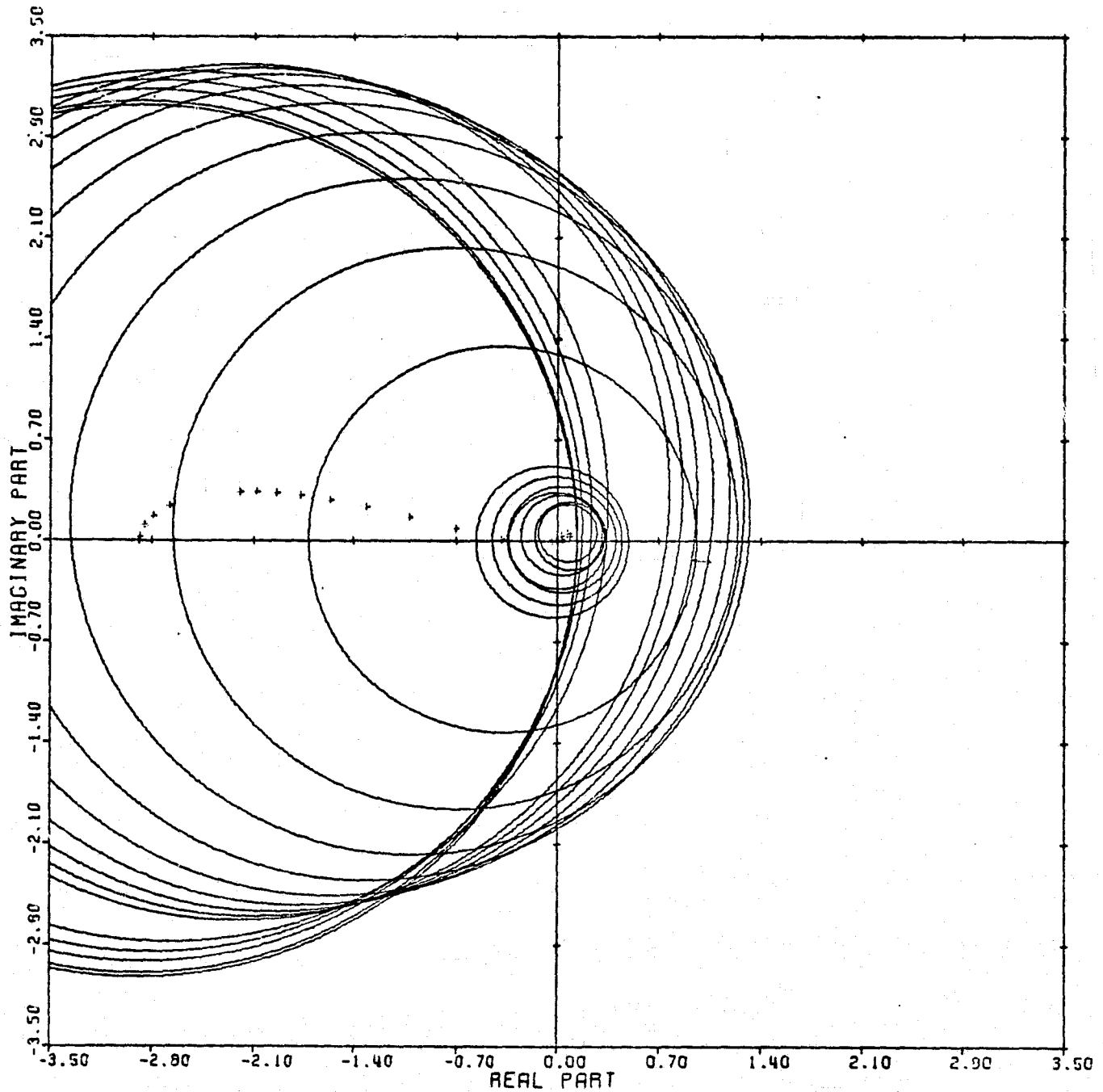
CARDIAD PLOT: 1,4 ENTRY: KMP 5, 6/24/78.

INPUTS = 4, SYSTEM ORDER = 6, ANALYSIS TYPE = 1

Figure 68
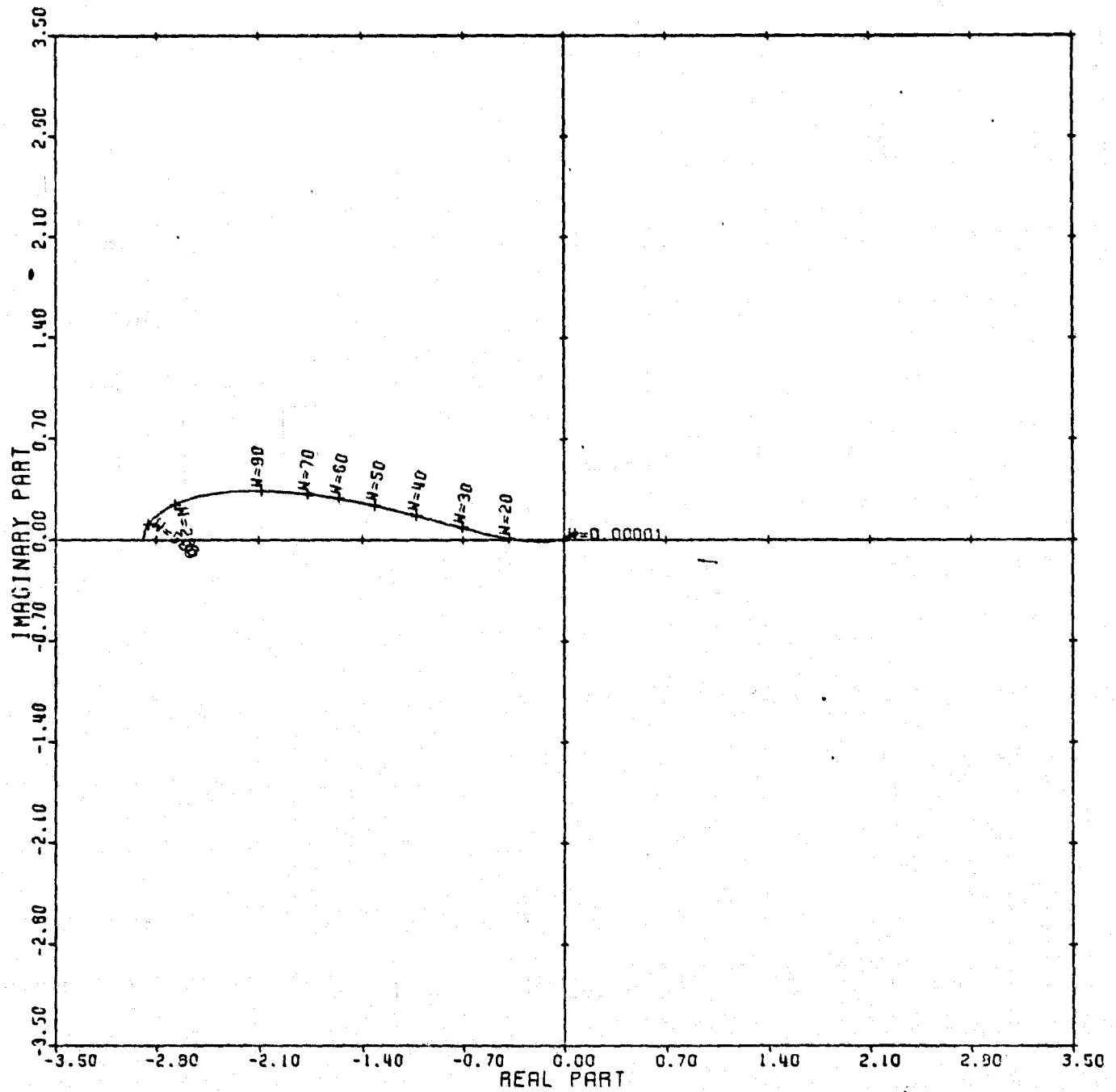
LOCUS OF CENTERS PLOT: 1,4 ENTRY: KMP 5, 6/24/78.

INPUTS = 4, SYSTEM ORDER = 6, ANALYSIS TYPE = 1

Figure 69
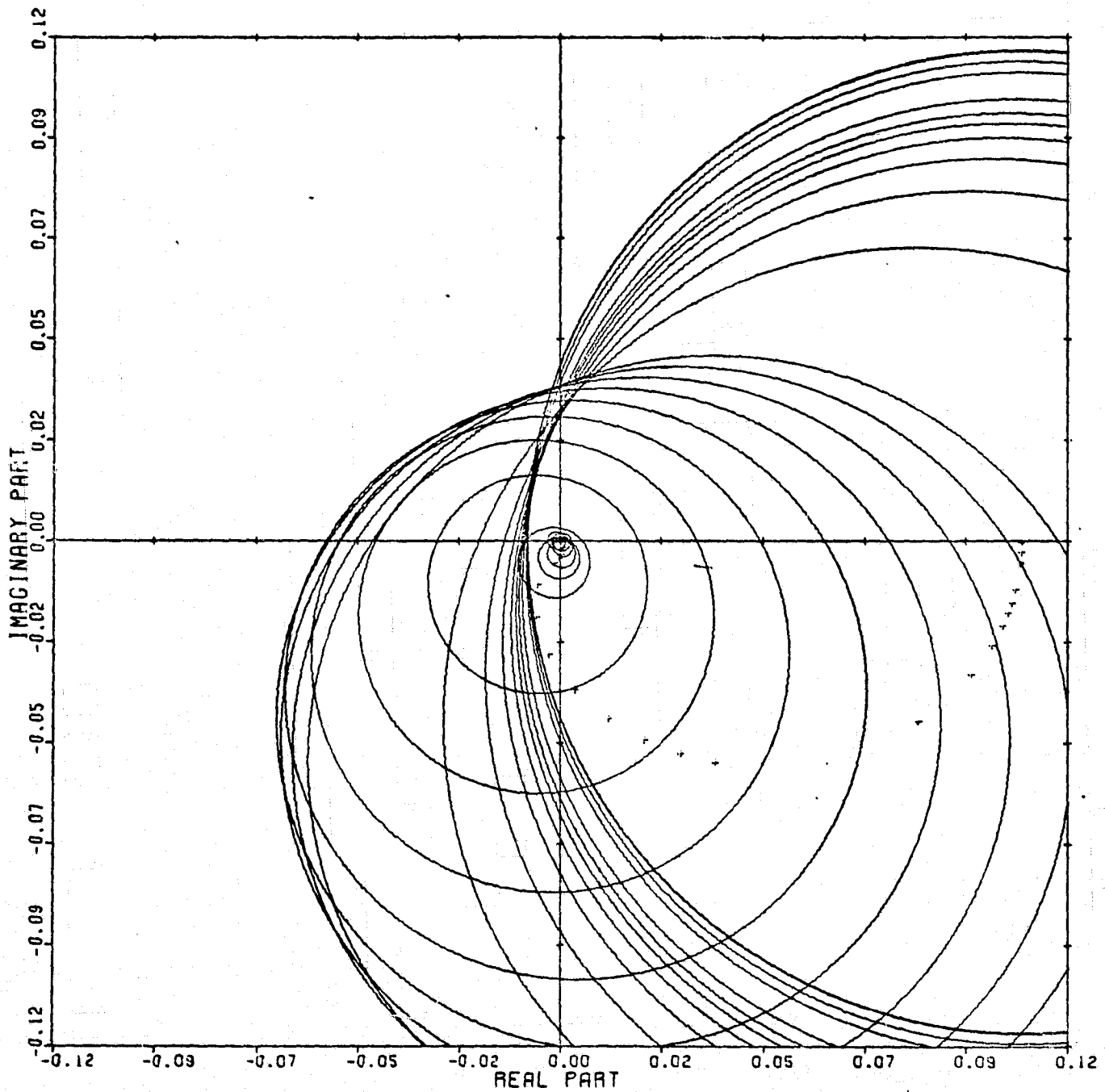
CARDIAD PLOT: 2,4 ENTRY: KMP 5, 6/24/78.

INPUTS = 4, SYSTEM ORDER = 6, ANALYSIS TYPE = 1

Figure 70
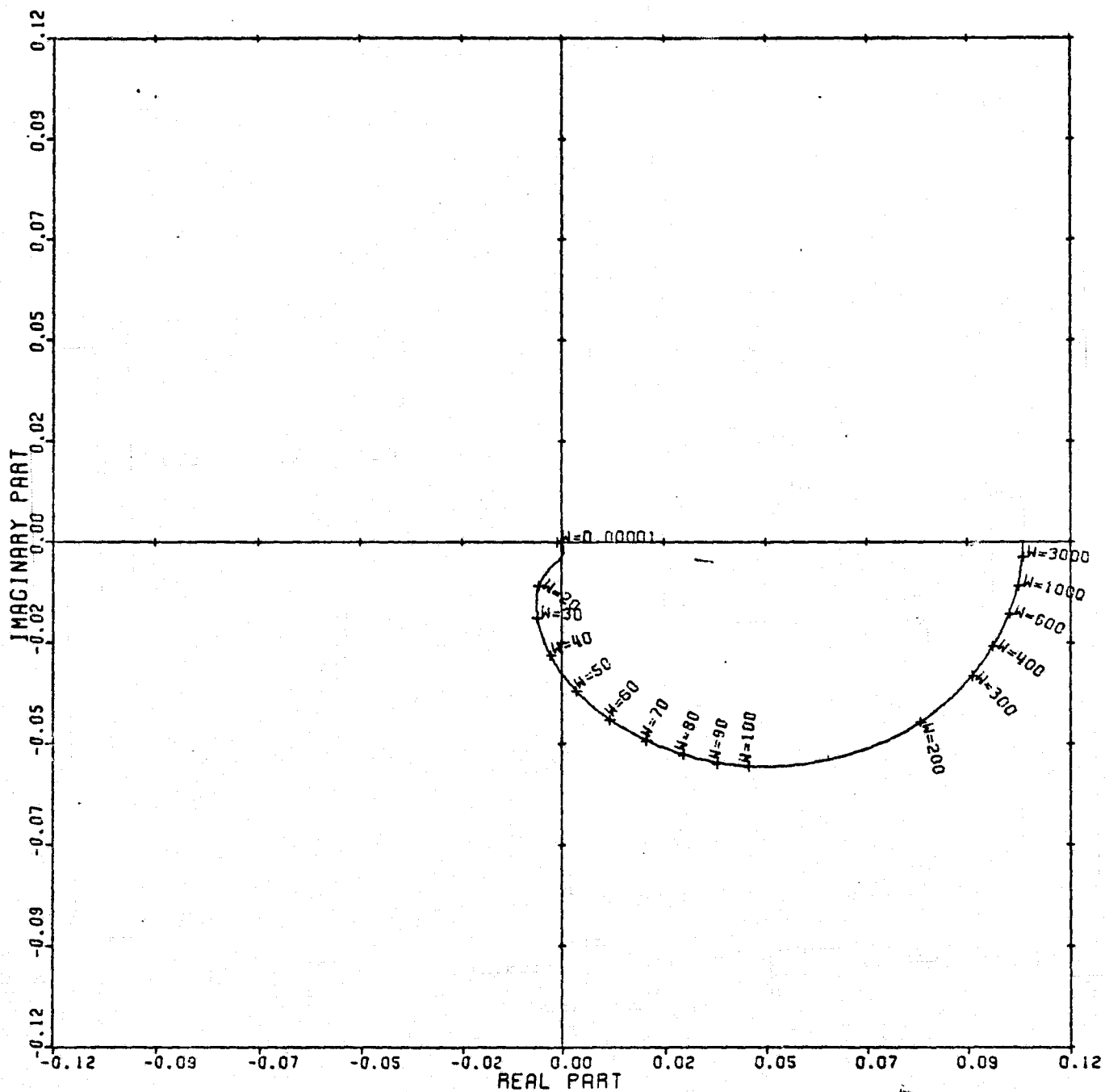
LOCUS OF CENTERS PLOT: 2,4 ENTRY: KMP 5, 6/24/78.

INPUTS = 4, SYSTEM ORDER = 6, ANALYSIS TYPE = 1

Figure 71
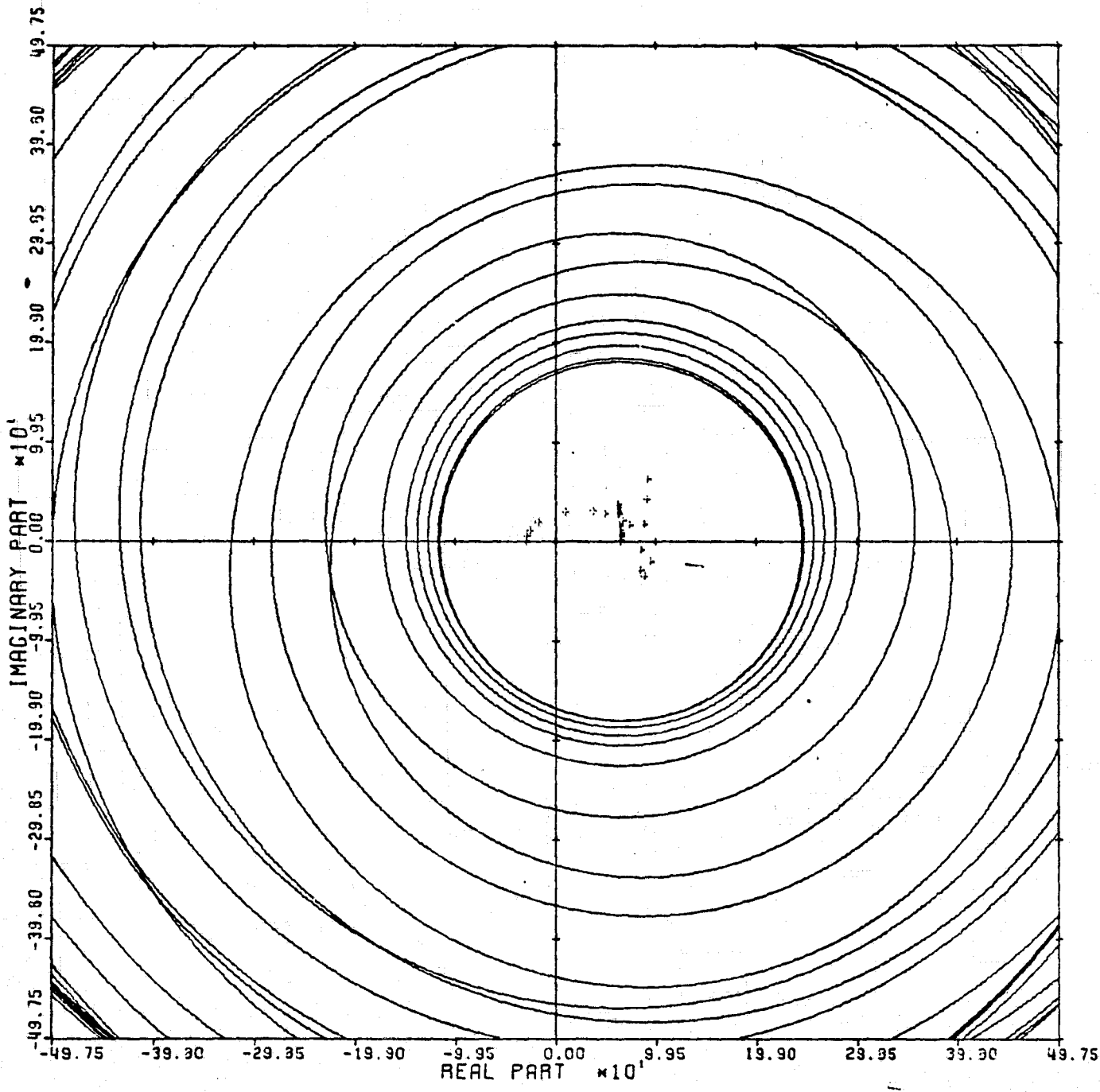
CARDIAD PLOT: 3.4 ENTRY: KMP 5, 6/24/78.

INPUTS = 4, SYSTEM ORDER = 6, ANALYSIS TYPE = 1

Figure 72
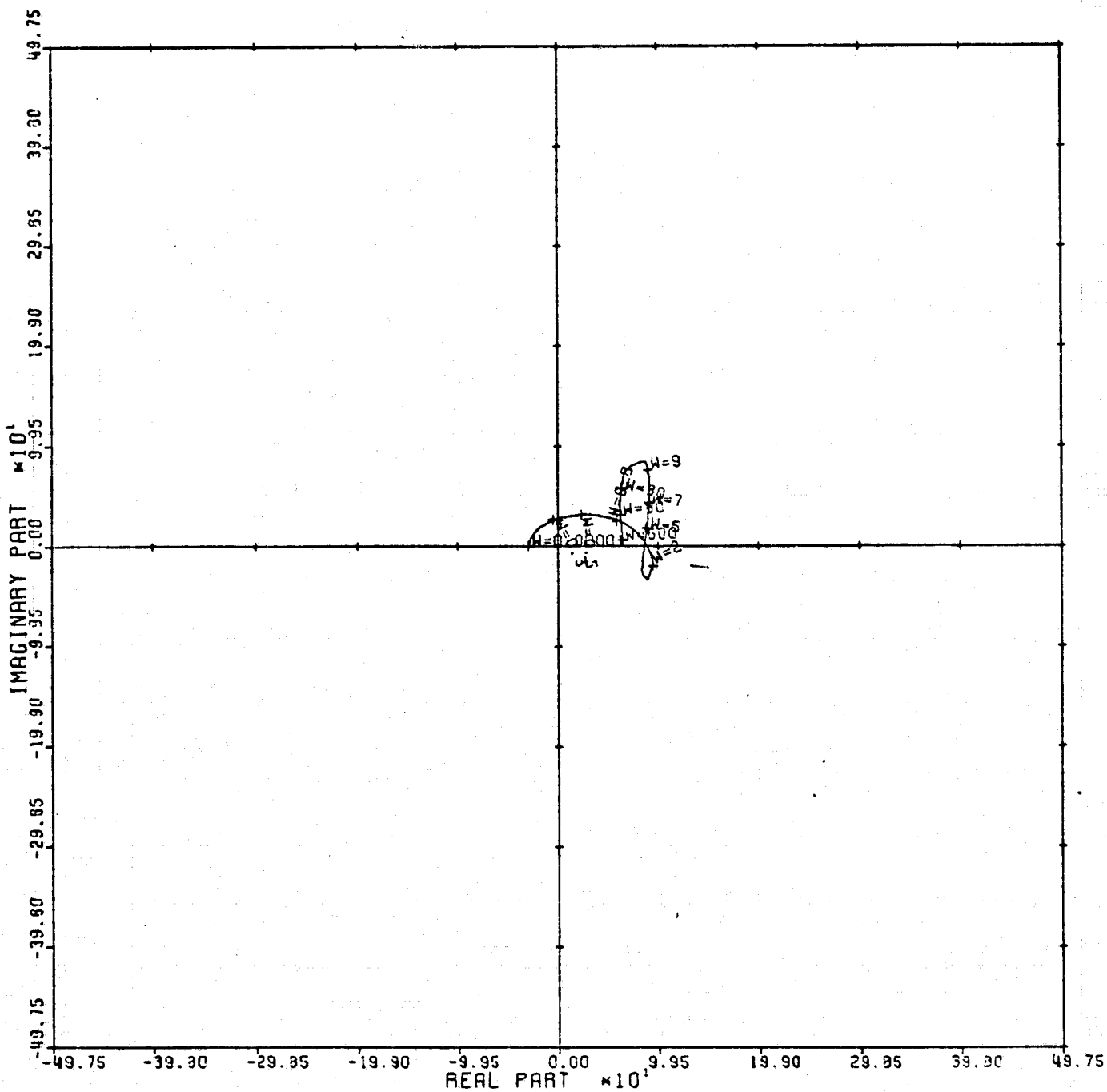
LOCUS OF CENTERS PLOT: 3,4 ENTRY: KMP 5, 6/24/78.

INPUTS = 4, SYSTEM ORDER = 6, ANALYSIS TYPE = 1

Figure 73
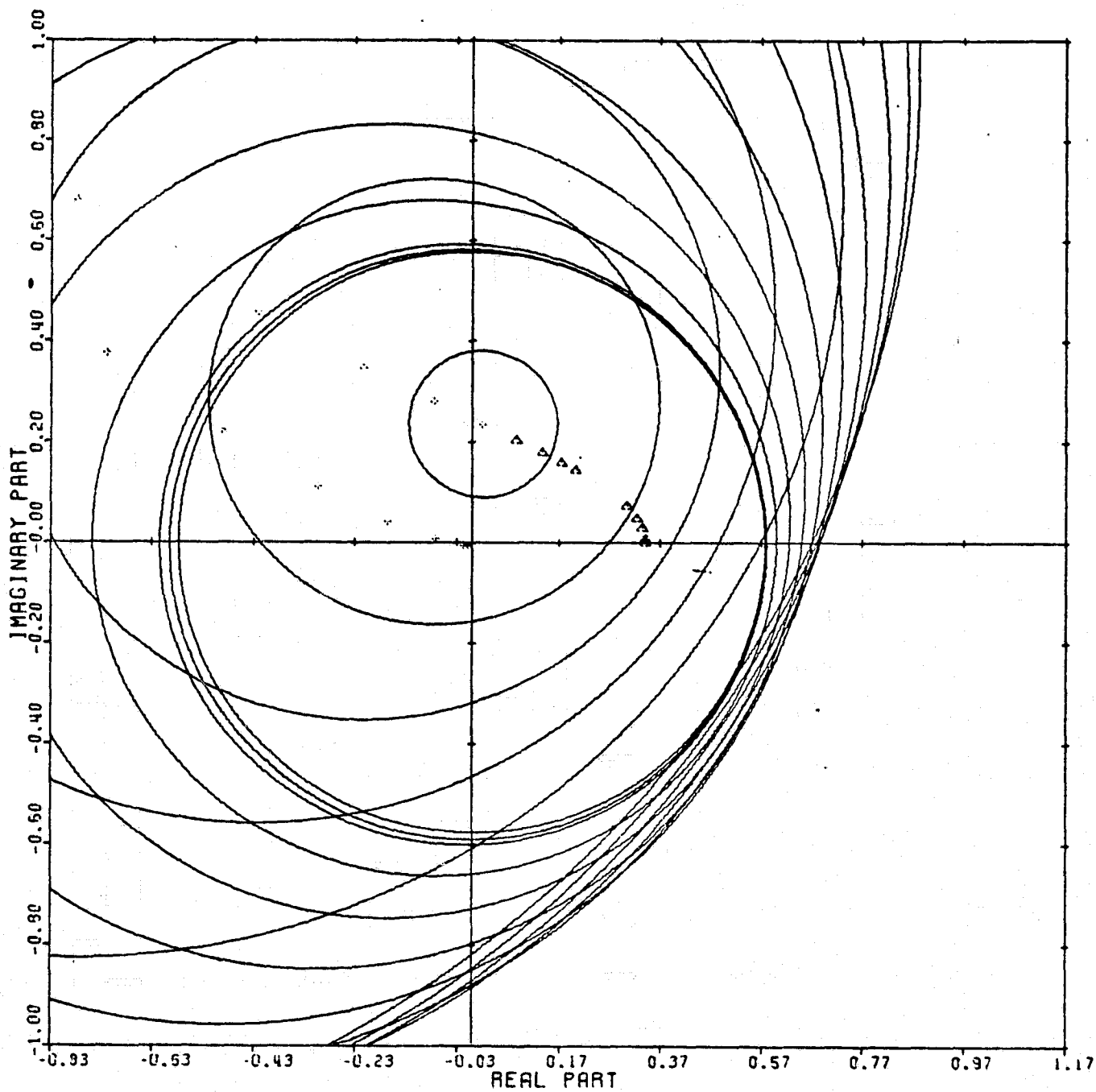
CARDIAO PLOT: 2.1 ENTRY: 1/G(0), 6/24/78.

INPUTS = 4, SYSTEM ORDER = 6, ANALYSIS TYPE = 11

Figure 74
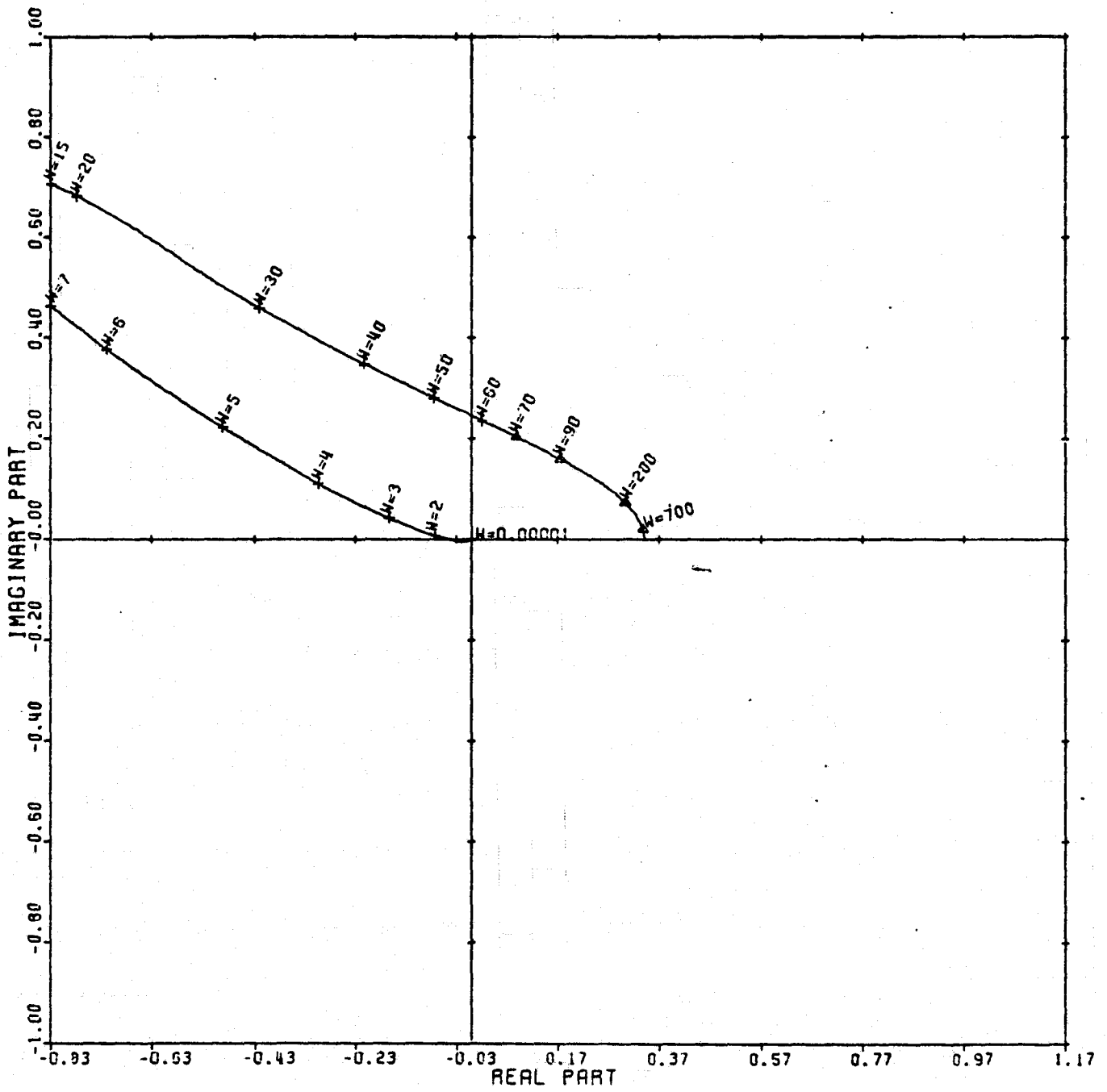
LOCUS OF CENTERS PLOT: 2,1 ENTRY: 1/G(0), 6/24/78.

INPUTS = 4, SYSTEM ORDER = 6, ANALYSIS TYPE = 11

Figure 75
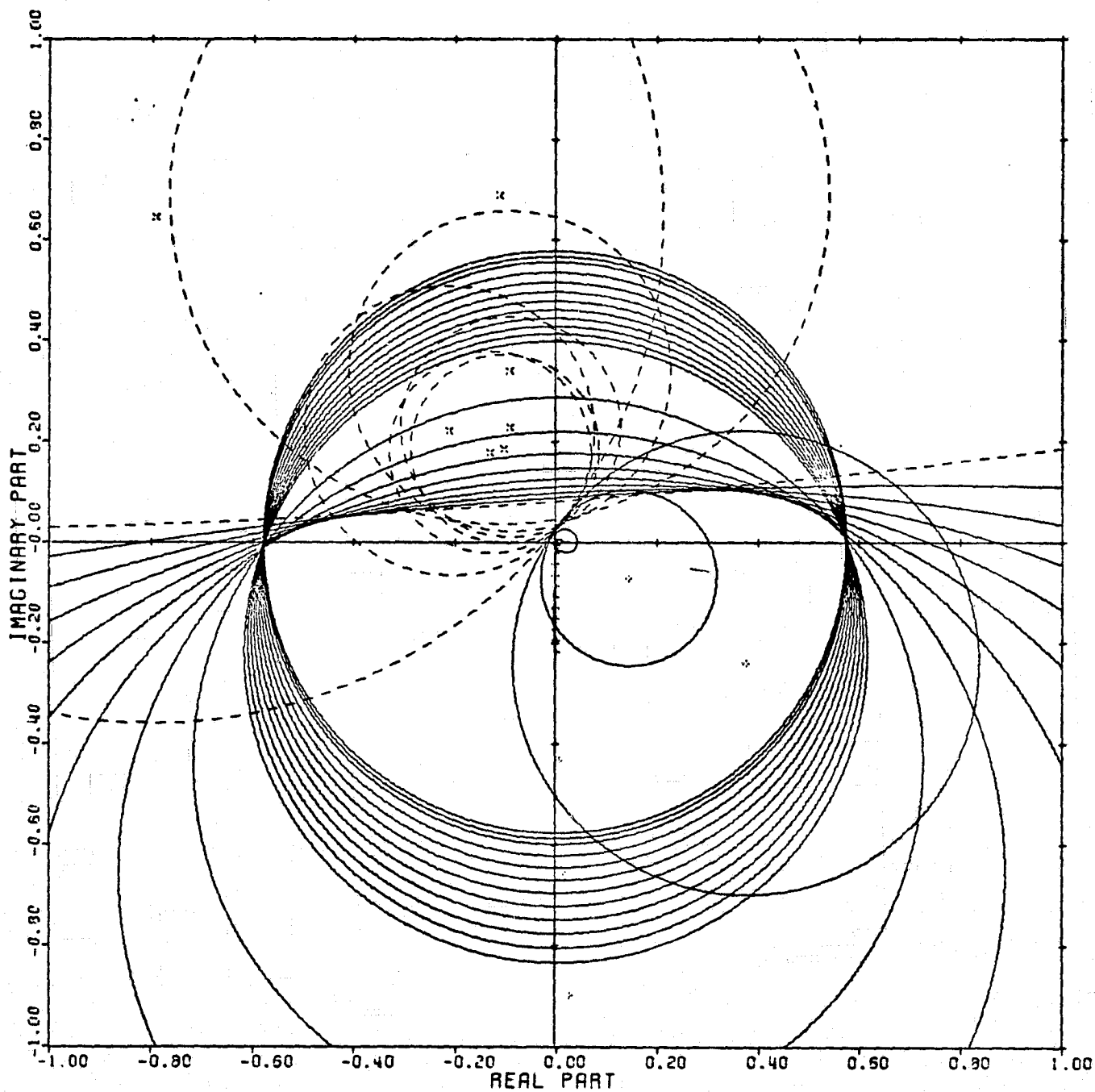
CARDIAD PLOT: 3.1 ENTRY: 1/G(0), 6/24/78.

INPUTS = 4, SYSTEM ORDER = 6, ANALYSIS TYPE = 11

Figure 76
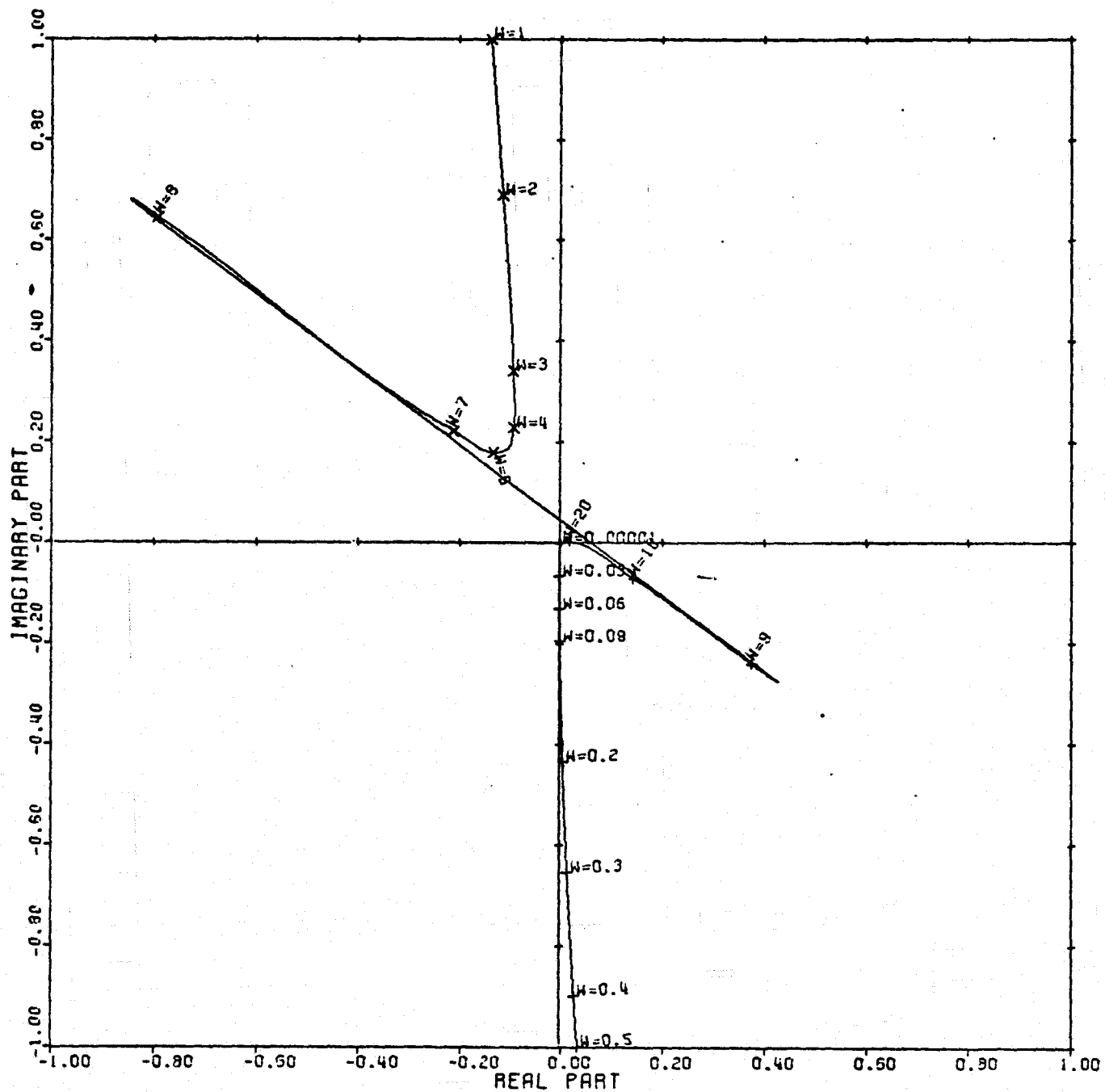
LOCUS OF CENTERS PLOT: 3.1 ENTRY: 1/G(0), 6/24/78.

INPUTS = 4, SYSTEM ORDER = 6, ANALYSIS TYPE = 11

Figure 77
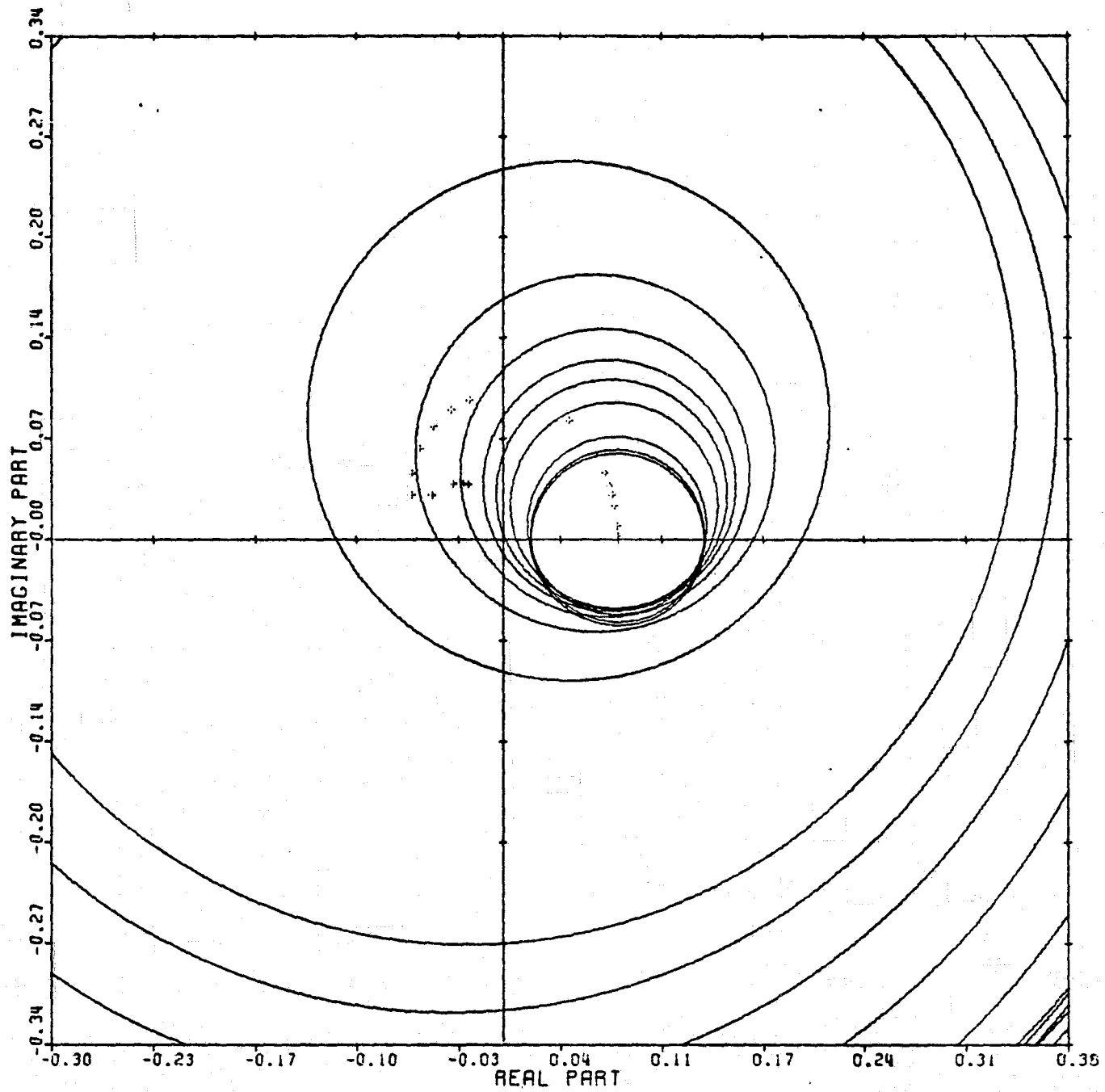
CARDIAD PLOT: 4,1 ENTRY: 1/G(0), 6/24/78.

INPUTS = 4, SYSTEM ORDER = 6, ANALYSIS TYPE = 11

Figure 78
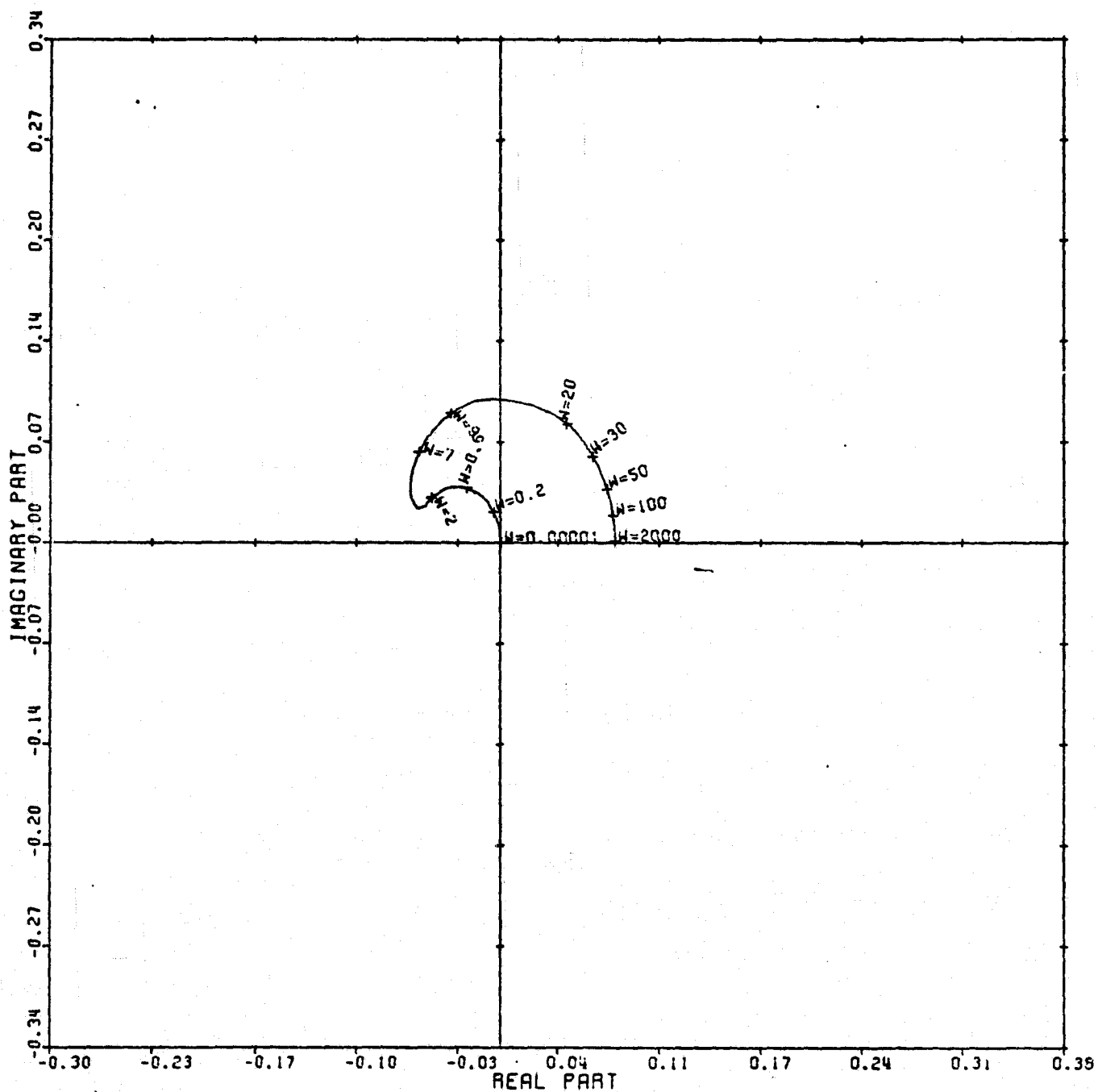
LOCUS OF CENTERS PLOT: 4,1 ENTRY: 1/G(0), 6/24/78.

INPUTS = 4, SYSTEM ORDER = 6, ANALYSIS TYPE = 11

Figure 79
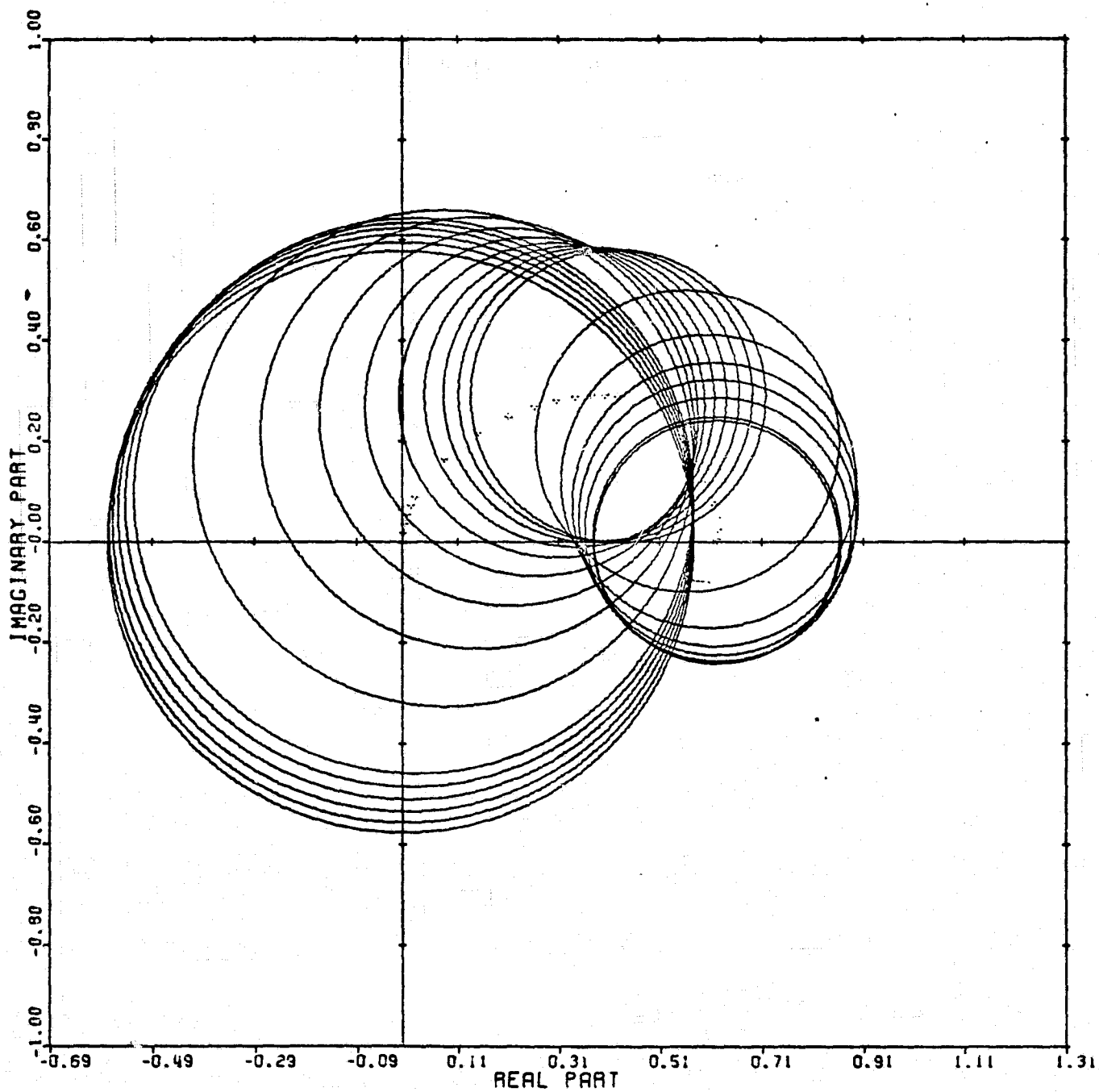
CARDIAD PLOT: 1,2 ENTRY: 1/G(0). 6/24/78.

INPUTS = 4, SYSTEM ORDER = 6, ANALYSIS TYPE = 11

Figure 80
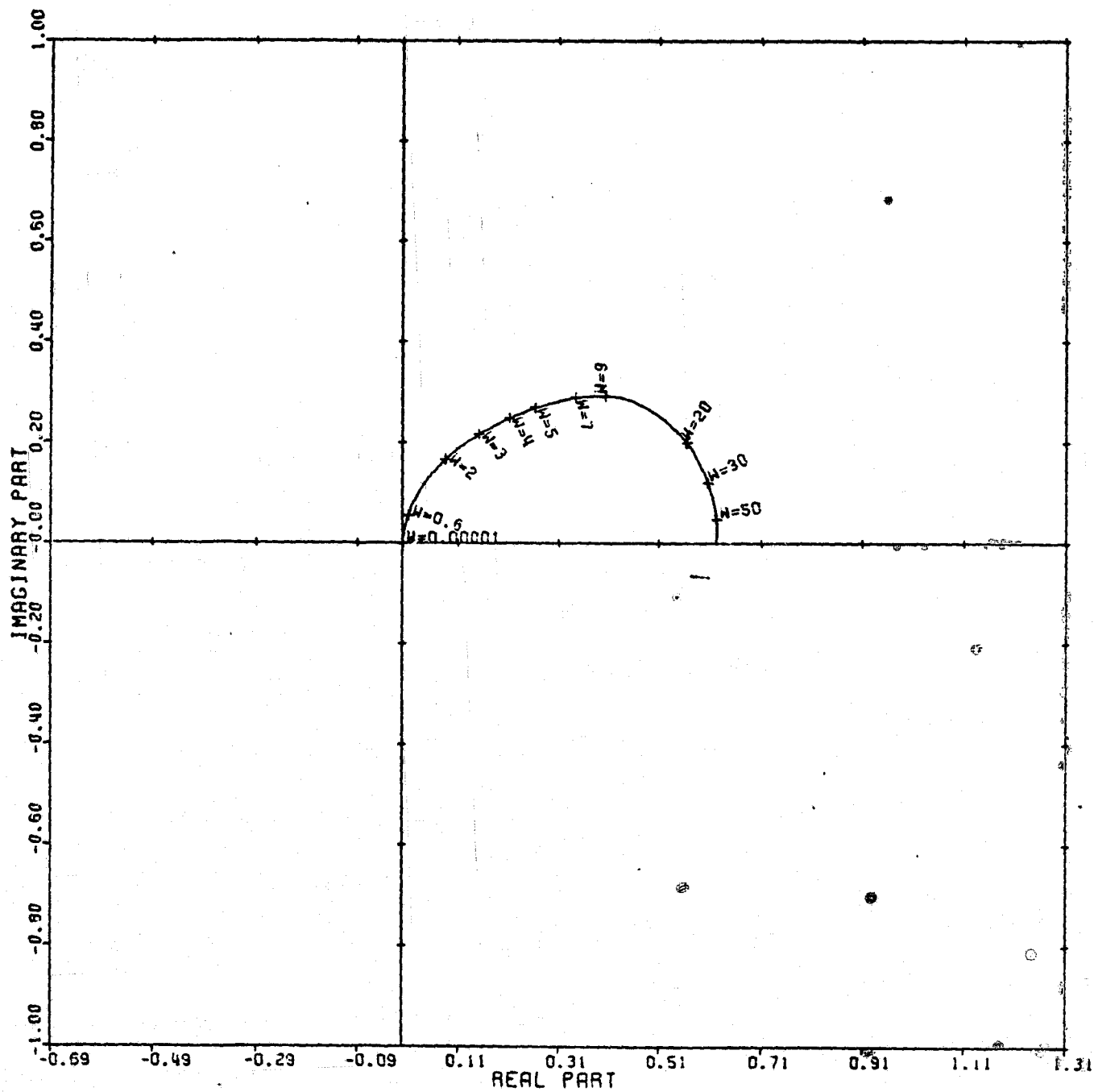
LOCUS OF CENTERS PLOT: 1,2 ENTRY: 1/G(0), 6/24/78.

INPUTS = 4, SYSTEM ORDER = 6, ANALYSIS TYPE = 11

Figure 81
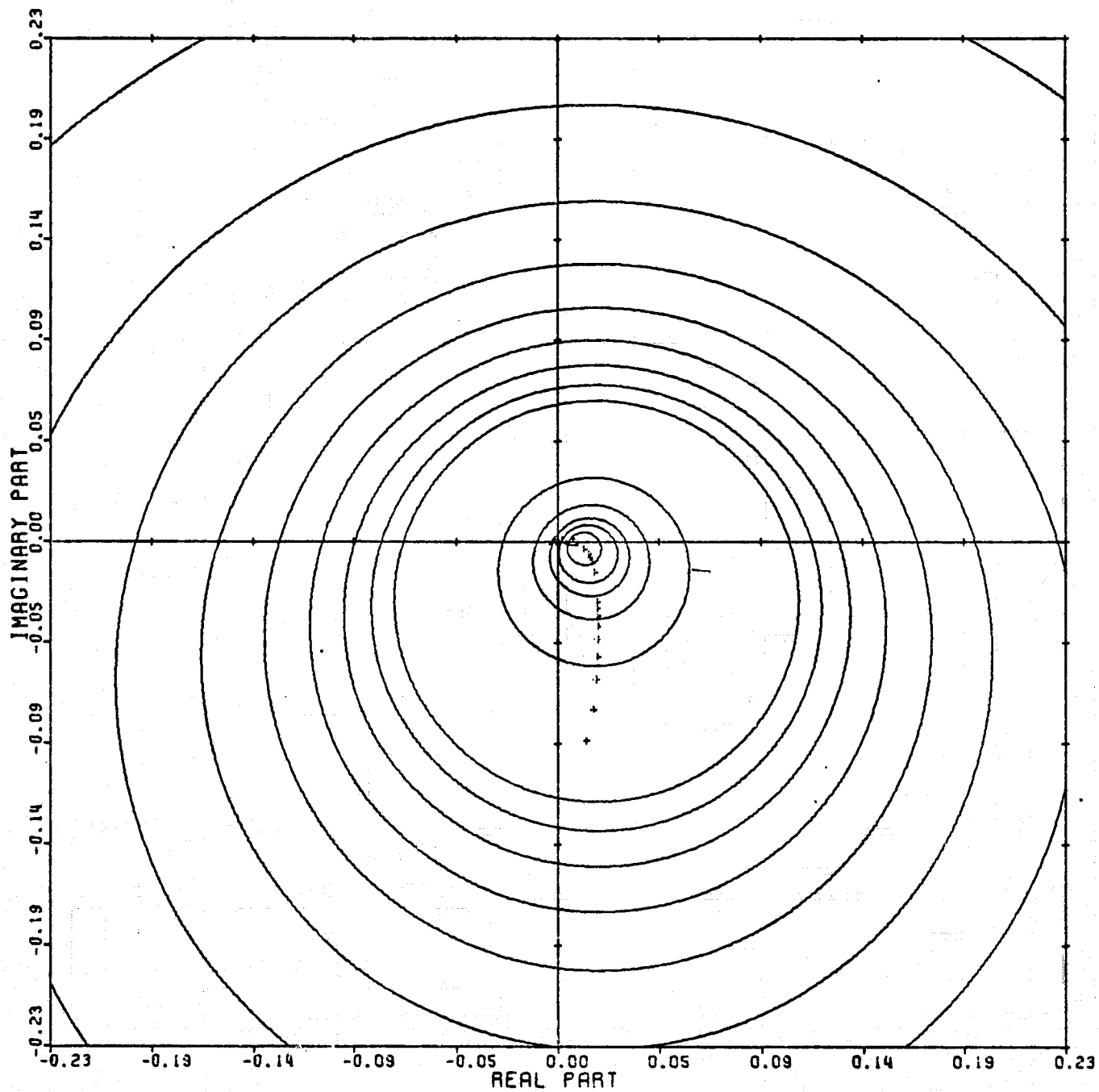
CARDIAD PLOT: 3,2 ENTRY: 1/G(0), 6/24/78.

INPUTS = 4, SYSTEM ORDER = 6, ANALYSIS TYPE = 11

Figure 82
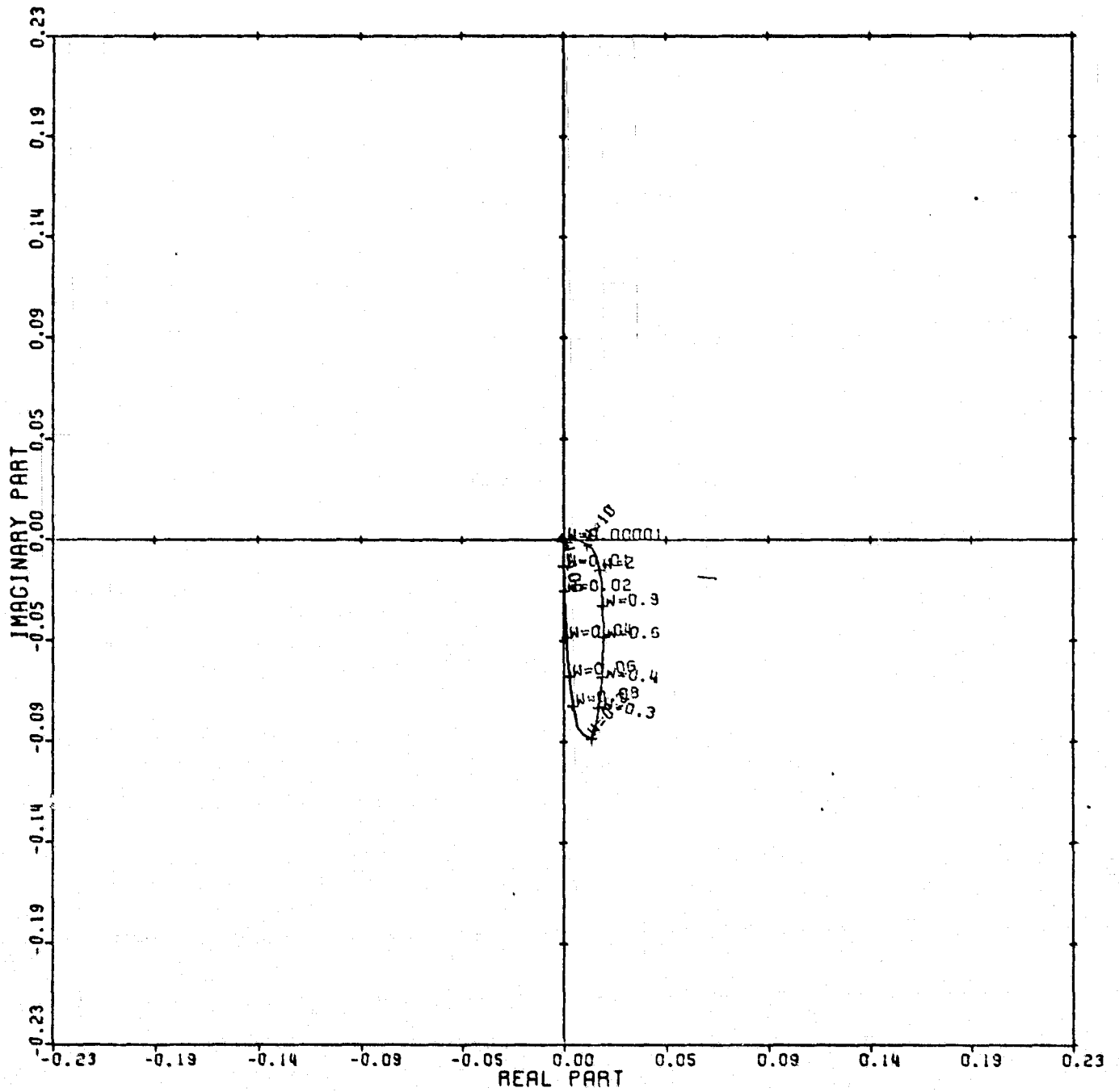
LOCUS OF CENTERS PLOT: 3.2 ENTRY: 1/G(0), 6/24/78.

INPUTS = 4, SYSTEM ORDER = 6, ANALYSIS TYPE = 11

Figure 83
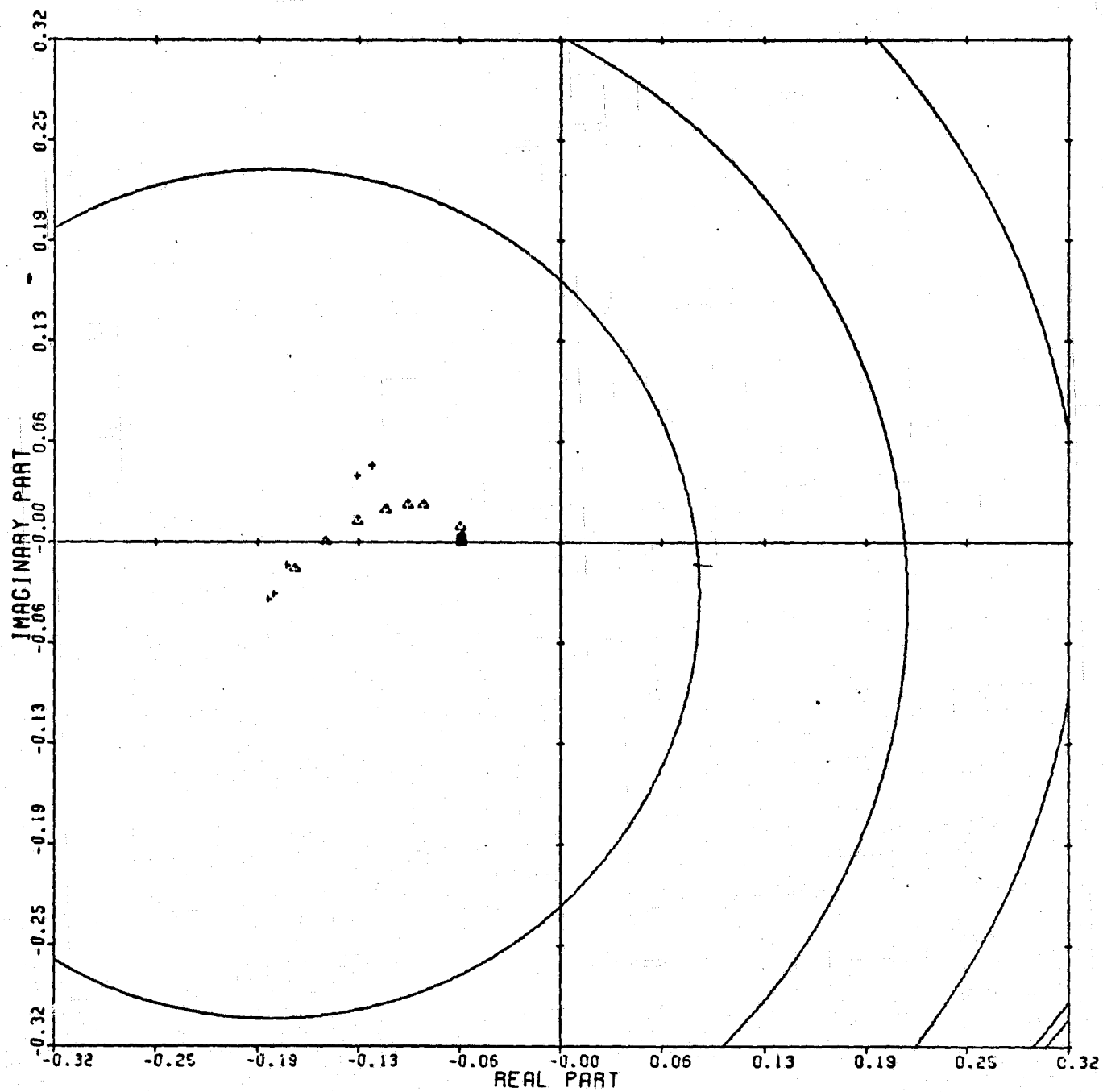
CARDIAD PLOT: 4,2 ENTRY: 1/G(0), 6/24/78.

INPUTS = 4, SYSTEM ORDER = .6, ANALYSIS TYPE = 11

Figure 84
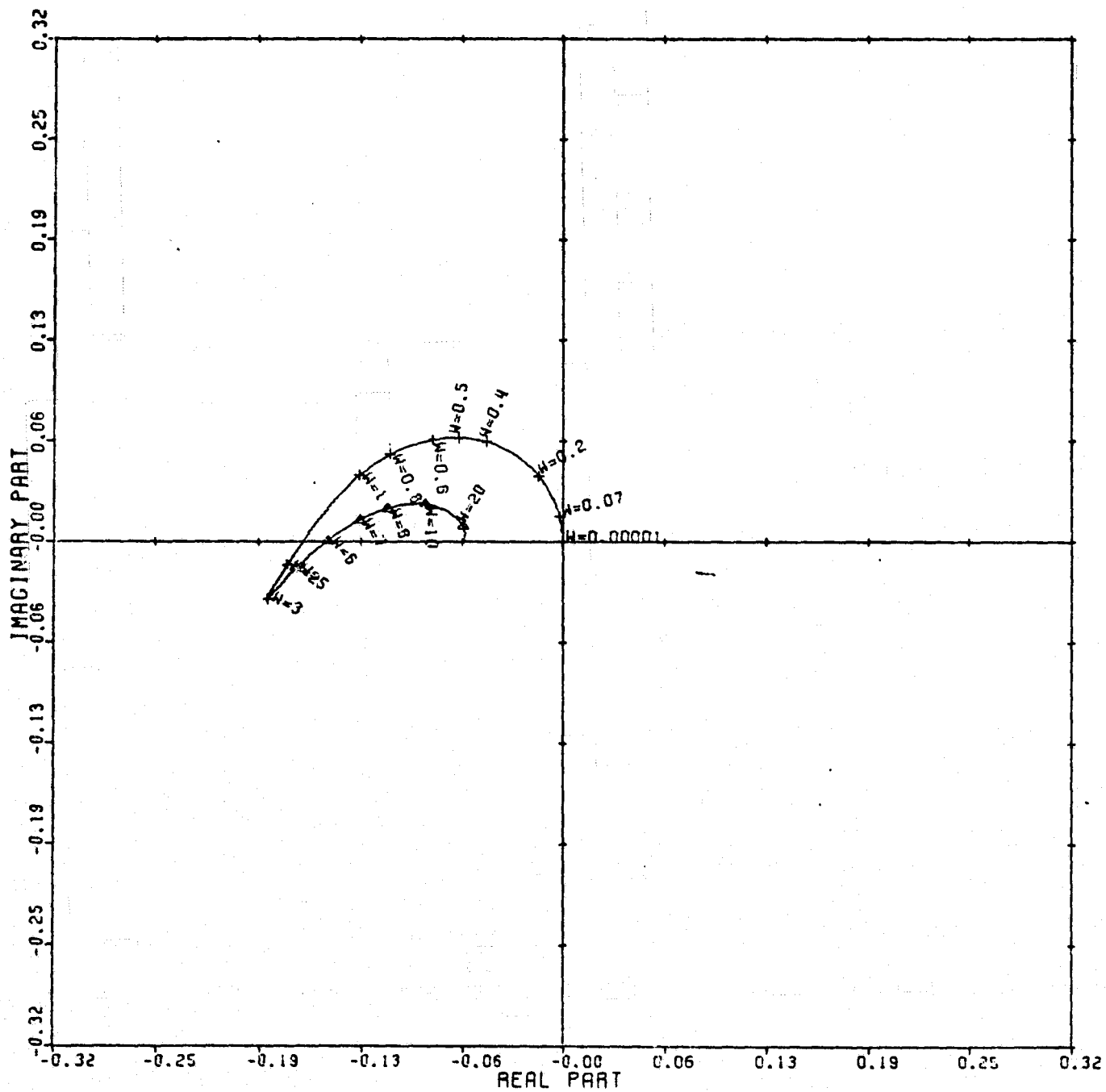
LOCUS OF CENTERS PLOT: 4,2 ENTRY: 1/G(0), 6/24/78.

INPUTS = 4, SYSTEM ORDER = 6, ANALYSIS TYPE = 11

Figure 85
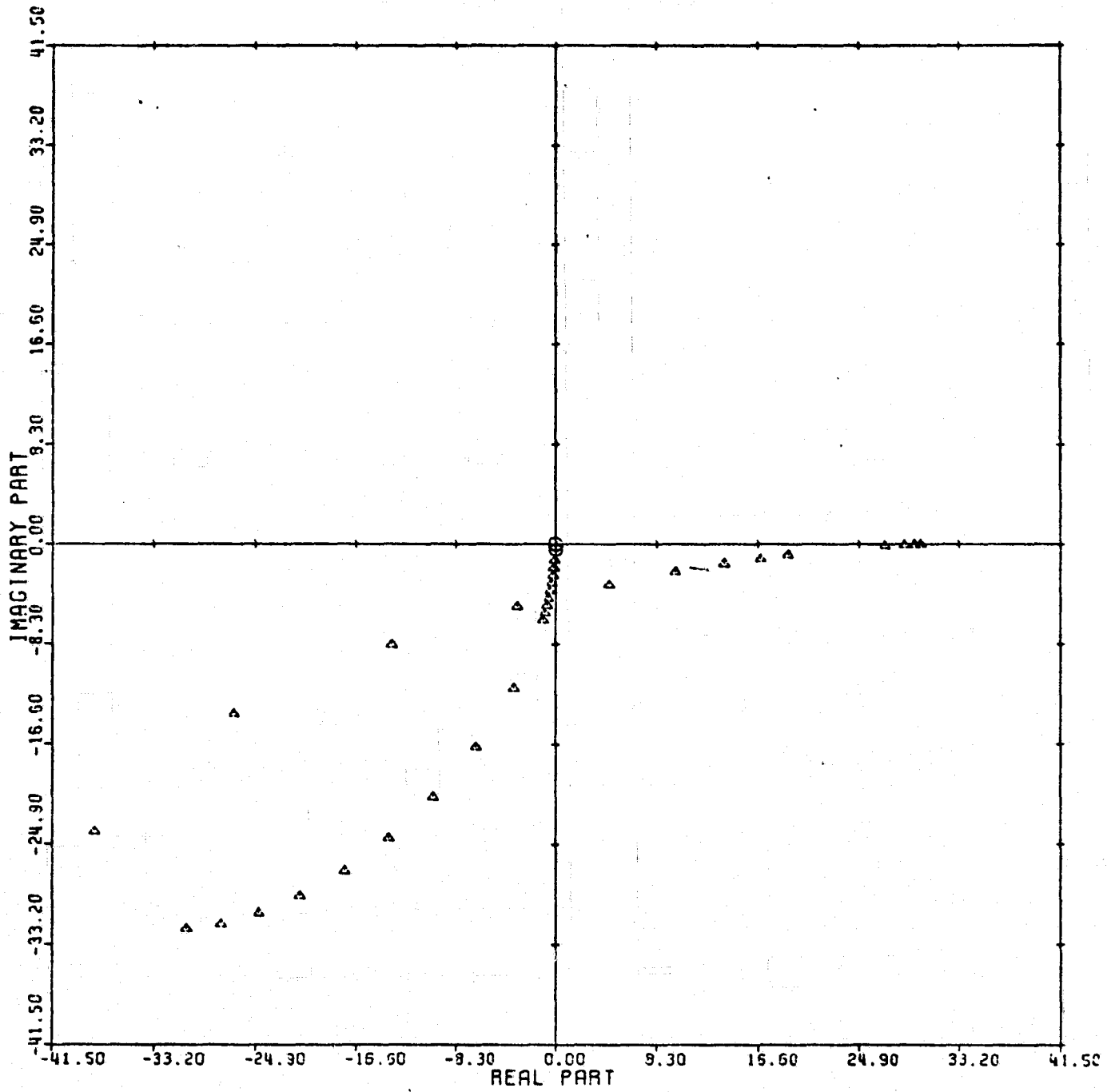
CARDIAD PLOT: 1,3 ENTRY: 1/G(0), 6/24/78.

INPUTS = 4, SYSTEM ORDER = 6, ANALYSIS TYPE = 11

Figure 86
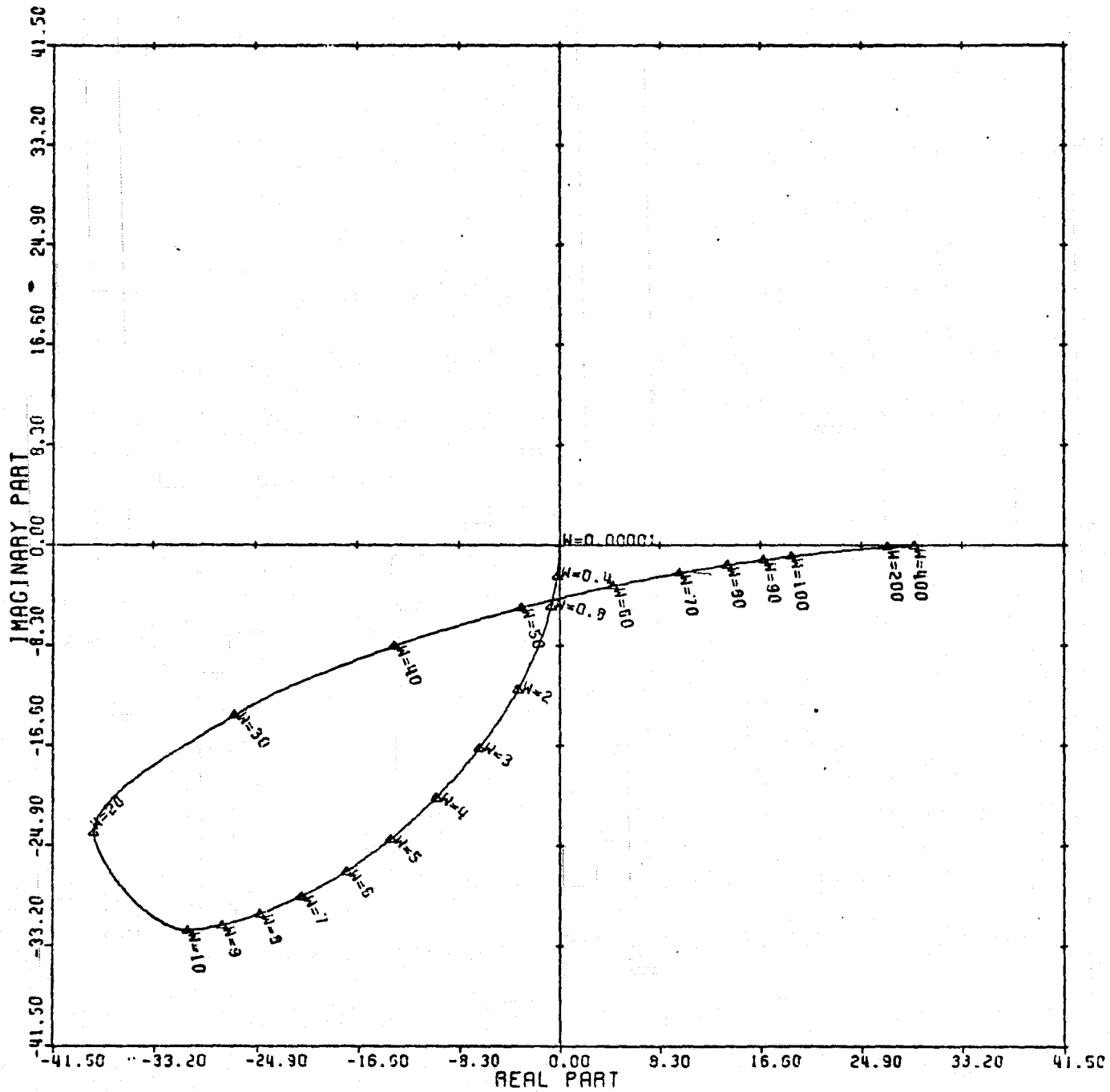
LOCUS OF CENTERS PLOT: 1,3 ENTRY: 1/G(0), 6/24/78.

INPUTS = 4, SYSTEM ORDER = 6, ANALYSIS TYPE = 11

Figure 87
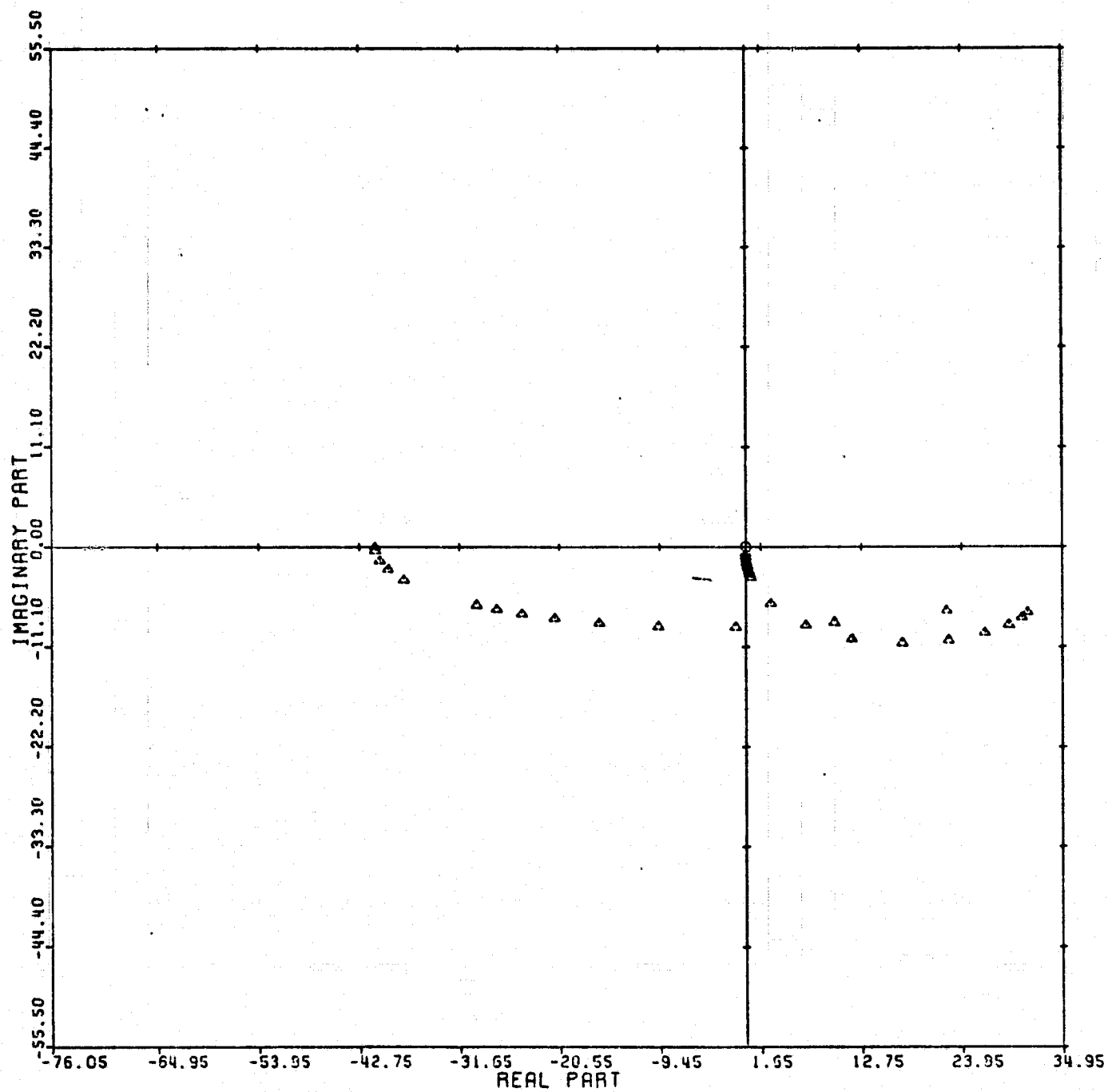
CARDIAD PLOT: 2,3 ENTRY: 1/G(0), 6/24/78.

INPUTS = 4, SYSTEM ORDER = 6, ANALYSIS TYPE = 11

Figure 88
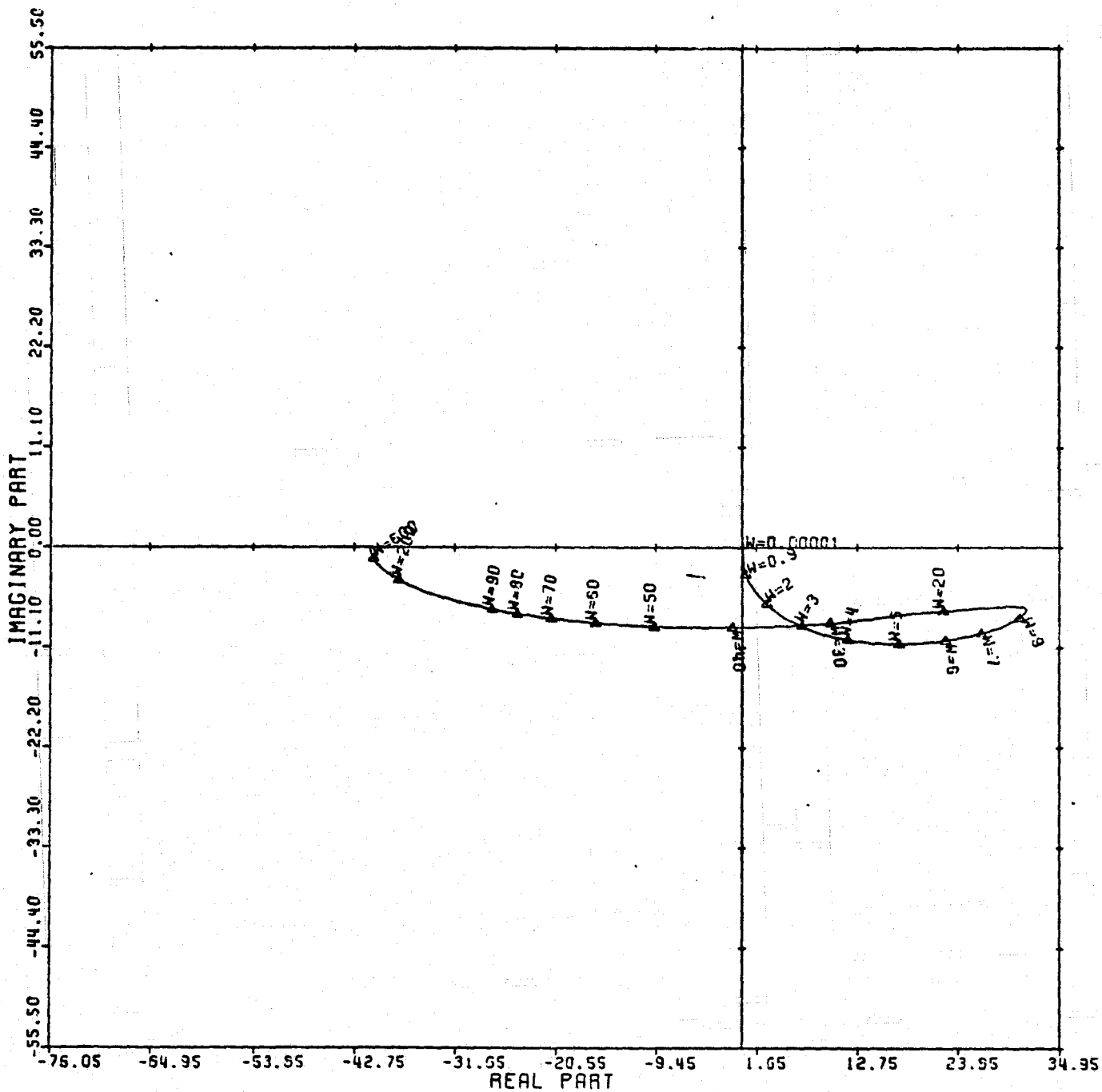
LOCUS OF CENTERS PLOT: 2,3 ENTRY: 1/G(0), 6/24/78.

INPUTS = 4, SYSTEM ORDER = 6, ANALYSIS TYPE = 11

Figure 89
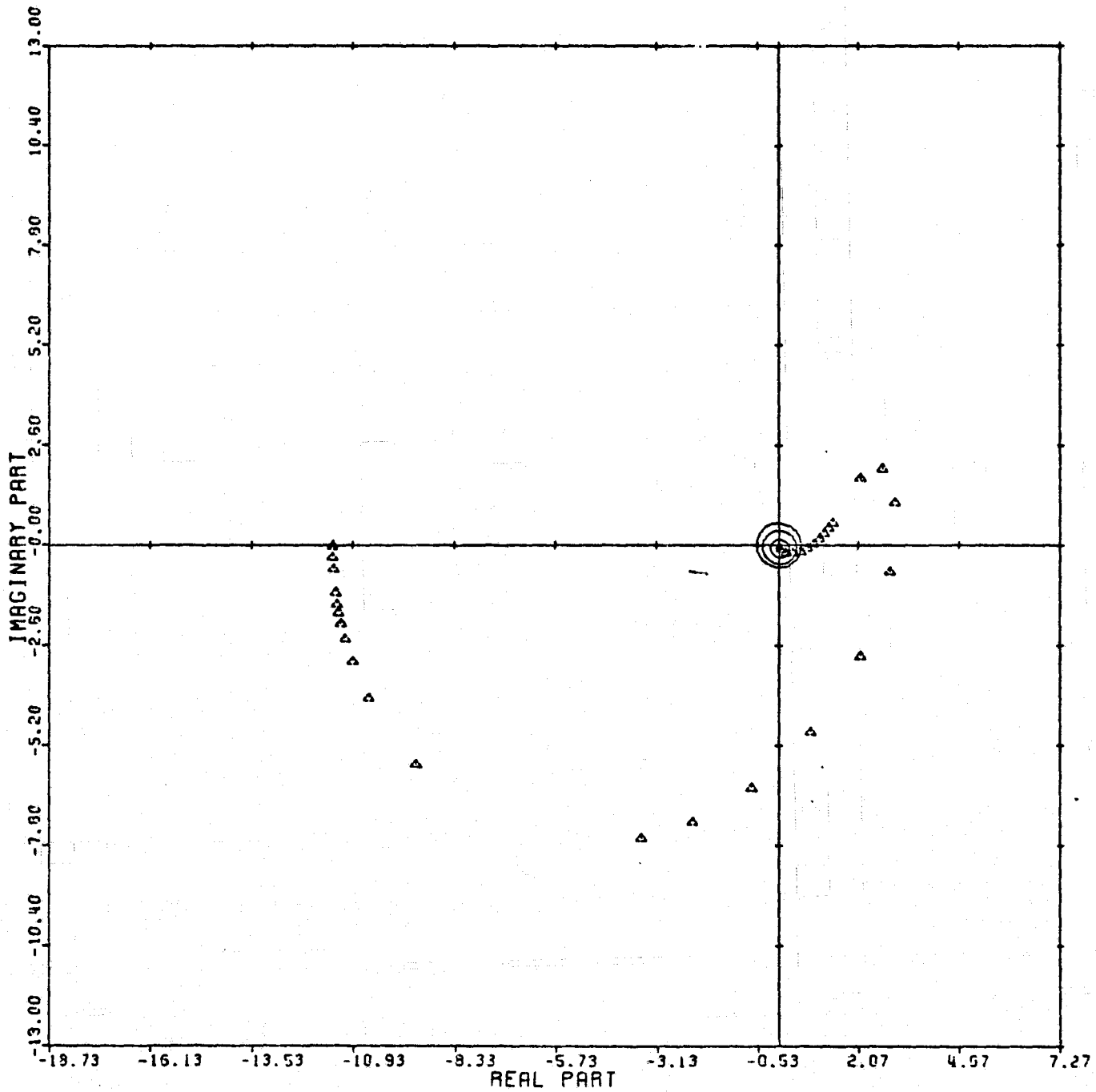
CARDIAD PLOT: 4,3 ENTRY: 1/G(0), 6/24/78.

INPUTS = 4, SYSTEM ORDER = 6, ANALYSIS TYPE = 11

Figure 90
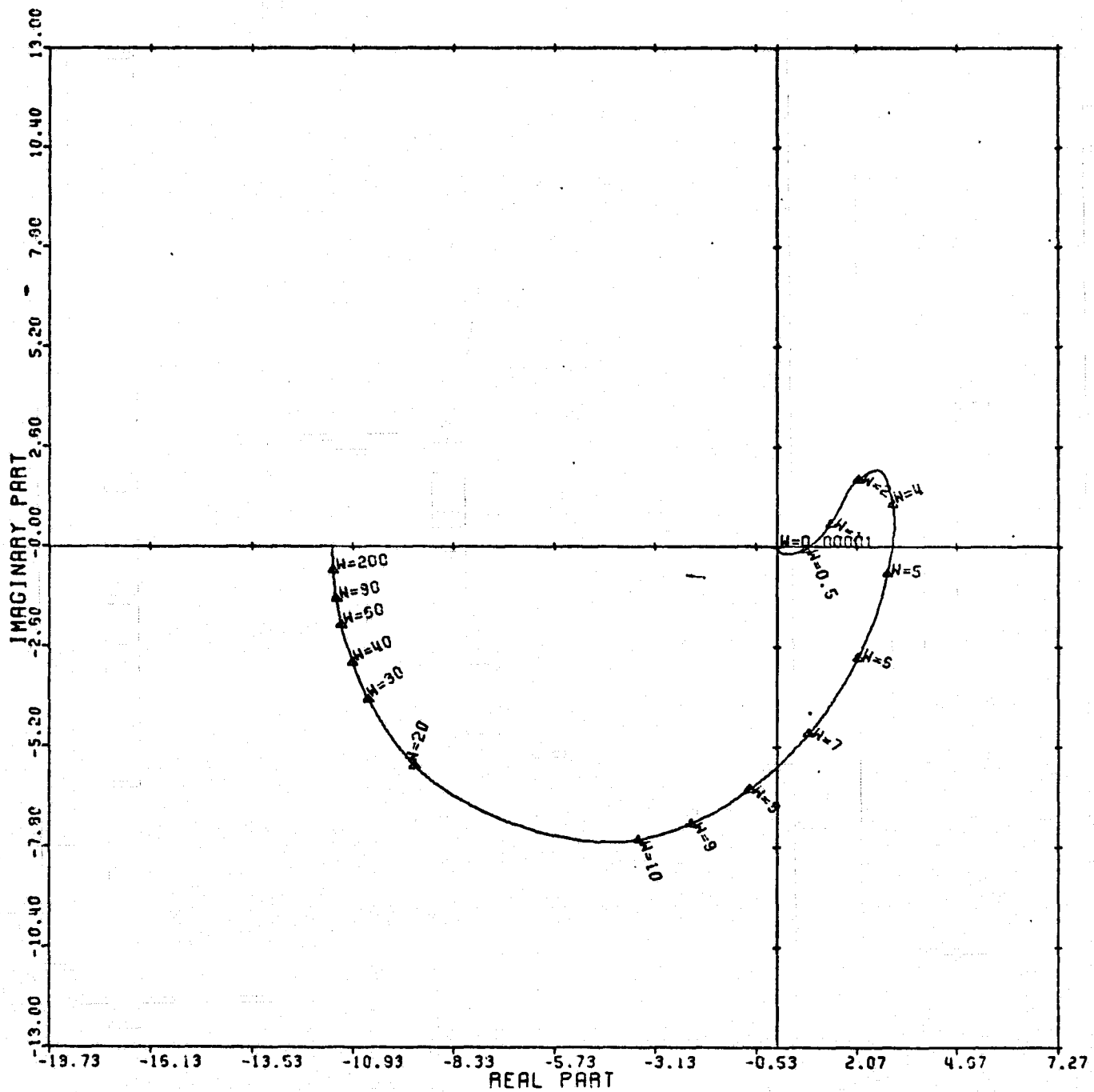
LOCUS OF CENTERS PLOT: 4.3 ENTRY: 1/G(0), 6/24/78.

INPUTS = 4, SYSTEM ORDER = 6, ANALYSIS TYPE = 11

Figure 91
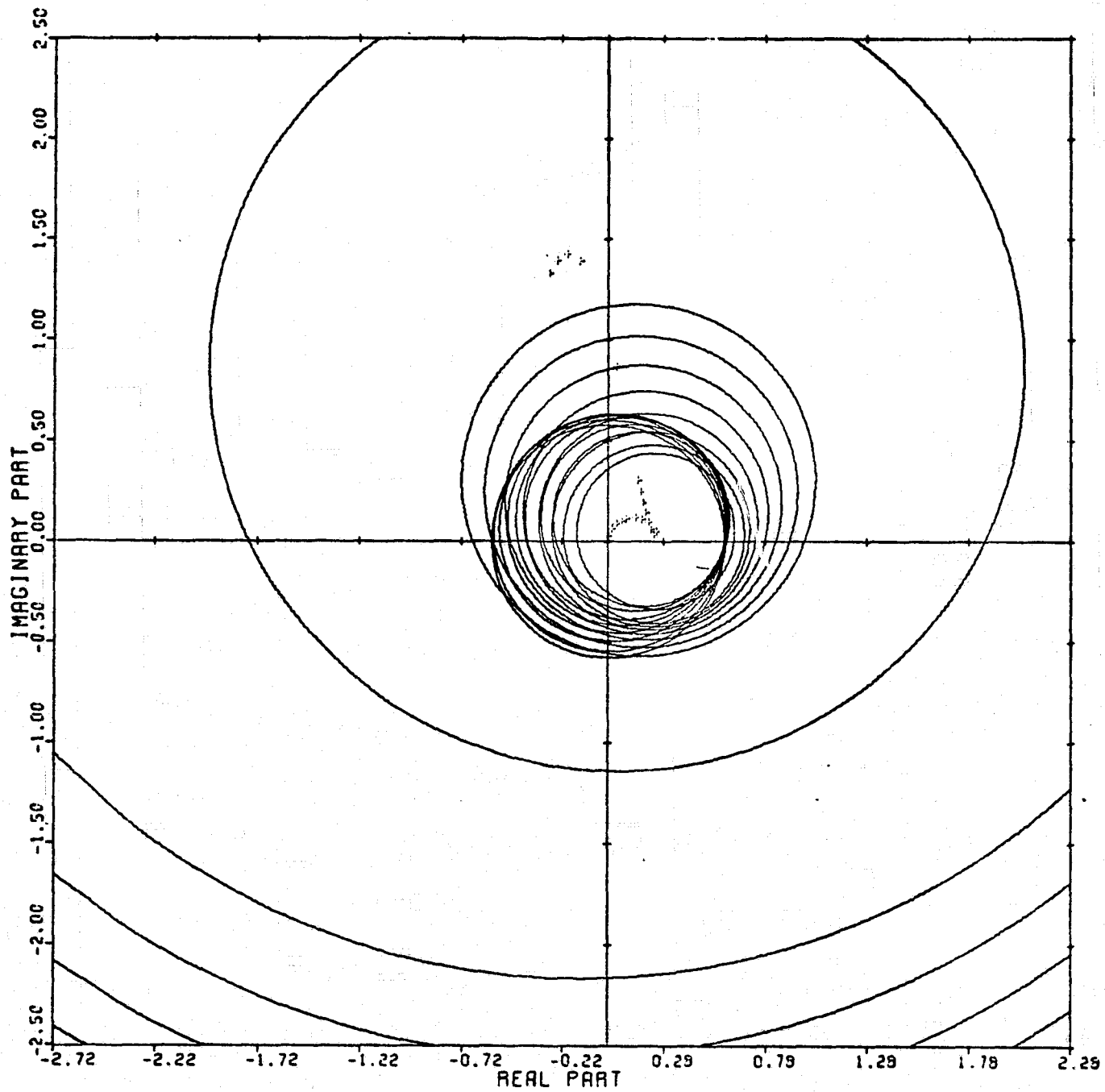
CARDIAD PLOT: 1.4 ENTRY: 1/G(0). 6/24/78.

INPUTS = 4. SYSTEM ORDER = G. ANALYSIS TYPE = 11

Figure 92
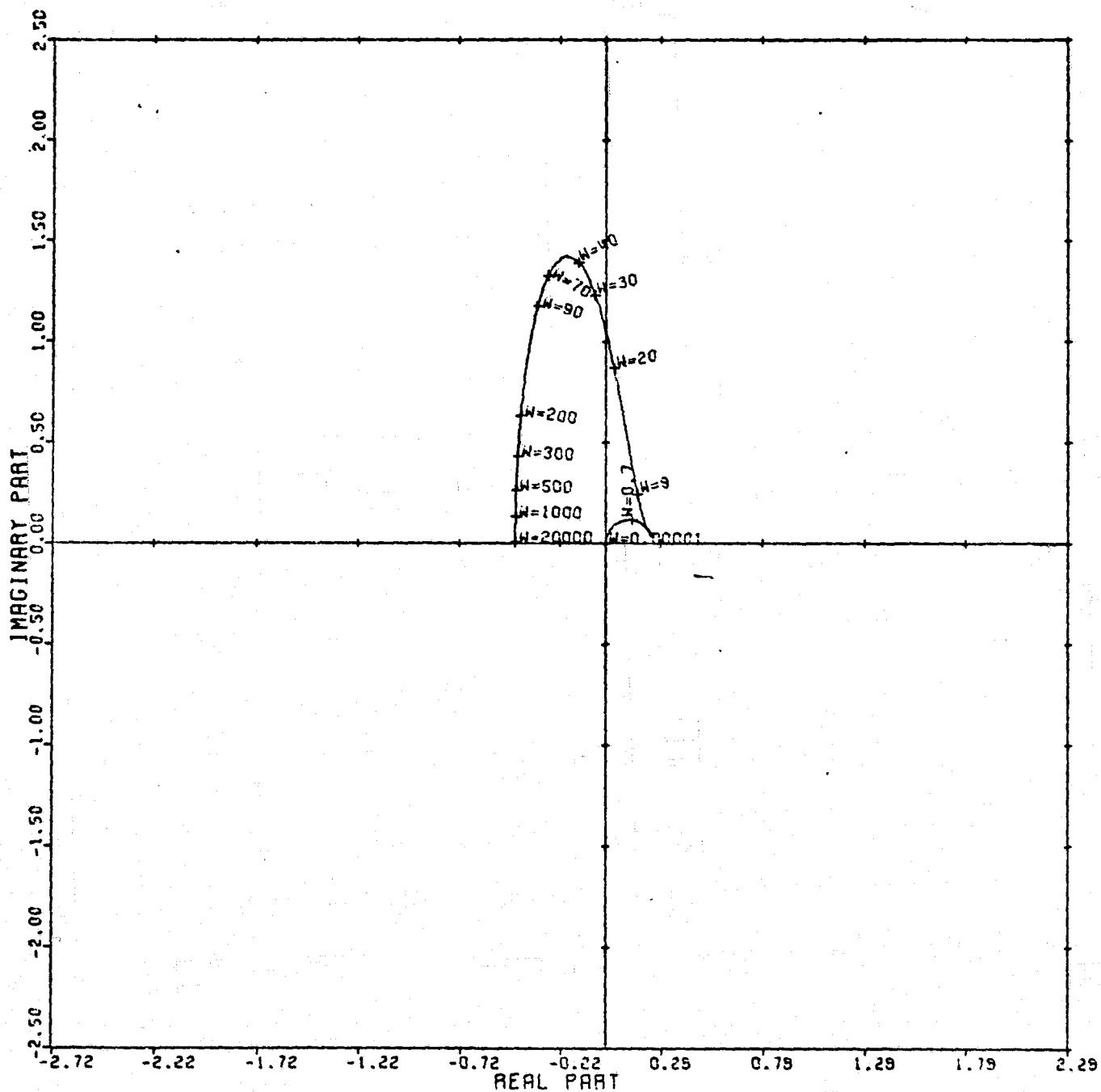
LOCUS OF CENTERS PLOT: 1,4 ENTRY: 1/G(0), 6/24/78.

INPUTS = 4, SYSTEM ORDER = 6, ANALYSIS TYPE = 11

Figure 93
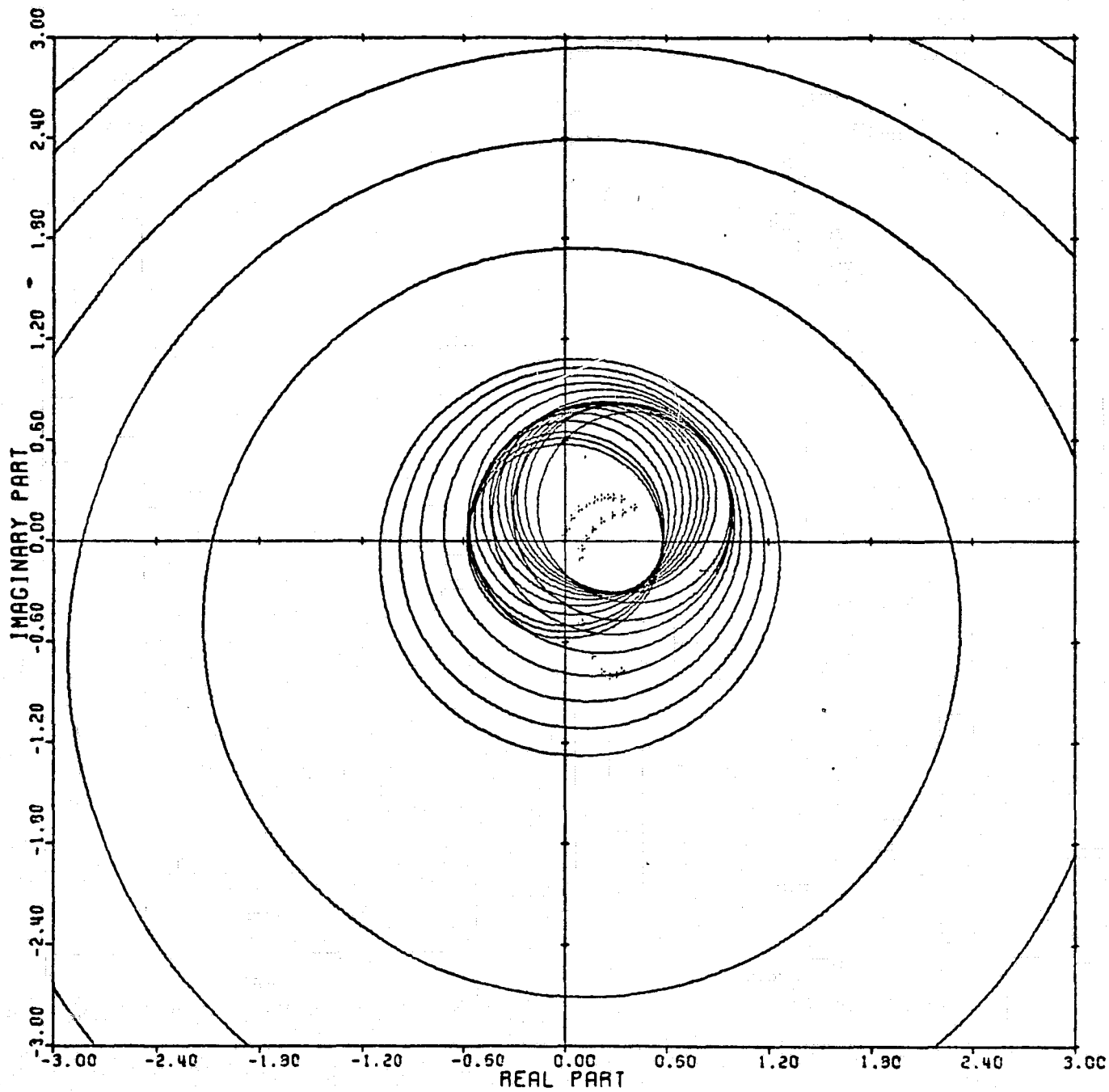
CARDIAD PLOT: 2.4 ENTRY: 1/G(0), 6/24/78.

INPUTS = 4, SYSTEM ORDER = 6, ANALYSIS TYPE = 11

Figure 94
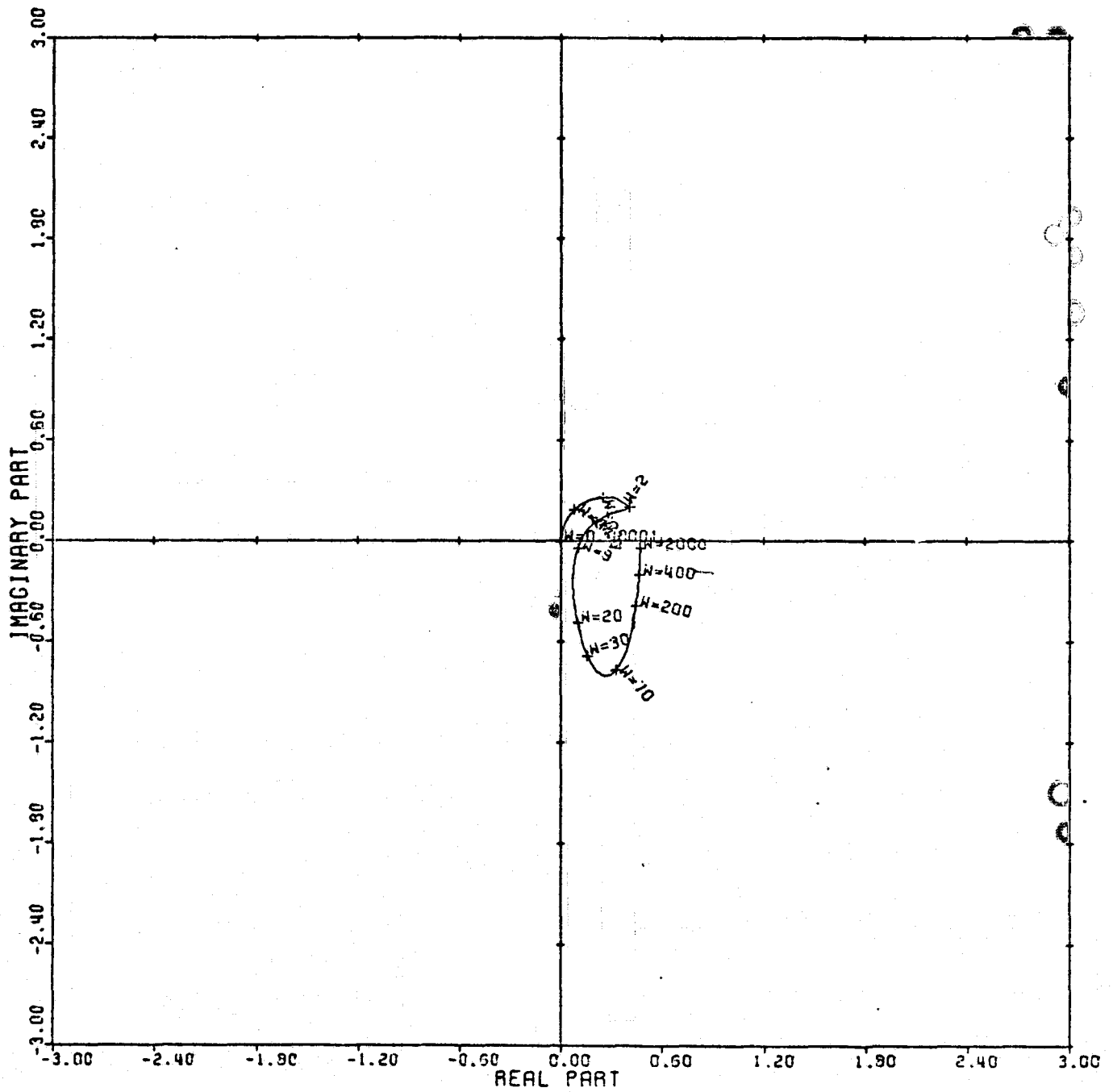
LOCUS OF CENTERS PLOT: 2.4 ENTRY: 1/G(0), 6/24/78.

INPUTS = 4, SYSTEM ORDER = 6, ANALYSIS TYPE = 11

Figure 95
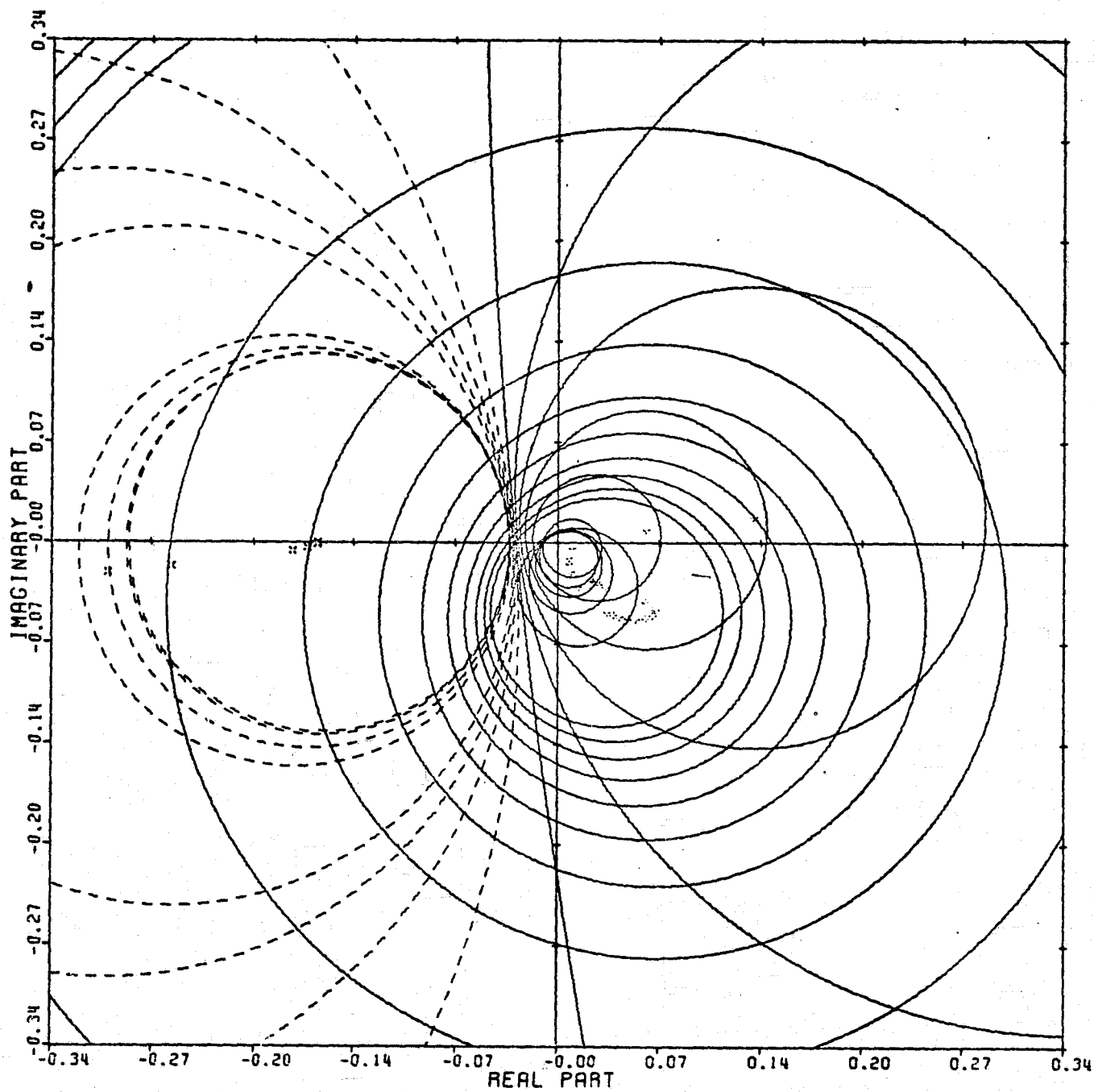
CARDIAD PLOT: 3.4 ENTRY: 1/G(0). 6/24/78.

INPUTS = 4, SYSTEM ORDER = 6, ANALYSIS TYPE = 11

Figure 96
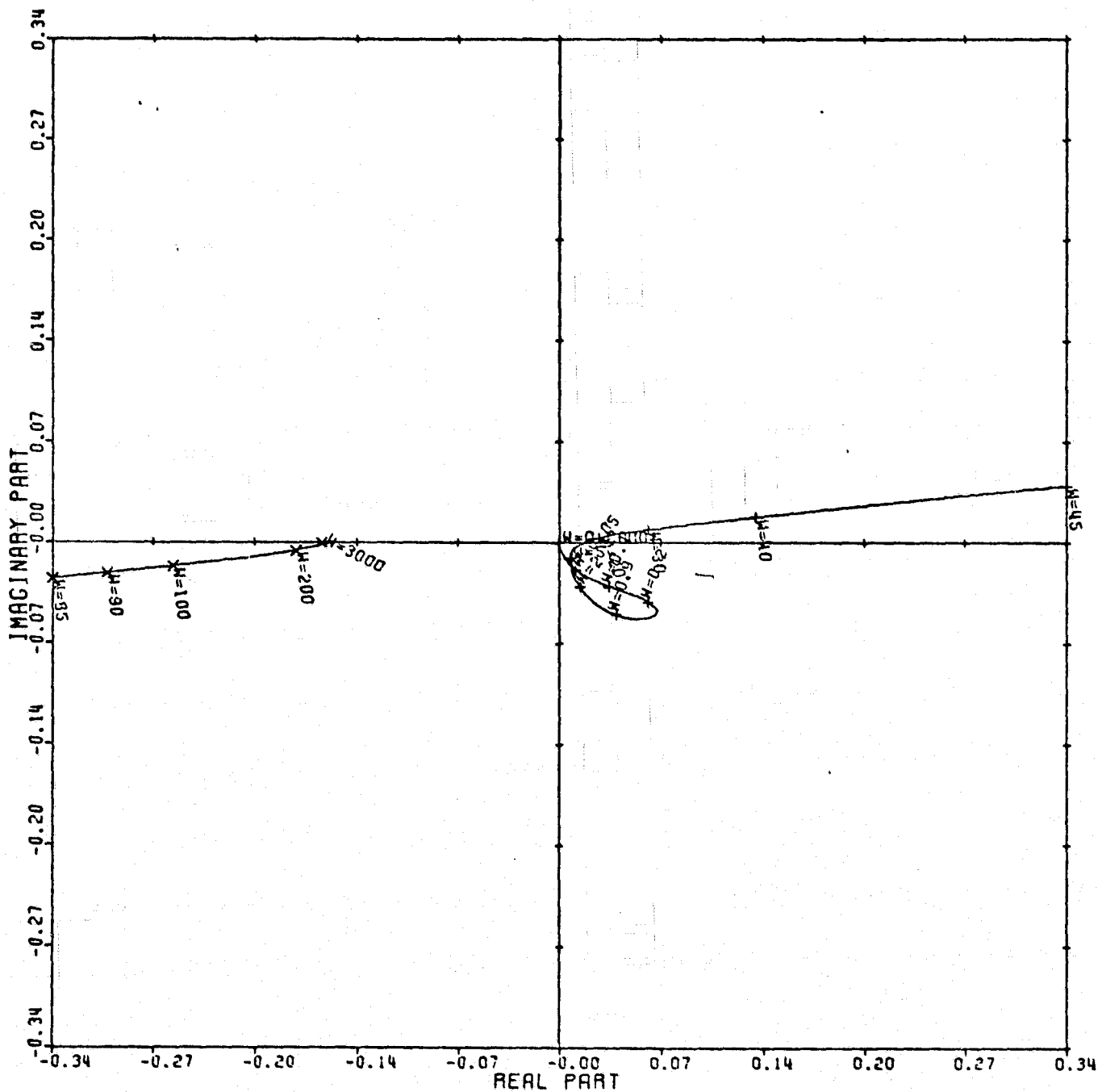
LOCUS OF CENTERS PLOT: 3,4 ENTRY: 1/G(0). 6/24/78.

INPUTS = 4, SYSTEM ORDER = 6, ANALYSIS TYPE = 11

Figure 97
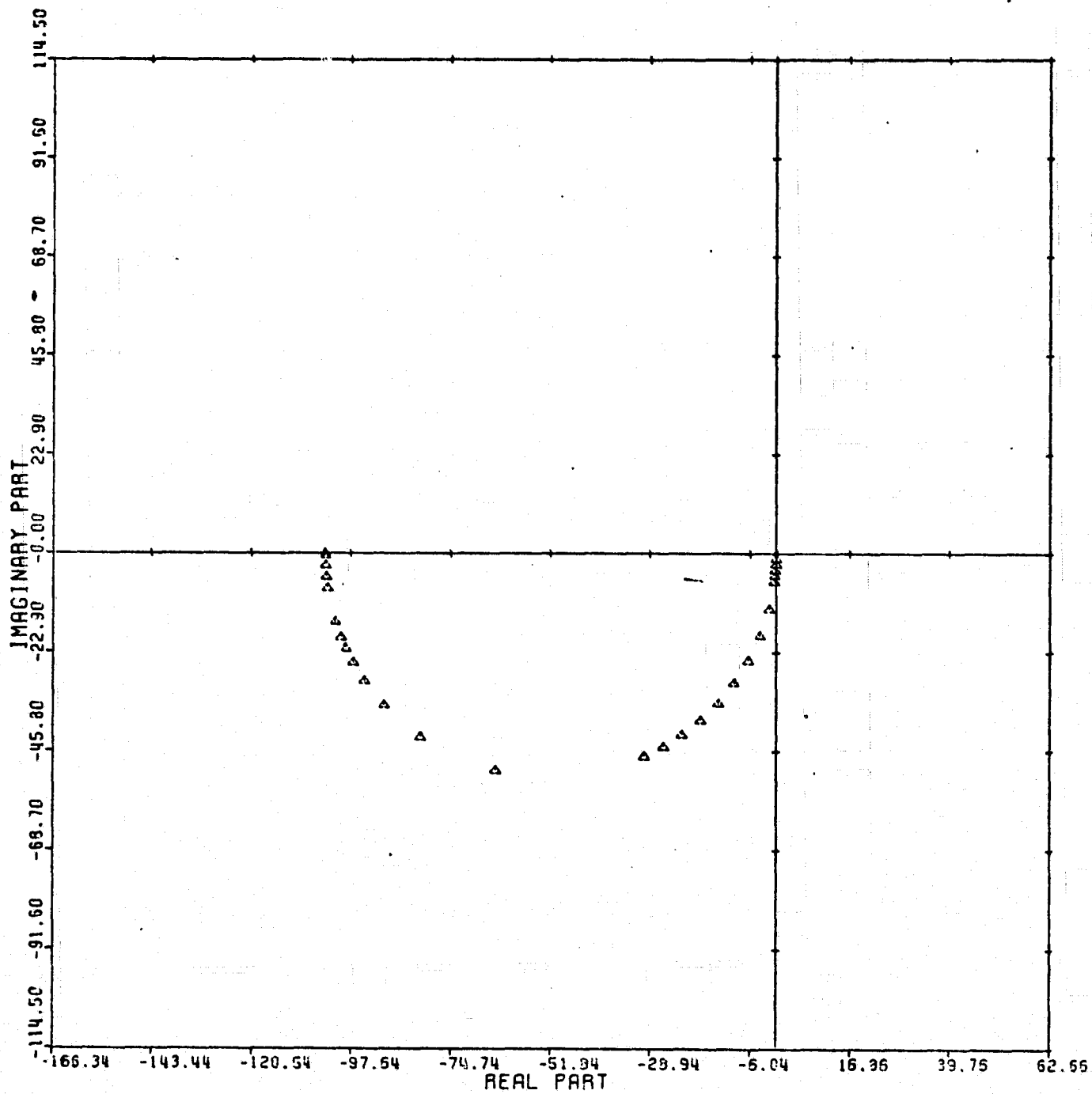
CARDIAD PLOT: 1,3 ENTRY: 1/G (0), 6/24/78.

INPUTS = 4, SYSTEM ORDER = 6, ANALYSIS TYPE = 12

Figure 98
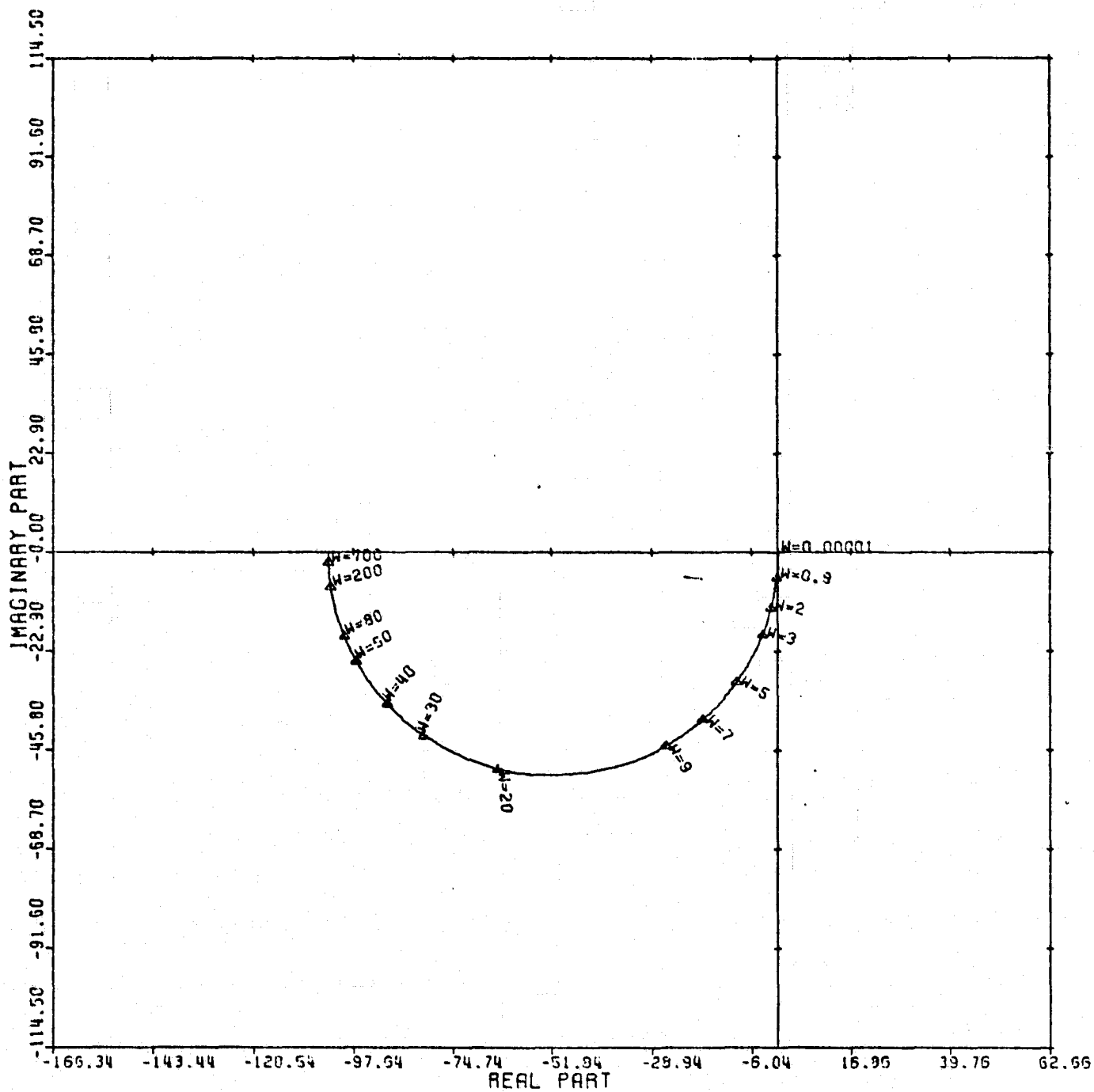
LOCUS OF CENTERS PLOT: 1,3 ENTRY: 1/G(0), 6/24/78.

INPUTS = 4, SYSTEM ORDER = 6, ANALYSIS TYPE = 12

Figure 99
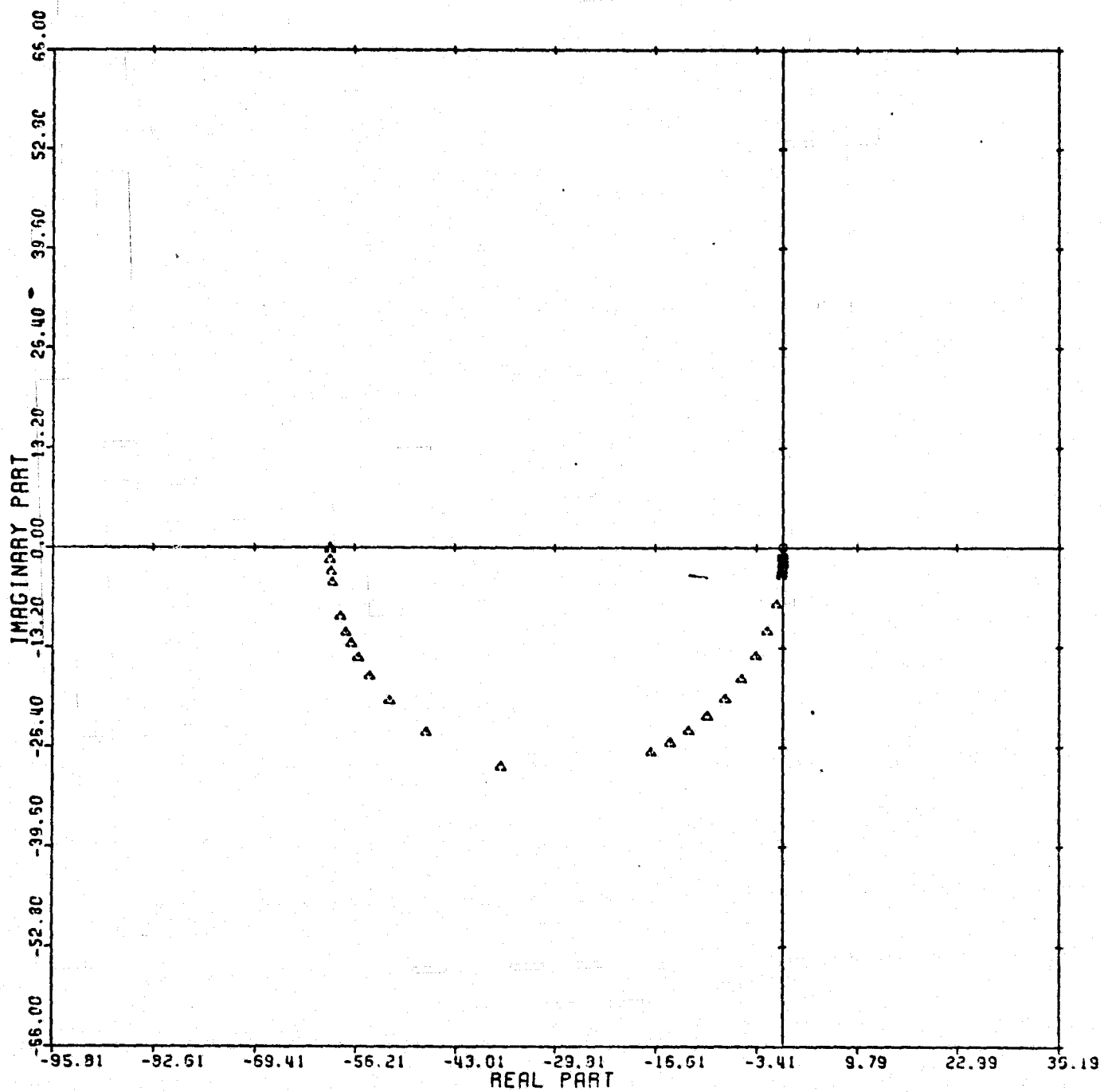
CARDIAD PLOT: 2.3 ENTRY: 1/G(0), 6/24/78.

INPUTS = 4, SYSTEM ORDER = 6, ANALYSIS TYPE = 12

Figure 100
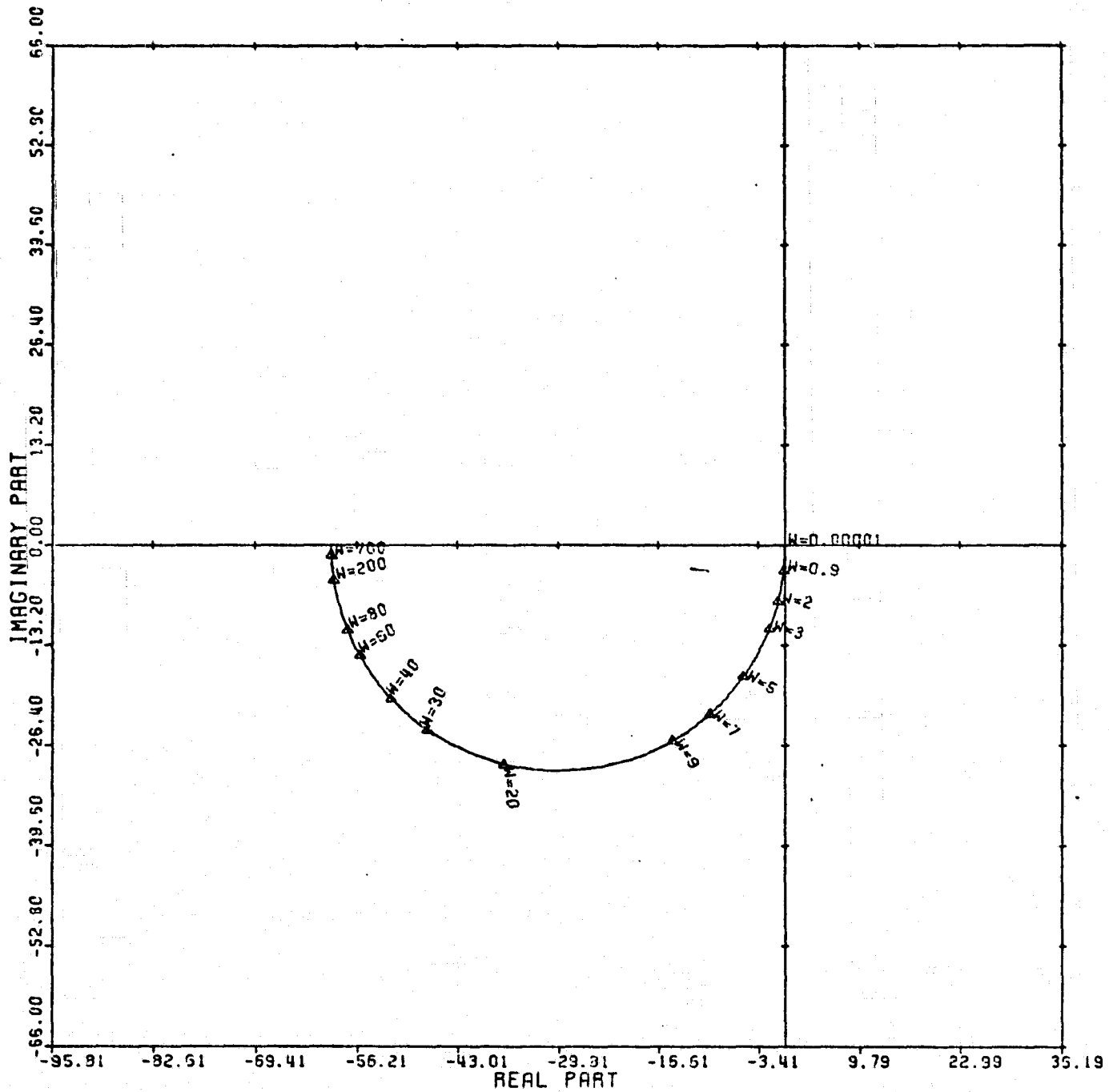
LOCUS OF CENTERS PLOT: 2,3 ENTRY: 1/G(0), 6/24/78.

INPUTS = 4, SYSTEM ORDER = 6, ANALYSIS TYPE = 12

Figure 101
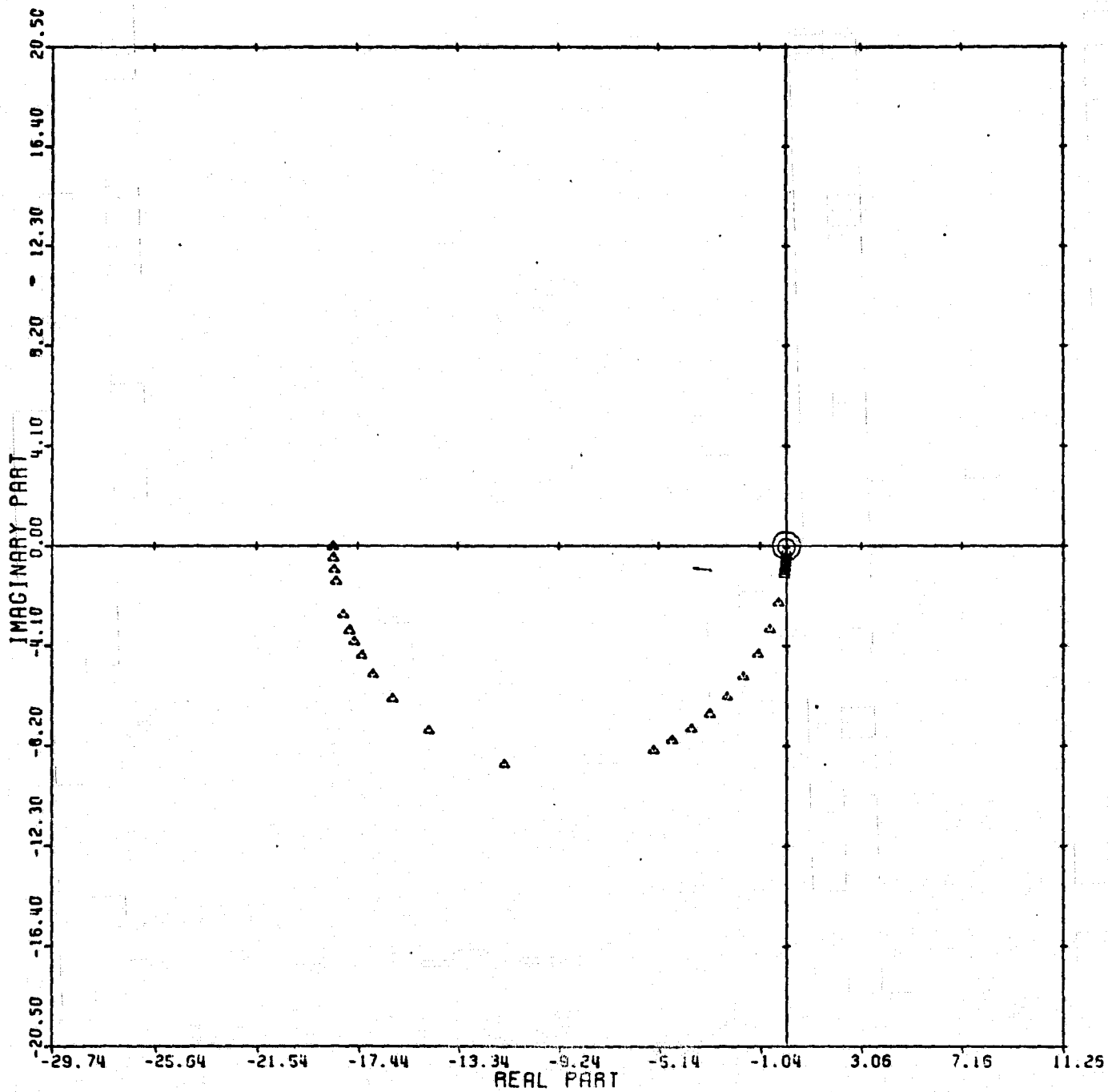
CARDIAO PLOT: 4,3 ENTRY: 1/G(0), 6/24/78.

INPUTS = 4, SYSTEM ORDER = 6, ANALYSIS TYPE = 12

Figure 102
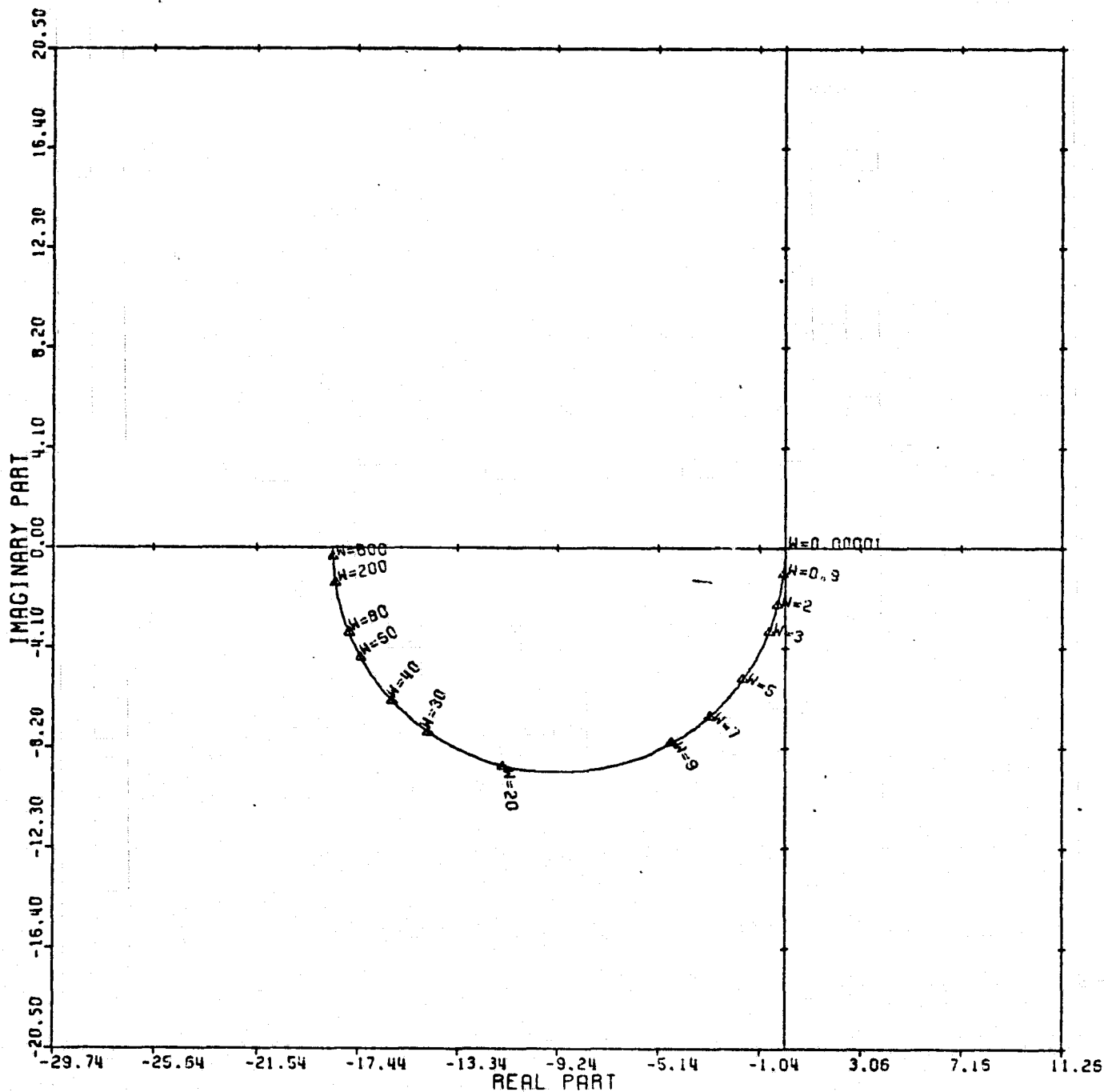
LOCUS OF CENTERS PLOT: 4.3 ENTRY: 1/G(0), 6/24/78.

INPUTS = 4, SYSTEM ORDER = 6, ANALYSIS TYPE = 12

Figure 103
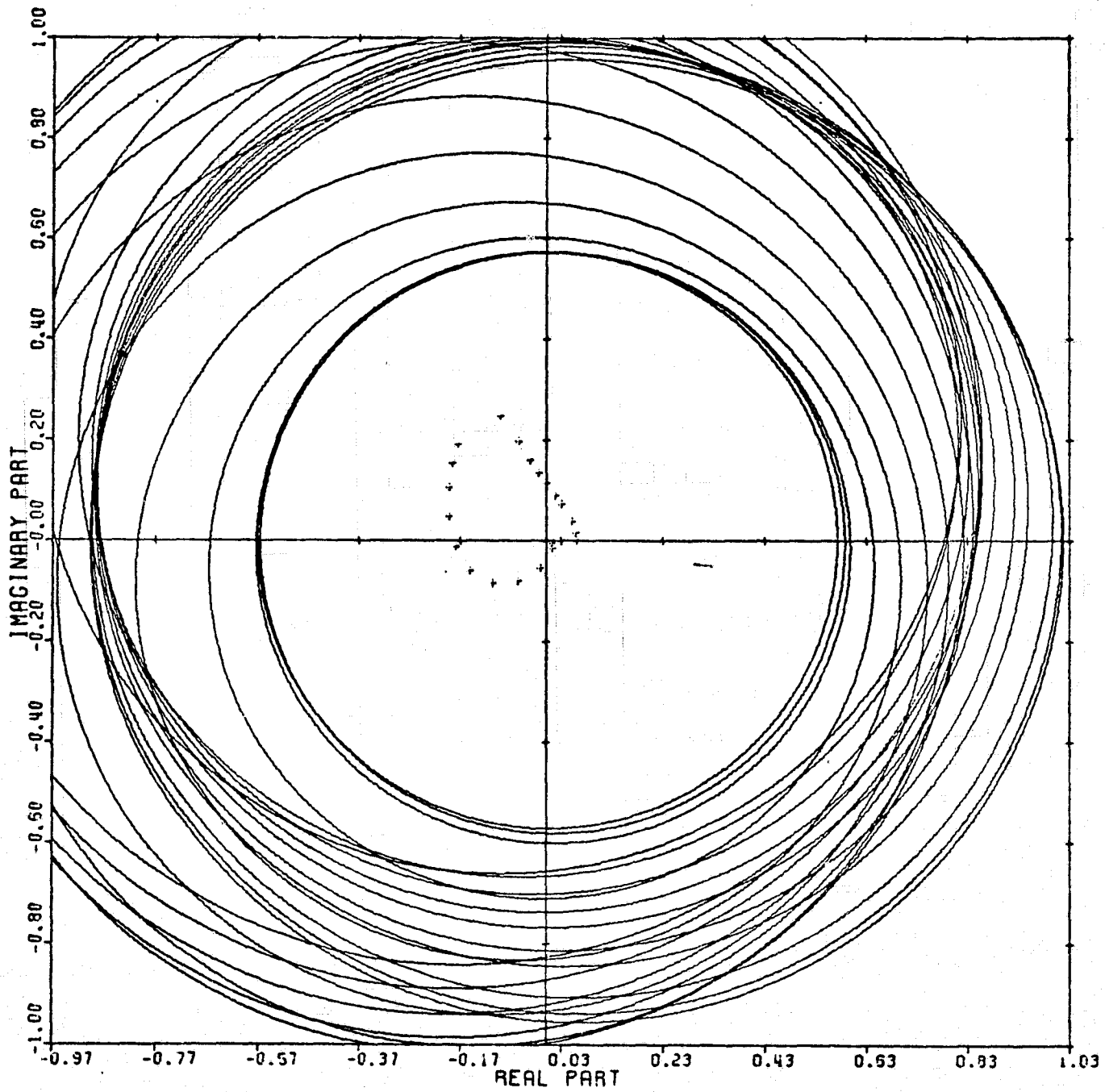
CARDIAD PLOT: 2,1 ENTRY: KMP 1, 1/G(0), 6/25/78.

INPUTS = 4, SYSTEM ORDER = 6, ANALYSIS TYPE = 11

Figure 104
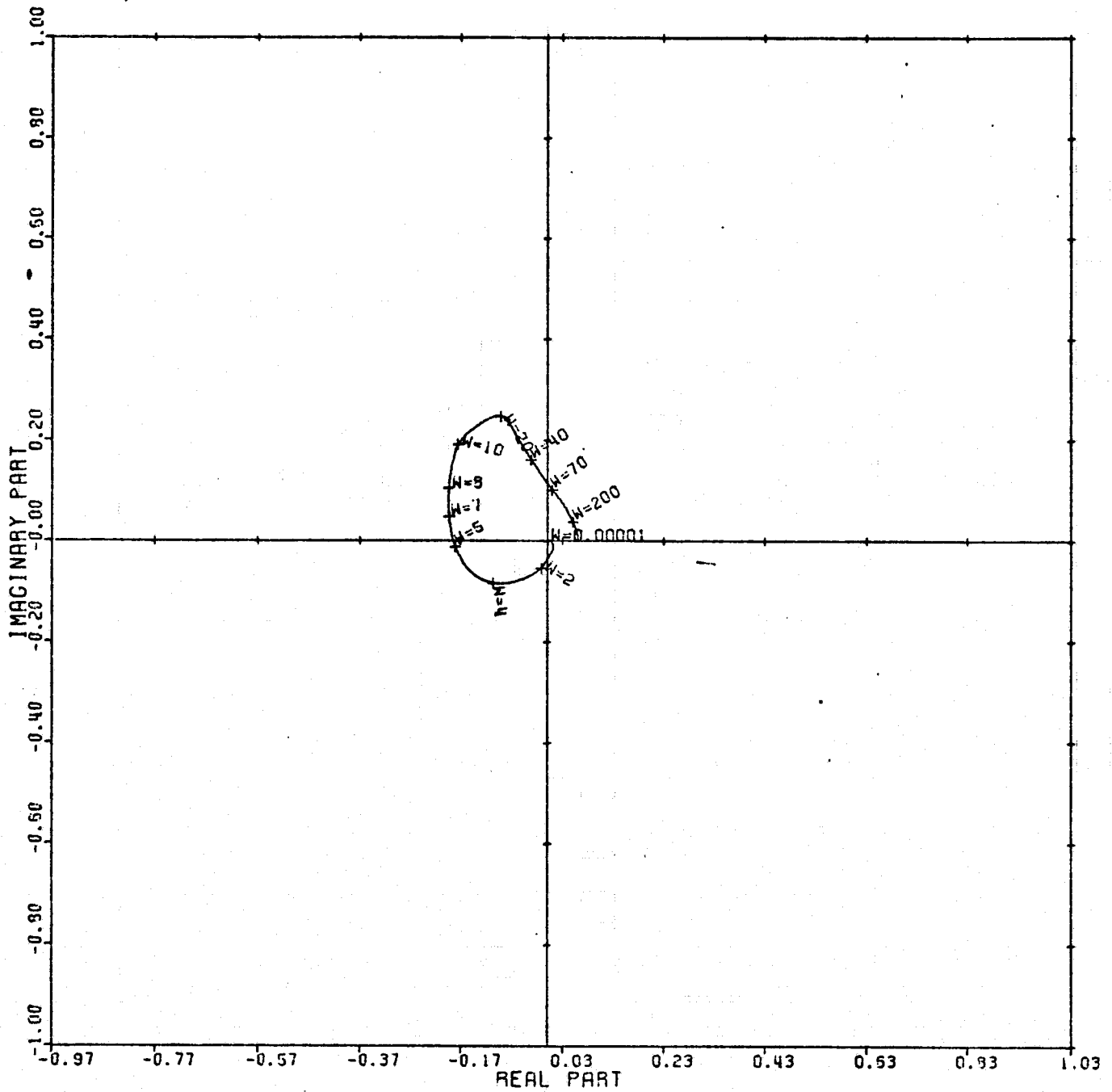
LOCUS OF CENTERS PLOT: 2,1 ENTRY: KMP 1, 1/G(0), 6/25/78.

INPUTS = 4, SYSTEM ORDER = 6, ANALYSIS TYPE = 11

Figure 105
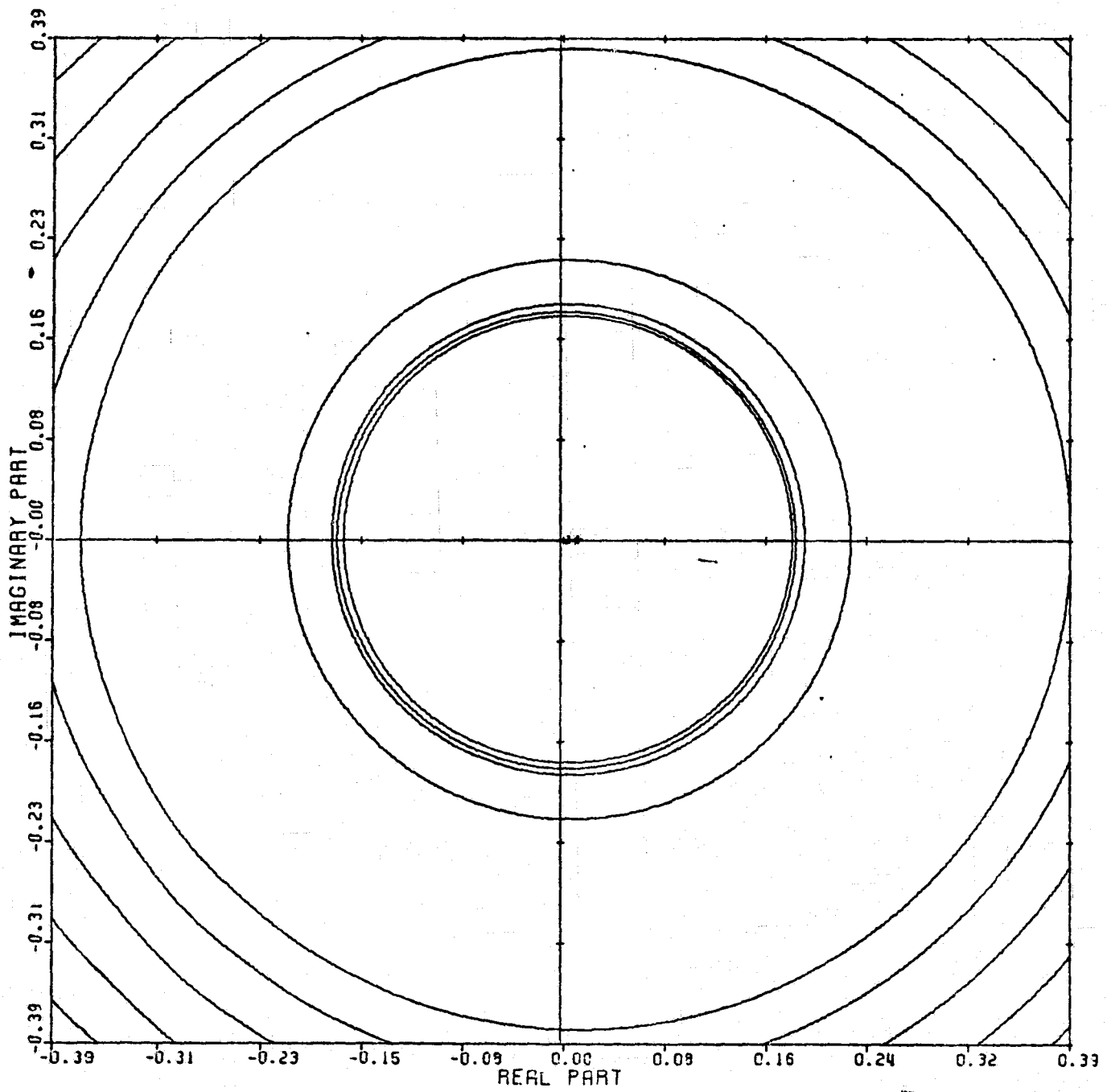
CARDIAD PLOT: 3,1 ENTRY: KMP 1, 1/G(0), 6/25/78.

INPUTS = 4, SYSTEM ORDER = 6, ANALYSIS TYPE = 11

Figure 106
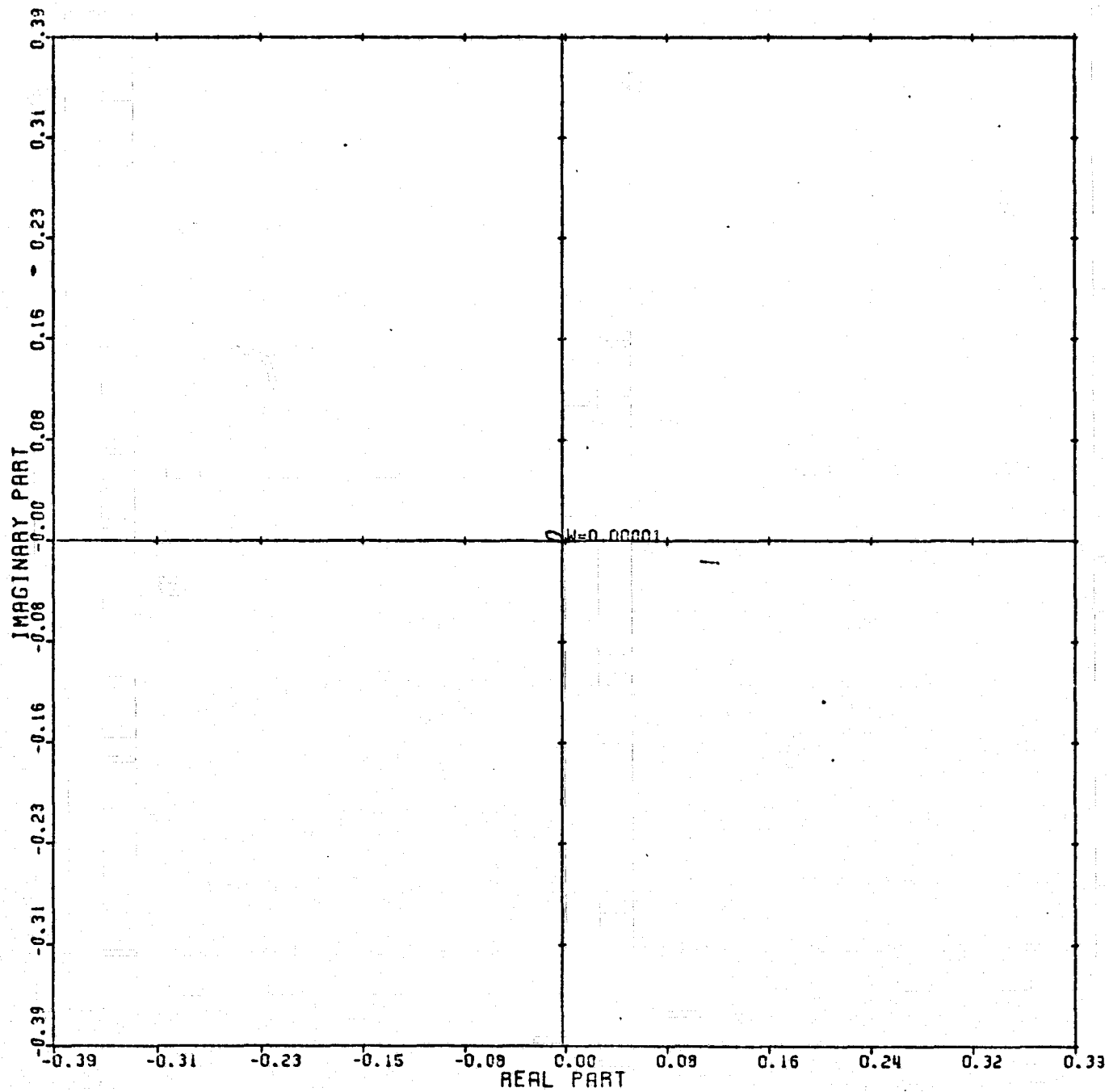
LOCUS OF CENTERS PLOT: 3.1 ENTRY: KMP 1, 1/G(0), 6/25/78.

INPUTS = 4, SYSTEM ORDER = 6, ANALYSIS TYPE = 11

Figure 107
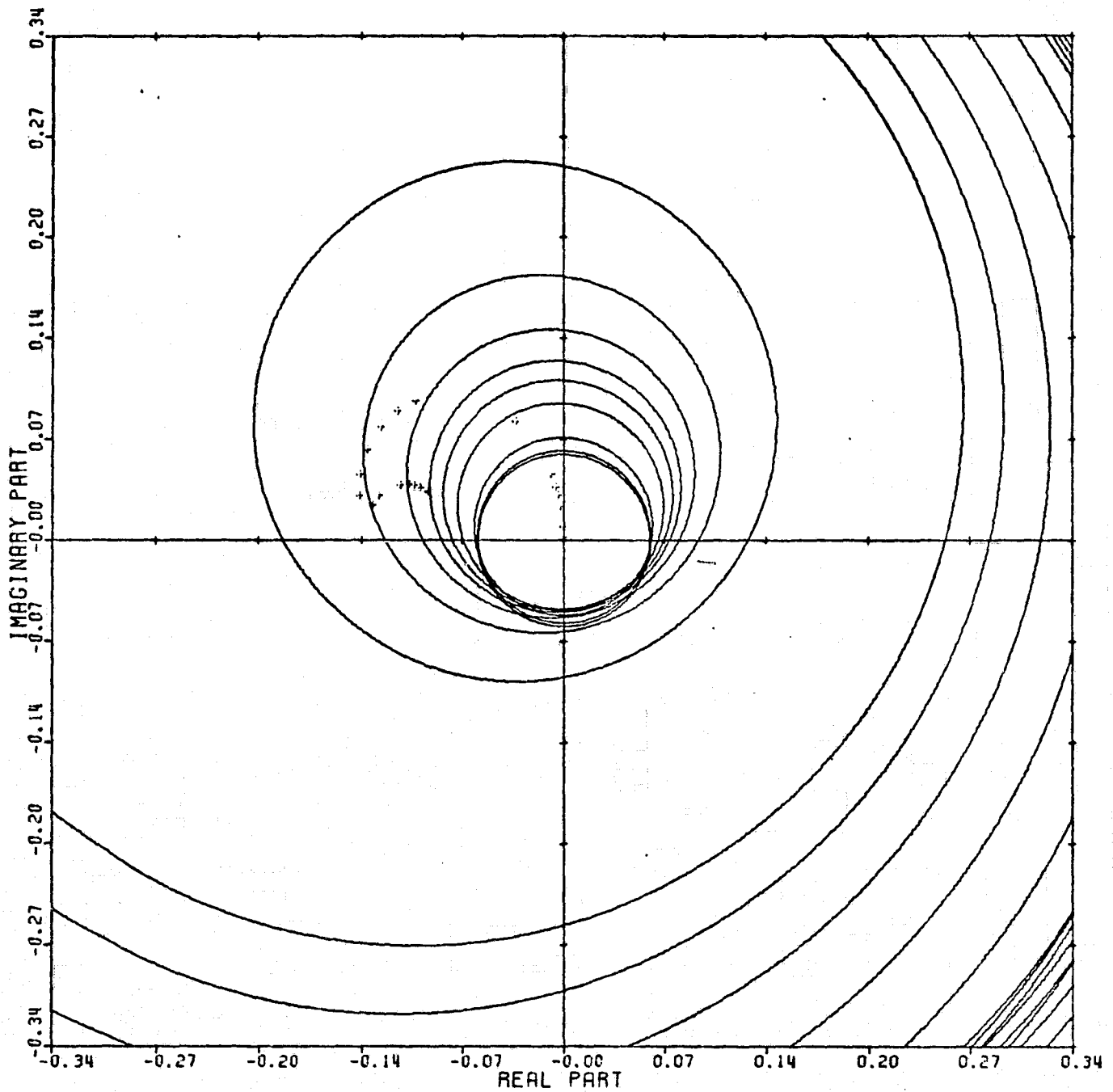
CARDIAD PLOT: 4.1 ENTRY: KMP 1, 1/G(0), 6/25/78.

INPUTS = 4, SYSTEM ORDER = 6, ANALYSIS TYPE = 11

Figure 108
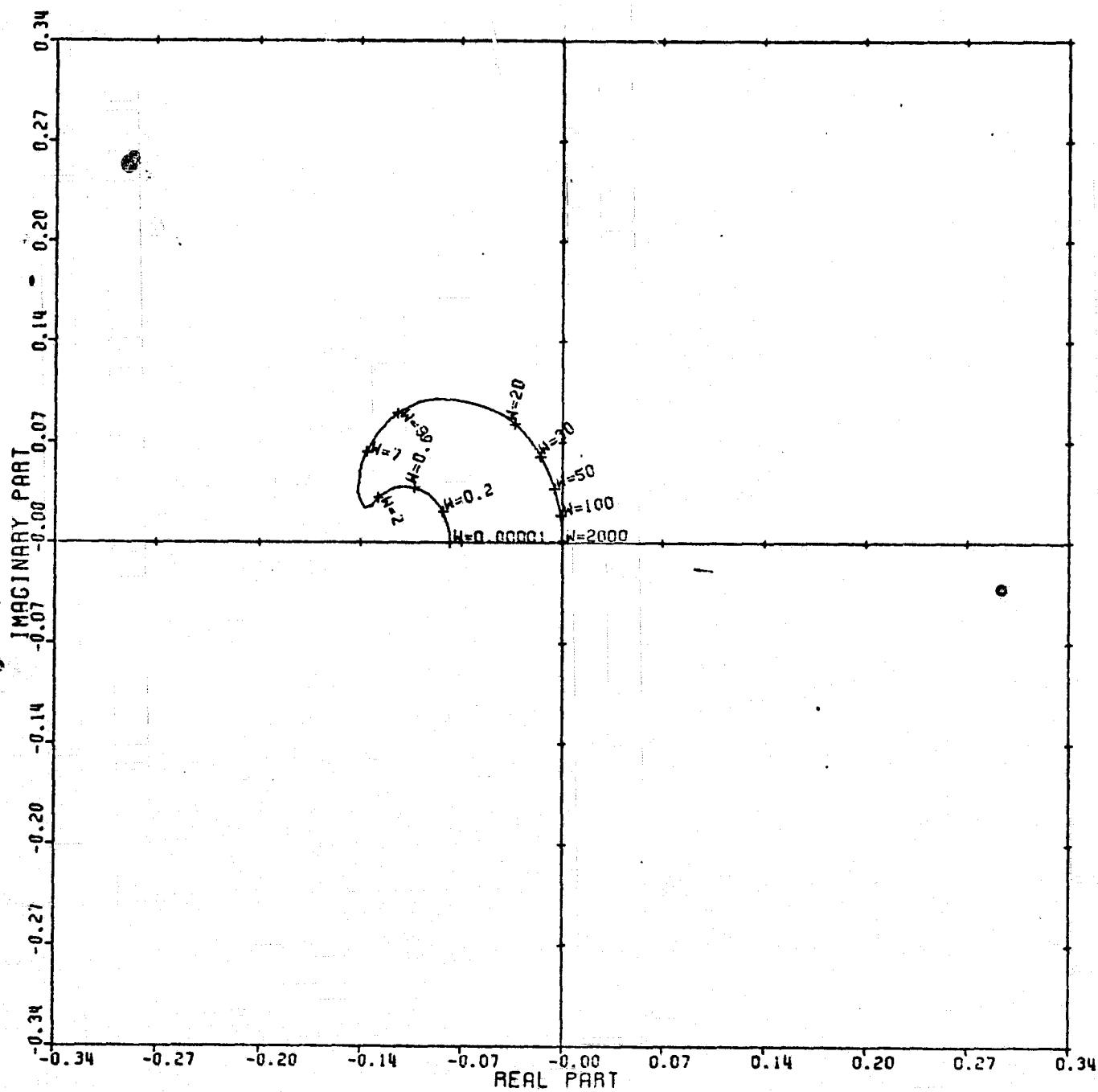
LOCUS OF CENTERS PLOT: 4,1 ENTRY: KMP 1, 1/G(0), 6/25/78.

INPUTS = 4, SYSTEM ORDER = 6, ANALYSIS TYPE = 11

Figure 109
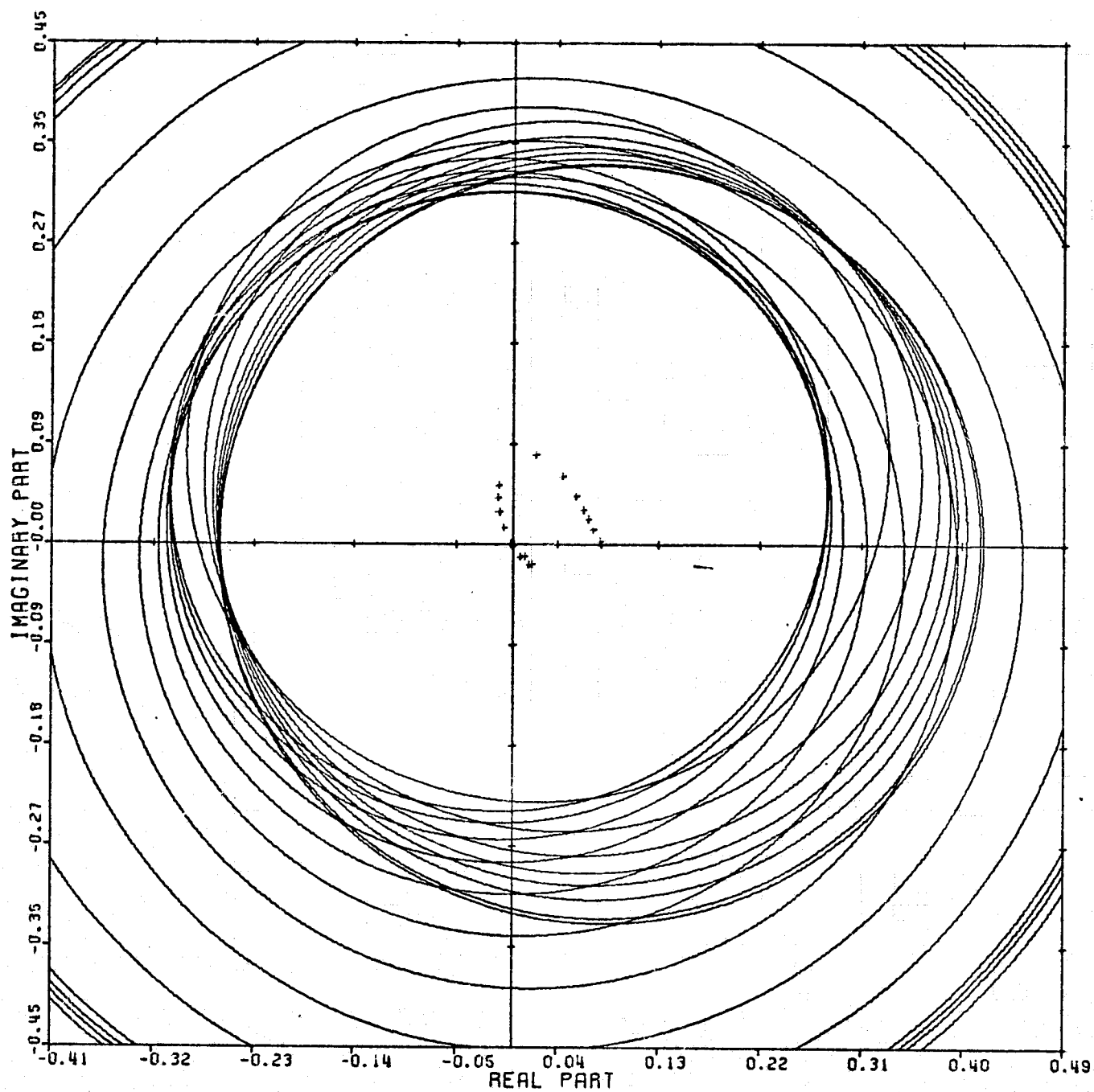
CARDIAD PLOT: 1,2 ENTRY: KMP 1, 1/G(0), 6/25/78.

INPUTS = 4, SYSTEM ORDER = 6, ANALYSIS TYPE = 11
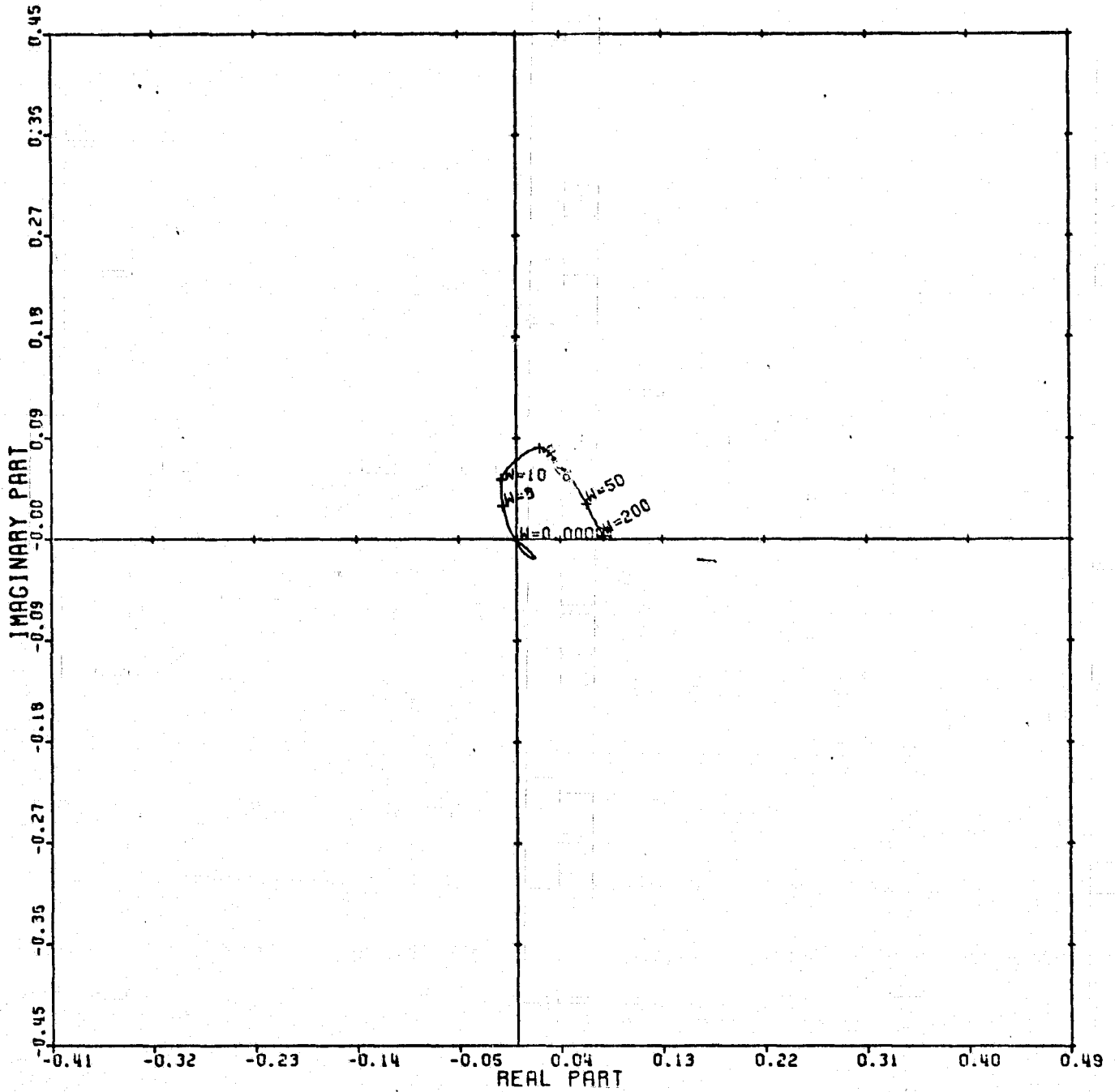
Figure 110

LOCUS OF CENTERS PLOT: 1,2 ENTRY: KMP 1, 1/G(0), 6/25/78.

INPUTS = 4, SYSTEM ORDER = 6, ANALYSIS TYPE = 11

Figure 111
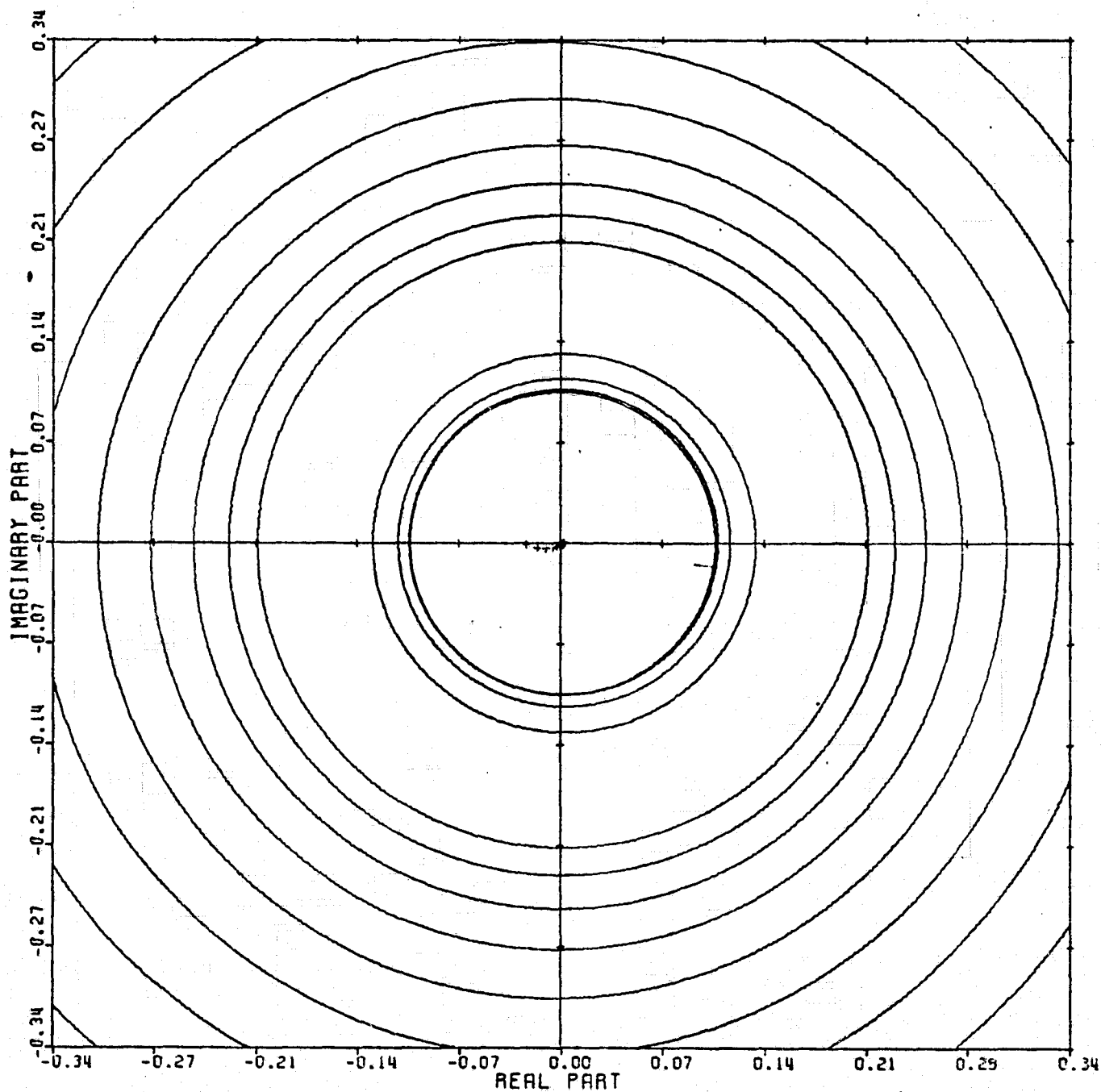
CARDIAD PLOT: 3.2 ENTRY: KMP 1, 1/G(0), 6/25/78.

INPUTS = 4, SYSTEM ORDER = .G, ANALYSIS TYPE = 11

Figure 112
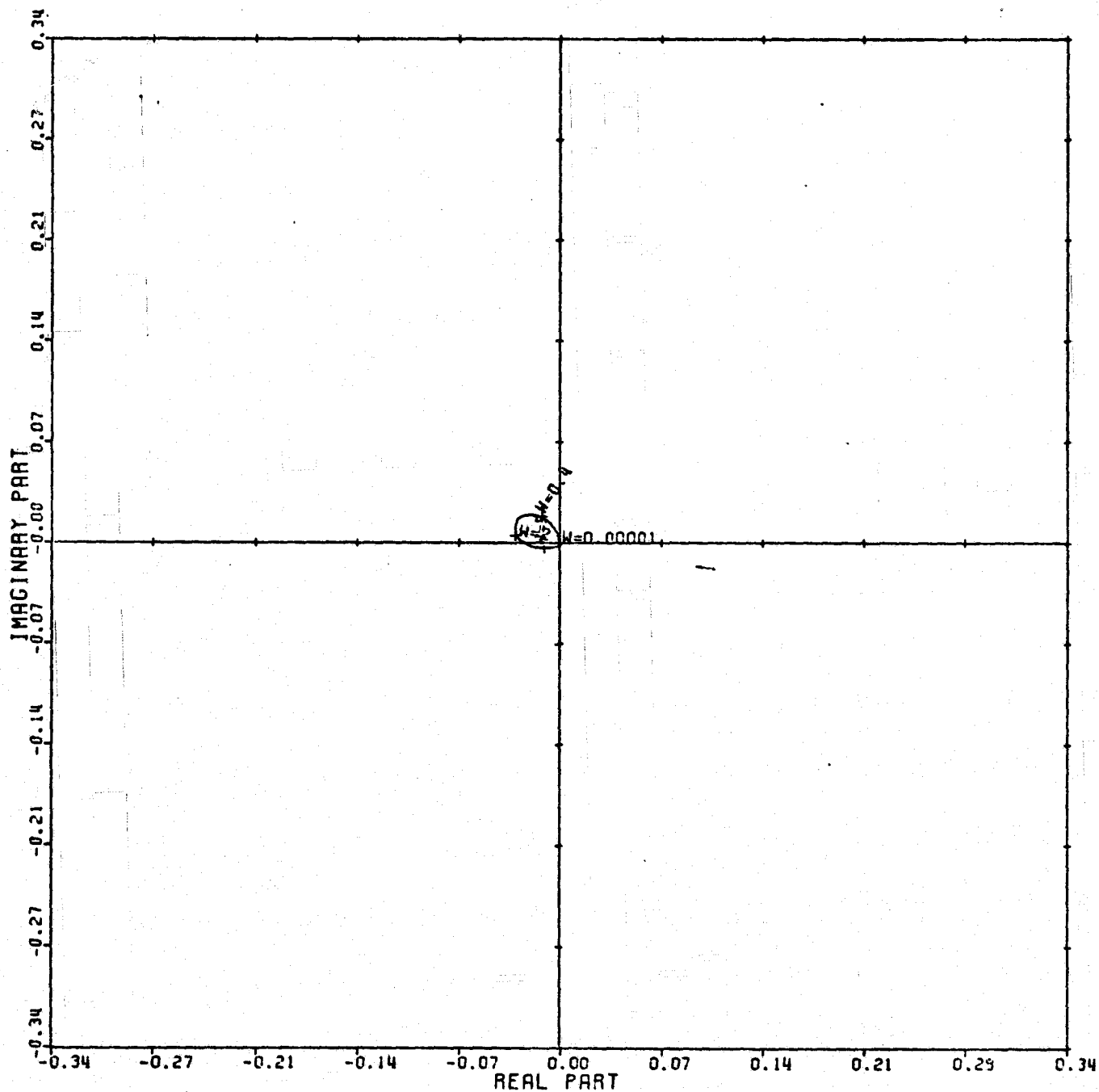
LOCUS OF CENTERS PLOT: 3.2 ENTRY: KMP 1, 1/G(0), 6/25/78.

INPUTS = 4, SYSTEM ORDER = 6, ANALYSIS TYPE = 11

Figure 113
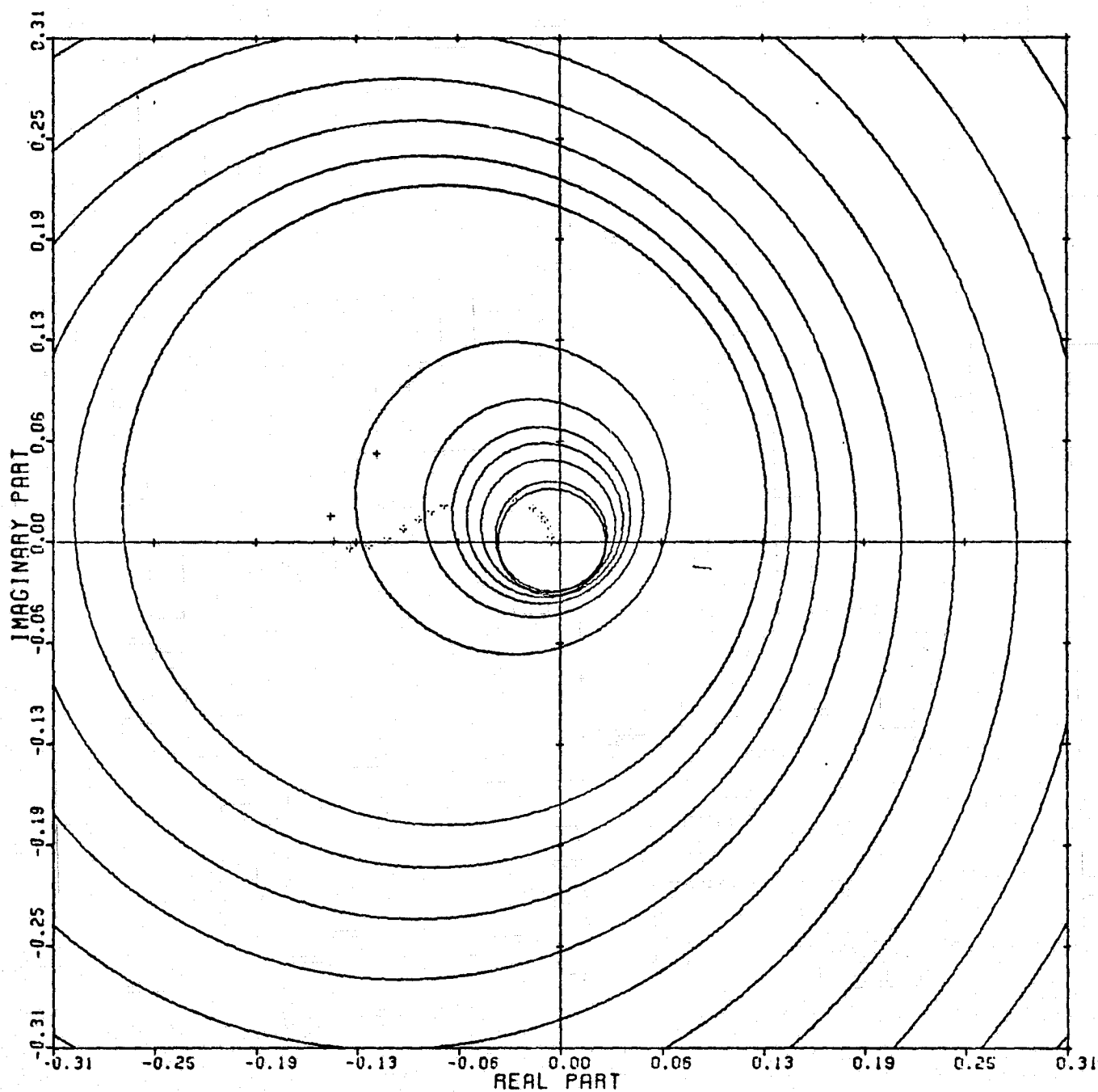
CARDIAD PLOT: 4,2 ENTRY: KMP 1, 1/G (O), 6/25/78.

INPUTS = 4, SYSTEM ORDER = 6, ANALYSIS TYPE = 11

Figure 114
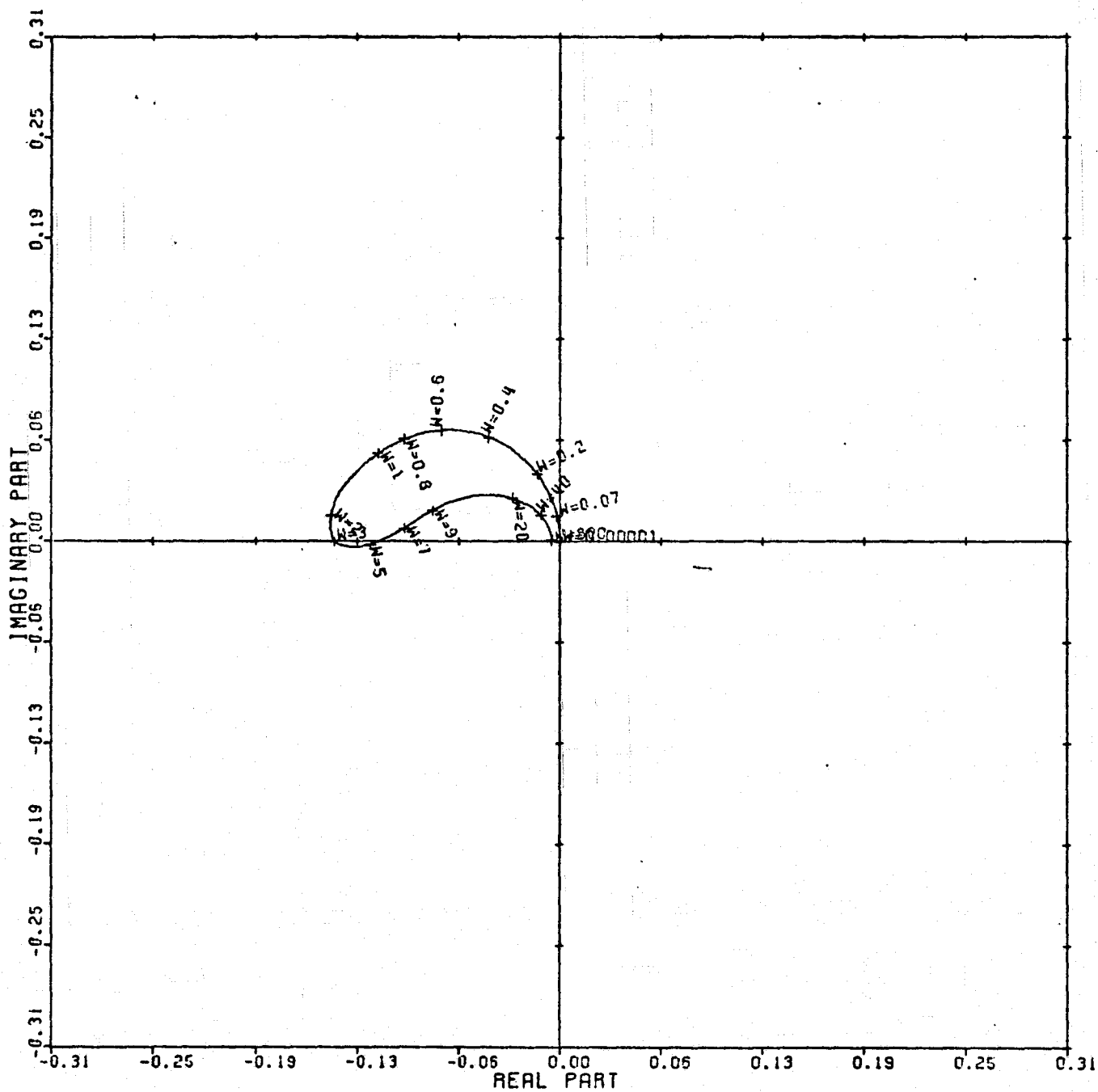
LOCUS OF CENTERS PLOT: 4,2 ENTRY: KMP 1, 1/G(0), 6/25/78.

INPUTS = 4, SYSTEM ORDER = 6, ANALYSIS TYPE = 11

Figure 115
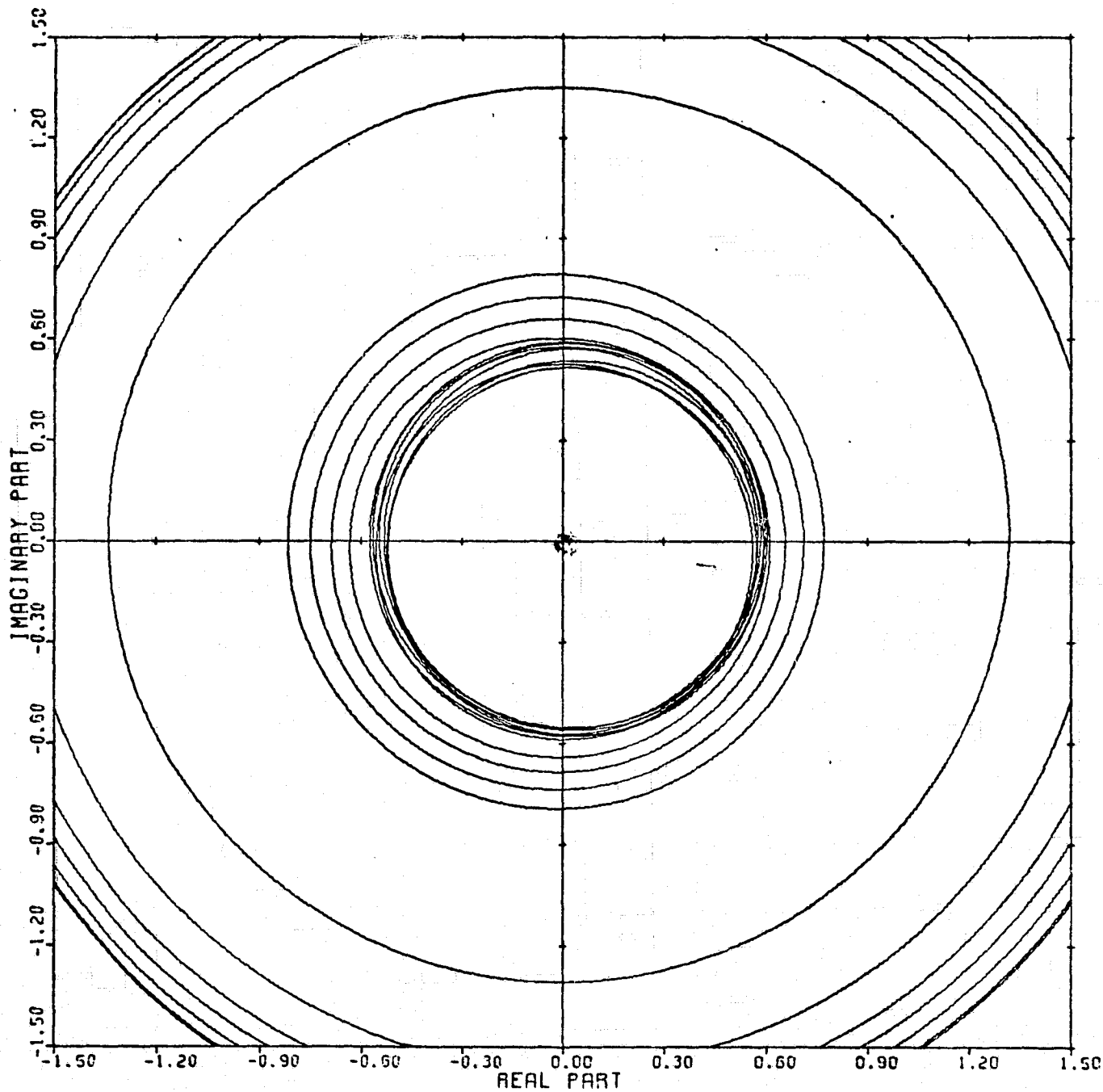
CARDIAD PLOT: 1,3 ENTRY: KMP 1, 1/G(0), 6/25/78.

INPUTS = 4, SYSTEM ORDER = 6, ANALYSIS TYPE = 11

Figure 116
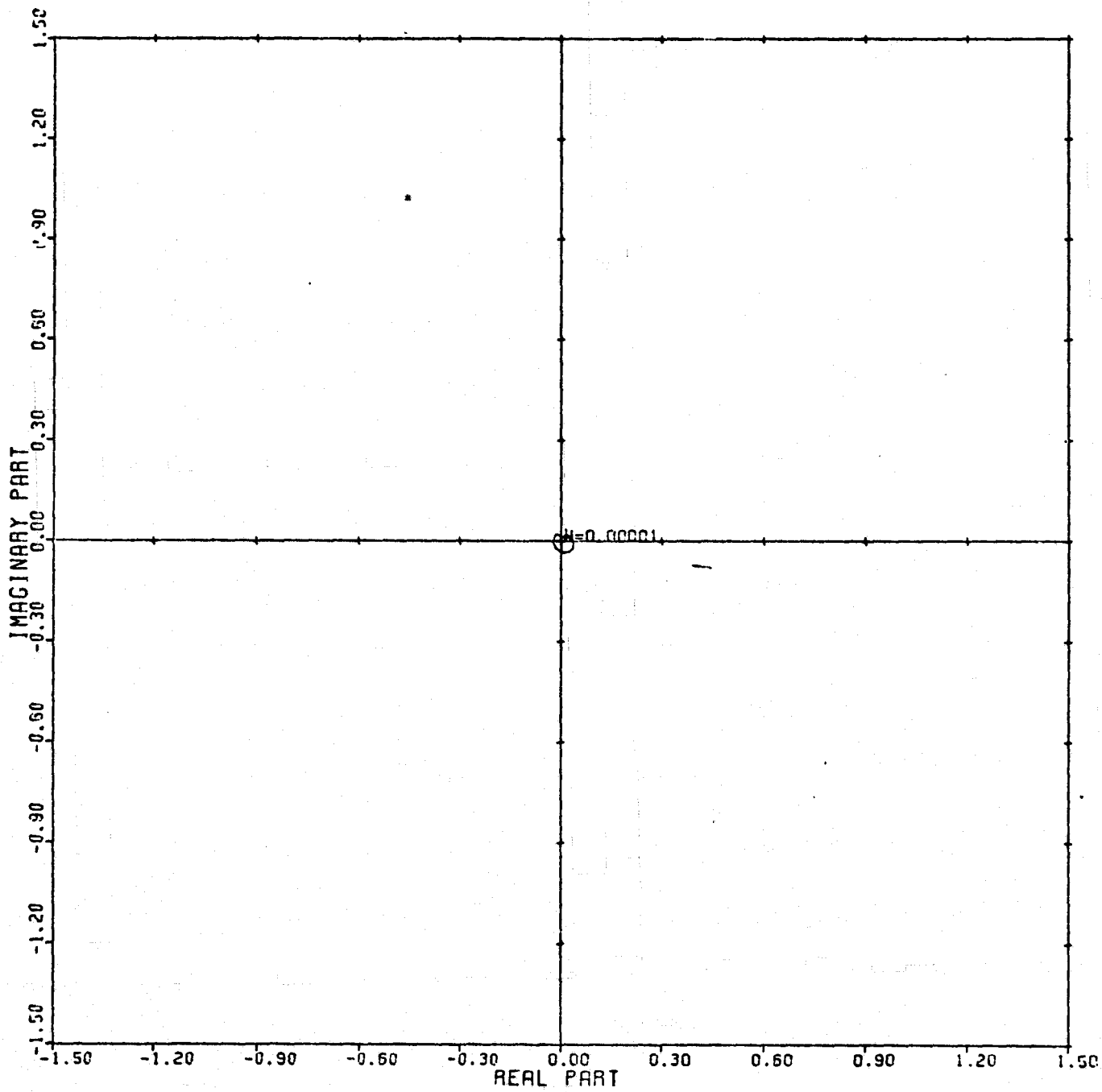
LOCUS OF CENTERS PLOT: 1,3 ENTRY: KMP 1, 1/G(0), 6/25/78.

INPUTS = 4, SYSTEM ORDER = 6, ANALYSIS TYPE = 11

Figure 117
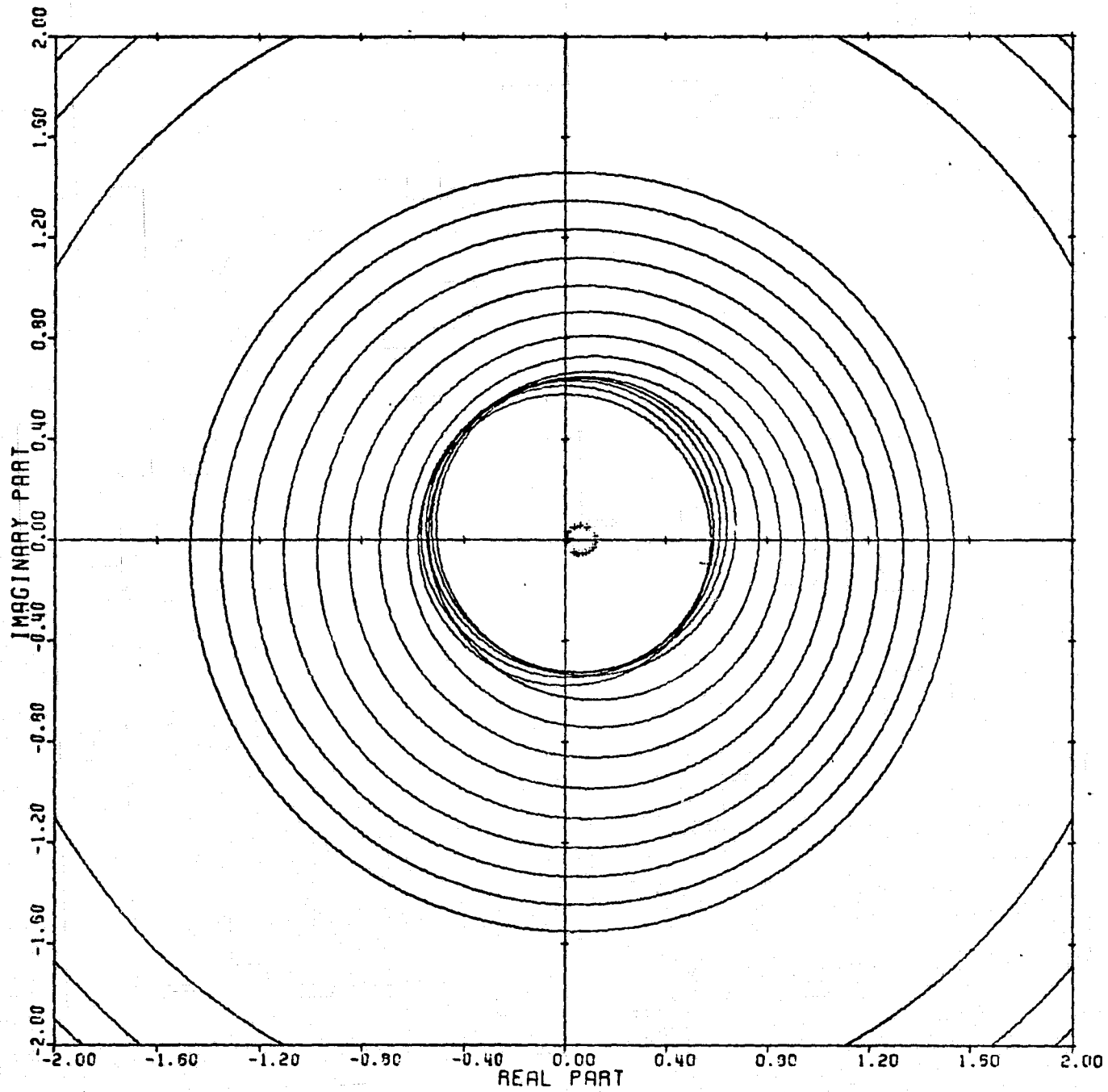
CARDIAD PLOT: 2,3 ENTRY: KMP 1, 1/G(0), 6/25/78.

INPUTS = 4, SYSTEM ORDER = 6, ANALYSIS TYPE = 11

Figure 118
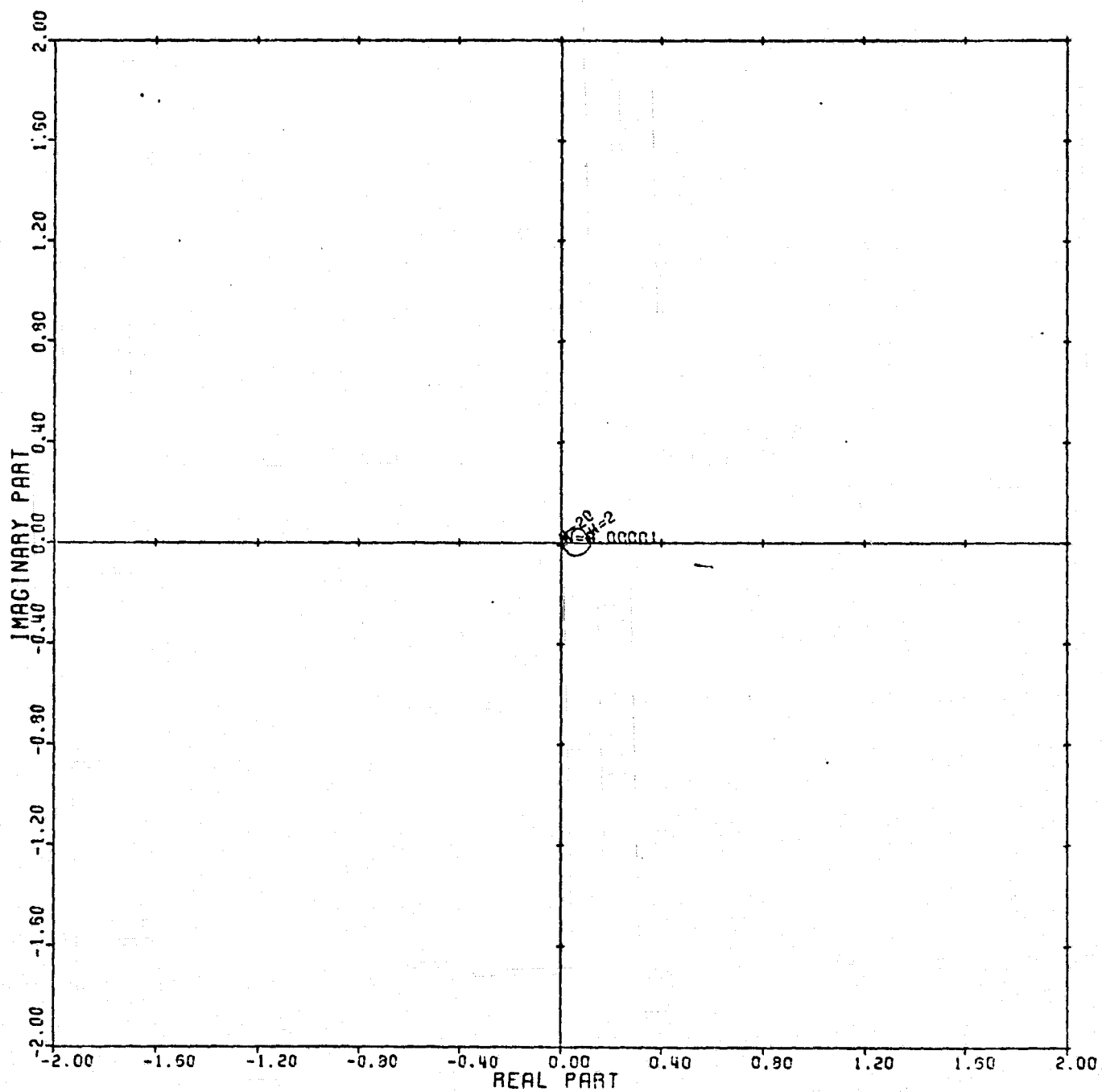
LOCUS OF CENTERS PLOT: 2,3 ENTRY: KMP 1, 1/G(0), 6/25/78.

(INPUTS = 4, SYSTEM ORDER = 6, ANALYSIS TYPE = 1)
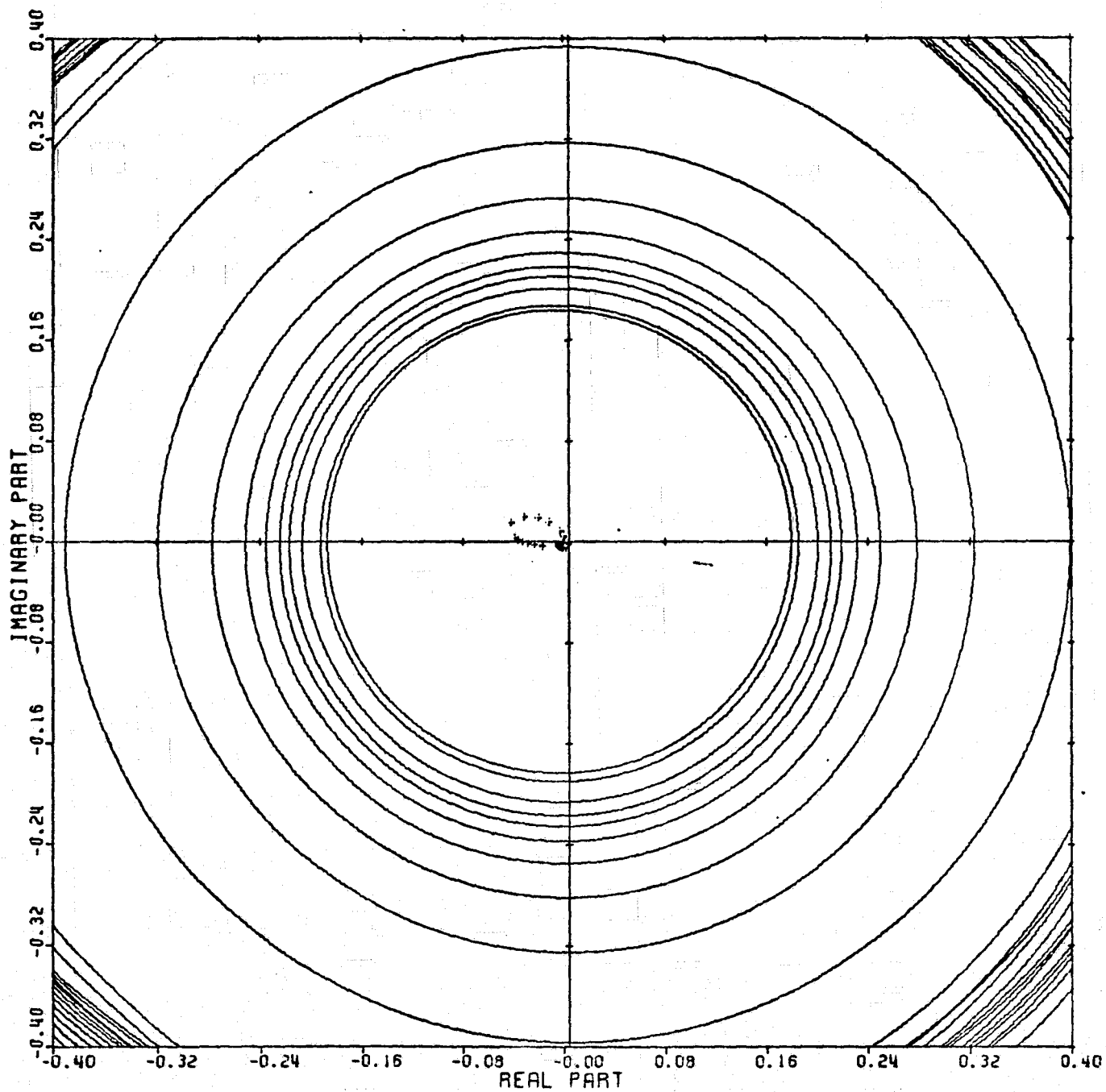
Figure 119

CARDIAD PLOT: 4,3 ENTRY: KMP 1, 1/G(0), 6/25/78.

INPUTS = 4, SYSTEM ORDER = 6, ANALYSIS TYPE = 11

Figure 120
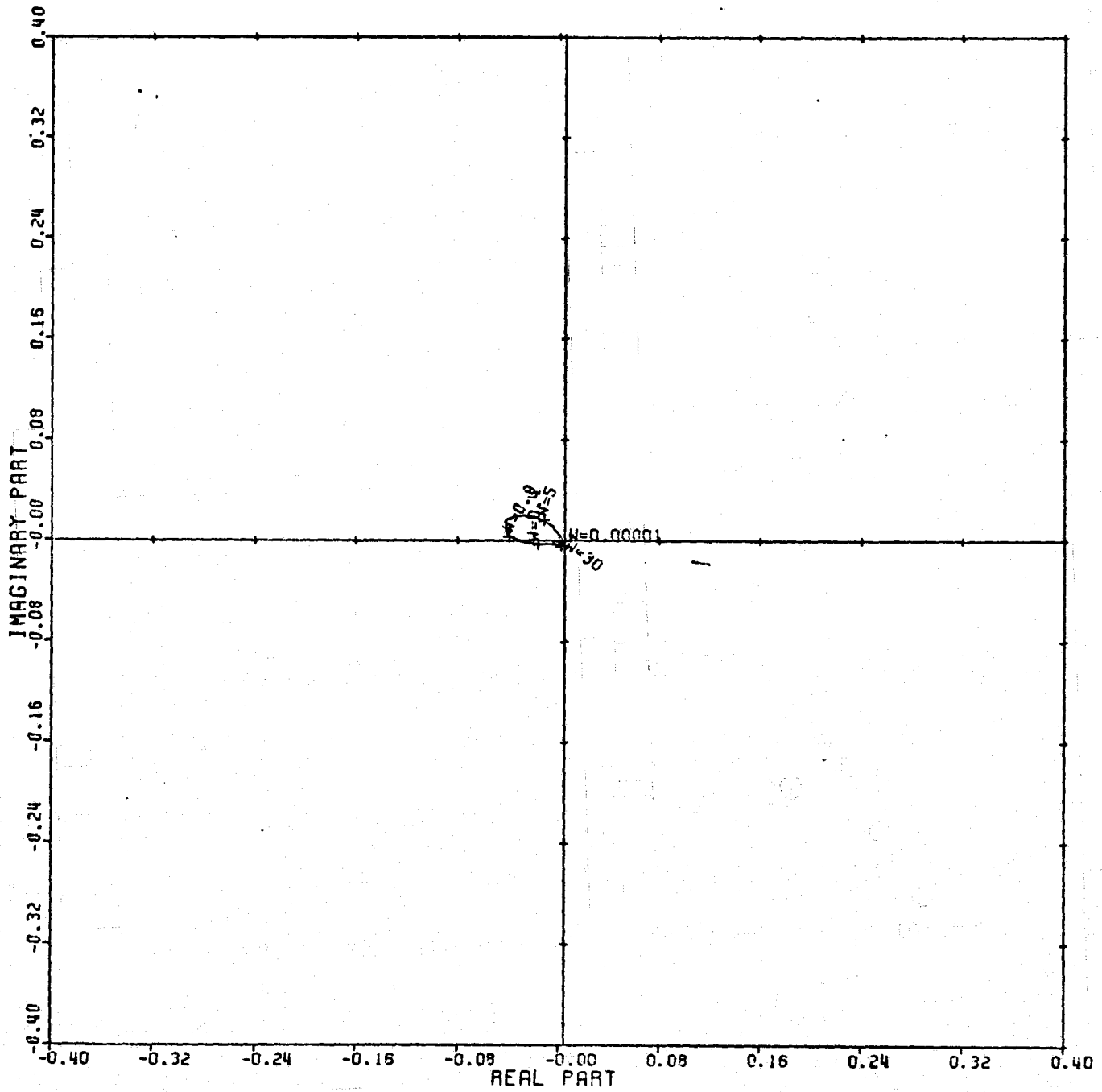
LOCUS OF CENTERS PLOT: 4,3 ENTRY: KMP 1, 1/G(0), 6/25/78.

INPUTS = 4, SYSTEM ORDER = 6, ANALYSIS TYPE = 11

Figure 121
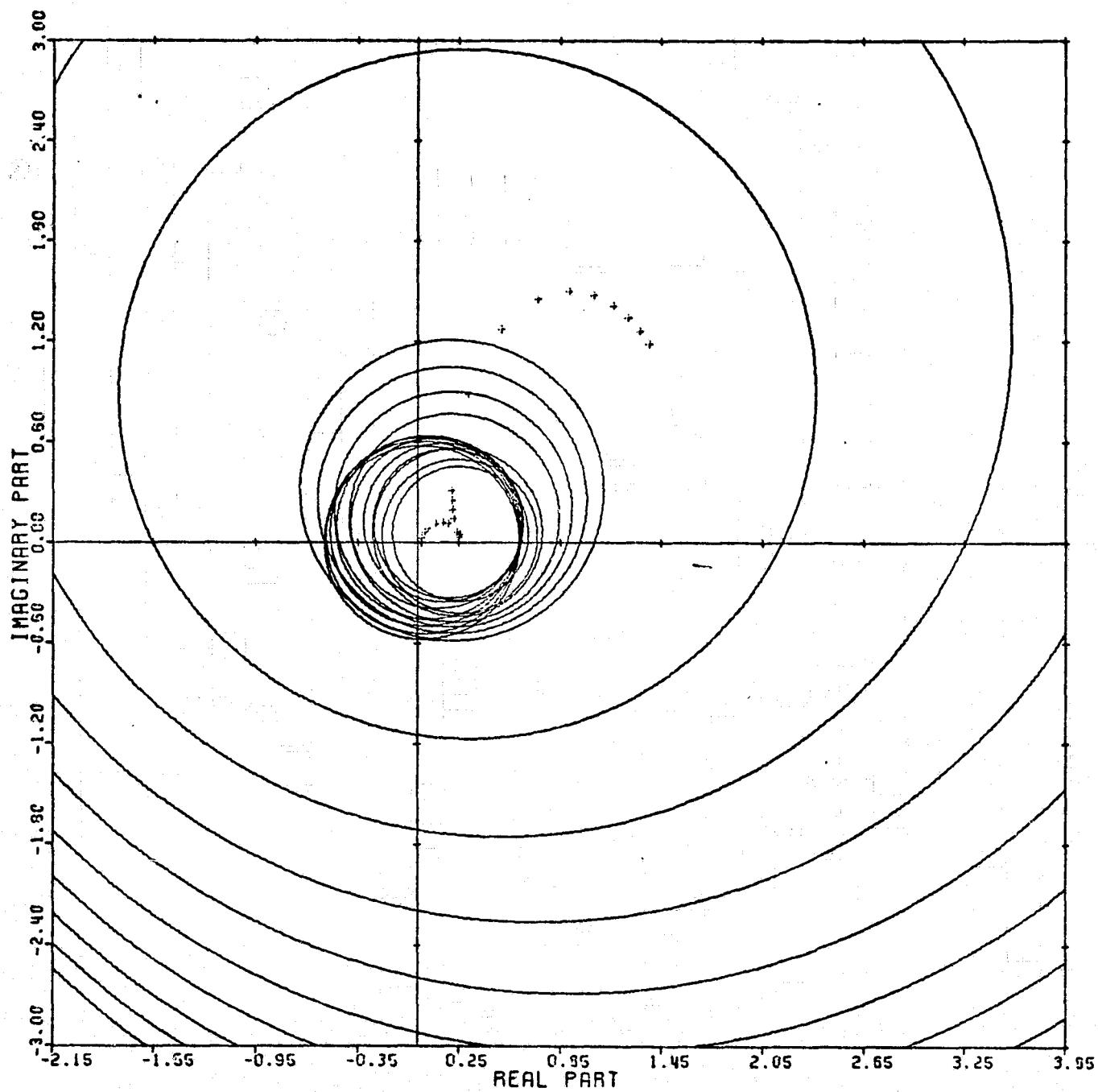
CARDIAD PLOT: 1,4 ENTRY: KMP 1, 1/G(0), 6/25/78.

INPUTS = 4, SYSTEM ORDER = 6, ANALYSIS TYPE = 11

Figure 122
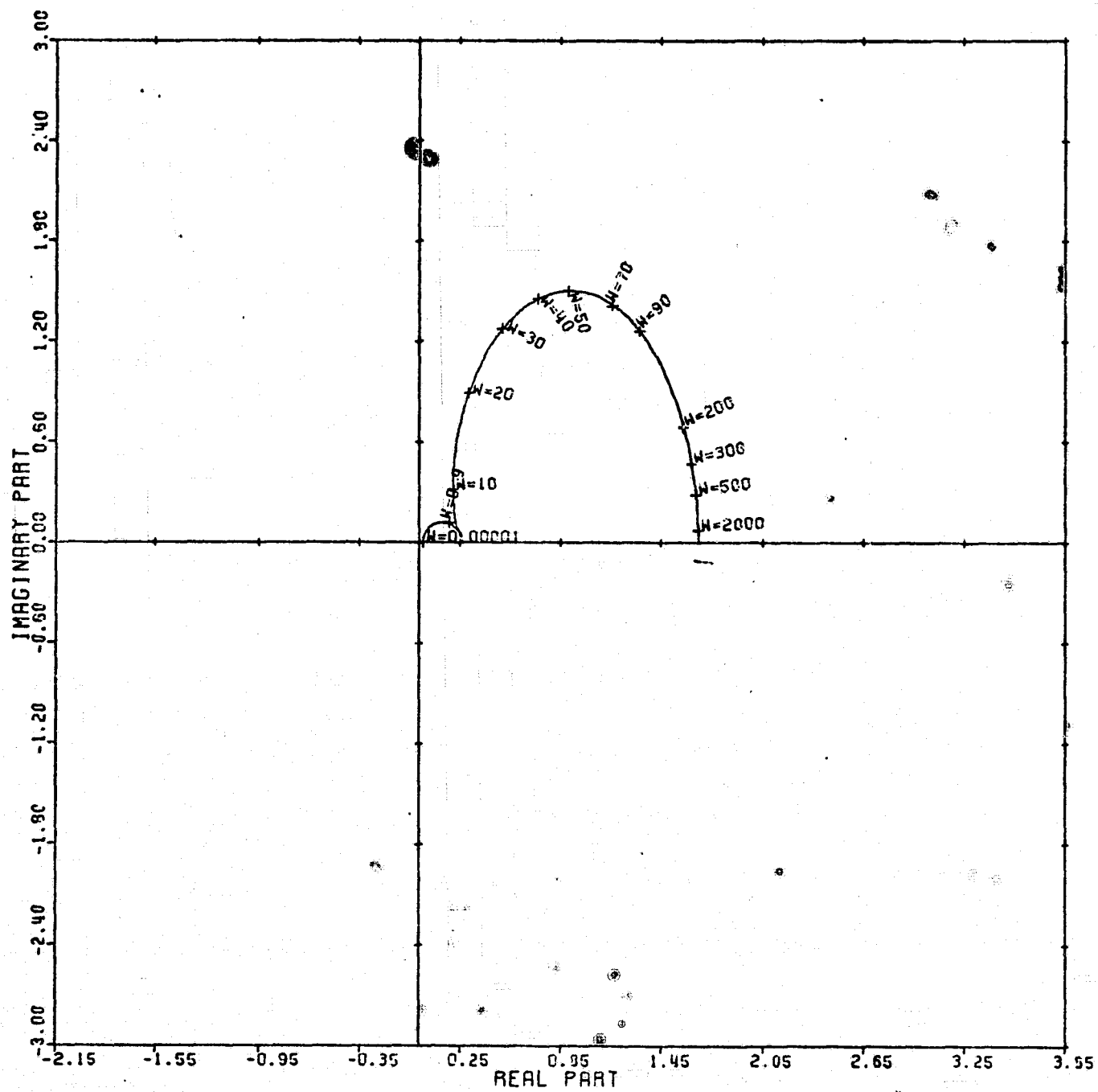
LOCUS OF CENTERS PLOT: 1,4 ENTRY: KMP 1, 1/G(0), 6/25/78.

INPUTS = 4, SYSTEM ORDER = 6, ANALYSIS TYPE = 11

Figure 123
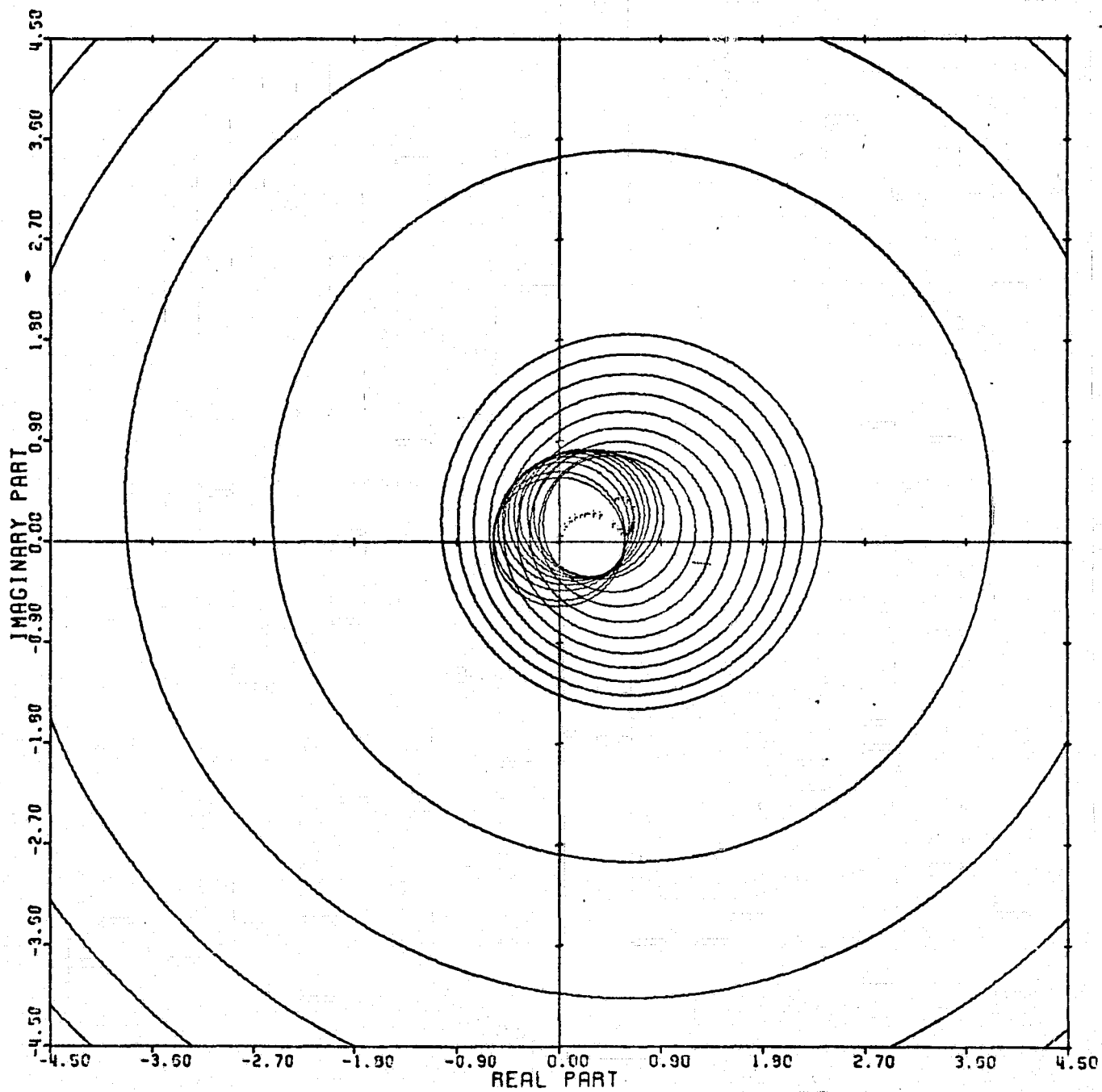
CARDIAD PLOT: 2,4 ENTRY: KMP 1, 1/G(0), 6/25/78.

INPUTS = 4, SYSTEM ORDER = 6, ANALYSIS TYPE = 11

Figure 124
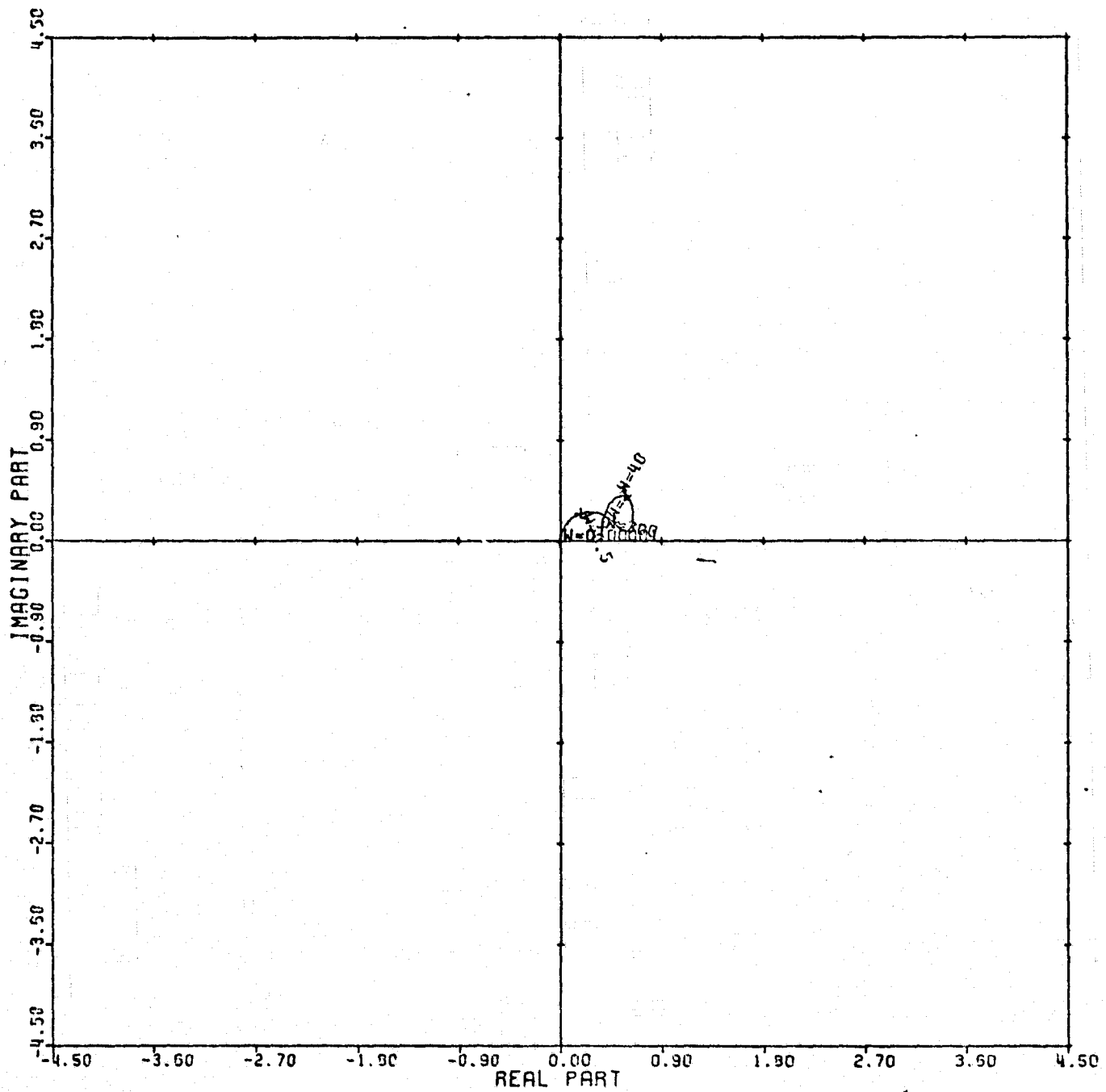
LOCUS OF CENTERS PLOT: 2,4 ENTRY: KMP 1, 1/G(0), 6/25/78.

INPUTS = 4, SYSTEM ORDER = 6, ANALYSIS TYPE = 11

Figure 125
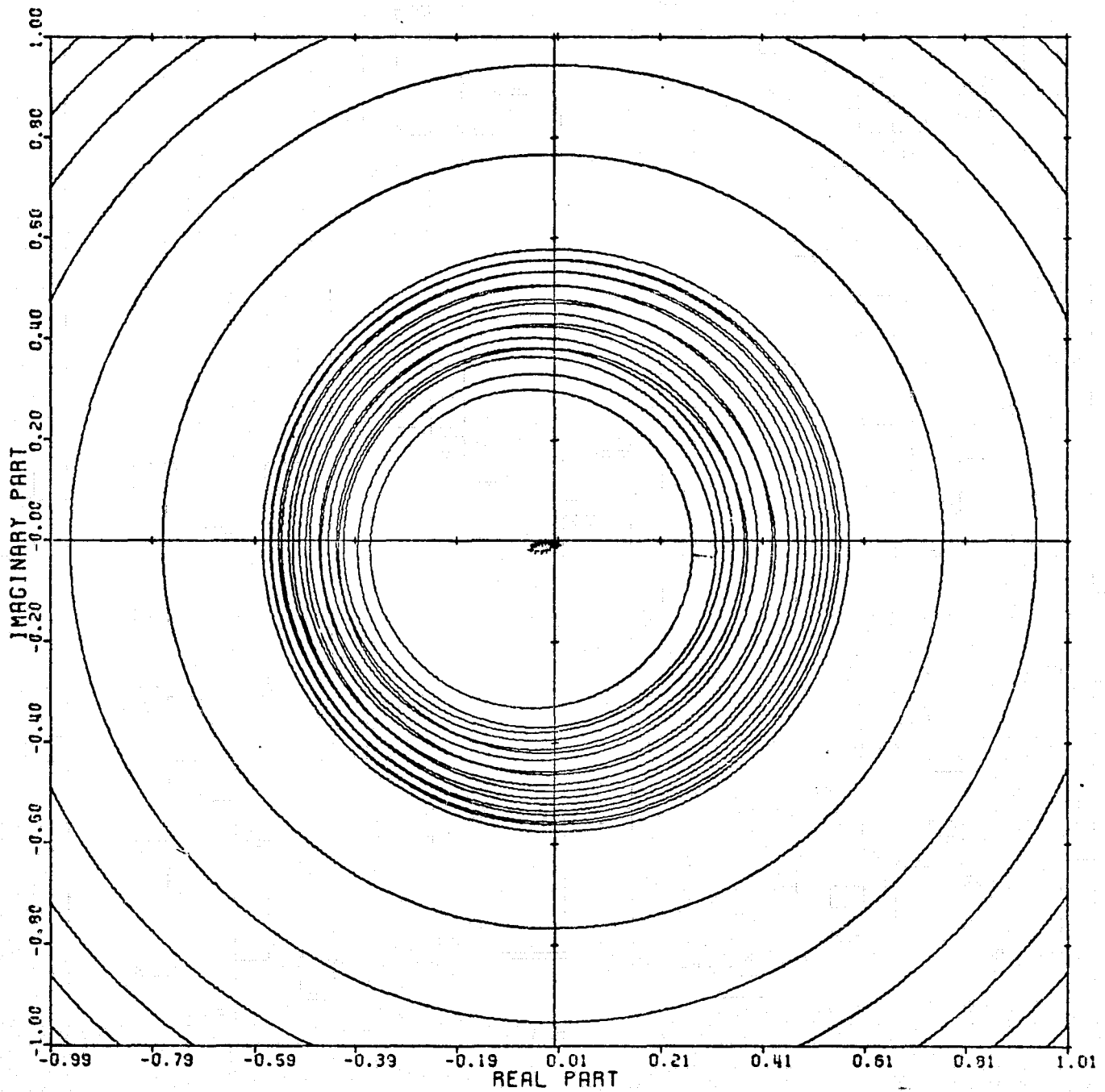
CARDIAD PLOT: 3,4 ENTRY: KMP 1, 1/G(0), 6/25/78.

INPUTS = 4, SYSTEM ORDER = 6, ANALYSIS TYPE = 11

Figure 126
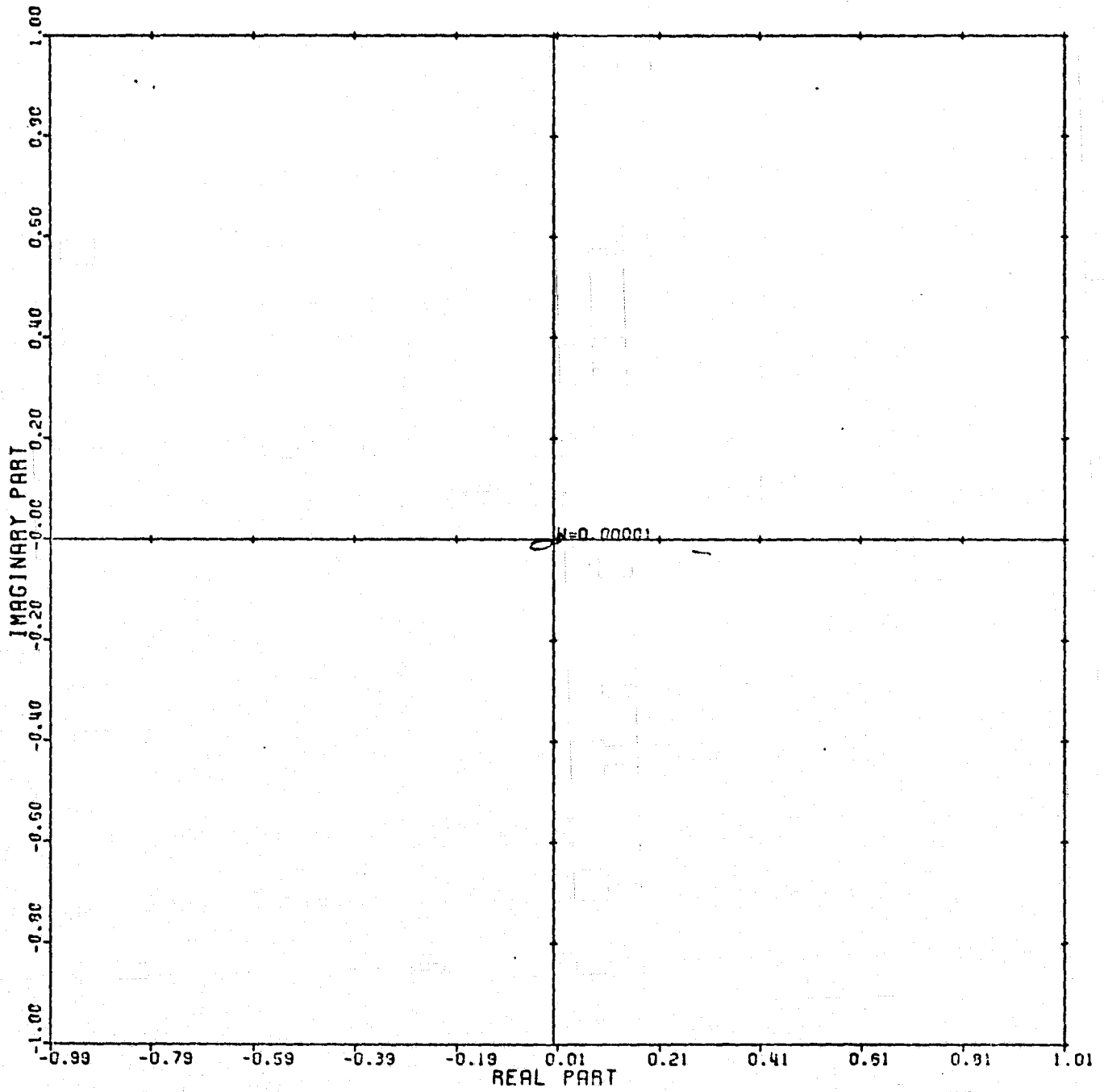
LOCUS OF CENTERS PLOT: 3,4 ENTRY: KMP 1, 1/G(0), 6/25/78.

INPUTS = 4, SYSTEM ORDER = 6, ANALYSIS TYPE = 11

APPENDIX C

PLANNED CONTENTS FOR M.S. THESIS

BY J.G. COMISKEY

Time Optimal Jet Engine Control

Using a Hermite Interpolation Model

TABLE OF CONTENTS

APPENDIX D

J.G. COMISKEY M.S. THESIS

CHAPTERS I-V

CHAPTER I

INTRODUCTION

The scope of this work will be to make preliminary efforts to generate
non-linear numerical models of a two-spooled turbofan jet engine, and sub-
ject these models to a known method of generating global, non-linear, time
optimal control laws. The models will be derived numerically, directly from
empirical data, as a first step in developing an automatic modelling proce-
dure.

A hierarchy of models, including analytical and numerical models, will
be established. The numerical models will be described in detail, and their
step responses compared to those of the hypothetical jet engine from which
they were derived. A method of generating time optimal control laws will be
explained, programmed, and applied to the numerical models. Finally, these
control laws will be tested, both on the models from which they were gener-
ated, and on the hypothetical jet engine.

This is the third in a series of similar works, whose ultimate goal
is the development of an automated modelling method. Even though DYNGEN,
an elaborate mathematical model, already exists, new models were developed
for two reasons. First, DYNGEN uses too much cpu time to be called re-
peatedly by an iterative method such as dynamic programming; a smaller,
faster model is required. Second, DYNGEN assumes the role of a physical
plant in this work, since access to a real jet engine is impossible.

In his paper, Basso [9] uses two methods of generating optimal control
sequences. The first is the dynamic programming successive approximations

technique. This actually generates a control law, from which a control sequence can be derived. The second is a modified Fletcher-Reeves conjugate gradient method. This method generates a control sequence that drives the system to the target in minimum time. The modification consists of the introduction of constraints into the original method.

His findings were that both methods yielded similar results, and that the number of computations necessary to solve a problem increases geometrically with system order for dynamic programming, but only arithmetically for the conjugate gradient method.

Longenbaker [1] applies the dynamic programming method to several models of the F-100 engine. His models include several linear systems, and one non-linear, analytical system of differential equations derived from physical and mathematical relationships among the state and control variables. Longenbaker concludes that the agreement between this analytical model and the DYNGEN simulator is not strong enough to justify great faith in the control law generated.

In this paper, the same dynamic programming method is applied with a modification introduced to reduce cpu time, to several numerical, non-linear models of the F-100 jet engine. The conclusions are that better numerical agreement with DYNGEN is achieved by this numerical models than by Longenbaker's analytical model, with a much smaller expenditure of man hours. However, complex interpolation techniques cause these models to use extravagant amounts of cpu time. Either larger data bases and less interpolation, or a more economical technique like Basso's conjugate gradient method should be explored in future work.

TWO SPOOL TURBOFAN JET ENGINE MODELS

2.1 Introduction

A form was chosen for the system model, which isolates static and dynamic portions of the system behavior, so that each of these can be modelled independently. Several methods of modelling these two portions were tried, resulting in a hierarchy of models. Each model was subjected to the same analysis for purposes of comparison.

In this chapter, the system model form is derived, and the modelling methods outlined. These methods will be treated in detail in later chapters.

2.2 Basic Approximation Approach [2]

Now consider a method for obtaining nonlinear models. Let

$$\dot{x} = f(x,u) \qquad (2.2\text{-}1)$$

with x an n vector and u an m vector denoting a dynamical system such as a jet engine, in which the state variables and parameters u remain positive throughout the system operation and there is a function $g(u)$ such that for each equilibrium point

$$f(x,u) = 0 \longleftrightarrow x = g(u) \qquad (2.2\text{-}2)$$

The steady state system analysis involves the study of the function $g(u)$.

We propose to approximate the system (2.2-1) by

$$\dot{x} = A(x,u)[x - g(u)] \qquad (2.2\text{-}3)$$

where $A(x)$ is a square matrix which varies as a function of x. Notice that if x_D is an equilibrium point of (2.2-1), $x_D = g(u_D)$, then a lin-

earization about this equilibrium point results in the linear system

$$\delta\dot{x} = A_D\delta x + B_D\delta u \qquad (2.2-4)$$

and a linearization of the approximating system (2) at $x_D = g(u_D)$ results in

$$\delta\dot{x} = A(x_D)\delta x + [-A(x_D) \frac{\delta g}{\delta u} (u_D)]\delta u \qquad (2.2-5)$$

Hence, the linearization of (2) will match the linearization of (1) if and only if

$$A(x_D) = A_D \quad , \quad -A_D \frac{\delta g}{\delta u} (u_D) = B_D \qquad (2.2-6)$$

Also, if A_D is invertible, as is often the case for jet engine models, equation yields

$$\frac{\delta g}{\delta u} (u_D) = -A_D^{-1}B_D \qquad (2.2-7)$$

These static and dynamic data are available from known algorithms [7], leaving only the choice of interpolation methods for generating non-linear models.

2.3 Hierarchy of Models

This work has resulted in the formation of a hierarchy of models, each a step in the development of an automated modelling method. They are classified as follows:

Model 0: The actual F-100 type engine (hypothetical)

Model 1: The DYNGEN [6] simulation program, coded with data presumed to have been taken from experimental measurements on Model 0. This model solves 16 nonlinear differential equations and uses data maps and thermodynamic tables which cannot be expressed analytically.

Model 2: The Longenbaker [1] model, a 5th order, nonlinear, analytical model. It includes the 5 state differential equations which govern the dynamical behavior of the system, along with 20 algebraic equations which express the relationship between various engine variables. This model is discussed in detail in [1].

Model 3A: The linear affine power law model, which is a fit of steady state data to a selected form with linear, nonlinear and constant terms.

Model 3B: The straight linear affine model, generated in the same manner as 3A, without the non-linear terms, to serve as a comparison.

Model 4: The Quasi-Hermite interpolation model. Also a fit to steady state data, this model employs value and derivative matching over a two dimensional subset of the state space.

Models 3 and 4 will be outlined briefly here, and detailed in later chapters.

2.4 Linear Affine Power Law Model   [2]

This model approximates the system by interpolating values of $A(x,u)$ from values of the matrix at two data points, and by generating values, for $g(u)$ by a fit of the form:

$$g_i(u) = c_{1i}u_1 + c_{2i}u_2 + c_{5i}u_1^{c_{3i}}u_2^{c_{4i}} + c_{6i} \quad , \quad i = 1,\ldots,5 \qquad (2.4\text{-}1)$$

to the same two data points.

2.5 Quasi-Hermite Interpolation Model

This model approximates the system by interpolating values of $A(x,u)$ from values of the matrix at five data points, and by interpolating values

of g(u) from 15 data points using a two dimensional adaptation of Hermite interpolation. This model represents new work for this thesis.

2.6 Summary

Having chosen to express the model in the form:

$$\dot{x} = A(x,u)[x - g(u)] \qquad (2.2\text{--}3)$$

it remains to derive the function g(u) and the matrix A(x,u) to correspond to empirical data. The function g(u) represents a mapping from the control space U into the state space X which yields steady state values for given controls. Empirical data available (i.e. DYGABCD output) includes both steady state values, and derivatives at those points with respect to the various inputs. It is desirable to choose functions which match as many of the available data as possible.

CHAPTER III

LINEAR AFFINE POWER LAW MODEL 3

3.1 Formation of A(x,u)   [2]

Values of $A(x,u)$ are interpolated from the values of $A_D = A(x_D, u_D)$

and $A_W = A(x_W, u_W)$ in the following manner:

$$A(x,u) = A_W \, \text{diag}\left(\frac{x_{Dj} - x_j}{x_{Dj} - x_{Wj}}\right) + A_D \, \text{diag}\left(\frac{x_j - x_{Wj}}{x_{D_j} - x_{Wj}}\right) \qquad (3.1\text{-}1)$$

where $\text{diag}(\cdot)$ is a diagonal matrix which causes the jth column of $A(x)$ to

be interpolated linearly between the jth columns of A_W and A_D with x_j

as the interpolation variable.

3.2 Approximation of g(u)   [2]

The parameter vector u is presumed to be made up of physical control

variables, and parameters such as fuel flow and nozzle area. The equilibrium

function is to be approximated in a manner such that both the equilibrium

values and the linearizations of the approximating system (3) match those

of system (1) at both x_D and x_W. This requires then that

$$g(u_D) = x_D \qquad g(u_W) = x_W \qquad (3.2\text{-}1)$$

and also

$$\frac{\delta g}{\delta u}(u_D) = -A_D^{-1} B_D \quad , \quad \frac{\delta g}{\delta u}(u_W) = -A_W^{-1} B_W . \qquad (3.2\text{-}2)$$

The method we propose here is to approximate each scalar component $g_i(u)$

of $g(u)$ by a _linear affine power law_ form

$$g(u) = c_1 u_1 + \ldots + c_m u_m + c_{2m+1} u_1^{c_{m+1}} u_2^{c_{m+2}} \ldots u_m^{c_{m+m}} + c_{2m+2} \qquad (3.2\text{-}3)$$

for which the jth partial derivative is

176

$$\frac{\delta g_i}{\delta u_j} = c_j + c_{2m+1} c_{m+j} \frac{u_1^{c_{m+1}} \ldots u_m^{c_{m+m}}}{u_j} . \tag{3.2-4}$$

Now, if the variables are normalized and scaled such that

$$u_D = (1,1,\ldots,1) = \underline{1} \qquad u_W = (a,a,\ldots,a) = \underline{a} \tag{3.2-5}$$

then, the conditions of (11) and (12) can be put in the form

$$k_j = \frac{\delta g_i}{\delta u_j} (\underline{1}) = c_j + c_{2m+1} c_{m+j}$$

$$k_{m+j} = \frac{\delta g_i}{\delta u_j} (\underline{a}) = c_j + c_{2m+1} c_{m+j} a^{\sum c_{m+j} - 1}$$

$$\tag{3.2-6}$$

$$k_{2m+1} = g_i(\underline{1}) = \sum c_j + c_{2m+1} + c_{2m+2}$$

$$k_{2m+2} = g_i(\underline{a}) = a \sum c_j + c_{2m+1} a^{\sum c_{m+j}} + c_{2m+2}$$

and summing the first two of these over j yields

$$\sum k_j = \sum c_j + c_{2m+1} \sum c_{m+j}$$

$$\sum k_{m+j} = \sum c_j + c_{2m+1} a^{\sum c_{m+j} - 1} \sum c_{m+j}$$

$$\tag{3.2-7}$$

$$k_{2m+1} = \sum c_j + c_{2m+1} + c_{2m+2}$$

$$k_{2m+2} = a \sum c_j + c_{2m+1} a^{\sum c_{m+j}} + c_{2m+2}$$

which is of the form

$$s_1 = r_1 + r_3 r_2$$

$$s_2 = r_1 + r_3 r_2 a^{r_2 - 1}$$

$$\tag{3.2-8}$$

$$s_3 = r_1 + r_3 + r_4$$

$$s_4 = a r_1 + r_3 a^{r_2} + r_4$$

which, incidentally is the $m=1$ condition also. This set of transcendental

equations is solved numerically for r_1, r_2, r_3, r_4 and (3.2-6) is then

used to solve for each c_j. In the event that (3.2-8) has no solution, a

best fit is made on the second equation by varying r_2 while the other con-

ditions are satisfied exactly.

3.3 Computational Algorithm [2]

In this section, we present an algorithm which serves to automate the

process of finding a nonlinear model for a system

$$\dot{x} = f(x,u) \tag{3.3-1}$$

to be approximated from $x_D, u_D, x_W, u_W, A_D, B_D, A_W, B_W$, by a normalized system.

The algorithm will automatically perform the normalization and, hence, ac-

tually approximate the system

$$\dot{\hat{x}} = \hat{f}(\hat{x}, \hat{u}) \tag{3.3-2}$$

where $\hat{x}_i = x_i/x_{D_i}$, $\hat{u}_j = u_j/u_{D_j}$. The approximating system is of the form

$$\dot{\hat{x}} = \hat{A}(\hat{x})[\hat{x} - \hat{g}(\hat{u})] \tag{3.3-3}$$

where

$$\hat{A}(\hat{x}) = \hat{A}_W \operatorname{diag} \frac{\hat{x}_{D_i} - \hat{x}_i}{\hat{x}_{D_i} - \hat{x}_{W_i}} + \hat{A}_D \operatorname{diag} \frac{\hat{x}_i - \hat{x}_{W_i}}{\hat{x}_{D_i} - \hat{x}_{W_i}} \tag{3.3-4}$$

and

$$\hat{g}_i = \sum_j c_j^i u_j^* + c_{2m+1}^i \prod_j u_j^{*c_{m+j}^i} + c_{2m+2}^i \tag{3.3-5}$$

where

$$u_j^* = \alpha_j \hat{u}_j + \beta_j. \tag{3.3-6}$$

Algorithm I.

1. Input: $x_D, u_D, A_D, B_D, m, n, a, \varepsilon, x_W, u_W, A_W, B_W$

   where m = number of controls

   n = number of states

2. Calculate:

$$\hat{A}_D = \text{diag}(1/x_{D_i}) \, A_D \text{diag}(x_{D_i})$$

$$\hat{A}_W = \text{diag}(1/x_{D_i}) \, A_W \text{diag}(x_{D_i})$$

$$\hat{B}_D = \text{diag}(1/x_{D_i}) \, B_D \text{diag}(u_{D_i})$$

$$\hat{B}_W = \text{diag}(1/x_{D_i}) \, B_W \text{diag}(u_{D_i})$$

3. Calculate:

$$\alpha_j = (1-a)u_{D_j}/(u_{D_j}-u_{W_j})$$

$$\beta_j = (au_{D_j}-u_{W_j})/(u_{D_j}-u_{W_j}) \qquad j = 1,\ldots,m$$

4. Calculate:

$$k_j^i = (-\hat{A}_D^{-1}\hat{B}_D)_{ij} \qquad k_{2m+1}^i = 1 = \hat{x}_{D_i} \qquad j = 1,\ldots,m$$

$$k_{m+j}^i = (-\hat{A}_W^{-1}\hat{B}_W)_{ij} \qquad k_{2m+2}^i = x_{W_i}/x_{D_i} = \hat{x}_{W_i} \qquad i = 1,\ldots,n$$

5. Calculate:

$$s_1^i = \sum_{j=1}^{m} \qquad\qquad s_2^i = \sum_{j=1}^{m} k_{m+j}^i$$

$$s_2^i = k_{2m+1}^i \qquad\qquad s_4^i = k_{2m+2}^i \qquad i = 1,\ldots,n$$

6. Go to Algorithm II.

   Send: s_1^i, s_2^i, s_3^i, s_4^i, a, ε

   Receive: r_1^i, r_2^i, r_3^i, r_4^i, γ $\qquad i = 1,\ldots,n$

7. Calculate:

$$c_{2m+1}^i = r_3^i \qquad\qquad c_{2m+2}^i = r_4^i \qquad j = 1,\ldots,m$$

$$c_{m+j}^i = \frac{k_{m+j}^i - k_j^i + \gamma}{r_j^i(a^{r_2^i-1}-1)} \qquad c_j^i = k_j^i - r_3^i c_{m+j}^i \qquad i = 1,\ldots,n$$

8. Output:

$$c_1^i, \ldots, c_{2m+2}^i$$

$$\alpha_i, \; \beta_j$$

$$\hat{x}_{D_i}, \; \hat{x}_{W_i}$$

$$\hat{A}_D, \; \hat{A}_W$$

$$j = 1,\ldots,m$$

$$i = 1,\ldots,n$$

Algorithm II.

1. Input: $s_1, s_2, s_3, s_4, \varepsilon, a$

2. Calculate:

$$p_1 = s_1 - \frac{s_3-s_4}{1-a}$$

$$p_2 = s_2 - \frac{s_3-s_4}{1-a}$$

3. Minimize by line search:

$$\left| p_2 - p_1 \frac{ax^{x-1} - \frac{a^x-1}{a-1}}{x - \frac{a^x-1}{a-1}} \right|$$

for $-10 \le x \le 10, \qquad x \ne 0, \qquad x \ne 1$

4. Calculate:

$$r_2 = x \qquad r_3 = \frac{p_1}{r_2 - \frac{a^{r_2}-1}{a-1}}$$

$$r_1 = \frac{s_3 - s_4 + r_3(a^{r_2}-a)}{1-a} \qquad \gamma = \frac{1}{m}(s_1-s_2 + r_2 r_3(a^{r_2-1}-1))$$

$$r_2 = \frac{s_4 - as_3 - r_3(a^2-a)}{1-a}$$

5. Return to Algorithm I.6

3.4 Straight Linear Affine Model

As a check that the Power law term has significant effect on the function g(u), a straight linear affine approximation to g(u) was generated. This model is then subjected to the same analysis as models 3A and 4.

3.5 Numerical Results [2]

The algorithm of the previous section was applied to data obtained using DYNGEN with x_D and u_D specified as in Section 2. An off-design point was obtained using u_W = (.72727, .72727), with the resulting normalized state $\hat{x}_W$ = (.9000, .7897, .7381, .9401, .9454). The normalized A and B matrices are

$$\hat{A}_D = \begin{bmatrix} -3.8 & -1.277 & 2.067 & -1.152 & 1.448 \\ 2.748 & -5.39 & 1.585 & -1.991 & 1.071 \\ 377.9 & 49.51 & -264.9 & 86.807 & 78.91 \\ 31.26 & 139.39 & -6.269 & -88.69 & 27.83 \\ -176.5 & 23.91 & -10.27 & -37.4 & -246.7 \end{bmatrix} \quad \hat{B}_W = \begin{bmatrix} -.00259 & .3553 \\ .2116 & -.31618 \\ 12.54 & -13.774 \\ -.6201 & -99.3 \\ 157.78 & 6.84 \end{bmatrix}$$

(3.5-1)

$$\hat{A}_W = \begin{bmatrix} -4.744 & -1.3888 & 3.2468 & -1.4591 & 1.1969 \\ .82.86 & -26.726 & 2.5585 & -1.8609 & .45548 \\ 475.73 & 137.55 & -328.91 & 27.791 & 91.495 \\ -50.103 & 110.91 & 63.188 & -116.69 & 8.2883 \\ -186.77 & -67.682 & -41.681 & 24.586 & -243.23 \end{bmatrix} \quad \hat{B}_W = \begin{bmatrix} -.04546 & .0013 \\ .0086 & -.0121 \\ 2.434 & -.613 \\ .67865 & -97.467 \\ 203.44 & .64755 \end{bmatrix}$$

(3.5-2)

Using the parameter value a = .7, the c_j^i coefficients which specify the equilibrium functions $\hat{g}(\hat{u})^i$ as in Section 3 are given by the matrix

$$C = \begin{bmatrix} .24267 & -.00218 & 1.90082 & 8.09916 & .02864 & .73088 \\ 1.01593 & .85407 & .89872 & .66919 & -.81879 & -.05121 \\ .73445 & .10133 & 6.90586 & 3.09409 & .011495 & .15272 \\ .77234 & -.35905 & 2.45867 & 2.87415 & -075198 & .66191 \\ .39503 & -.27262 & -3.44682 & 13.4468 & .01838 & .85921 \end{bmatrix} \qquad (3.5-3)$$

This matrix together with the values $\alpha=1.1$ and $\beta=0.1$ and the matrices $\hat{A}_D$ and $\hat{A}_W$ completely specify Model 3A.

Another model which we will call Model 3B is easily obtained by using a _linear_ _affine_ approximation to $\hat{g}(\hat{u})$ such that $\hat{g}(\hat{u}_D) = \hat{x}_D$, $\hat{g}(\hat{u}_W) = \hat{x}_W$. Model 3B is specified by $a = e^{-1}$, $\alpha = 2.31778$, $\beta = -1.31778$ and the co-efficient matrix

$$C = \begin{bmatrix} .1553 & .0028 & 1.0 & 1.0 & 0. & .8418 \\ .1619 & .1707 & 1.0 & 1.0 & 0. & .6674 \\ .5351 & -.1208 & 1.0 & 1.0 & 0. & .5857 \\ .5878 & -.49313 & 1.0 & 1.0 & 0. & .9053 \\ .2962 & -.2099 & 1.0 & 1.0 & 0. & .9137 \end{bmatrix} \qquad (3.5-4)$$

CHAPTER IV

QUASI-HERMITE INTERPOLATION MODEL 4

4.1 Introduction

A known method for matching a polynomial to the values and derivatives of a function at several points is Hermite interpolation. However, this method is formulated in general only for the one dimensional case. [3] Some works exist which apply this method to an n dimensional case, but only under certain narrow restrictions. [5] The single variable case, its restricted application in n dimensions, and a modified application in two dimensions, are discussed in this chapter.

4.2 Hermite Interpolation for a Single Variable

This presentation of the Hermite interpolation method is drawn from Hildebrand. [3] His notation is preserved, as closely as possible, here and in the resultant computer program.

If the values of $g(u)$ are known at m points, $u = u^1, u^2, \ldots, u^m$, define:

$$\pi(u) = (u - u^1)(u - u^2)\ldots(u - u^m) \qquad (4.2.1)$$

and:

$$\ell^i(u) = \frac{\pi(u)}{(u-u^i)\ \pi'(u^i)} \qquad (4.2.2)$$

with the properties:

$$\pi(u^j) = 0 \qquad j = 1,\ldots,m \qquad (4.2.3)$$

and:

$$\ell^i(u^j) = \delta_{ij} \qquad i = 1,\ldots,m \qquad j = 1,\ldots,m \qquad (4.2.4)$$

where δ_{ij} is the Kronecker delta ($\delta_{ii} = 1$, $\delta_{ij} = 0$ for all $i \neq j$).

With these defined, the polynomial of degree $m-1$ which takes on the values $g(u^1)$, $g(u^2)$,...,$g(u^m)$ can be expressed as:

$$y(u) = \sum_{k=1}^{m} \ell^k(u) g(u^k) \tag{4.2.5}$$

Suppose both $g(u)$ and $g'(u)$ are known for $u = u^1$, u^2,...,u^m, it is possible to determine a polynomial of degree $2m-1$ with these values and derivatives. We shall assume this polynomial is expressible in the form:

$$y(u) = \sum_{k=1}^{m} h^k(u)\, g(u^k) + \sum_{k=1}^{m} \bar{h}^k(u)\, g'(u^k) \tag{4.2.6}$$

where $h^i(u)$ and $\bar{h}^i(u)$, $i = 1,...,m$ are polynomials of maximum degree $2m-1$. The requirement $y(u^j) = g(u^j)$ will be satisfied if:

$$h^i(u^j) = \delta_{ij} \quad \text{and} \quad \bar{h}^i(u^j) = 0 \tag{4.2.7}$$

and the requirement $y'(u^j) = g'(u^j)$ will be satisfied if:

$$h'^i(u^j) = 0 \quad \text{and} \quad \bar{h}'^i(u^j) = \delta_{ij} \tag{4.2.8}$$

Since $\ell^i(u)$ is a polynomial of degree $m-1$ which satisfied (4.2.4), then $[\ell^i(u)]^2$ is a polynomial of degree $2m-2$ which satisfies (4.2.4) and whose derivative is zero at $u_i^{\,j}$ when $i \neq j$. So if $h^i(u)$ and $\bar{h}^i(u)$ are polynomials of degree $2m-1$, then:

$$h^i(u) = r^i(u)\,[\ell^i(u)]^2 \quad \text{and} \quad \bar{h}^i(u) = s^i(u)\,[\ell^i(u)]^2 \tag{4.2.9}$$

where $r^i(u)$ and $s^i(u)$ are linear functions of u, so that (4.2.7) and (4.2.8) will be satisfied when $i \neq j$. These four conditions, when $i = j$, then yield:

$$r^i(u^i) = 1 \quad r^{-i}(u^i) + 2 \ell^{-i}(u^i) = 0 \qquad (4.2.10)$$

$$s^i(u^i) = 0 \quad s^{-i}(u^i) = 1 \qquad (4.2.11)$$

from which follows:

$$r^i(u) = 1 - 2 \ell^{-i}(u^i)(u - u^i) \quad \text{and} \quad s^i(u) = (u - u^i) \qquad (4.2.12)$$

So, by combining (4.2.6), (4.2.9), and (4.2.12) we obtain the desired polynomial in the form:

$$y(u) = \sum_{k=1}^{m} h^k(u) \, g(u^k) + \sum_{k=1}^{m} \bar{h}^k(u) \, g^\cdot(u^k) \qquad (4.2.13)$$

where:

$$h^i(u) = r^i(u) [\ell^i(u)]^2 \quad \text{and} \quad \bar{h}^i(u) = s^i(u) [\ell^i(u)]^2 \qquad (4.2.14)$$

and:

$$r^i(u) = 1 - 2 \ell^{-i}(u^i)(u - u^i) \quad \text{and} \quad s^i(u) = (u - u^i) \qquad (4.2.15)$$

This result is known as Hermite's interpolation formula, or the formula for osculating interpolation.

4.3 Problems of Hermite Interpolation in n Dimensions

If Hermite Interpolation were to be applied in n dimensions, the task would be to determine m sets of n+1 polynomials with properties similar to h and $\bar{h}$. Specifically, if we assume that the desired polynomial can be expressed in the form:

$$y(u) = \sum_{k=1}^{m} h^k(u) \, g(u^k) + \sum_{j=1}^{n} \sum_{k=1}^{m} \bar{h}^{jk}(u) \, \frac{dg}{du^j}(u^k) \qquad (4.3.1)$$

then these polynomials must have the properties:

$$h^i(u^j) = \delta_{ij} \quad \text{and} \quad \bar{h}^{ik}(u^j) = 0 \qquad (4.3.2)$$

and:

$$\frac{\delta h^i}{\delta u_j}(u^k) = 0 \quad \text{and} \quad \frac{\delta \bar{h}^{jk}}{\delta u_j}(u^k) = \delta_{jk} \tag{4.3.3}$$

corresponding to the conditions (4.2.7) and (4.2.8). However, the further condition:

$$\frac{\delta \bar{h}^{i\ell}}{\delta u_j}(u^k) = 0 \quad \text{for all} \quad i \neq k \tag{4.3.4}$$

must also be satisfied. This final condition cannot be satisfied by the polynomials described in the previous section. In [5], Niijima treats a special case, in which the existence of certain orthogonal polynomials allows the application of Hermite interpolation to carefully chosen data in two dimensions. However, this method is not universally applicable to arbitrary data.

4.4 Quasi-Hermite Approach for Two Controls

Given that no general method of Hermite interpolation in two variables was found, the following adaptation of the one dimensional case was applied. The value of control u_2 (nozzle area) was held constant at the design point value, and Hermite interpolation was applied to a set of points generated by varying u_1 (fuel flow). Both values, and derivatives with respect to u_1 were matched at these data points. Then, for each value of u_1, a value Δ was chosen, and control u_2 was varied by this amount, both plus and minus. A function was then chosen to match values at these new points, without altering the function at the original points. The resulting polynomial is of the form:

$$y(u) = \sum_{k=1}^{m} h^k(u_1) \, g(u_1^k, u_2^1) \, \theta^k(u_2) + \sum_{k=1}^{m} \bar{h}^k(u_1) \, g'(u_1^k, u_2^1) \tag{4.4.1}$$

where:

$$\theta^k(u_2) = 1 + [\frac{g(u_1^k, u_2^1 + \Delta^k) - g(u_1^k, u_2^1 - \Delta^k)}{2 \Delta^k g(u_1^k, u_2^1)}] u_2$$

$$+ [\frac{g(u_1^k, u_2^1 + \Delta^k) + g(u_1^k, u_2^1 - \Delta^k) - 2g(u_1^k, u_2^1)}{2(\Delta^k)^2 g(u_1^k, u_2^1)}] (u_2)^2 \qquad (4.4.2)$$

This function has the property that:

$$\theta^k(u_2) = 1 \quad \text{when} \quad u_2 = u_2^1 \qquad (4.4.3)$$

and:

$$\theta^k(u_2) = g(u_1^k, u_2^1 + \Delta^k)/g(u^k) \quad \text{when} \quad u_2 = u_2^1 + \Delta^k$$

$$\theta^k(u_2) = g(u_1^k, u_2^1 - \Delta^k)/g(u^k) \quad \text{when} \quad u_2 = u_2^1 - \Delta^k \qquad (4.4.4)$$

and since $h^i(u^j) = \delta_{ij}$, the resultant polynomial will match values and derivatives with respect to u_1 along the $u_2 = u_2^1$ line, and values at $u_2 = u_2^1 \pm \Delta^k$.

4.5 Formation of A(x,u)

Having chosen an approximation to $g(u)$, it remains to choose a method for interpolating values for $A(x,u)$ to complete the model. Lagrangian interpolation was used to match values only at three points along the $u_2 = u_2^1$ line, and at $u = (u_1^1, u_2^1 \pm \Delta^1)$. The results of this approach are embodied in the following equations. First define:

$$A1 = A(x,u) \quad \text{at} \quad u = u^1 = (u_1^1, u_2^1), \qquad x = g(u^1)$$

$$A3 = A(x,u) \quad \text{at} \quad u = u^3 = (u_1^3, u_2^3), \qquad x = g(u^3)$$

$$A5 = A(x,u) \quad \text{at} \quad u = u^5 = (u_1^5, u_2^5), \qquad x = g(u^5) \qquad (4.5.1)$$

$$AP = A(x,u) \quad \text{at} \quad u = u^P = (u_1^1, u_2^1 + \Delta^1), x = g(u^P)$$

$$AM = A(x,u) \quad \text{at} \quad u = u^M = (u_1^1, u_2^1 - \Delta^1), x = g(u^M)$$

and:

$$FR1 = [(x_1 - x_1^3)(x_1 - x_1^5)]/[(x_1^1 - x_1^3)(x_1^1 - x_1^5)]$$

$$FR3 = [(x_1 - x_1^1)(x_1 - x_1^5)]/[(x_1^3 - x_1^1)(x_1^3 - x_1^5)]$$

$$FR5 = [(x_1 - x_1^1)(x_1 - x_1^3)]/[(x_1^5 - x_1^1)(x_1^5 - x_1^3)]$$

$$FRP = [(u_2 - u_2^1)(u_2 - (u_2^1 - \Delta^1))]/[2(\Delta^1)^2]$$

$$FR = [(u_2 - (u_2^1 + \Delta^1))(u_2 - (u_2^1 - \Delta^1))]/[(-(\Delta^1)^2)]$$

$$FRM = [(u_2 - (u_2^1 + \Delta))(u_2 - u_2^1)]/[2(\Delta^1)^2]$$

$$(4.5.2)$$

then:

$$A_{ij}(x,u) = [FR1(A1_{ij}) + FR3(A3_{ij}) + FR5(A5_{ij})]$$

$$x \; [FRP(AP_{ij}/A1_{ij}) + FR + FRM(AM_{ij}/A1_{ij})]$$

$$(4.5.3)$$

CHAPTER V

MODEL RESPONSE COMPARISONS

5.1 Introduction

Before subjecting the models to the Dynamic Programming Algorithm,
some effort was made to examine their closeness of fit to DYNGEN data.
Steady state values of models 1 and 4 are compared, and fuel flow step re-
sponses of models 3A, 3B, and 4 are plotted in comparison to DYNGEN responses.
A description of the step response program is also included.

5.2 Steady State Comparison of Models 1 and 4

The function $g(u)$ represents a mapping from the control space into
the state space, relating fixed controls to steady states. It is not only
useful in the model form:

$$\dot{x} = A(x,u)[x - g(u)] \qquad\qquad (5.2\text{-}1)$$

but should also approximate the operating line of the plant.

Such a comparison is made here between $g(u)$ for model 4 and the
DYNGEN simulator. Nozzle area was held constant, as fuel flow was varied
from 9.0 to 1.1 by 0.02. All values are normalized. Percentage error is
also computed, and shows the model's excellent agreement in its range of
accuracy, and rapid deterioration outside that range.

189

Table 5.2-1

X(1) = NC

fuel flow	DYNGEN	Model 4	% error
0.90	.97275	.97288	0.01
0.92	.97761	.97790	0.03
0.94	.98326	.98326	0.00
0.96	.98887	.98892	0.01
0.98	.99445	.99461	0.02
1.00	1.0000	1.0000	0.00
1.02	1.0051	1.0051	0.00
1.04	1.0102	1.0113	0.11
1.06	1.0152	1.0230	0.77
1.08	1.0201	1.0513	3.06
1.10	1.0244	1.1195	9.28

C - 3

Table 5.2-2

$$X(2) = NF$$

fuel flow	DYNGEN	Model 4	% error
0.90	.97132	.97099	-0.03
0.92	.97883	.97817	-0.07
0.94	.98427	.98425	0.00
0.96	.98961	.98948	-0.01
1.00	1.0000	1.0000	0.00
1.02	1.0046	1.0011	-0.35
1.04	1.0091	.98046	-2.84
1.06	1.0136	.89094	-12.10
1.08	1.0180	.62787	-38.32
1.10	1.0221	-.013230	-101.29

Table 5.2-3

X(3) = P4

fuel flow	DYNGEN	Model 4	% error
0.90	.92038	.92042	0.00
0.92	.93623	.93633	0.01
0.94	.95225	.95225	0.00
0.96	.96821	.96824	0.00
0.98	.98413	.98434	0.02
1.00	1.0000	1.0000	0.00
1.02	1.0148	1.0125	−0.23
1.04	1.0295	1.0136	−1.54
1.06	1.0441	.98374	−5.78
1.08	1.0587	.88135	−16.75
1.10	1.0727	.62822	−41.44

Table 5.2-4

$$X(4) = P7$$

fuel flow	DYNGEN	Model 4	% error
0.90	.94118	.94109	-0.01
0.92	.95358	.95340	-0.02
0.94	.96532	.96531	0.00
0.96	.97697	.97693	0.00
0.98	.98853	.98856	0.00
1.00	1.0000	1.0000	0.00
1.02	1.0107	1.0081	-0.26
1.04	1.0213	1.0013	-1.96
1.06	1.0319	.94911	-8.02
1.08	1.0425	.78384	-24.81
1.10	1.0527	.37203	-64.66

Table 5.2-5

$$X(5) = U4$$

fuel flow	DYNGEN	Model 4	% error
0.90	.96625	.96624	0.00
0.92	.97304	.97308	0.00
0.94	.97992	.97992	0.00
0.96	.98670	.98665	-0.01
0.98	.99339	.99320	-0.02
1.00	1.0000	1.0000	0.00
1.02	1.0074	1.0089	0.15
1.04	1.0147	1.0248	1.00
1.06	1.0219	1.0573	3.46
1.08	1.0290	1.1231	9.14
1.10	1.0365	1.2494	20.54

5.3 Program Layout

The method chosen for generating time response data was a Euler inegration with a user varied time step. After specifying initial controls, the user provides a control sequence of time step, duration (in iterations), and controls.. This structure allows the user to provide smaller time increments for the steeper portions of the response, and to alter the controls during the response. The step response program creates a file of time-state n-tuples, which are plotted against similar DYNGEN data by another program.

5.4 Fuel Step Response for Models 3A, 3B, and 4

Each of the three models was subjected to a fuel flow step from 0.8 to 1.0, and the response plotted against the same response by DYNGEN. These graphs show that all three models match DYNGEN closely, but that model 4 is a better fit than either 3A or 3B.

STEP RESPONSE OF MODEL 3A VS. DYNGEN
FOR FUEL FLOW STEP FROM 0.8 TO 1.0
DYNGEN DENOTED BY ×
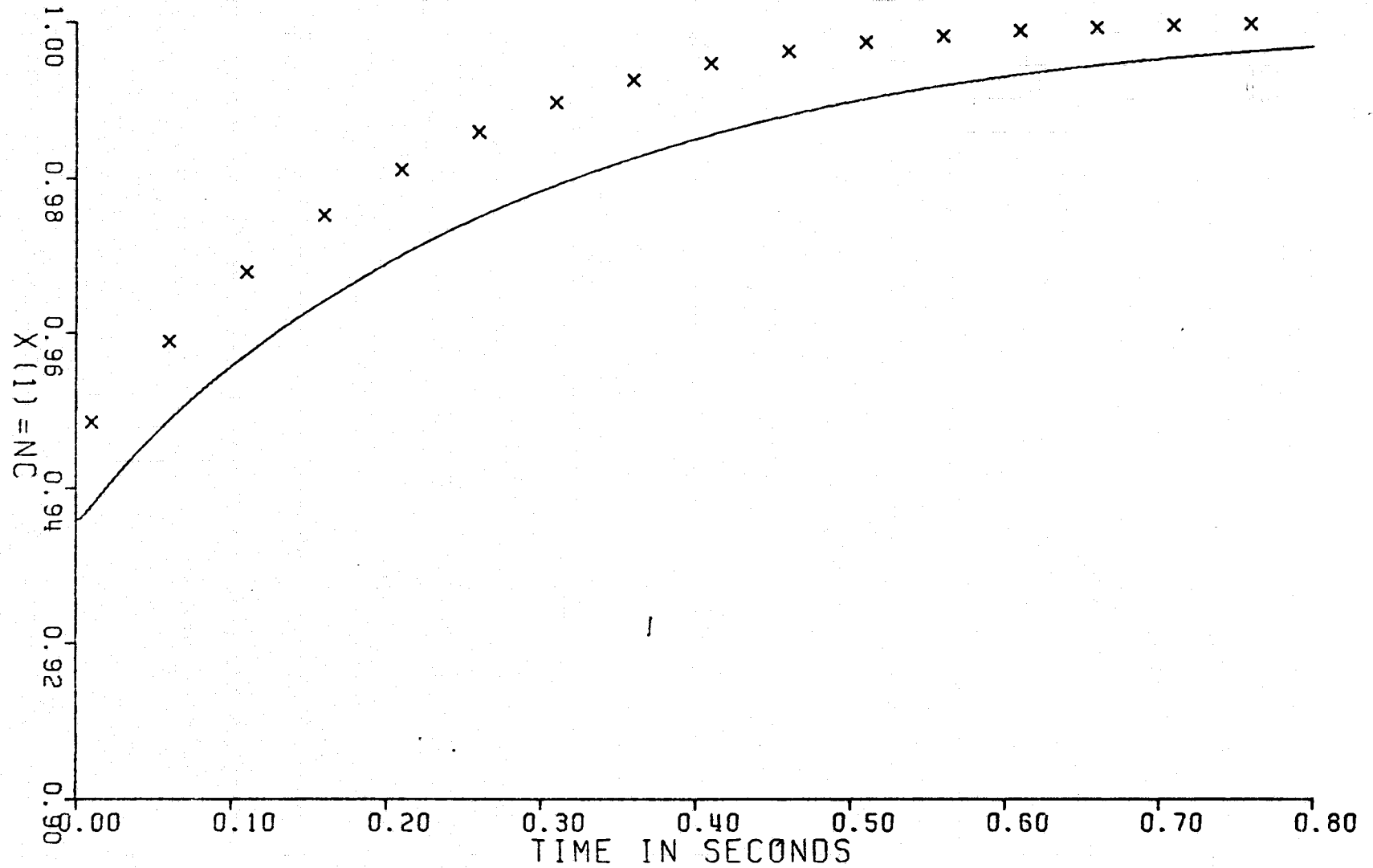
Figure 5.4-1

STEP RESPONSE OF MODEL 3A VS. DYNGEN
FOR FUEL FLOW STEP FROM 0.8 TO 1.0
DYNGEN DENOTED BY ×
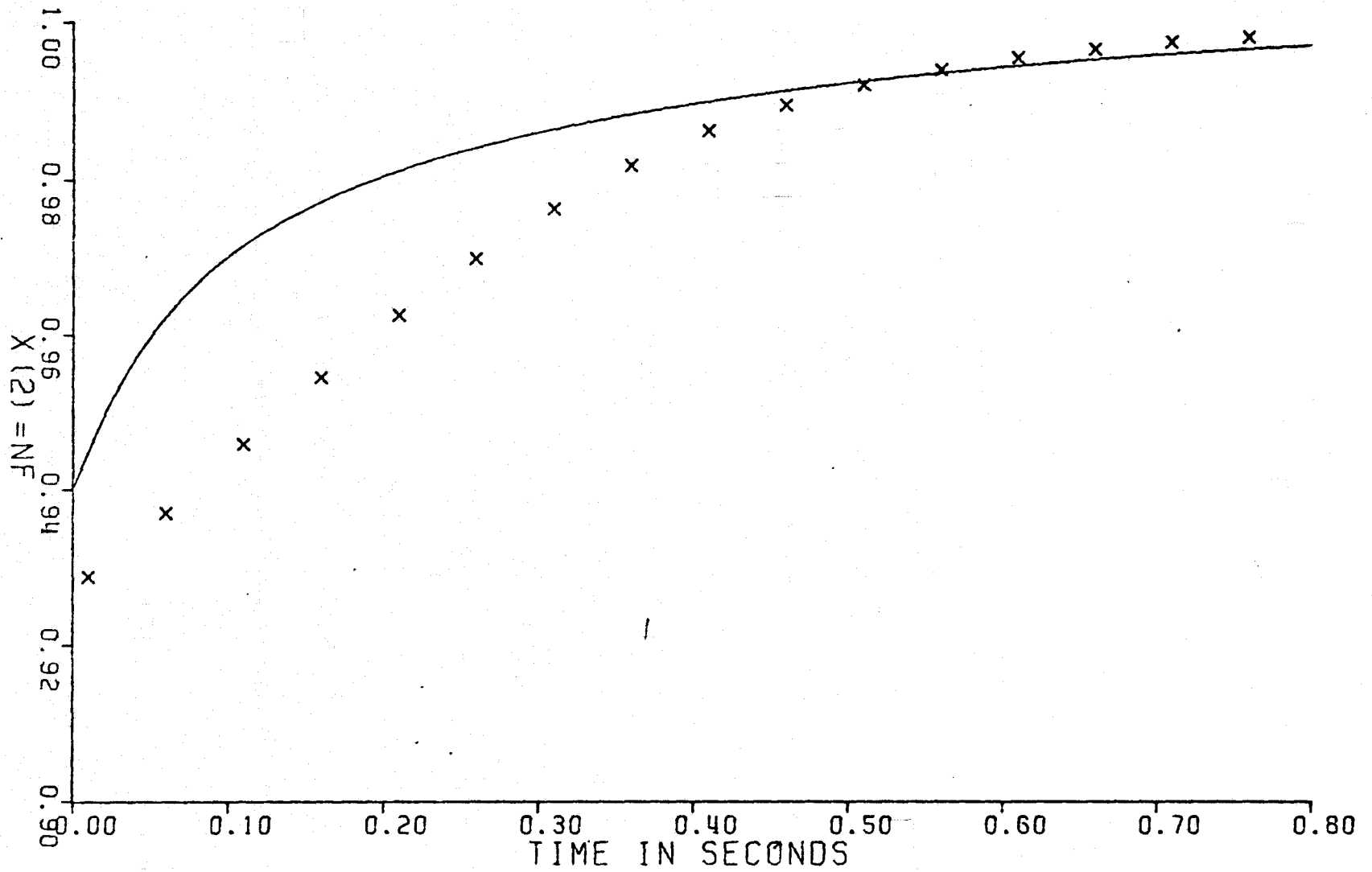
Figure 5.4-2

STEP RESPONSE OF MODEL 3A VS. DYNGEN
FOR FUEL FLOW STEP FROM 0.8 TO 1.0
DYNGEN DENOTED BY ×

X (3) = P4

TIME IN SECONDS
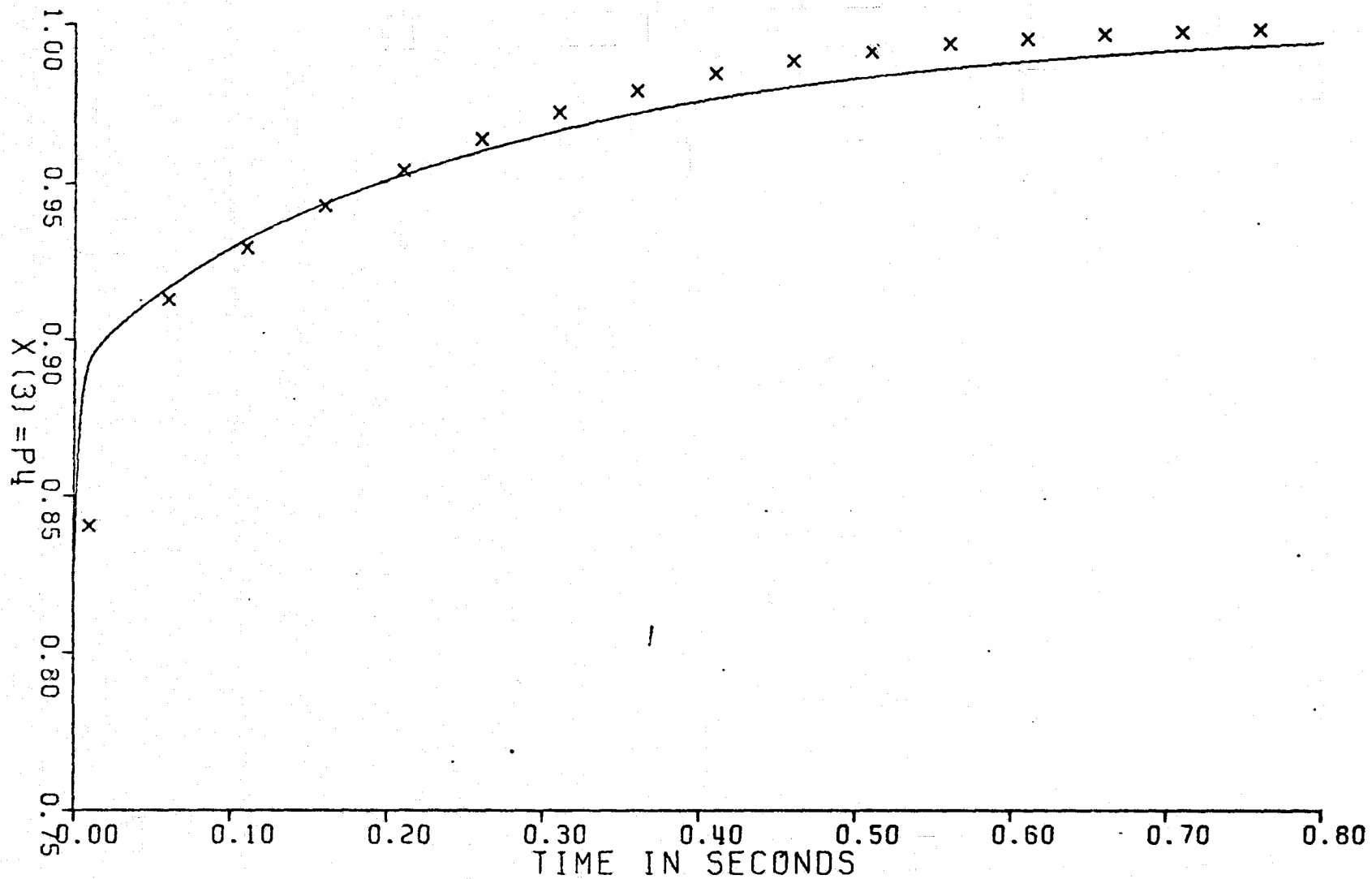
Figure 5.4-3

STEP RESPONSE OF MODEL 3A VS. DYNGEN
FOR FUEL FLOW STEP FROM 0.8 TO 1.0
DYNGEN DENOTED BY ✕
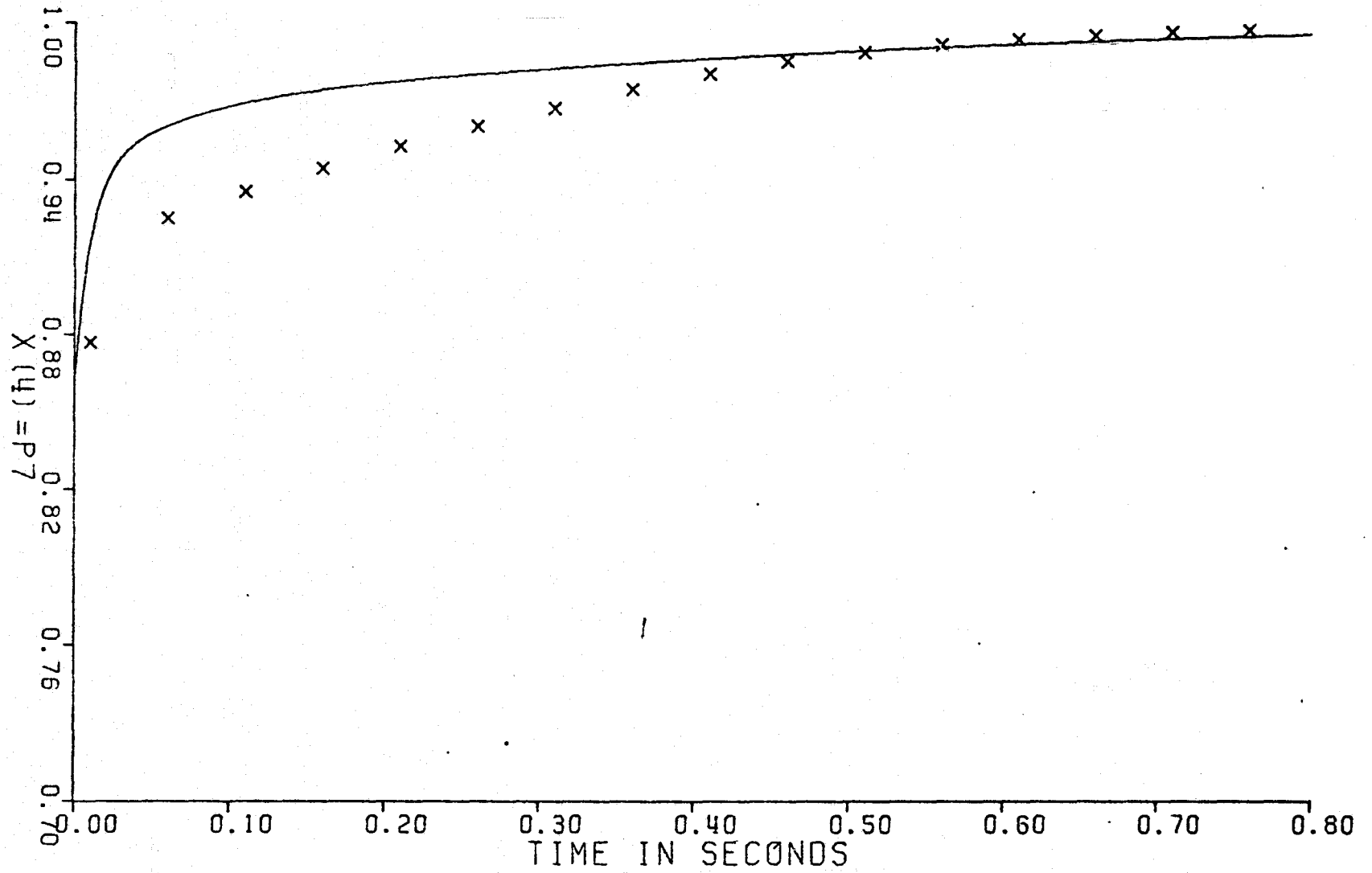
Figure 5.4-4

STEP RESPONSE OF MODEL 3A VS. DYNGEN
FOR FUEL FLOW STEP FROM 0.8 TO 1.0
DYNGEN DENOTED BY ✕
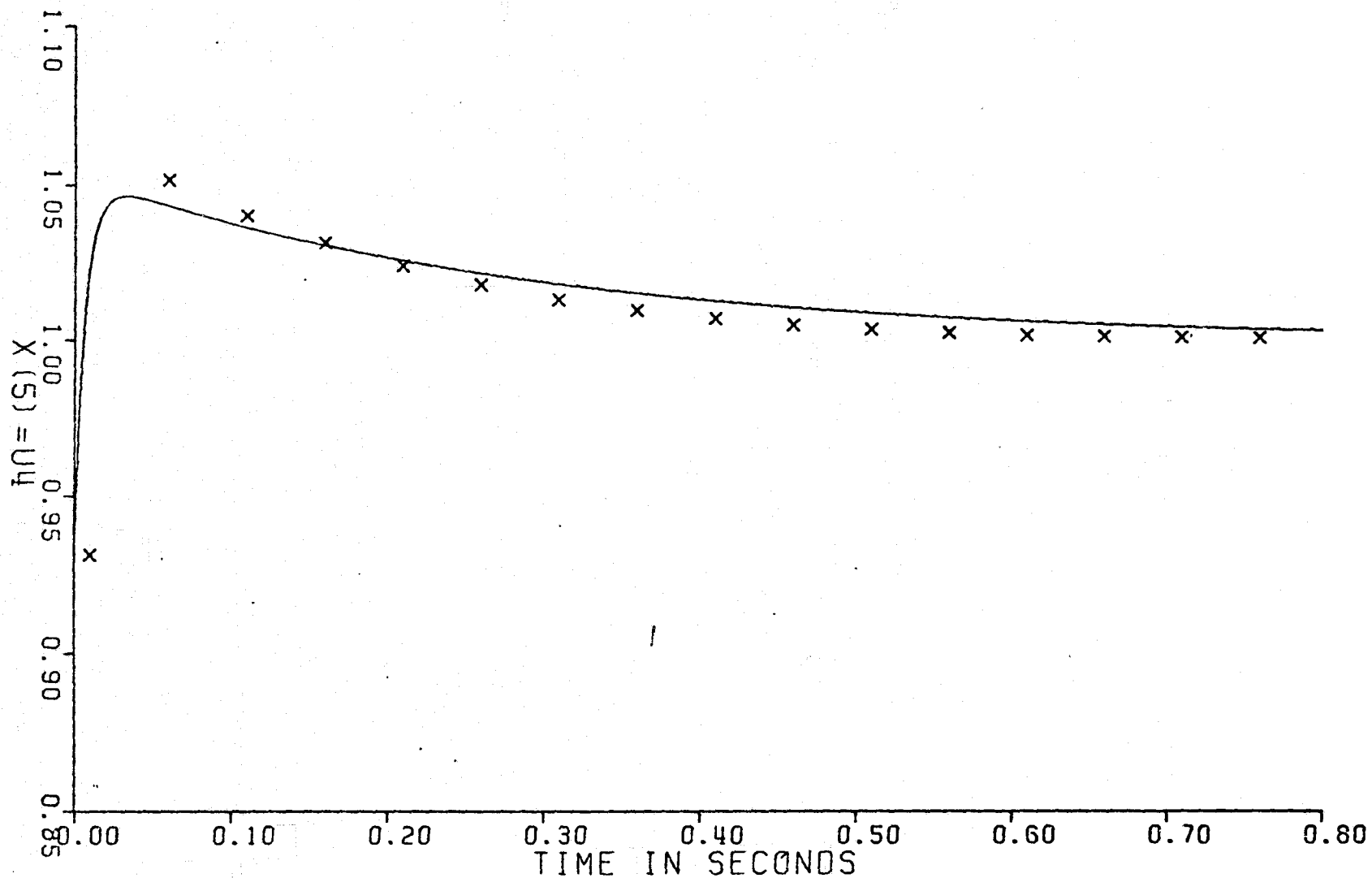
Figure 5.4-5

STEP RESPONSE OF MODEL 3B VS. DYNGEN
FOR FUEL FLOW STEP FROM 0.8 TO 1.0
DYNGEN DENOTED BY ✕
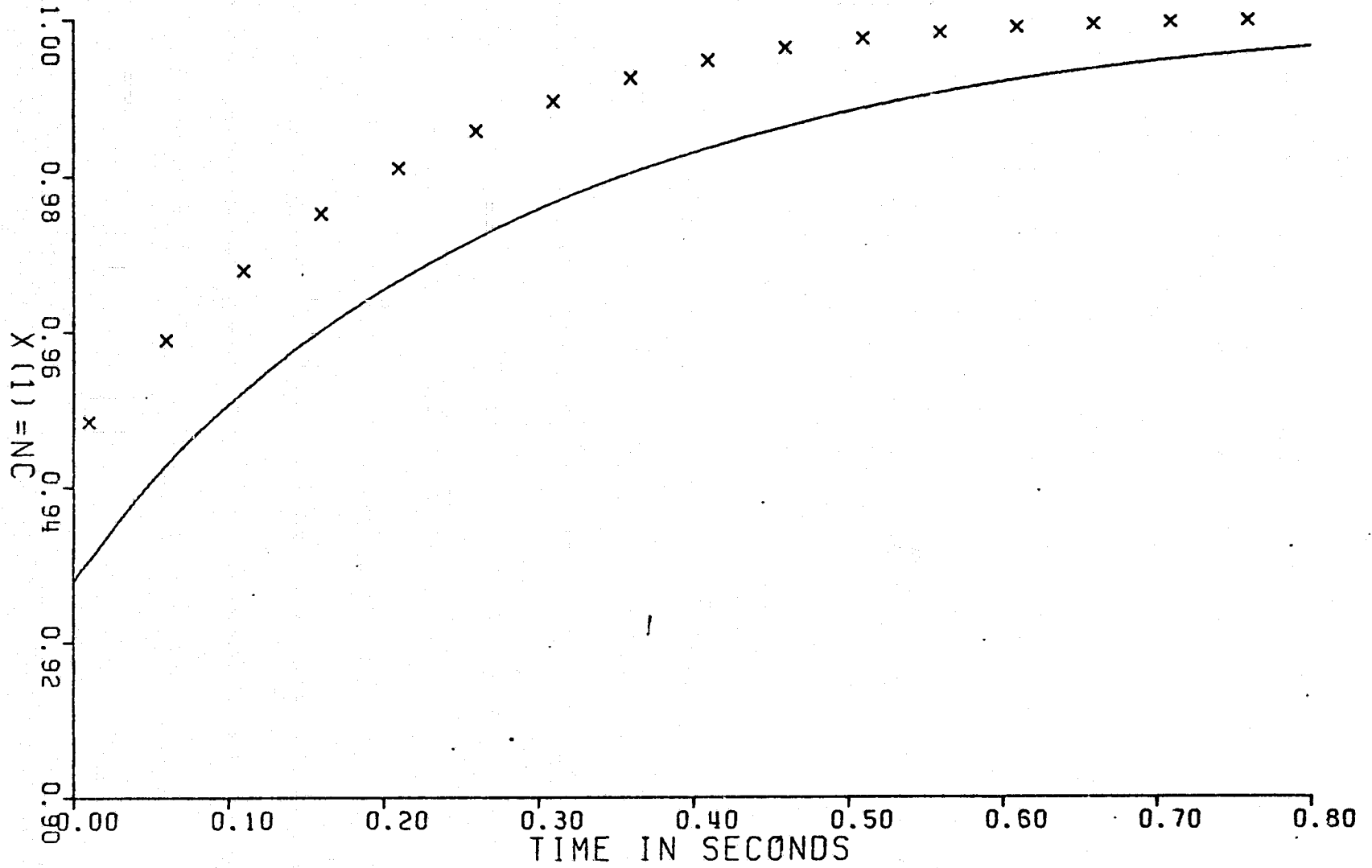
Figure 5.4-6

STEP RESPONSE OF MODEL 3B VS. DYNGEN
FOR FUEL FLOW STEP FROM 0.8 TO 1.0
DYNGEN DENOTED BY ✕
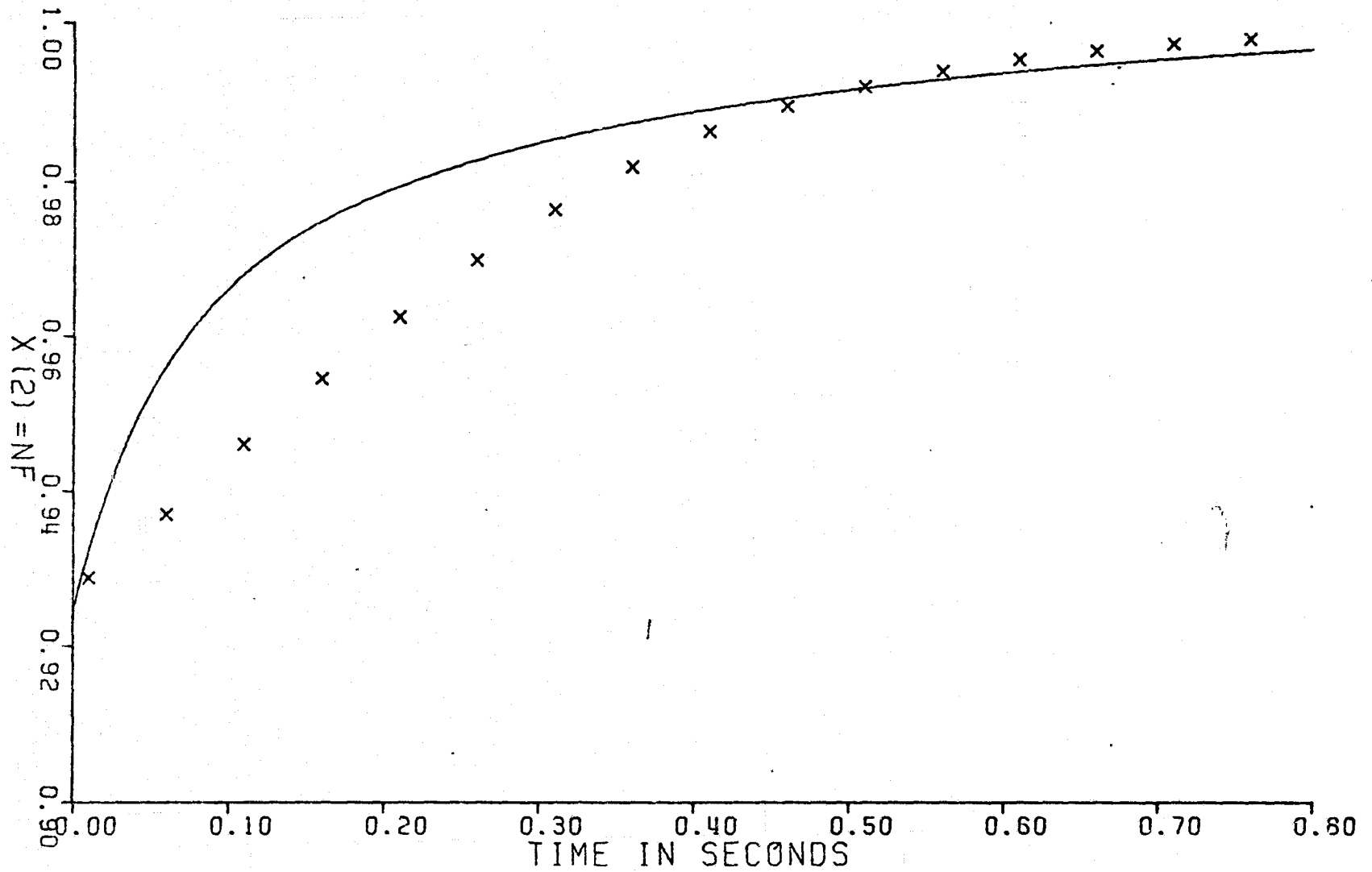
Figure 5.4-7

STEP RESPONSE OF MODEL 3B VS. DYNGEN
FOR FUEL FLOW STEP FROM 0.8 TO 1.0
DYNGEN DENOTED BY ×
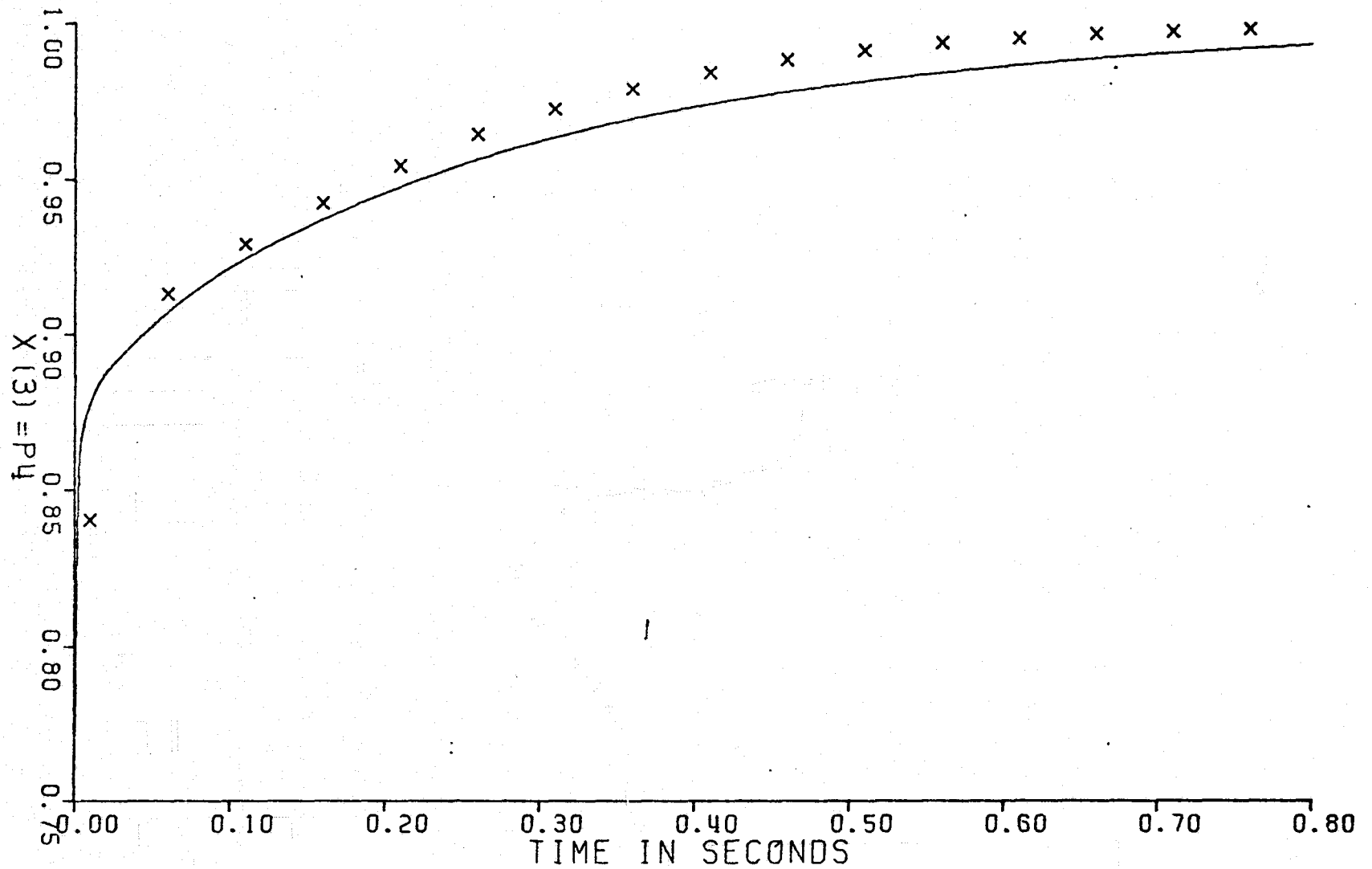
Figure 5.4-8

STEP RESPONSE OF MODEL 3B VS. DYNGEN
FOR FUEL FLOW STEP FROM 0.8 TO 1.0
DYNGEN DENOTED BY ✕
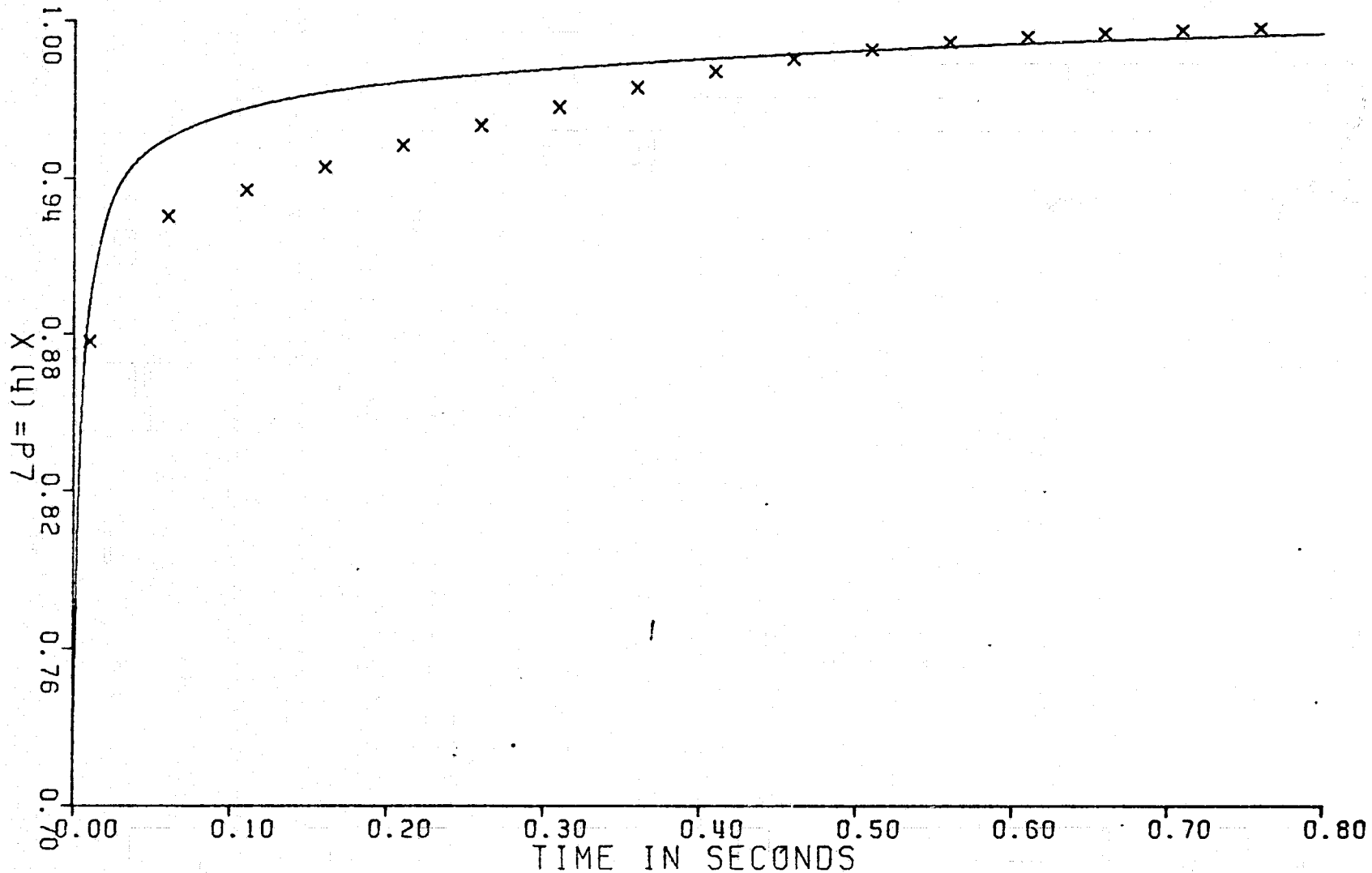
Figure 5.4-9

STEP RESPONSE OF MODEL 3B VS. DYNGEN
FOR FUEL FLOW STEP FROM 0.8 TO 1.0
DYNGEN DENOTED BY ×
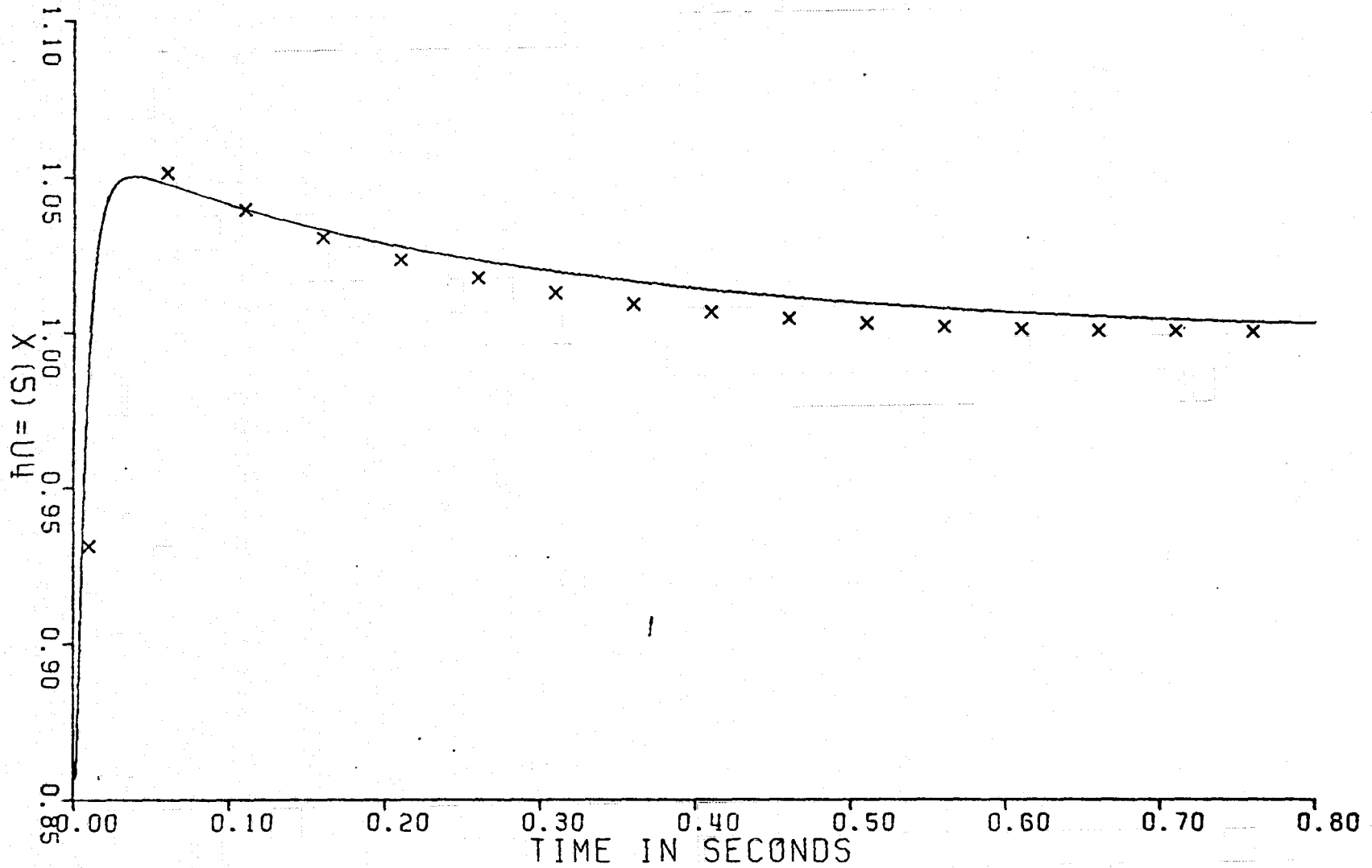
Figure 5.4-10

STEP RESPONSE OF MODEL 4 VS. DYNGEN
FOR FUEL FLOW STEP FROM 0.8 TO 1.0
DYNGEN DENOTED BY ✕
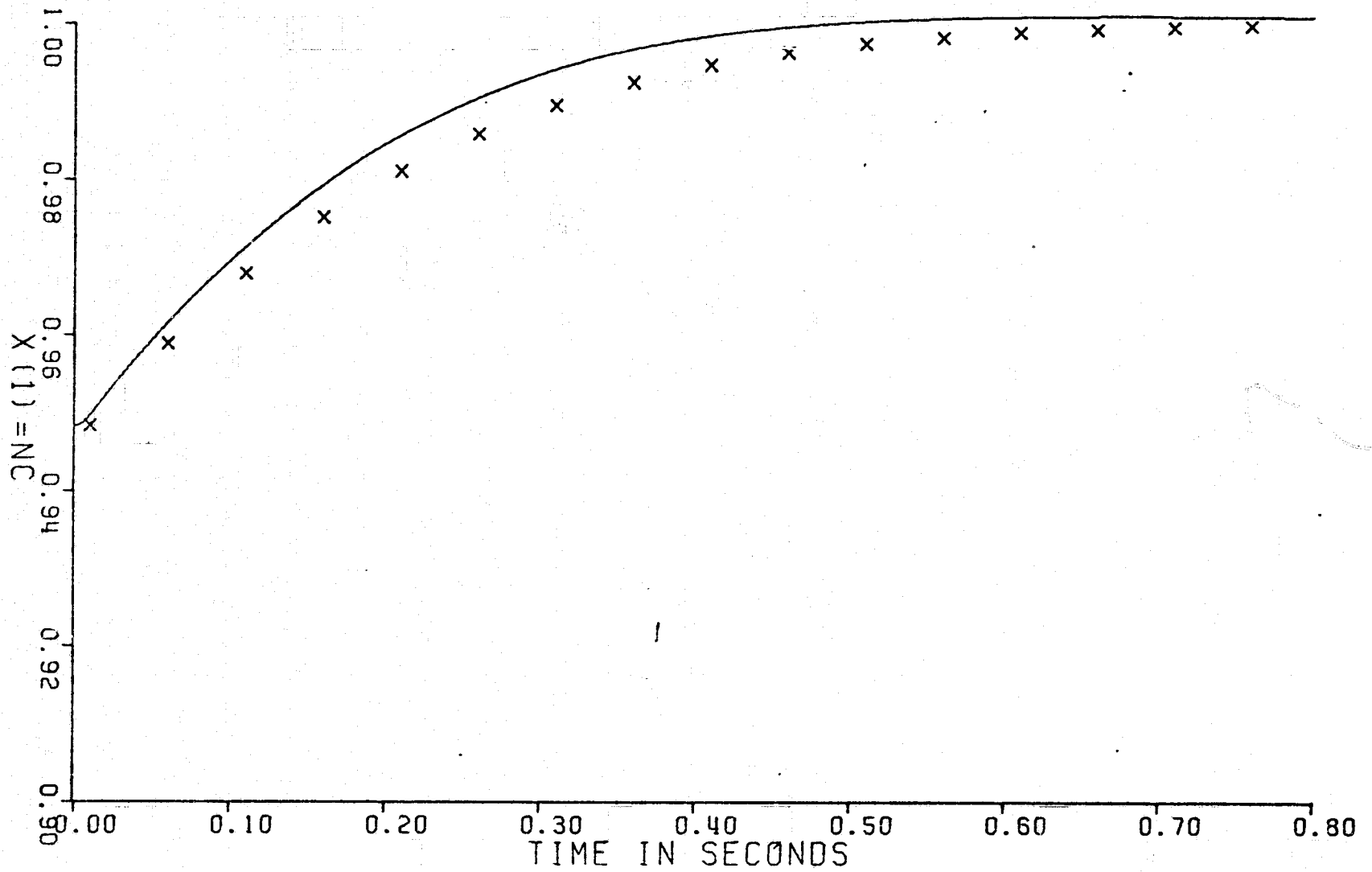
Figure 5.4-11

STEP RESPONSE OF MODEL 4 VS. DYNGEN.
FOR FUEL FLOW STEP FROM 0.8 TO 1.0
DYNGEN DENOTED BY ×
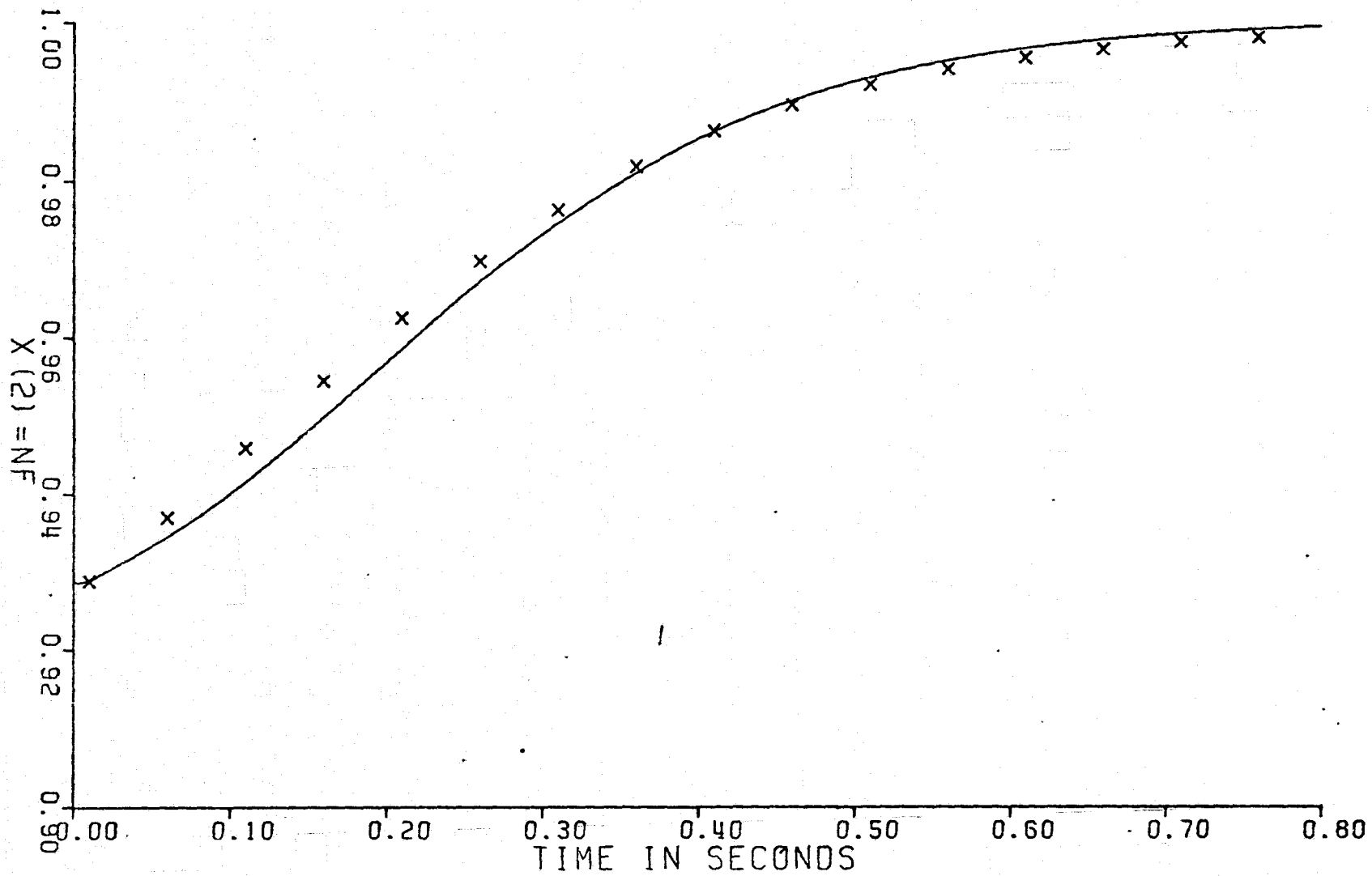
Figure 5.4-12

STEP RESPONSE OF MODEL 4 VS. DYNGEN
FOR FUEL FLOW STEP FROM 0.8 TO 1.0
DYNGEN DENOTED BY ×
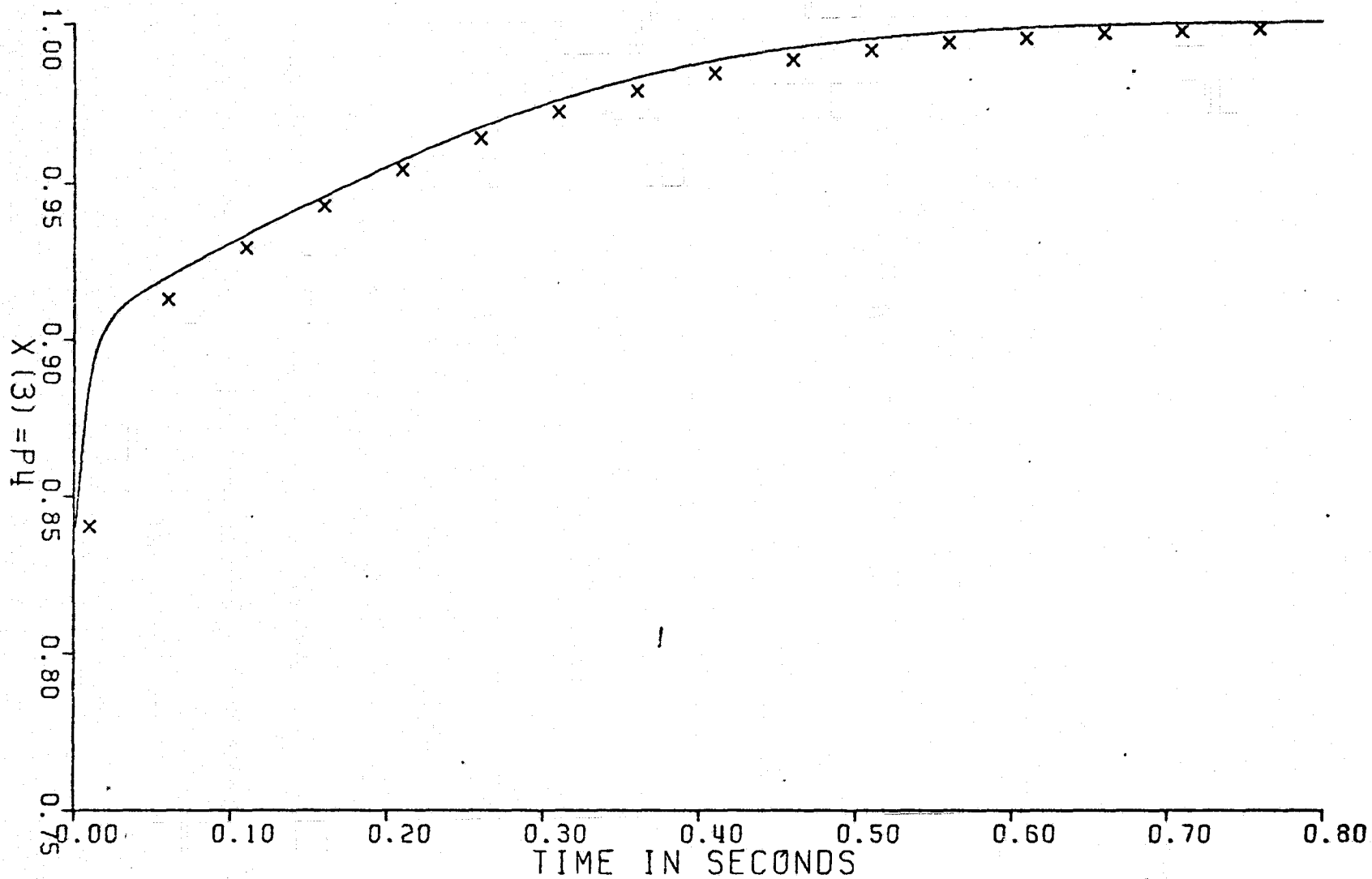
Figure 5.4-13

STEP RESPONSE OF MODEL 4 VS. DYNGEN
FOR FUEL FLOW STEP FROM 0.8 TO 1.0
DYNGEN DENOTED BY ✕
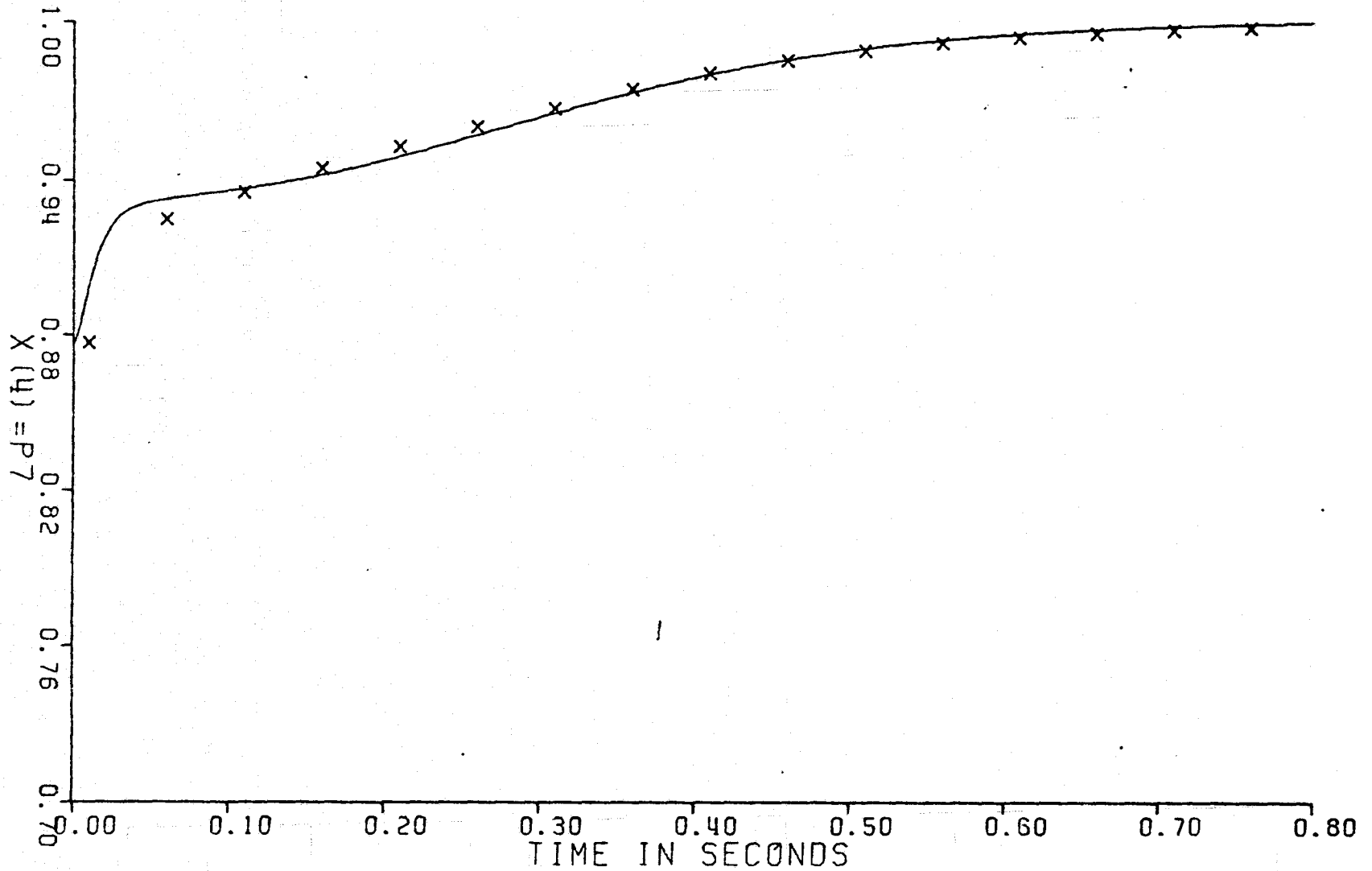
Figure 5.4-14

STEP RESPONSE OF MODEL 4 VS. DYNGEN
FOR FUEL FLOW STEP FROM 0.8 TO 1.0
DYNGEN DENOTED BY ✕

Figure 5.4-15